SYNTHETIC, SPECTROSCOPIC, AND ELECTROCHEMICAL STUDIES ON COMPLEXES OF RUTHENIUM AND OSMIUM

Vyvyan T. Coombe

Ph.D. Thesis

University of Edinburgh

1985

DECLARATION

Except where specific reference is made to other sources, the work presented in this thesis is the original work of the author. It has not been submitted, in whole or in part, for any other degree. Certain of the results have already been published.

V.T. Coombe

To my Mother, Father and Sister

and to my Wife

ACKNOWLEDGEMENTS

The author wishes to thank Dr. G.A. Heath and Dr. T.A. Stephenson for their unending help and encouragement throughout the couse of this work. I also wish to express my gratitude to Dr D.K. Vattis and Dr. L.J. Yellowlees for their invaluable contributions to this study.

In addition, I am grateful to Dr. D. Reed, Mr. J.A.A. Millar and Mr. L.H. Bell for recording ^{31}P, ^{13}C, and ^{1}H nmr spectra, to Mr. M. Grunbaum for performing microanalytical measurements and to Napier College of Commerce and Technology, Edinburgh, for the use of their spectrophotometric facilities.

I am deeply indebted to the S.E.R.C. for their financial support and to the University of Edinburgh for the use of facilities.

ABSTRACT

Chapter 1

Reviews triply halide bridged binuclear ruthenium systems of the type $[L_{(3-x)}Cl_xRuCl_3RuCl_yL_{(3-y)}]$ in oxidation states ranging from Ru_2(II/II) to Ru_2(III/III). In the present work, organo-soluble salts of $[Ru_2X_9]^{3-}$ (X = Cl,Br) are described and their electrochemical, magnetic and spectroscopic properties investigated. Electrosynthesis of the oxidised derivatives $[Ru_2X_9]^{2-}$ and $[Ru_2X_9]^{-}$, and their characterisation by electronic absorption spectroscopy and magnetic susceptibility measurements have helped to elucidate their electronic nature, leading to a greater understanding of the nature of ruthenium triple halide-bridged complexes in general.

Chapter 2

Mixed-valence triple chloro bridged binuclear complexes of ruthenium bearing NH_3 or H_2O terminal ligands such as $[Ru_2Cl_3(NH_3)_6]^{2+}$ and $[Ru_2Cl_3(H_2O)_6]^{2+}$ are discussed. A comprehensive examination of the redox properties of $[Ru_2Cl_3(NH_3)_6]^{2+}$ achieved in non-aqueous media, and of optical spectra in differing oxidation states, are reported. The underlying metal metal interactions are discussed in relation to the influence of terminal ligand basicity.

Chapter 3

A sequence of binuclear complexes of the type $[Ru_2Br_x(AsR_3)_{(9-x)}]$ (x = 5,6) have been synthesised and previous suggestions regarding their structure as indicated by esr studies and their electrochemical

behaviour, have been enhanced and reinforced.

Chapter 4

Electroreduction of mer $[OsCl_3(PMe_2Ph)_3]$ in a variety of coordinating media has produced a range of 6-coordinate Os(II) monomeric complexes in two separable isomeric forms. In non-coordinating solvents the Os(III) complex is found to expel chloride under most conditions, to give a detectable 5-coordinate intermediate, which can react under favourable conditions to produce doubly- and triply-bridged binuclear species. This series of electro-initiated reactions has so far yielded many separate complexes, identified by both spectroscopic methods and voltammetric data.

Appendix 1

Voltammetric measurements establish a reversible one-electron oxidation for the complex $[RuCl_5NO]^{2-}$. Bulk electrogeneration of the resulting oxidised species has allowed i.r, esr and magnetic susceptibility measurements to confirm its existance as the low-spin $[RuCl_5NO]^{-}$ ion, in contrast to previous reports.

Appendix 2

Electrochemical studies on $[Os_2(OCOR)_4Cl_2]$ (R = Et, ^{n}Pr) and $[Os_2(hp)_4Cl_2]$ (hp = hydroxypyridinate anion) establish a reversible one-electron reduction for these complexes, producing the first examples of species containing the Os_2^{5+} core. These derivatives have been characterised by voltammetry, electronic absorption spectroscopy, esr spectroscopy and magnetic susceptibility measurements.

CONTENTS page

LIST OF FIGURES page

LIST OF TABLES

A2.1 Magnetic Measurements (Evans' Method) on mer-$[OsCl_3(PMe_2Ph)_3]$ in CH_2Cl_2 at Differing Field Strengths

CHAPTER 1

Synthesis and Characterisation of $[Ru_2X_9]^{n-}$ Complexes (X = Cl, Br) in Differing Oxidation States

1.1 Introduction

Since the early 1970's much work has been carried out in our laboratories on the synthesis and characterisation of redox-active triple-bridged binuclear complexes of ruthenium and osmium [1,2,3,4,5,6]. These compounds take the form of a confacial bioctahedron as shown in Figure 1.1. The three bridging ligands are usually small anionic moieties such as halide ion, OH^- or SEt^- with the remaining six terminal sites occupied by soft neutral ligands such as PR_3, AsR_3, CO or CS, or harder neutral ligands *i.e.* NH_3 or H_2O, frequently with one or more terminal halide ligands.

The first of these compounds produced in 1961 by Chatt and co-workers [7] were of the $[M_2Cl_3(PR_3)_6]^+$ family (M = Ru, Os; PR_3 = a variety of tertiary phosphine ligands). The compounds were synthesised by heating commercial ruthenium trichloride ($RuCl_3.xH_2O$) or $Na_2[OsCl_6]$ in a polar solvent under N_2 in the presence of an excess of PR_3, illustrating the first example of a general pathway for the production of these species. The confacial bioctahedral structure of these compounds was confirmed by Raspin in 1969 [8] with the published structure of $[Ru_2Cl_3(PEt_2Ph)_6][RuCl_3(PEt_2Ph)_3]$. Electrochemical studies of $[Ru_2Cl_3(PR_3)_6]^+$ compounds in this department have revealed that they undergo two reversible one-electron oxidations [9], (*e.g.* $[Ru_2Cl_3(PMe_2Ph)_6]Cl$ undergoes an oxidation at +1.33V and an oxidation at +1.87V *vs.* Ag/AgCl; separation 0.54V), thus illustrating the possible changes in oxidation state of the complex without loss in

overall structure.

Since the first reports by Chatt et al. many more species have been synthesised, virtually all containing bulky terminal PR_3 or AsR_3 ligands either alone or together with CO or CS. A notable further category is the series of π-bonded arene systems of the type $[ArRuCl_3RuAr]^+$ [6]. Significantly, many of the new complexes richer in terminal halide ligation exhibited metal centres in higher oxidation states than $M_2(II/II)$, such as the $[M_2Cl_5(QR_3)_4]$ family (M = Ru; QR_3 = $AsPh_3$, $As(p\text{-tolyl})_3$, $As(PhCl)_3$, PEt_2Ph, PMe_2Ph: M = Os; QR_3 = $AsPh_3$, $As(p\text{-tolyl})_3$, PPh_3) and the $[Ru_2Cl_6(QR_3)_3]$ family (QR_3 = $AsPh_3$, $As(p\text{-tolyl})_3$) [10,11,12]. In the former family of complexes the M_2 unit exists in a II/III mixed-valence oxidation state and there are three possible geometric isomers consistent with the confacial bioctahedral structure, i.e. both terminal Cl^- ligands attached to one metal centre (asymmetric, type I) or one per metal centre at either end of the molecule (symmetric, type II or III) (see Figure 1.2).

In 1967 Nicholson described the isolation and crystallographic structure of $[Ru_2Cl_5(P^nBu_3)_4]$ [13]. Interestingly where QR_3 = tertiary phosphine, this is the only report of a symmetric (type II) isomer. Despite numerous attempts we have never been able to duplicate this preparation although an analogous complex of the type $[(AsR_3)_2ClRuCl_3RuCl(AsR_3)_2]$ (R = p-tolyl) has been discovered and characterised [11].

A major question which arises in the consideration of

Figure 1.1 Structure of the Generalised Triple Bridged Confacial Bioctahedron

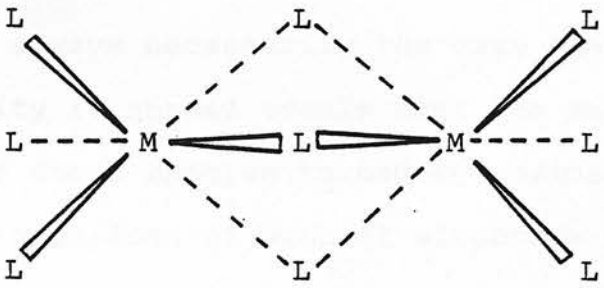

Figure 1.2 Possible Isomeric Structures of $[M_2Cl_5(QR_3)_4]$ Complexes (M = Ru, Os; QR_3 = Tertiary Arsine or Phosphine Ligand)

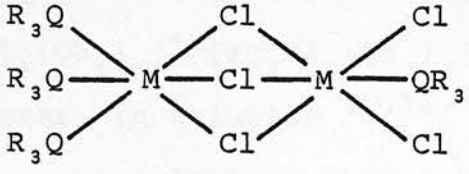

Type I

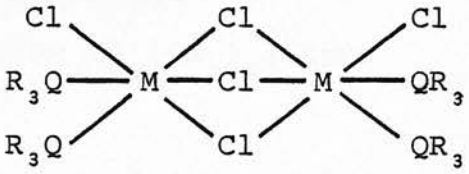

Type II

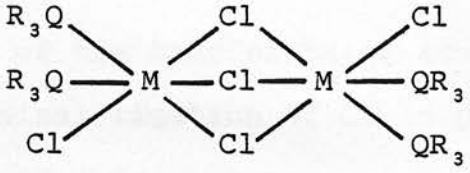

Type III

molecules such as the $[Ru_2Cl_5L_4]$ system outlined above is the nature of the electronic interaction between the metal centres, especially where formally mixed-valence metal ions occur in one molecule. It has been found that it is certainly not always necessarily the case that the electron density is spread evenly over the metal centres. The ability of these species to undergo oxidations and reductions without loss of overall structure has meant that electrochemistry, coupled with spectroscopic techniques, has proved an ideal probe for investigating their electronic properties.

In our laboratory spectroscopic measurements have previously been undertaken on an extensive range of compounds which either naturally occur in a mixed oxidation state such as the $[Ru_2Cl_5L_4]$ type outlined above or which can be electrochemically oxidised or reduced to produce a mixed oxidation state, such as the $[Ru_2Cl_3(QR_3)_6]^+$ $[Ru_2Cl_4(QR_3)_5]$ and $[Ru_2Cl_6(QR_3)_3]$ type complexes, in solution [9,12,14].

Two major factors have been found to influence the potentials at which metal-based redox processes occur in the previously mentioned complexes:

a) The isomeric form of the complex being studied and

b) The degree of terminal ligation of Cl in place of soft neutral ligands e.g. PR_3.

For example, on investigation of the electrochemical behaviour of the complex $[Ru_2Cl_5(As\{p\text{-}tol\}_3)_4]$ [11], the effect of the isomeric form on the electrochemistry of these species was immediately apparent. While the

symmetric form has a separation between oxidation and reduction of ca. 0.70V, moving a terminal Cl^- ligand from one end of the molecule to the other to produce the asymmetric complex makes both the reduction and the oxidation more inaccessible, increasing their separation to ca. 1.5V.

Similarly the electrochemical behaviour of $[Ru_2Cl_5(PR_3)_4]$ complexes, of which only the asymmetric form was available, showed a wide separation of ca. 1.55V between the oxidation and reduction potentials [10] characteristic of all such asymmetric complexes so far investigated.

The electrochemical behaviour of $[Ru_2Cl_6(AsPh_3)_3]$ [10] and $[Ru_2Cl_6(As\{p\text{-}tol\}_3)_3]$ [11] on the other hand, which have both been shown to have the structure illustrated in Figure 1.3, exhibits a separation between the two reductions of ca. 1.05V.

These observations led us to an intensive investigation into the correlation of the potentials at which redox activity occurs, with the specific structure of the particular complex being studied, i.e. the extent of terminal ligation of Cl^- ,(y+x), and the asymmetry of Cl^- ligation, (y-x), for a whole range of complexes of the general type $[L_{(3-x)}Cl_xMCl_3MCl_yL_{(3-y)}]$ (M = Ru, Os: L = soft neutral ligand e.g. PR_3, AsR_3) [9,10,11,12,14].

The data obtained showed that the relationship between redox potential separation and the degree of asymmetry, (y-x), of terminal halide ligation, as outlined above for the complexes of the $[Ru_2Cl_5L_4]$ family, holds true for

Figure 1.3 Structure of $[Ru_2Cl_6(AsPR_3)_3]$ (R = Ph, p-tolyl)

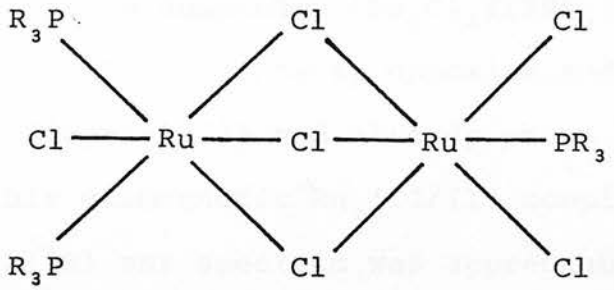

other complexes of the type $[L_{(3-x)}Cl_xMCl_3MCl_yL_{(3-y)}]$. As the asymmetry between the two metal centres increases, the separation between the two redox couples also increases, by ca. 0.5V per excess Cl^-. Furthermore it appeared that all the results obtained on investigation of the change in redox potential with differing terminal halide ligation, (y+x), could be interpreted using a few simple empirical rules based on the available electrochemical data. Nmr spectroscopic data on complexes $[Ru_2Cl_4Y(PPh_3)_4]$ (Y = CO, CS) (terminal Y and Cl ligands at opposite ends of the molecule, (see figure 1.4)) had already shown [9] that on oxidation of this diamagnetic Ru_2(II/II) complex only one half of the $^{31}P\{^1H\}$ nmr spectrum was appreciably disturbed, that is, only the AB pattern resulting from the end of the molecule containing the terminal chloride collapses, leaving the AB pattern resulting from the end containing the terminal CO or CS ligand, almost unperturbed. This strongly suggested that the two ruthenium centres in the molecule are distinct, so that on oxidation of the complex from the II/II to the II/III species, only one of the metal centres (i.e. the centre with the coordinated terminal Cl^- ligand) undergoes any appreciable change in oxidation state.

It appeared that if all the binuclear compounds investigated electrochemically were regarded in a similar manner, i.e. with two distinct centres, capable of sequential redox change, then the electrochemical data could be interpreted using three simple empirical rules.

Figure 1.4 $^{31}P\{^{1}H\}$ n.m.r. Spectra of $[Ru_2Cl_4(CO)(PPh_3)_4]$ Before and After Oxidation

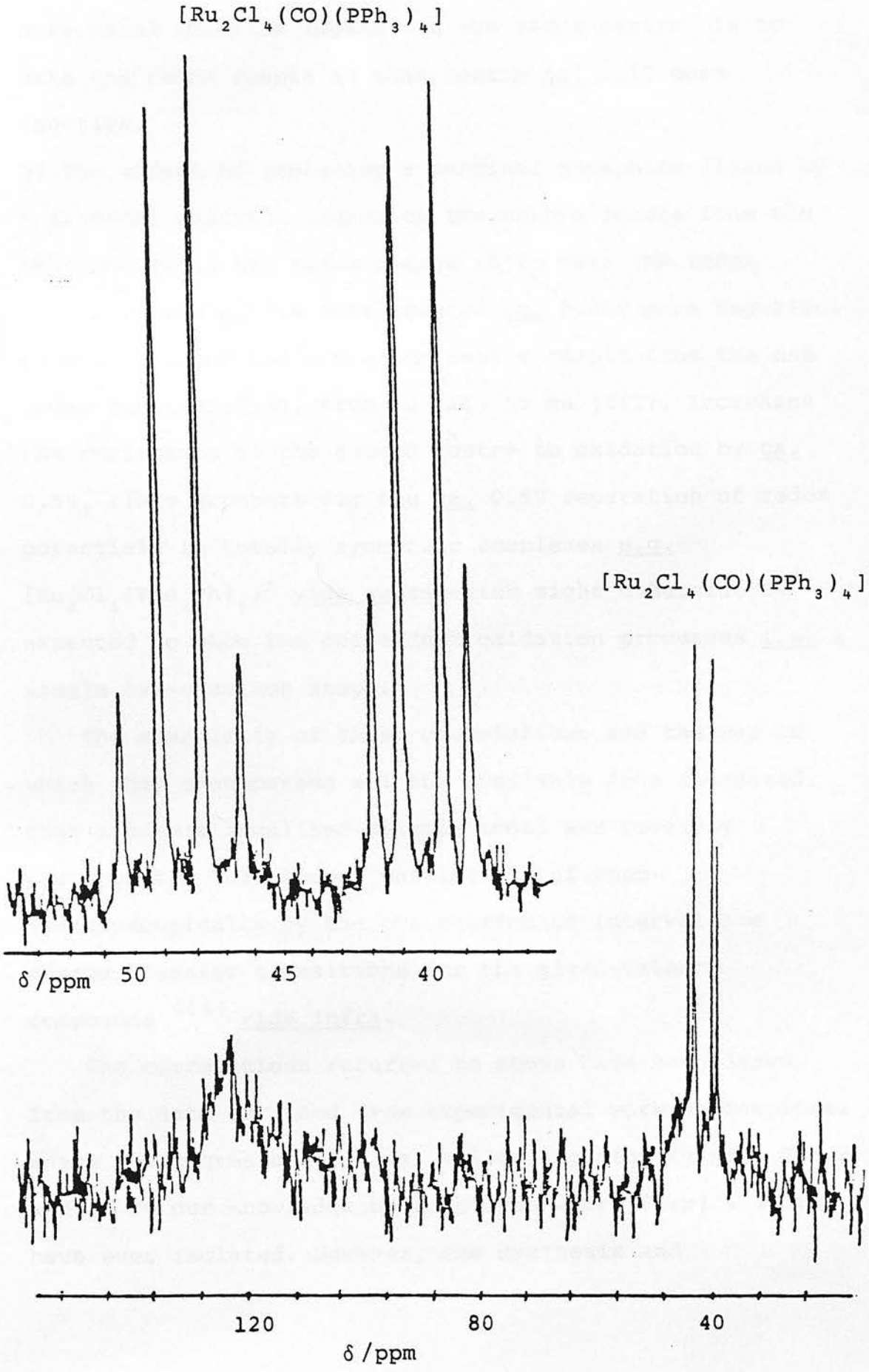

Thus:

a) The effect of replacing one neutral phosphine ligand by a terminal chloride ligand on the redox centre is to make the redox couple at that centre *ca.* 0.7V more negative.

b) The effect of replacing a terminal phosphine ligand by a terminal chloride ligand on the centre remote from the one undergoing the redox change is to make the redox couple of the *active* metal centre *ca.* 0.25V more negative.

c) Oxidation of the ruthenium centre remote from the one under consideration, from Ru (II) to Ru (III), increases the resistance of the second centre to oxidation by *ca.* 0.5V, (This accounts for the *ca.* 0.5V separation of redox potentials in totally symmetric complexes *e.g.* $[Ru_2Cl_3(PMe_2Ph)_6]^+$ *vide supra* which might otherwise be expected to show two coincident oxidation processes *i.e.* a single two-electron step).

The simplicity of these correlations and the way in which they encompassed all the available data suggested that a simple localised-valence model was possibly appropriate. This theory was later confirmed spectroscopically by the observation of intervalence charge transfer transitions for the mixed-valence compounds [14] *vide infra*.

The correlations referred to above have been drawn from the data obtained from experimental work on complexes where the degree of terminal halide ligation (y+x) = 0,1,2 and 3. To our knowledge no complexes where (y+x) = 4 or 5 have ever isolated. However, the synthesis and

characterisation of complexes where (x+y) = 6, i.e. $[Ru_2Br_9]^{3-}$ (15) and more recently $[Ru_2Cl_9]^{3-}$ (16) have been documented in the literature.

By following the rules outlined earlier, on the change in redox potential incurred by the substitution of soft neutral ligands by halide ions the expected shift in redox potential on exhaustive substitution of, for example, $[Ru_2Cl_3(PMe_2Ph)_6]^+$ to produce $[Ru_2Cl_9]^{3-}$, can be estimated. Thus we might expect a shift of ca. -((3x0.7)+(3x0.25)) = ca. -2.8V in the 35/34 valence electron couple to accompany the aforementioned substitution. Previous studies on complexes such as $[Ru_2Cl_3(PMe_2Ph)_6]Cl$ and $[Ru_2Br_3(PMe_2Ph)_6]Br$ have shown that substitution of Br^- for Cl^- makes almost no difference to the observed redox potentials of these compounds (9), thus considerable interest was aroused concerning the electrochemical behaviour of both the $[Ru_2Br_9]^{3-}$ and $[Ru_2Cl_9]^{3-}$ trianions and the majority of the present chapter is devoted to the results and discussion of that behaviour.

Esr and magnetic measurements on the oxidised symmetric and asymmetric binuclear complexes (5,11,14) have also helped to elucidate their electronic nature. Measurements on a number of Ru_2(III/III) complexes show that as the degree of asymmetry in the molecule, (y-x), increases the degree of metal-metal interaction decreases, giving rise to increased magnetic moments (14). Thus while the $[(As\{p\text{-}tol\}_3)_2ClRuCl_3RuCl(As\{p\text{-}tol\}_3)_2]^+$ cation ((y-x) = 0) exhibits a moment of only 0.91 BM per ruthenium at

233K, as the asymmetry increases i.e. as in $[(As\{p\text{-}tol\}_3)_2ClRuCl_3RuCl_2(As\{p\text{-}tol\}_3)]$, ((y-x) = 1) and increases still further as in $[(As\{p\text{-}tol\}_3)_3RuCl_3RuCl_2(As\{p\text{-}tol\}_3)]^+$, ((y-x) = 2), the increase in magnetic moment to 1.45 BM per ruthenium at 229K and 2.01 BM per ruthenium at 233K, respectively, is readily apparent.

Extensive studies, prior to those in our laboratory, have already been carried out, concerning the X-ray structure and magnetic properties of a number of transition metal $[M_2X_9]^{3-}$ ions. Within the general $[M_2X_9]^{3-}$ family certain trends become apparent on analysis of these data. For example in the Cr, Mo, W triad, both the X-ray structural data and the measured magnetic moments of the $[M_2X_9]^{3-}$ ions indicate an increasing metal-metal interaction on proceeding down the triad, (see table 1.1 and figure 1.5). Thus the X-ray crystal structure of $Cs_3[Cr_2X_9]$, (X = Cl,Br), [17,18] shows a marked displacement of the metal atoms away from the centres of their octahedra towards the plane of the terminal halide ligands, (d'/d" > 1, (see figure 1.5)), caused by a net repulsive force between the two metal centres in the absence of any bonding interaction. The corresponding magnetic data clearly show three unpaired electrons.

By contrast, the $[W_2Cl_9]^{3-}$ ion shows a marked metal-metal interaction, with a shortening of the M-M bond distance, [19] (cf. the Cr_2(III/III) analogue), (d'/d" < 1, (see figure 1.5 and table 1.1)). The magnetic data also indicate a severely depressed moment [20], commensurate with the greater degree of metal-metal

Figure 1.5 + Table 1.1
Selected Structural and Magnetic Data for
Some $[M_2X_9]^{3-}$ Complexes

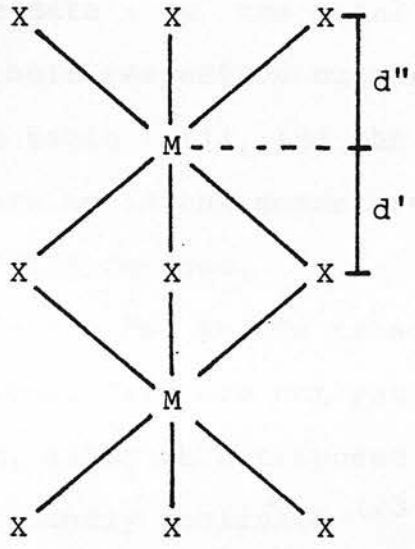

Complex	d' (A)	d" (A)	d'/d"	μeff at ca. 300K (per molecule)	ref
$Cs_3[Cr_2Cl_9]$	1.56	1.27	1.23	3.76	20
$Cs_3[Cr_2Br_9]$	1.66	1.30	1.28	3.81	20
$Cs_3[Fe_2Cl_9]$	1.71	1.145	1.49	6.03	25
$Cs_3[Mo_2Cl_9]$	1.328	1.351	0.98	0.43	21
$Cs_3[Mo_2Br_9]$	1.41	1.46	0.97	0.52	21
$Cs_3[Ru_2Cl_9]$	1.362	1.339	1.02	0.51	16
$Cs_3[Ru_2Br_9]$	1.43	1.59	0.90	1.01	15
$Cs_3[W_2Cl_9]$	1.205	1.35	0.89	0.43	20

interaction.

The $[Mo_2X_9]^{3-}$, (X = Cl,Br), ions appear to exhibit behaviour part-way between the two extremes. The X-ray crystallographic data show the metal atoms very close to the centres of their respective octahedra [18], (d'/d" ≃ 1, (see table 1.1)), and the magnetic data [21,22] show some depression in the moment required for two isolated metal (III) centres.

Provisionally the Fe, Ru, Os triad appears to follow much the same trend. Data are not yet available for the $[Os_2X_9]^{3-}$ system, although a proposed synthesis of $[Os_2Br_9]^{3-}$ was recently published [23]. The X-ray crystallographic [24] and magnetic [25] data for the iron complex, (see Table 1.1), suggest that like the chromium complex, $[Fe_2Cl_9]^{3-}$ shows little or no interaction between the metal ions resulting in a net electrostatic repulsion between the two metal centres. $[Ru_2Cl_9]^{3-}$ on the other hand shows a marked decrease in the internuclear M-M distance, (see Table 1.1), and a severely depressed magnetic moment [16], fully in accord with an increased metal-metal interaction. This has led Cotton and co-workers [26] to calculate a ground state valence electron structure of a'2 e'4 e"4 by the SCF-Xα-SW molecular orbital method [27].

Thus while previous electrochemical studies in our laboratory on the $[Ru_2Cl_x(QR_3)_{9-x}]$, (x = 3,4,5,6), systems show them to contain relatively localised non-interactive metal centres, X-ray and magnetic data on the $[Ru_2X_9]^{3-}$, (X = Cl, Br), trianions indicates a much greater degree of

metal-metal interaction, to the extent where a molecular orbital model appears to describe the electronic structure of the systems. The aim of the following study was to explore the relationship between the contrasting systems and if possible to extend the range of (RuX_3Ru)-containing structures.

1.2 Results and Discussion

1.2.1 Preparation of the $[Ru_2Br_9]^{3-}$ and $[Ru_2Cl_9]^{3-}$ Anions

The $[Ru_2Br_9]^{3-}$ anion is readily prepared by a number of methods and apparently dominates ruthenium bromo chemistry to a large degree. The salt $K_3[Ru_2Br_9]$ was prepared by the method of Fergusson and Greenaway [15], (see Experimental section), but is freely soluble only in water, (in which electrochemical studies are very limited). However, treatment of an aqueous solution of the potassium salt with $[^{n}Bu_4N]Br$ or $[Ph_3PhCH_2P]Br$ induces the precipitation of the alkyl ammonium and phosphonium salts respectively, which are readily soluble in a variety of organic media.

The synthesis of the $[Ru_2Cl_9]^{3-}$ anion was first unequivocally shown by Darriet in 1981 [16]. The method involved heating CsCl and $RuCl_3.xH_2O$ together at extreme temperatures, (*ca.* 850°C), whereupon the formation of small reddish-brown crystals of $Cs_3[Ru_2Cl_9]$ was observed.

The $[Ru_2Cl_9]^{3-}$ ion had previously been mentioned briefly in the literature, firstly in 1960 [28] and again in 1978 by Fergusson and Greenaway [15] although in both

cases details were lacking. Because of the extreme conditions of Darriet's synthesis it was decided to explore the method touched upon by Fergusson and Greenaway, of heating the complex $A_2[RuCl_5(H_2O)]$, (A = Cs, Rb, K). They suggested that the green compound they obtained on heating $A_2[RuCl_5(H_2O)]$ to 200°C under N_2 might be $A_3[Ru_2Cl_9]$ and that further heating produced the brown complex $A_3[RuCl_6]$, but these assignments are confused.

In our laboratory it was found that heating $K_2[RuCl_5(H_2O)]$ <u>in vacuo</u> in a sealed Carius tube at 260°C for prolonged periods, (see Experimental section), produced only a dark brown powder which on cooling was found to be wet. On drying the product the weight loss was found to correspond precisely to that expected for the loss of one mole of water per mole of $K_2[RuCl_5(H_2O)]$, suggesting a reaction in accord with equation 1.1.

<u>Equation 1.1</u>

$$2K_2[RuCl_5(H_2O)] \xrightarrow{\Delta} K_3[Ru_2Cl_9] + KCl + 2H_2O$$

Infrared spectra of the brown powder showed strong absorption peaks at 310 and 344 cm^{-1} indicating Ru-Cl(terminal) stretching modes and a weaker peak at 275 cm^{-1}, indicative of of a Ru-Cl(bridging) vibration.

Since, like its bromo analogue $K_3[Ru_2Br_9]$, the chloro compound was freely soluble only in water, and since production of $K_3[Ru_2Cl_9]$ by the method outlined above would entail contamination with KCl, the complex was dissolved in water and added to an aqueous solution of $[^{n}Bu_4N]NO_3$. Immediate precipitation of a light brown solid occurs and this may be removed by filtration and dried in

air. This solid, which is analytically pure $[^{n}Bu_4N]_3[Ru_2Cl_9]$, is soluble in a variety of organic solvents including CH_2Cl_2, thf and CH_3CN.

1.2.2 Electrochemistry of the $[Ru_2Br_9]^{3-}$ and $[Ru_2Cl_9]^{3-}$ Anions

Cyclic voltammetry (c.v.), linear stirred voltammetry (s.v.) and alternating current voltammetry (a.c.v.) at a platinum electrode in CH_2Cl_2 establish that at 233K, $[^{n}Bu_4N]_3[Ru_2Br_9]$ undergoes two reversible stepwise one-electron oxidations and a partially reversible reduction, (see Figure 1.6 and table 1.2). At room temperature the cyclic voltammetric step corresponding to the reduction wave becomes completely irreversible, (see Table 1.3 for full reversibility criteria), due to the rapid breakdown of the $[Ru_2Br_9]^{4-}$ ion.

The one-electron nature of the redox steps is indicated by the equal heights of the low-temperature s.v. waves, the peak widths at half height of the a.c. waves (72mV, independent of a.c. frequency, (ω), in the range 40-400Hz), the characteristic diffusion coefficient ($D = 4.73 \times 10^{-6}$ cm^2 s^{-1} at 285K measured at +1.00V) [29], and finally by coulometric measurements which show that the first oxidation step corresponds to the loss of 1.0 electron per molecule of $[Ru_2Br_9]^{3-}$. These observations establish a sequence of metal-based redox interconversions as shown in Scheme 1.1.

Figure 1.6 Voltammetry of $[^{n}Bu_4N]_3[Ru_2Br_9]$ in CH_2Cl_2 at 233K

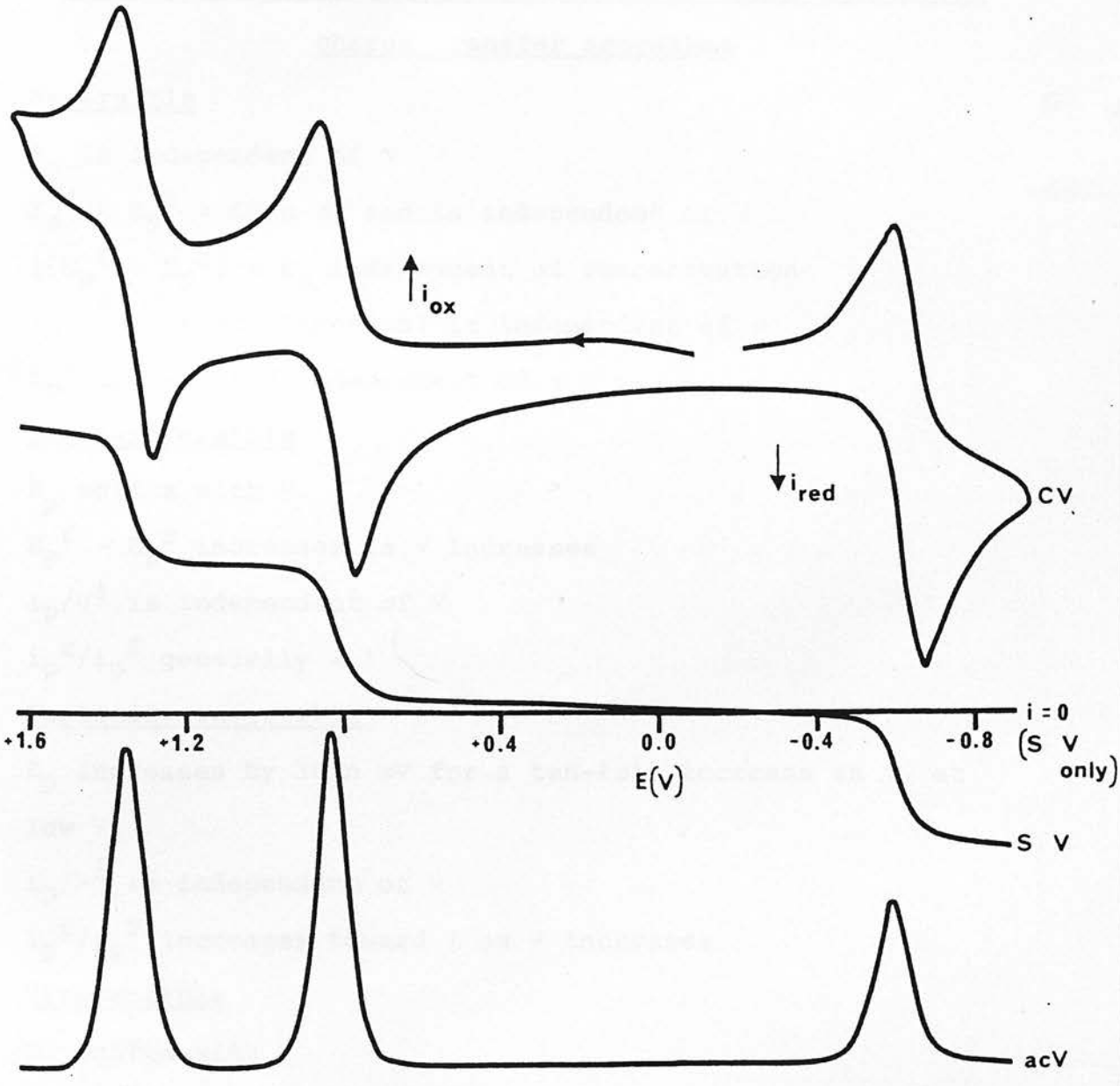

Table 1.2 Redox Potentials for the $[Ru_2Br_9]^{n-}$ and $[Ru_2Cl_9]^{n-}$ Ions

	II/III	III/III	III/III	III/IV	III/IV	IV/IV
$[Ru_2Br_9]^{n-}$		-0.55V		+0.83V		+1.36V
$[Ru_2Cl_9]^{n-}$		-0.57V		+0.92V		+1.58V

All potentials vs. Ag/AgCl reference electrode against which ferrocene is oxidised at +0.55V

Table 1.3

Cyclic voltammetric criteria for reversible, quasi-reversible, partially-reversible and irreversible charge transfer processes

Reversible

E_p is independent of ν

$E_p^f - E_p^r = 59/n$ mV and is independent of ν

$\frac{1}{2}[E_p^f + E_p^r] = E_{\frac{1}{2}}$ independent of concentration

$i_p/\nu^{\frac{1}{2}}$ (current function) is independent of ν

$i_p^r/i_p^f = 1$ and independent of ν

Quasi-reversible

E_p shifts with ν

$E_p^f - E_p^r$ increases as ν increases

$i_p/\nu^{\frac{1}{2}}$ is independent of ν

i_p^r/i_p^f generally = 1

Partially-reversible

E_p increases by 30/n mV for a ten-fold increase in ν, at low ν

$i_p/\nu^{\frac{1}{2}}$ is independent of ν

i_p^r/i_p^f increases toward 1 as ν increases

Irreversible

E_p shifts with ν

$i_p/\nu^{\frac{1}{2}}$ is independent of ν

There is no current on the reverse scan

ν = sweep rate in mVs^{-1}

n = number of electrons involved in the redox process

E_p^f and i_p^f are the potential and the net current at the maximum of the forward curve respectively. E_p^r and i_p^r are the corresponding parameters for the reverse curve.

Scheme 1.1 Redox Interconversions of the $[Ru_2Br_9]^{3-}$ Anion

$$[Ru_2(II/III)Br_9]^{4-} \underset{}{\overset{-0.60V}{\rightleftharpoons}} [Ru_2(III/III)Br_9]^{3-} \overset{+0.83V}{\rightleftharpoons}$$

35e 34e

$$[Ru_2(III/IV)Br_9]^{2-} \overset{+1.36V}{\rightleftharpoons} [Ru_2(IV/IV)Br_9]^{-}$$

33e 32e

C.v, a.c.v and s.v. measurements on the $[^{n}Bu_4N]_3[Ru_2Cl_9]$ compound in CH_2Cl_2, show virtually identical behaviour to the bromo analogue i.e. a single, one-electron reduction, (irreversible at 293K and partially reversible at 223K), and two one-electron oxidations, (reversible at all temperatures up to 293K), (see Figure 1.6 and Table 1.2).

Thus we conclude that the brown compound formed as a result of the thermolysis of $K_2[RuCl_5(H_2O)]$ does indeed contain the $[Ru_2Cl_9]^{3-}$ anion.

This new information now allows direct comparison of these binuclear complexes with the tertiary phosphine and arsine substituted analogues discussed earlier. The sequence of redox steps bears out the redox behaviour expected on exhaustive substitution of phosphine or arsine ligands by halide. The higher degree of halide ligation stabilises the higher oxidation states of the metal atoms even to the extent of the unusually high $Ru_2(III/IV)$ and $Ru_2(IV/IV)$ states in the $[Ru_2X_9]^{2-}$ and $[Ru_2X_9]^{-}$ anions respectively, both of which appear indefinitely stable in CH_2Cl_2 at 223K.

Conversely the lower oxidation states are destabilised

in these species, the Ru_2(II/III) only being accessible electrochemically at 200K and even then only transiently. This precludes the electrogeneration of the $[Ru_2X_9]^{4-}$ anion in bulk, (vide infra). The Ru_2(II/II) oxidation state, $[Ru_2X_9]^{5-}$, has never been observed electrochemically even at temperatures as low as 180K. This is perhaps not surprising in view of the extreme negative charge such a species would have to carry and the ease with which that charge could be dissipated by the expulsion of one or more X^- ligands.

As mentioned above, the estimation of the shift in redox potential of the 35/34 electron couple on exhaustive substitution of phosphine or arsine ligands by chloride ion, using the rules outlined earlier, produces an expected shift of -2.8V. The shift in fact observed is ca. -2.4V, ($E_{\frac{1}{2}}$ for $[Ru_2Cl_3(PMe_2Ph)_6]^{2+/3+}$ (II/III—III/III) = +1.82V and for $[Ru_2Cl_9]^{3-/4-}$ (III/III—III/II) = -0.57V both vs. Ag/AgCl reference electrode), a remarkable correlation considering the gross extent of the substitution, although the redox step occurs somewhat more easily than might have been expected. A more serious departure is the complete lack of evidence for a 35/36 valence electron couple. However since despite stringent efforts in dry non-coordinating media, this reduction has never been observed, we can at least say that the process is unexpectedly difficult.

This comparatively large separation that must exist between the 36/35 electron couple and the 35/34 electron couple for the $[Ru_2X_9]^{n-}$ anions, (compared to for example

that found between the analogous redox couples of $[Ru_2Cl_3(PMe_2Ph)_6]^{n+}$ (ΔV = 0.55V)), indicates that there has been a change in the nature of the bimetallic core, leading to an increase in interaction between the two metal centres, on substituting the six terminal phosphine ligands by halide ions.

On reflection this might be expected on replacement of π-acid, electron-withdrawing QR_3 groups, (Q = As, P), with relatively π-basic, negatively charged chloride ligands. The additional electron density on each metal centre might overcome the trapped electronic behaviour exemplified by the $[Ru_2X_3(QR_3)_6]^{2+} \longrightarrow [Ru_2X_6(QR_3)_3]^-$ series of compounds. This increased interaction is also manifest in the magnetic properties of the $[Ru_2X_9]^{3-}$ anions, (compared to their related Ru_2(III/III) arsine substituted analogues), and this will now be discussed in more detail.

1.2.3 Electrogeneration of the $[Ru_2X_9]^{n-}$ Anions and a Study of Their Magnetic Properties.

In order to explore further the structural and electronic changes which accompany the stepwise electron-transfer processes of the $[Ru_2X_9]^{3-}$ anions we have sought to electrogenerate the $[Ru_2X_9]^{n-}$ ions (n = 4,2,1) on a preparative scale and examine their magnetic properties by the Evans' solution nmr method, (see Appendix 3 for full explanation of this method).

The compounds $A_3[Ru_2Br_9]$ (A = Cs,Rb,K) had already been subjected to a solid-state magnetic study [15] where values of 0.75, 0.92 and 1.01 BM/Ru were recorded for

A = K, Rb and Cs respectively at 296K. These data agree well with our experimentally determined value of 1.13 BM/Ru for $[^{n}Bu_4N]_3[Ru_2Br_9]$ at 299K using the Evans' method. The magnetic moment of $Cs_3[Ru_2Cl_9]$ is also severely depressed, and is temperature-independent above 50K, being reported as only 0.51 BM per ruthenium at 300K whereas a value of 1.7-2.3 BM might be expected for an isolated low spin monomer of ruthenium(III) [30].

Unfortunately bulk electrosyntheses of the $[Ru_2X_9]^{4-}$ ions have not been accomplished because of their very low stability. However controlled-potential electrolysis in CH_2Cl_2/0.5M $[^{n}Bu_4N][BF_4]$ at +1.00V *vs.* Ag/AgCl and 233K of $[^{n}Bu_4N]_3[Ru_2X_9]$ (X = Cl,Br) proceeds smoothly with the expected exponential decay of current. The percentage conversion was measured by stirred voltammetry and essentially quantitative conversion was attained. The $[Ru_2Br_9]^{2-}$ ion is quite stable up to temperatures of *ca.* 270K while the $[Ru_2Cl_9]^{2-}$ ion appears to be stable up to even higher temperatures, showing no signs of decomposition after short exposures to temperatures as high as 300K.

The magnetic moments of the $[Ru_2X_9]^{2-}$ ions were measured by the Evans' method in solution and the results are shown in Tables 1.4 and 1.5. Plots of $1/\chi_m$, *vs.* T are shown in Figures 1.7 and 1.8.

Immediately evident is the fact that the electrogenerated dianions in this system have three unpaired electrons, an observation not consistent within the molecular orbital model, from oxidation of either

Table 1.4

Variable Temperature Evans' Magnetic Measurements on the $[Ru_2Cl_9]^{2-}$ Ion in CH_2Cl_2

T/K	Δf (Hz)	χ_g (÷ 10^{-6})	$\chi_{m'}$ (÷ 10^{-3})	μeff (per molecule)
300	49.4	24.8	5.90	3.78
290	52.1	25.8	6.11	3.78
280	54.3	26.6	6.27	3.76
270	57.3	27.8	6.50	3.76
260	61.2	29.3	6.82	3.78
250	63.7	30.1	6.98	3.75
240	67.1	31.3	7.23	3.74
230	71.6	33.1	7.58	3.74
220	76.7	35.0	7.97	3.76
210	83.8	37.8	8.53	3.80
200	91.8	40.9	9.15	3.84

$m = 2.35 \times 10^{-3}$ g atoms Ru cm^{-3}

f = 200 MHz (superconducting)

$\alpha = 1.2 \times 10^{-3}$

$\chi_0 = -5.49 \times 10^{-7}$

Diamagnetic Corrections = 896×10^{-6}

Table 1.5

Variable Temperature Evans' Magnetic Measurements on the $[Ru_2Br_9]^{2-}$ Ion in CH_2Cl_2

T/K	Δf (Hz)	χ_g (÷ 10^{-6})	$\chi_{m'}$ (÷ 10^{-3})	μeff (per molecule)
273	14.0	39.2	8.90	4.43
263	14.8	40.9	9.26	4.43
252	15.5	42.3	9.53	4.40
242	16.0	43.1	9.70	4.35
231	16.7	44.9	10.1	4.33
220	17.2	45.1	10.1	4.23
210	17.9	46.3	10.3	4.19
200	18.5	47.2	10.5	4.12
190	19.0	47.9	10.7	4.04

$m = 1.64 \times 10^{-3}$ g atoms Ru cm^{-3}

$f = 100$ MHz

$\alpha = 1.2 \times 10^{-3}$

$\chi_0 = -5.49 \times 10^{-7}$

Diamagnetic Corrections $= 986 \times 10^{-6}$

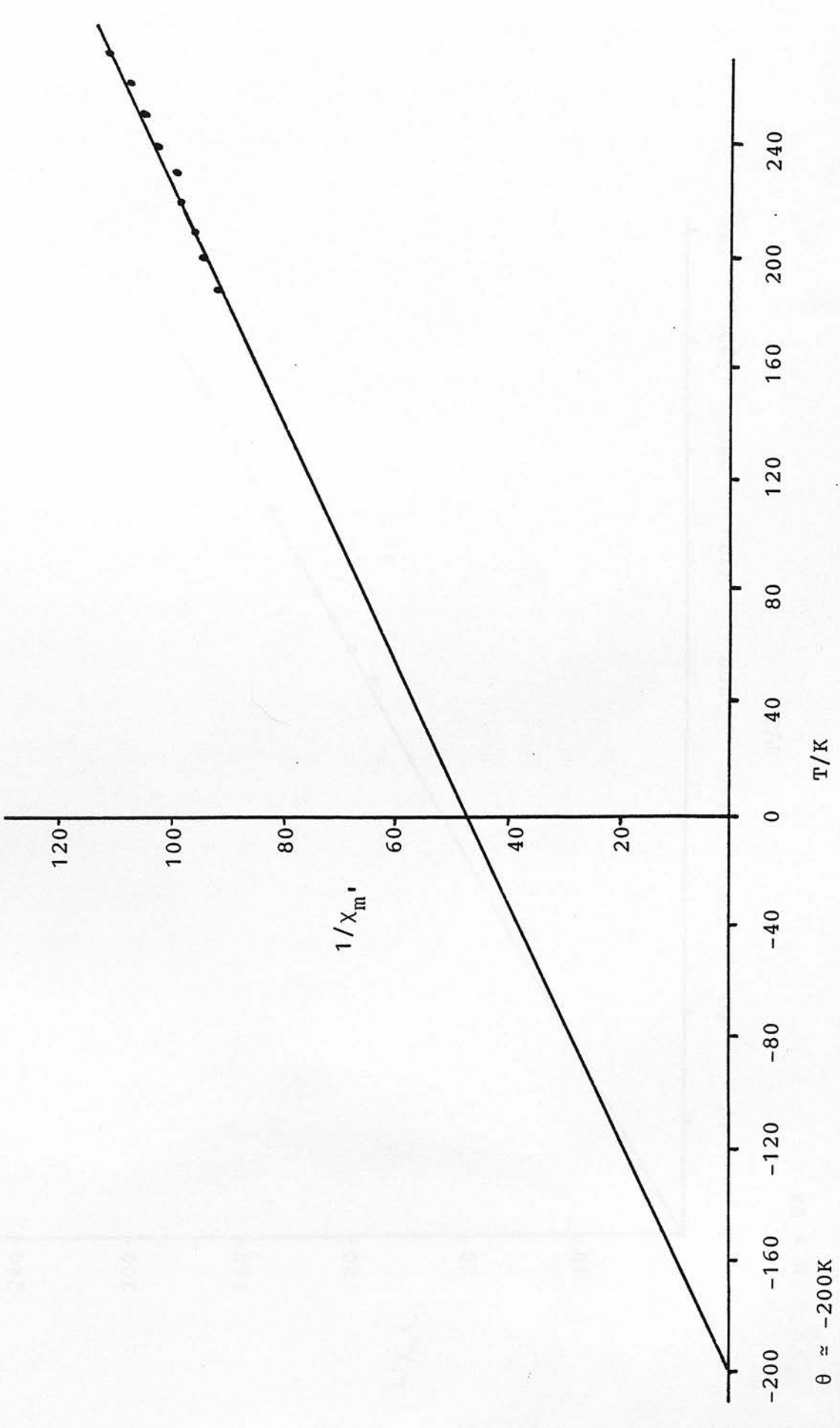

Figure 1.7 Plot of $1/\chi_m'$ vs T for the $[Ru_2Br_9]^{2-}$ Ion

Figure 1.8 Plot of $1/\chi_m$, vs T for the $[Ru_2Cl_9]^{2-}$ Ion

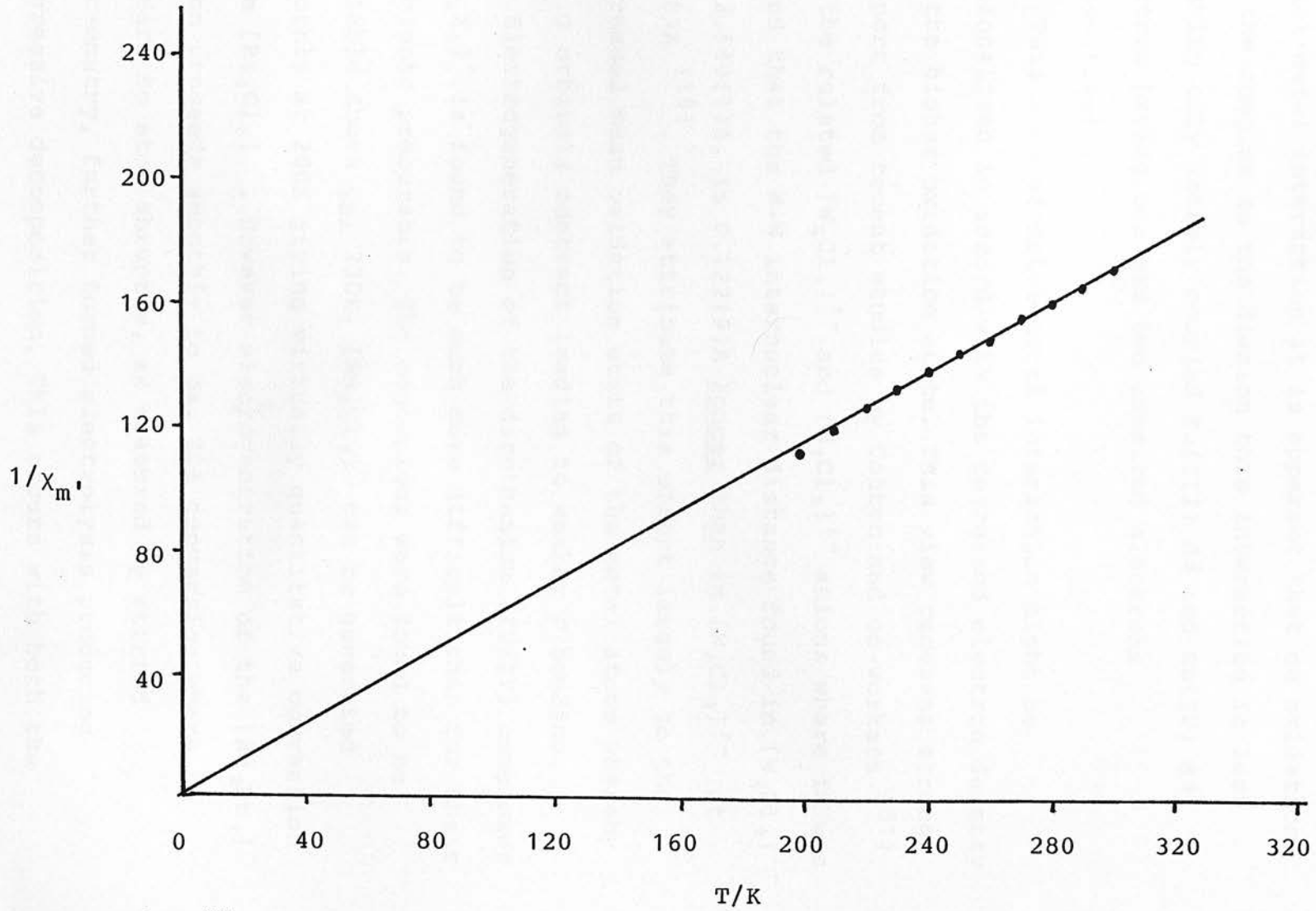

$\theta \simeq 0K$

a'2 e'4 e"4 or a'2 e'4 e"3 a"1 states of $[Ru_2X_9]^{3-}$, where in both instances, only one unpaired electron might have been anticipated. Thus while the 34 valence electron $[Ru_2X_9]^{3-}$ ions appear to exhibit a large degree of metal-metal interaction it is apparent that on oxidation of the complex to the dianion this interaction is lost leaving only loosely coupled Ru(III) d5 and Ru(IV) d4 centres having one and two unpaired electrons respectively.

This loss of metal-metal interaction might be rationalized in accord with the decreased electron density of the higher oxidation state. This view receives strong support from recent studies by Cotton and co-workers [31] on the related $[W_2Cl_9]^{3-}$ and $[W_2Cl_9]^{2-}$ anions where it was found that the W-W internuclear distance found in $[W_2Cl_9]^{2-}$ at 2.540(1)A, is 0.122(9)A longer than in $[W_2Cl_9]^{3-}$ at 2.409A [19]. They attribute this effect largely to the increased mean oxidation state of the metal atoms whereby the d orbitals contract leading to weaker σ bonding.

Electrogeneration of the diruthenium (IV/IV) complexes $[Ru_2X_9]^{-}$ is found to be much more difficult than for their dianionic precursors. The monoanions were found to be unstable above ca. 230K. $[Ru_2Cl_9]^{-}$ can be generated smoothly at 200K giving virtually quantitative conversion from $[Ru_2Cl_9]^{-}$. However electrogeneration of the $[Ru_2Br_9]^{-}$ anion proceeds smoothly to ca. 80% conversion where it appears to stop abruptly, as measured by stirred voltammetry, further forced electrolysis producing progressive decomposition. This occurs with both the

$[^{n}Bu_4N]^+$ and $[Ph_3PhCH_2P]^+$ salts and it is surmised that it may be caused by a slight degree of dissociation of Br^- from the complex, which may be electrochemically induced. This would thermodynamically limit the conversion of the remaining $[Ru_2Br_9]^{2-}$ ion, which requires an oxidation potential considerably more positive than that of free bromide.

Magnetic measurements were carried out on the monoanions, (appropriate corrections being made in the case of $[Ru_2Br_9]^-$ to take account of the 20% $[Ru_2Br_9]^{2-}$ still present in the solution), and the results are shown in Tables 1.6 and 1.7. Although quantitative discussion is perhaps unwarranted in view of the inherently higher degree of error associated with these data the results show that the ruthenium centres are still non-interactive producing no depression in magnetic moment. This result is in accord with our above postulate. The further increase in positive charge on the ruthenium core causes further d orbital contraction and increases the mutual repulsion between the two metal centres. It therefore appears that on oxidation of the ruthenium atoms in the $[Ru_2X_9]^{3-}$ anion, the orthodox molecular orbital description of the species which implies symmetrical charge distribution between the two metal centres may be inappropriate.

This being the case the $[Ru_2X_9]^{2-}$ ions might be expected to show behaviour similar to their Ru_2(II/III) mixed valence arsine and phosphine substituted analogues which have already been shown to exhibit bands due to optically excited intervalence charge-transfer, (IVCT),

Table 1.6

Variable Temperature Evans' Magnetic Measurements on the $[Ru_2Br_9]^-$ Ion in CH_2Cl_2

T/K	Δf§ (Hz)	χ_g ($\div 10^{-6}$)	$\chi_{m'}$ ($\div 10^{-3}$)	μ_{eff} (per molecule)
233	7.9	31.6	7.37	3.72
223	8.2	32.4	7.53	3.68
213	8.2	31.9	7.44	3.57
203	8.1	31.1	7.27	3.34
193	8.3	31.4	7.34	3.38

(§ Note: These Δf values have been corrected to exclude the effect of the 20% $[Ru_2Br_9]^{2-}$ still present at the end of the electrogeneration of the $[Ru_2Br_9]^-$ Ion)

m $[Ru_2Br_9]^-$ = 1.09×10^{-3} g atoms Ru cm^{-3}

m $[Ru_2Br_9]^{2-}$ = 3.28×10^{-4} g atoms Ru cm^{-3}

f = 100 MHz

$\alpha = 1.2 \times 10^{-3}$

$\chi_0 = -5.49 \times 10^{-7}$

Diamagnetic Corrections = 981×10^{-6}

Table 1.7

Variable Temperature Evans' Magnetic Measurements on the $[Ru_2Cl_9]^-$ Ion in CH_2Cl_2

T/K	Δf (Hz)	χ_g (÷ 10^{-6})	$\chi_{m'}$ (÷ 10^{-3})	μeff (per molecule)
255	73.7	35.2	8.00	4.06
245	76.6	36.1	8.19	4.02
235	77.4	36.0	8.17	3.94
225	72.0	33.0	7.57	3.71
215	67.8	30.7	7.1	3.51
206	66.1	22.5	6.86	3.38
195	76.2	33.6	7.68	3.48

$m = 2.35 \times 10^{-3}$ g atoms Ru cm^{-3}

$f = 200$ MHz (superconducting)

$\alpha = 1.2 \times 10^{-3}$

$\chi_0 = -5.49 \times 10^{-7}$

Diamagnetic Corrections = 891×10^{-6}

transitions in the near-infrared region of the electronic spectrum [14]. For this reason the electronic spectrum of the $[Ru_2Cl_9]^{2-}$ ion was extensively investigated and the results will now be discussed.

1.2.4

Intervalence Charge-Tranfer Behaviour of the $[Ru_2Cl_9]^{2-}$ Ion

In 1967 Hush [32] defined intervalence charge transfer as an optical transition which involves transfer of an electron from one nearly localised site to an adjacent one, the donor and acceptor being metal ions which possess more than one accessible oxidation state. Through the Theory of Radiative and Radiationless Transfer, Hush provided explanations for the characteristic features of IVCT bands and developed the method for calculation of the degree of electron delocalisation, α^2, for weakly interacting systems according to the equation

$$\alpha^2 = \frac{4.24 \times 10^{-4} \ \varepsilon max \ \nu^{\frac{1}{2}}}{\nu max \ . \ d^2}$$

where εmax is the maximum extinction coefficient, νmax is the position of the band centre, $\nu^{\frac{1}{2}}$ is the full width of the band at half height and d is the internuclear distance between the metal centres.

Robin and Day [33] used the degree of delocalisation, α^2, to help more fully characterise mixed-valence compounds and Table 1.8 shows their classification into four distinct groups ranging from fully localised, isolated valence, class I behaviour to fully delocalised, average-valence class IIIB behaviour.

Table 1.8 Characteristics of the Four Classes of Mixed-Valence Compounds

Class I	Class II	Class III-A	Class III-B
1. Metal ions in ligand fields of very different symmetry and/or strength, ie, tetrahedral vs octahedral	1. Metal ions in ligand fields of nearly identical symmetry, relative distortion $\lesssim$ 50 pm	1. Metal ions indistinguishable but grouped into polynuclear clusters	1. All metal ions indistinguishable
2. $\alpha=0$; valences very firmly trapped	2. $\alpha>0$; valences distinguishable, but with slight delocalisation	2. α maximal locally	2. α maximal; complete delocalisation over the cationic sublattice
3. Insulator; resistivity of 10^{10} Ωcm or greater	3. Semiconductor; resistivity in the range $10-10^{7}$ Ωcm.	3. Probably insulating	3. Metallic conducitivity; resistivity in the range $10^{-2}-10^{-6}$ Ωcm
4. No mixed-valence transitions in the visible region	4. One or more mixed-valence transitions in the visible region	4. One or more mixed-valence transitions in the visible region	4. Absorption edge in the infrared, opaque with metallic reflectivity in the visible region.
5. Clearly shows spectra of constituent ions, IR, UV, Mössbauer	5. Shows spectra of contituent ions at very nearly normal frequencies	5. Spectra of constituent ions not discernable	5. Spectra of constituent ions not discernable
6. Magnetically dilute, paramagnetic or diamagnetic to very low temperatures	6. Magnetically dilute, with both ferromagnetic and antiferromagnetic interactions at low temperatures	6. Magnetically dilute	6. Either ferromagnetic with a high Curietemperature or diamagnetic, depending on the presence of absence of local moments

The possibility of the existence of an IVCT band in the electronic spectrum of the 33-electron $[Ru_2Cl_9]^{2-}$ ion was investigated using an Optically Transparent Thin Layer Electrode (OTTLE) cell (see Experimental section) on the $[Ph_3PhCH_2P]_3[Ru_2Cl_9]$ complex in $CH_2Cl_2/0.5M[^nBu_4N][BF_4]$ at 240K. The spectra of the $[Ru_2Cl_9]^{3-}$ and $[Ru_2Cl_9]^{2-}$ ions are shown in Figure 1.9. The two prominent bands of the $[Ru_2Cl_9]^{3-}$ ion at 398nm (ε = 7,780) and 442nm (9,435) partially collapse on oxidation and a new weaker band at 537nm (ε= 3,570) appears. In the near infrared region, interestingly,a characteristic new band appears at 970nm (2,500) and this is believed to be the optically excited IVCT band.

Since the ligands around each metal atom in the $[Ru_2Cl_9]^{2-}$ ion are identical a simple energy-configurational coordinate diagram may be drawn for the system as shown in Figure 1.10 . E_{fc} is the Franck-Condon energy, which for totally symmetric mixed-valence complexes, is equal to E_{op} the optical transition energy required for charge transfer. Hush [34] demonstrated that for these symmetric complexes E_{ad} (the adiabatic or thermal transition energy) = $E_{fc}/4$ and Mayoh and Day [35] have shown that they may belong to either the 'trapped-valence' (class II) category of complexes or the 'average-valency' (class III) type depending on the magnitude of the resonance interaction H_{res} between the two metal sites (see Figure 1.10). If H_{res} is large when compared with E_{ad} then delocalised class III behaviour results whereas if it is small cf. E_{ad}, class II localised behaviour results.

Figure 1.9 U.V./Visible/near ir Spectra of $[Ru_2Cl_9]^{3-/2-}$ in CH_2Cl_2 at -40°C

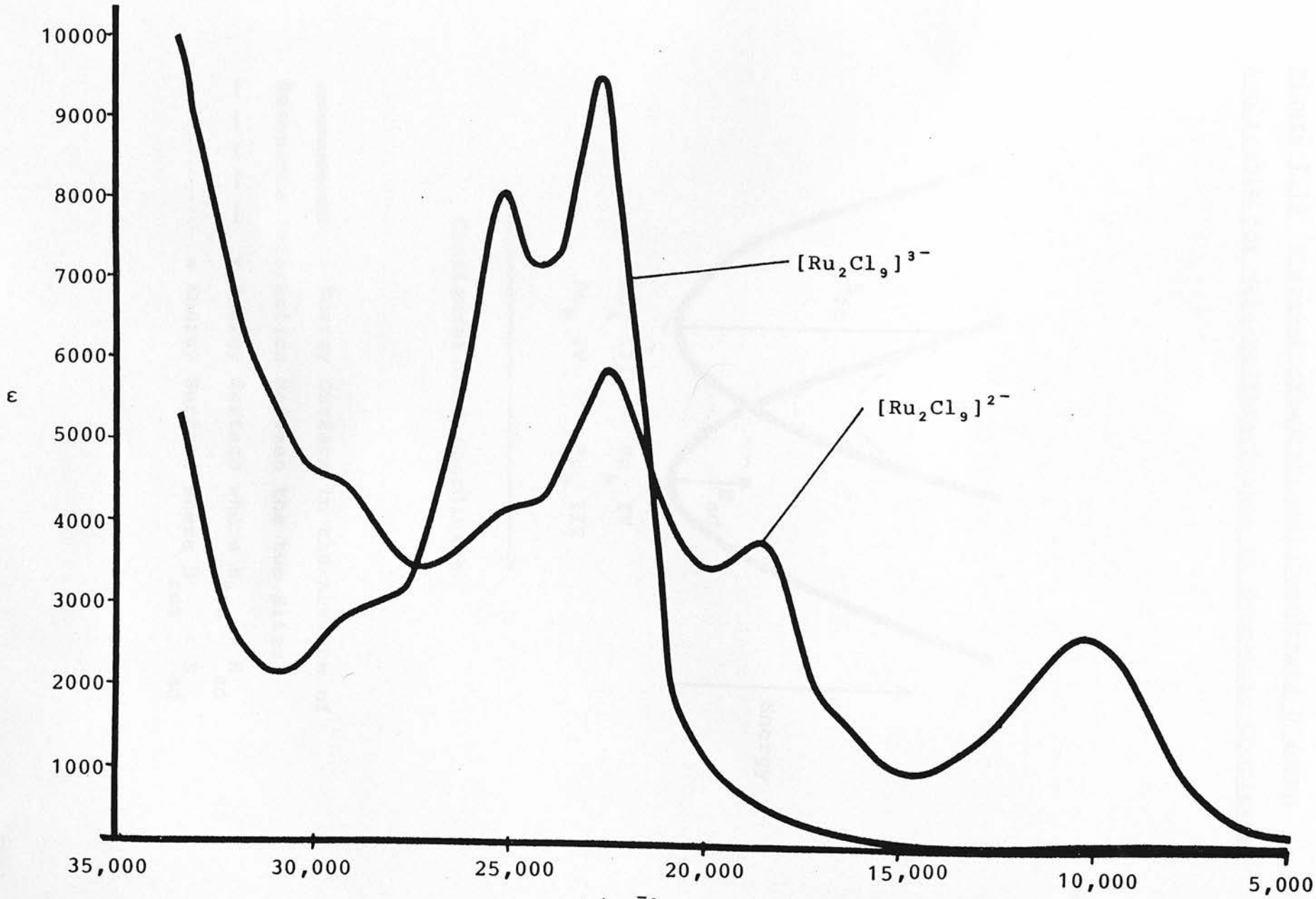

Figure 1.10 Energy-Configurational Coordinate Diagram Applicable for Valence Interchange in Symmetric Complexes

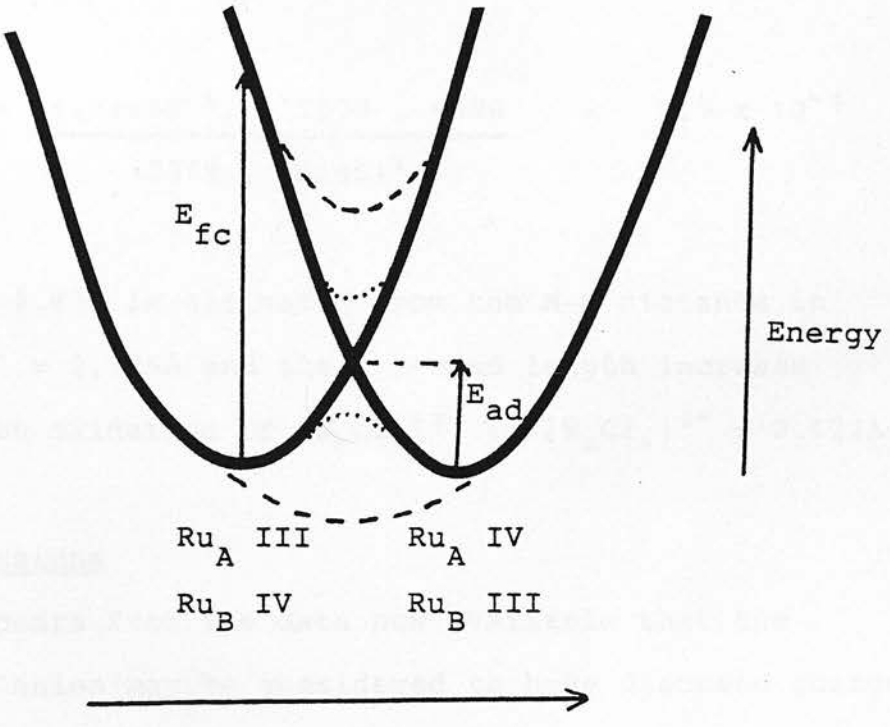

——— = Energy Surface in the Absence of Resonance Interaction Between the two Sites

– – – – – = Energy Surface where $H_{res} > E_{ad}$

..... = Energy Surface where $H_{res} < E_{ad}$

Mayoh and Day [35] have shown that the criterion $\alpha < 1/4$ should be satisfied for trapped valence behaviour so that any experimentally determined value of α^2 between 0.07 and 0.5 (0.5 being the maximal value of α^2 in a fully delocalised system) would invalidate the valence-trapping criterion. From the data obtained for the $[Ru_2Cl_9]^{2-}$ ion in CH_2Cl_2 (see Figure 1.9) the value of α^2 may be calculated as

$$\alpha^2 = \frac{(4.24 \times 10^{-4}) \cdot 2500 \cdot 4690}{10310 \cdot (2.85)^2} = 5.9 \times 10^{-2}$$

(N.B. d = 2.85A is estimated from the M-M distance in $[Ru_2Cl_9]^{3-}$ = 2.725A and the M-M bond length increase incurred on oxidation of $[W_2Cl_9]^{3-}$ to $[W_2Cl_9]^{2-}$ = 0.122A).

1.3 Conclusions

It appears from the data now available that the $[Ru_2Cl_9]^{2-}$anion may be considered to have discrete charge centres, displaying only weak interaction, in accord with the model proposed by Hush. In comparing this result with the data from the symmetric and asymmetric arsine and phosphine substituted analogues described earlier, three factors must be taken into account.

a) The asymmetry of ligand ligation. Previous studies on Ru_2(II/III) complexes where (y-x) = 1 or 2 have shown that ligand asymmetry greatly increases the tendency towards localisation. This is lost when (y-x) = 0 in for example $[Ru_2Cl_3(PEt_2\ Ph)_6]^{2+}$ where 'relatively delocalised'

although not 'average valence' behaviour is observed [9,14]

b) The electron donating/withdrawing properties of the ligands. The localised behaviour observed in the phosphine and arsine substituted complexes is undoubtedly assisted by the π-acidity of these ligands. This aids the withdraw of electron density from the metal centres, diminishing the tendency toward delocalised behaviour. Substitution of these ligands for more π-basic ones such as Cl^- should tend to increase delocalisation.

c) The oxidation states of the metal centres. As the oxidation state increases the tendency towards delocalisation should diminish on two counts. Firstly the decreased electron density on the metal atoms should cause contraction of the d-orbitals leading to a lesser degree of interaction (c.f. Cotton et al studies on related $[W_2Cl_9]^{3-}$ and $[W_2Cl_9]^{2-}$ [31]). Secondly the increase in formal positive charge on the metal centres should increase the purely electrostatic, mutual repulsion experienced by the two ions, again leading to a lesser degree of interaction.

In attempting to compare the mixed-valence behaviour of the 33 electron $[Ru_2Cl_9]^{2-}$ species with, for example the 35 electron $[Ru_2Cl_3(PEt_2Ph)_6]^{2+}$ species, it appears that the increase in metal oxidation state associated with the dianion outweighs the tendency towards delocalisation caused by the greater π-basicity of the Cl^- ligands. However, the localised behaviour is not nearly so marked as in the phosphine and arsine substituted analogues with (y-x) = 1 or 2, where asymmetry appears to have a

dominating influence. The striking possibility exists that the Ru_2(III/IV) complexes $[Ru_2X_9]^{2-}$ may have a flickering asymmetric geometry caused by rapid exchange of the trapped spin centres.

The nature of the 34-electron $[Ru_2X_9]^{3-}$ anions remains uncertain. Although the magnetic properties may be explained in terms of a molecular orbital model such as that proposed by Cotton and others, the data do not exclude the possibility of discrete but magnetically correlated charge centres. What is obvious is that the degree of metal-metal interaction will be increased thus almost certainly taking the complex outside the scope of Hush's weakly interactive model *c.f.* $[Ru_2X_9]^{2-}$.

At present the search for possible intervalence charge-transfer absorptions associated with the 35 electron Ru_2(II/III) $[Ru_2X_9]^{4-}$ species has not been successful due to the severe constraints imposed by their instability. However the possibility of the existence of such a band is not excluded by the present data. A much greater degree of metal-metal interaction than in the related 35 electron phosphine and arsine analogues would be expected, caused both by the maximal symmetry that the $[Ru_2X_9]^{4-}$ complexes enjoy, and by the loss of the exceptional π-electron withdrawing capabilities of the tertiary phosphine and arsine groups present in previous examples, thus increasing electron density on the metal core and augmenting the interaction capability.

Obviously the synthesis and study of new compounds where (y+x) = 7 or 8, the other terminal ligand sites

being occupied by tertiary phosphines or arsines, would be extremely valuable, since they should be intermediate in electronic character between the presently available phosphine and arsine substituted species and fully halo-coordinated complexes, and their preparation is presently being attempted.

The best analogues of the $[Ru_2X_9]^{2/3-}$ species that are currently available are the $[Ru_2Cl_3(H_2O)_6]^{2/3+}$ and $[Ru_2Cl_3(NH_3)_6]^{2/3+}$ systems, investigated by Mercer and others, and these will be discussed in more detail in the following chapter.

1.4 Experimental

Microanalyses were performed by the Chemistry Department, University of Edinburgh, and the Butterworth Microanalytical Consultancy. Melting points (uncorrected) were determined with a Kofler hot-stage microscope and conductivity measurements with a Portland Electronics Model 310 conductivity bridge. Infrared spectra were recorded on a Perkin-Elmer 577 grating spectrometer using Nujol mulls on caesium iodide plates (4000-250 cm^{-1}). Solution magnetic measurements (Evans' method) were obtained in 2% TMS/CH_2Cl_2 solutions on Varian HA100 (continuous wave) and Bruker WP200SY (pulse/Fourier transform) nmr spectrometers, both equipped with variable temperature probes.

Electron spin resonance (esr) experiments were carried out in the Department of Biochemistry, University of Edinburgh, on a Varian E4 spectrometer employing 100KHz

magnetic field modulation.

Investigative electrochemistry was performed using a PAR model 170 potentiostat and programmer and 0.50 M $[^{n}Bu_4N][BF_4]/CH_2Cl_2$ solutions, with Pt working and auxiliary electrodes and Ag/AgCl reference electrode (against which ferrocene is oxidised at $E_{\frac{1}{2}} = 0.55V$). Scan rates were from 50 to $500mVs^{-1}$ (c.v.) and $10mVs^{-1}$ (a.c.v.) with $\omega = 205Hz$.

Electrosyntheses were carried out in a three-compartment cell with a Pt gauze working electrode using a Hi-Tek potentiostat type DT2101 in conjunction with a Hi-Tek waveform generator type PPR1 (see Figure 1.11 for cell design). Electrogenerated species were transferred by syringe, with rigorous exclusion of air, to pre-cooled nmr or esr tubes.

Fast scan voltammograms ($\nu > 500mVs^{-1}$) were monitored using a Physical Data Inc. model 512A digital transient store in conjunction with a Telequipment model D66A oscilloscope with subsequent playback to a Hewlett Packard 704A X-Y recorder. Low temperature studies were carried out in a jacketed cell cooled by a Haake F3Q refrigerated circulation unit.

The chilled Optically Transparent Thin Layer Electrode (OTTLE) cell used in the present study was designed and built in the Department of Chemistry, University of Edinburgh, in accordance with the original principles of Murray *et al* [36]. The OTTLE cell consists of a fine Pt gauze working electrode (transparency *ca.* 40%) fitted into a standard Infrasil quartz UV/visible/near ir cell of 0.1

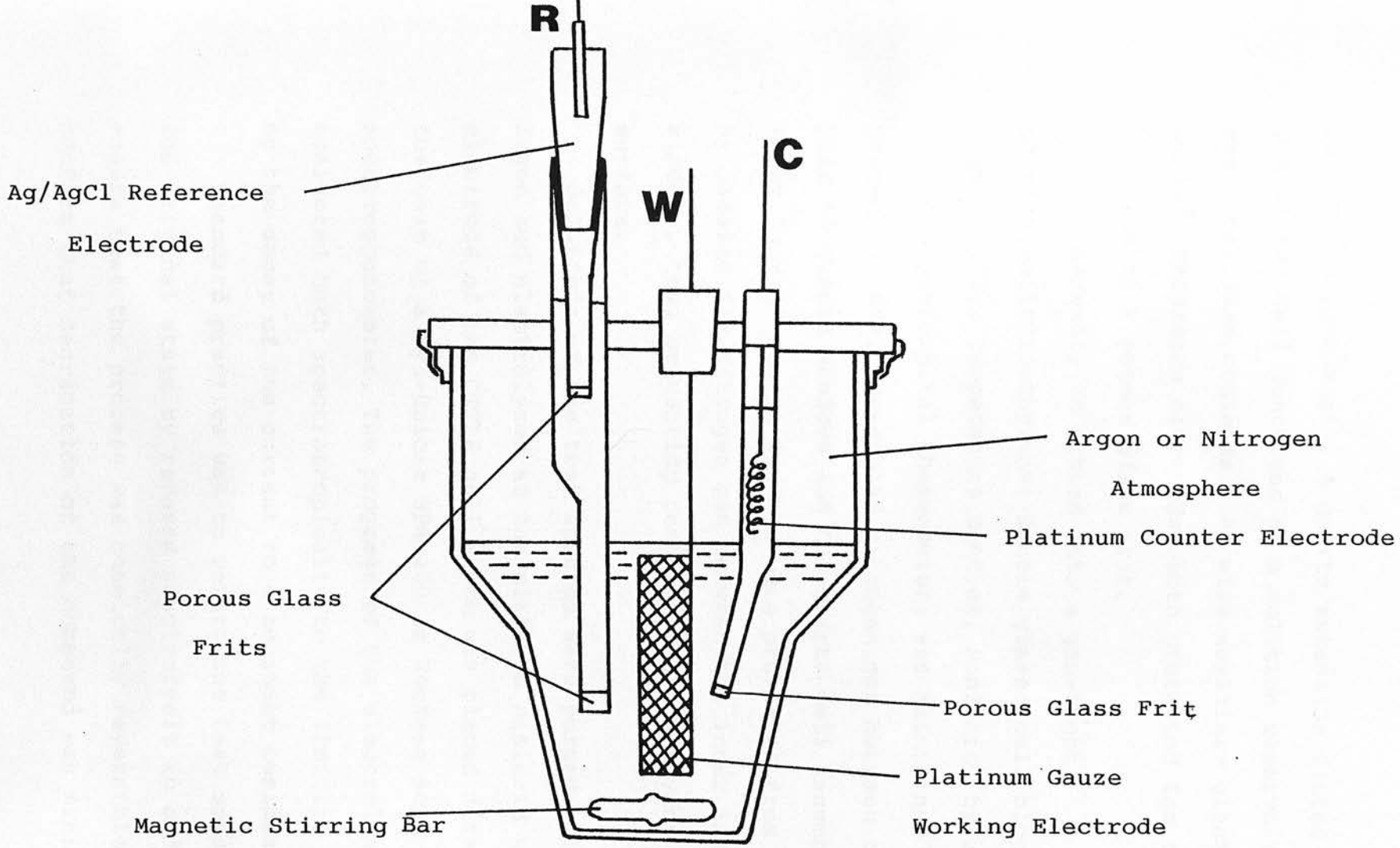

Figure 1.11 Schematic Representation of the Three Compartment Cell used for Bulk Electrosynthesis

or 0.05 cm pathlength. A quartz extension fitted to the top of the cell functions as a solution reservoir. The reservoir also contains a Pt wire auxiliary electrode and Ag/Ag^{+} reference electrode, both protected fom the bulk solution by a porous glass frit.

The assembly is fitted into a gas-tight poly(tetrafluoroethylene) double glazed cell block (see Figure 1.12). Temperature control, monitored by a thermocouple/digital thermometer, was maintained by the passage of dry, pre-cooled nitrogen gas between the inner pair of quartz windows and the quartz cell assembly. The inner pair of quartz windows were prevented from fogging by passing dry nitrogen gas between the inner and outer windows, thus preventing contact of air with any cooled surface.

Solutions of the test species were purged with dry argon and electrolysed at the platinum minigrid working electrode of the OTTLE cell which was placed directly in the beam of a Pye-Unicam SP8-400 or Beckman Acta MkIV spectrophotometer. The progress of the electrolysis was monitored both spectroscopically to the limiting curve and by the decay of the current to a constant residual value.

Standard practice was to return the test species to the original state by reverse electrolysis in order to ensure that the process was chemically reversible and to confirm that degradation of the compound was minimal.

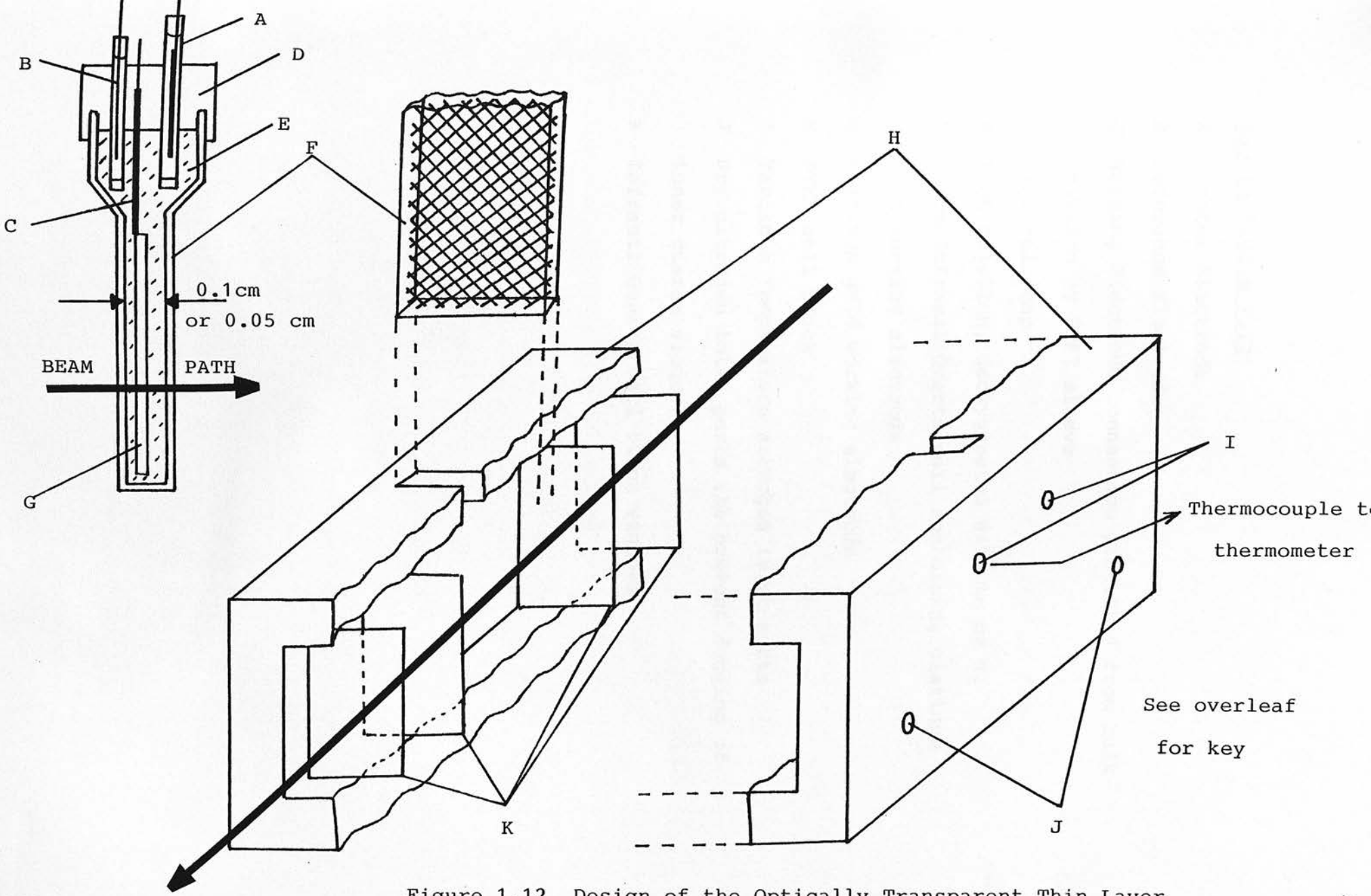

Figure 1.12 Design of the Optically Transparent Thin Layer Electrode

Key to Figure 1.12

A Counter Electrode

B Reference Electrode

C Working Electrode connection protected from bulk solution by PTFE sleeve

D PTFE cell cap

E Test solution, deoxygenated with Ar or N_2

F 0.1cm Infrasil Quartz cell containing platinum grid working electrode

G Platinum grid working electrode

H PTFE cell block

I Variable Temperature nitrogen inlet ports

J Dry nitrogen inlet ports (to prevent fogging of inner quartz windows)

K Infrasil Quartz cell block windows

Reagents

Acetonitrile was purified by the method of Walter and Ramalay [37] and was freshly distilled from P_2O_5 before use. Methylene chloride was allowed to stand for one week over KOH pellets and dried by distillation over P_2O_5. All other solvents were used as supplied without further purification. $RuCl_3.xH_2O$ (Johnson Matthey plc), $[Ph_3PhCH_2P]Br$, $[Ph_3PhCH_2P]Cl$, $[^{n}Bu_4N]NO_3$ and $[^{n}Bu_4N]Br$ (Aldrich Chemicals). $K_2[RuCl_5(H_2O)]$ was prepared by the method of Mercer and Buckley [38].

Potassium Tri-μ-bromo-hexabromodiruthenate (III/III)

The compound was prepared by a variant of the method of Fergusson and Greenaway [15]. The compound $RuCl_3.xH_2O$ (0.50g) was dissolved in 100ml of a mixture (1:1 v/v) of concentrated HBr (48%) and ethanol and heated under reflux, under a nitrogen atmosphere, for 2 hours. A stoichiometric amount of KBr (0.34g) was then added and on concentration and cooling of the solution the black microcrystalline product precipitated. This was filtered off, washed with ethanol and diethyl-ether, and dried *in vacuo*

[Yield 0.80g (80%)]

Electronic spectrum (in water, 40,000-10,000 cm^{-1}) 35,710 (ε = 21,090), 32,050 (14,140), 24,390 (3,970), 20,330 (4,540 $dm^3\ mol^{-1}\ cm^{-1}$).

Tetra-n-butylammonium Tri-μ-bromo-hexabromo-diruthenate (III/III)

This was prepared from the potassium salt by treatment of an aqueous solution of the latter with an excess of $[^{n}Bu_4N]Br$. The precipitated purple solid was washed with water and diethyl-ether and dried in vacuo at 40°C.

Yield: quantitative.

MP = 194°C

Analysis Required for $C_{48}H_{108}Br_9N_3Ru_2$:

C 34.9; H 6.6; N 2.6%

Found: C 35.1; H 6.6; N 2.7%

Λ: (0.95×10^{-3} mol dm^{-3}) in CH_3NO_2 = 177 Ω^{-1} cm^{-2} mol^{-1}

Electronic spectrum: (in CH_2Cl_2, 40,000-10,000 cm^{-1}) 34,720 (ε = 26,740), 30,960 (18,200), 23,360 (4,120), 19,720 (6,050 dm^3 mol^{-1} cm^{-1}).

Benzyltriphenylphosphonium Tri-μ-bromo-hexabromo-diruthenate (III/III)

This was similarly prepared by treatment of aqueous solutions of $K_3[Ru_2Br_9]$ with an excess of $[Ph_3PhCH_2P]Br$.

MP = 135-137°C (decomp)

Yield: quantitative

Analysis Required for $C_{75}H_{66}Br_9P_3Ru_2$:

C 45.4; H 3.3; Br 36.3 P 4.6%

Found: C 44.3; H 3.4; Br 36.3 P 4.4%

Λ: (1.0×10^{-3} mol dm^{-3} in CH_3NO_2) = 232 Ω^{-1} cm^{-2} mol^{-1}

Electronic spectrum (in CH_2Cl_2, 40,000-10,000 cm^{-1}) 34,970 (ε = 27,460), 31,250 (19,350), 23,470 (4,970) and 19,680 (6,270 dm^3 mol^{-1} cm^{-1})

Potassium Tri-μ-chloro-hexachlorodiruthenate (III/III)

$K_2[RuCl_5(H_2O)]$ (1.07g) was sealed *in vacuo* in a Carius tube and heated at 260°C for 130 hours. On cooling the tube was opened and the dark brown product dried at 90°C *in vacuo* for two hours.

Yield ($K_3[Ru_2Cl_9]$ + KCl): 1.01g (100%)

Tetra-n-butylammonium Tri-μ-chloro-hexachloro-diruthenate (III/III)

This was prepared in the same manner as the analogous bromo compound *vide supra* by using a solution of $[^{n}Bu_4N][NO_3]$ and the KCl-contaminated product in water.

Yield: quantitative

Analysis Required for $C_{48}H_{108}Cl_9N_3Ru_2$:
C 46.2; H 8.7; N 3.4%

Found: C 46.1; H 8.7; N 3.4%

Electronic Spectrum (in CH_2Cl_2, 40,000-10,000 cm^{-1}) 25,130 (ε =7,780); 22,620 (9,435 $dm^3\ mol^{-1}\ cm^{-1}$).

Benzyltriphenylphosphonium Tri-μ-chloro hexachloro-diruthenate (III/III)

This was prepared in the same manner as above *vide supra*

Yield: quantitative

Analysis Required for $C_{75}H_{66}Cl_9P_3Ru_2$: C 56.9; H 4.2%

Found: C 56.8; H 4.2%

Chapter 1 References

1. P.W. Armit, T.A. Stephenson and E.S. Switkes, J.Chem.Soc., Dalton Trans., 1974, 1134.
2. P.W. Armit, W.J. Sime and T.A. Stephenson, J.Chem.Soc., Dalton Trans., 1976, 2121.
3. D.R. Robertson and T.A. Stephenson, J.Organometal.Chem., 1976, 116 C29.
4. W.J. Sime and T.A. Stephenson, J.Organometal.Chem. 1978, 116, 245.
5. G.A. Heath, G. Hefter, D.R. Robertson, W.J. Sime and T.A. Stephenson, J.Organometal.Chem., 1978, 152, C1.
6. T. Arthur and T.A. Stephenson, J.Organometal.Chem., 1981, 208, 369.
7. J. Chatt and R.G Hayter, J.Chem.Soc., Dalton Trans., 1961, 896.
8. K.A. Raspin, J.Chem.Soc., A, 1969, 3, 461.
9. A.J. Lindsay, Ph.D. Thesis, University of Edinburgh, 1982.
10. T. Arthur, R. Contreras, G.A. Heath, G. Hefter, A.J. Lindsay, D.J.A. Riach and T.A. Stephenson J.Organometal.Chem., 1979, 179, C49.
11. R. Contreras, G.G. Elliot, R.O. Gould, G.A. Heath, A.J. Lindsay and T.A. Stephenson J.Organometal.Chem., 1981, 215, C6.
12. R. Contreras-Zarate, Ph.D. Thesis, University of Edinburgh, 1981.
13. J.K. Nicholson, Angew.Chem., 1967, 6, 264.
14. G.A. Heath, A.J. Lindsay, T.A. Stephenson and D.K. Vattis, J.Organometal.Chem., 1982, 233, 353.

15. J.E. Fergusson and A.M. Greenaway, Aust.J.Chem., 1978, 31, 497.

16. J. Darriet, Rev.Chim.Miner., 1981, 18, 27.

17. D.J.W. Ijdo and G.J. Wessel, Acta.Cryst., 1957, 10, 446.

18. K. Folting, R.B.Jackson, R. Saillant, W.E. Streib and R.A.D. Wentworth, Inorg.Chem., 1971, 10, 1453.

19. J. Waser and J.H. Watson Jr., Acta.Cryst., 1958, 11, 689.

20. R. Saillant and A.D. Wentworth, Inorg.Chem., 1968, 7, 1606.

21. I.E. Grey and P.W. Smith, Aust.J.Chem., 1969, 22, 121.

22. R. Saillant and R.A.D. Wentworth, Inorg.Chem., 1969, 8, 1226.

23. K. Emerson and J.E. Fergusson, Proc.Mont.Acad.Sci., 1983, 42, 101.

24. M.T. Kovsarnechan, D. Mascherpa-Corral and J. Roziere, J.Inorg.Nucl.Chem., 1978, 40, 2009.

25. A.P. Ginsberg and M.B. Robin, Inorg.Chem., 1963, 2, 817.

26. B.E. Bursten, F.A. Cotton and A. Fang, Inorg.Chem., 1983, 22, 2127.

27. K.H. Johnson, Ann.Rev.Phys.Chem., 1975, 26, 39.

28. D.J.W. Ijdo, Ph.D. Thesis, University of Leiden, 1960.

29. 'Electrochemical Methods' A.J. Bard and L.R. Faulkner, pub. Wiley N.Y. 1980.

30. "Theory and Applications of Molecular Paramagnetism", Wiley Interscience, New York,

31. F.A. Cotton, L.R. Falvello, G.N. Mott, R.R. Schrock and L.G. Sturgeoff, Inorg.Chem.,

32. G.C. Allen and N.S. Hush, Prog.in Inorg.Chem., 8, 357.

33. P. Day and M.B. Robin, Advan.Inorg.Chem.Radiochem., 1967, 10, 267.

34. N.S. Hush, Prog.in Inorg.Chem., 8, 391.

35. P. Day and B. Mayoh, J.Am.Chem.Soc., 1972, 94, 2885.

36. W.R. Heinemann, R.W. Murray and G.W. O'Dom, Anal.Chem., 1967, 39, 1666.

37. L. Ramaley and M. Walter, Anal.Chem., 1973, 45, 165.

38. R.R. Buckley and E.E. Mercer, Inorg.Chem., 1965, 4, 1692.

CHAPTER 2

Synthesis and Study of Triple Chloro-Bridged Binuclear Complexes Containing 'Harder' Terminal Ligands

2.1 Introduction

Following the studies on confacial bioctahedral diruthenium complexes where soft neutral terminal ligands of previously studied systems [1,2,3,4] were exhaustively replaced by halide ions [5], (see Chapter 1), we sought to increase our knowledge of these systems even further by again changing the identity of the terminal ligands.

Mercer and Dumas [6] were the first workers to postulate that the blue complexes formed on electroreduction of $[RuCl_5(H_2O)]^{2-}$ in dilute acid solution were in fact binuclear complexes containing formally mixed oxidation state metal atoms, although as long ago as 1959, Russian workers suggested that the blue colours obtained on reduction of hydrochloric acid solutions of ruthenium (IV) by ethanol was due to ruthenium (III) in the presence of other lower valencies of ruthenium [7]. Mercer and Dumas isolated three blue species which they postulated as $[Ru_2Cl_3(H_2O)_6]^{2+}$, $[Ru_2Cl_4(H_2O)_5]^{+}$ and $[Ru_2Cl_5(H_2O)_4]$, which could be separated by ion exchange chromatography, (see Experimental section), and found that each could be oxidised to a yellow product i.e. $[Ru_2Cl_3(H_2O)_6]^{3+}$, $[Ru_2Cl_4(H_2O)_5]^{2+}$ and $[Ru_2Cl_5(H_2O)_4]^{+}$ respectively [6]. Characterisation of both the blue and yellow complexes was carried out using charge per ion determinations, using the membrane equilibration method of Wallace [8], (which indicated the charges given above), and by chloride analysis which showed the Cl:Ru ratio to be 1.5, 2.0 and 2.5 respectively, for both the oxidized and reduced forms of each complex.

Potentiometric titrations were performed to verify that the blue complexes indeed contained both ruthenium (II) and ruthenium (III) and that oxidation to the yellow solutions corresponded to the removal of one electron per two ruthenium atoms [6].

The magnetic moment found by Mercer and Dumas for the blue complexes was *ca.* 900 x 10^{-6} esu per gram atom of ruthenium, (*ca.* 1.7 BM per molecule), consistent with one unpaired electron per two ruthenium atoms. They thus assigned to the complexes the *triple chloro-bridged* structure described previously. The electrochemical behaviour of the three blue complexes was studied polarographically in various 0.1 M acid solutions using a dropping mercury electrode, (see Table 2.1). Each complex exhibited a reduction and an oxidation, the reductions however being only partially resolved from the hydrogen discharge wave, electrosynthesis at -0.50V (*vs.* sce) causing no diminution in the height of the wave. This led Mercer and Dumas to speculate that the product of the electrochemical reduction was probably reoxidised chemically, to its initial form.

Previous to this work, Wilkinson and coworkers [9] had published data relating to a species which they suggested to be the $[Ru_5Cl_{12}]^{2-}$ cluster anion, formed by the reduction of $RuCl_3.xH_2O$ by hydrogen in H_2O, MeOH or dmf in the presence of a platinum catalyst. A blue solid could be precipitated from the resulting solution by addition of a solution of (o-phenylmethylene)bis(triphenylphosphonium) dichloride. Wilkinson was unable however to account for

Table 2.1

Redox Potentials of Selected Binuclear Ruthenium Complexes

Complex		(II/II)/(II/III)*	(II/III)/(III/III)*	Separation	Ref
$[Ru_2Cl_3(H_2O)_6]^{2+}$		-0.44V	+0.55V	0.99V	6
$[Ru_2Cl_4(H_2O)_5]^{+}$	(in 0.1 M	-0.48V	+0.45V	0.93V	6
$[Ru_2Cl_5(H_2O)_4]$	acid)	-0.52V	+0.42V	0.94V	6
$[Ru_2Cl_3(NH_3)_6]^{2+}$	(in 1M H_2SO_4)	-0.61V	+0.32V	0.93V	10
$[Ru_2Cl_3(NH_3)_6]^{2+}$	(in MeCN)	-0.51V	+0.72V	1.23V	
$[Ru_2Cl_3(PMe_2Ph)_6]^{+}$		+1.26V	+1.81V	0.55V	1

(* All $E_{\frac{1}{2}}$ values *vs.* SCE reference electrode)

the observed magnetic moment of ca. 1.3 BM per five ruthenium atoms in what should have nominally been a 5 x t_2g6 electron system containing no unpaired electrons.

2.2 Results and Discussion

2.2.1 Preparation of the Blue Ruthenium-Aquo Complexes

In our laboratories the preparation and separation of the reduced ruthenium blue solutions was carried out as outlined by Mercer and Dumas, (see Experimental section). Very few variations occurred between our work and the results previously published [6] although one or two points of interest may be examined here. Preparations were undertaken in p-toluenesulphonic acid, in tetrafluoroboric acid and, in a departure from Mercers' work, in hydrochloric acid. Interestingly it was discovered that even in hydrochloric acid solution, after the initial electroreduction stage, there appear to be no substitution processes of H_2O by Cl^- or vice versa, i.e. once the various binuclear complexes have been formed. Thus the solution, once formed by reduction in hydrochloric acid and loaded onto a cation exchange column, forms distinct bands which show no signs of dispersion, and the characteristic uv/visible spectra, (vide infra), of the separated cations show no change, even after prolonged periods in the HCl medium.

2.2.2 E.s.r. Studies on the $[Ru_2Cl_x(H_2O)_{(9-x)}]^{(5-x)+}$ Complexes

The esr. spectra for the three blue complexes isolated i.e. $[Ru_2Cl_5(H_2O)_4]$, $[Ru_2Cl_4(H_2O)_5]^+$ and $[Ru_2Cl_3(H_2O)_6]^{2+}$ were recorded for the eluted solutions as aqueous glasses at -120°C, in the presence of either HCl or p-$MeC_6H_4SO_3H$. The composition of the counterion/electrolyte system did not affect the esr spectrum in any significant manner, either in shape or in the g values observed.

The spectra, typified by the example in Figure 2.1, are all very similar and appear to be those of species of near axial symmetry, (see Table 2.2). They also show a striking resemblance to the spectrum reported by Wilkinson et al [9] for the proposed cluster anion $[Ru_5Cl_{12}]^{2-}$.

Table 2.2

E.s.r. Values for $[Ru_2Cl_x(H_2O)_{(9-x)}]^{(5-x)+}$ Complexes (x = 3,4,5)

	$g_\perp$	$g_{//}$
$[Ru_2Cl_5(H_2O)_4]$	2.08	1.94
$[Ru_2Cl_4(H_2O)_5]^+$	2.07	1.94
$[Ru_2Cl_3(H_2O)_6]^{2+}$	2.08	1.96

The 2g value spectra observed are as expected for $[Ru_2Cl_3(H_2O)_6]^{2+}$ and $[Ru_2Cl_4(H_2O)_5]^+$ which only have one possible configuration consistent with a triple chloro-bridged confacial bioctahedron, each having an axial plane of symmetry as shown in Figure 2.2.

Figure 2.1 E.s.r. Spectrum of $[Ru_2Cl_4(H_2O)_5]Cl$ in Aqueous Glass at 150K

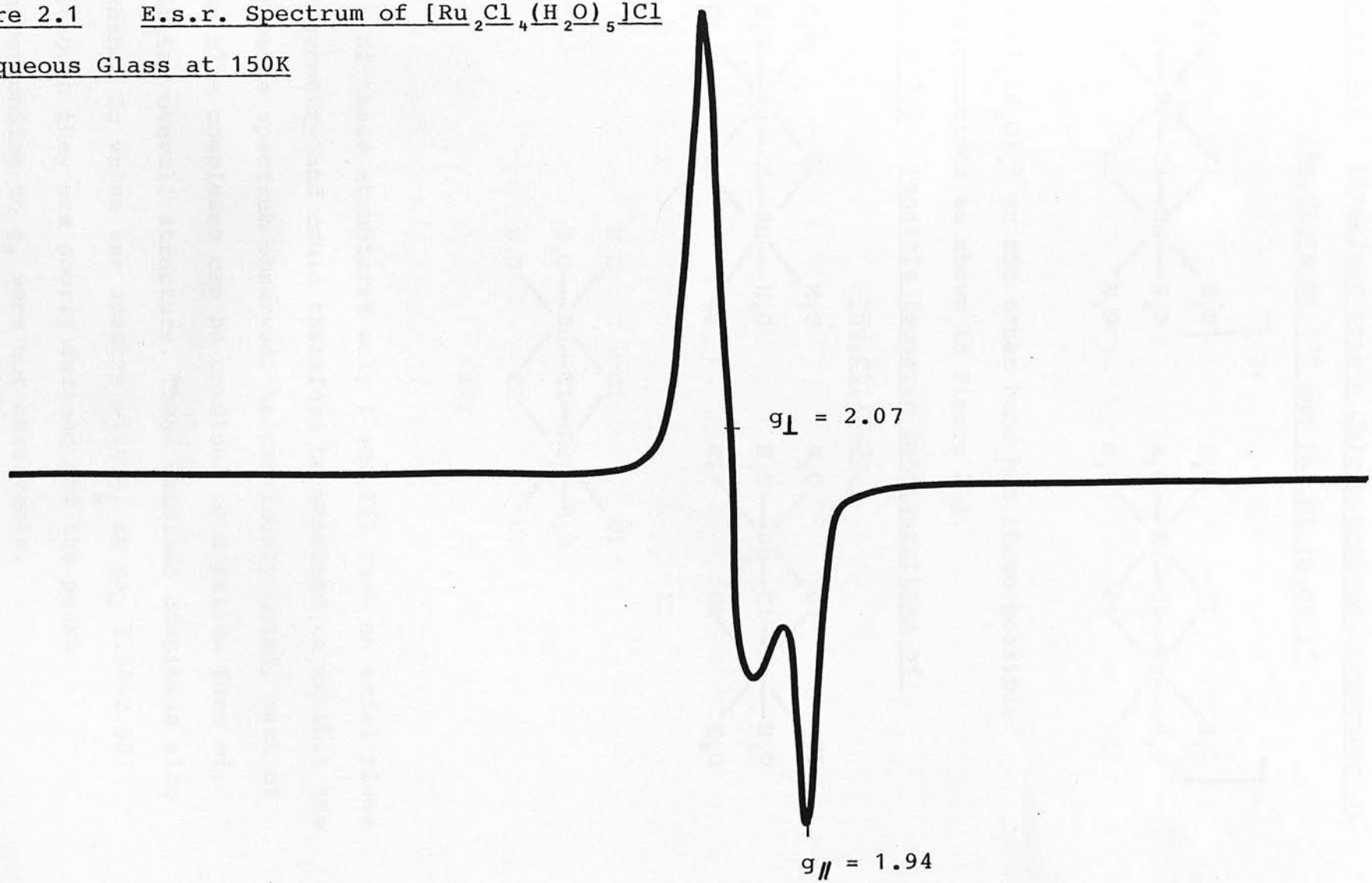

Figure 2.2 Binuclear Triple Chloro-Bridged Structures of $[Ru_2Cl_3(H_2O)_6]^{2+}$ and $[Ru_2Cl_4(H_2O)_5]^{+}$

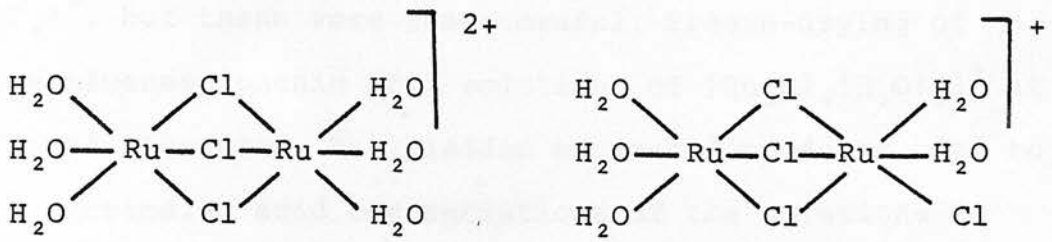

$[Ru_2Cl_5(H_2O)_4]$ on the other hand has three possible configurations as shown in Figure 2.3.

Figure 2.3 Possible Isomeric Configurations of $[Ru_2Cl_5(H_2O)_4]$

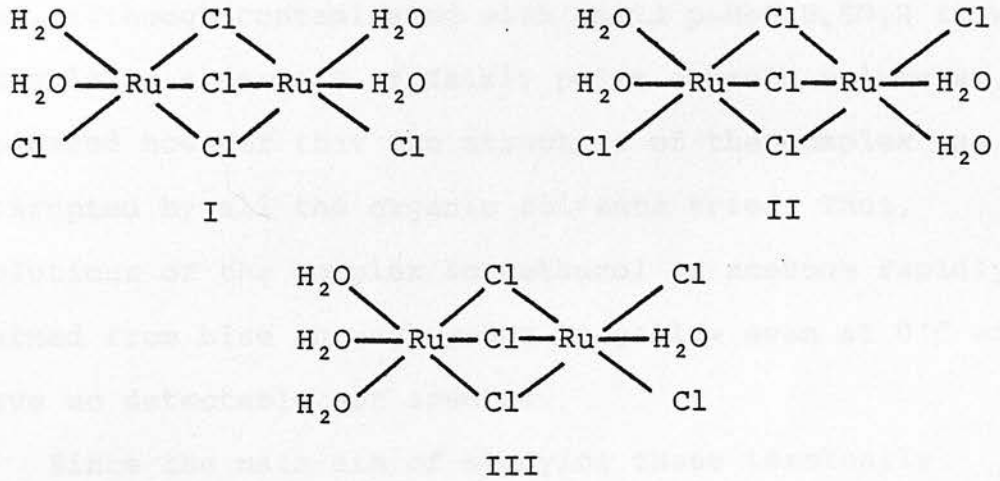

Of these structures only I and III have an axial plane of symmetry and could therefore be expected to exhibit the 2g value spectrum observed. As previously noted, each of the blue complexes can be oxidised to a yellow form of similar overall structure. These oxidised complexes also exhibit 2g value esr spectra with $g_{\perp}$ at *ca.* 2.50-2.60 although they are poorly defined and the peaks corresponding to $g_{\parallel}$ were not observable.

Numerous attempts were made to try to precipitate the

two blue cationic complexes from their separated aqueous solutions using large counteranions such as $[BPh_4]^-$ and $[PF_6]^-$, but these were unsuccessful. Freeze-drying of paratoluenesulphonic acid solutions of $[Ru_2Cl_4(H_2O)_5]^+$ at 0°C was attempted, but yielded no useful products, due to the increasing acid concentrations of the solutions as their volumes were reduced. On freeze-drying a solution of $[Ru_2Cl_3(H_2O)_6]^{2+}$ ion in the presence of p-$MeC_6H_4SO_3H$ a blue solid was eventually precipitated which could be collected under nitrogen and dried at 0°C *in vacuo*. The solid appeared to be stable in air at room temperature and, although contaminated with solid p-$MeC_6H_4SO_3H$ it was soluble in a variety of fairly polar organic solvents. It appeared however that the structure of the complex was disrupted by all the organic solvents tried. Thus, solutions of the complex in methanol or acetone rapidly turned from blue through green to yellow even at 0°C and gave no detectable esr spectra.

Since the main aim of studying these terminally aquated complexes was the characterisation of their uv/visible/near ir spectra in varying oxidation states, (*vide infra*), in conjunction with investigation of their redox chemistry and its correlation with electronic structure, the inability to extract the complexes from their aqueous media proved a severe handicap. Although Mercer and Dumas had studied these complexes [6] polarographically in aqueous solution, water has a very poor electrochemical range, particularly in the reducing region where even at only -0.50V they could not fully

resolve the reduction wave due to the complexes, from the hydrogen discharge wave due to the solvent. Despite these difficulties with the aquo-based complexes, we turned our attention to the analogous hexamine complexes hoping that investigations might yield an isolable species which could be transferred to a non-aqueous medium where more powerful physico-chemical methods were available.

2.3 Preparation and Characterisation of the Mixed-valence Ruthenium (II/III) Complex $[Ru_2Cl_3(NH_3)_6]^{2+}$

2.3.1 Introduction

In a subsequent paper [10] Mercer gave cogent evidence of a triple chloro-bridged binuclear hexammine species, formed by the action of hydrochloric acid on ruthenium (II) solutions containing N-donor ligands. Given the previous confusion of contemporary literature a short summary is given here.

Endicott and Taube reported the results of their studies of the redox reactions of ruthenium ammine complexes in the early 1960's [11,12] which indicated facile redox couples between $[Ru(NH_3)_6]^{2+} \rightleftarrows [Ru(NH_3)_6]^{3+} + e^-$ and $[Ru(NH_3)_5Cl]^{2+} \rightleftarrows [Ru(NH_3)_5Cl]^{3+} + e^-$. Later Lever and Powell [13] isolated a blue solid from the reaction of $[Ru(II)(NH_3)_6][ZnCl_4]$ with hydrochloric acid which they formulated as $[Ru(III)(NH_3)_3Cl_2H_2O]_2[ZnCl_4]$.

This complex was later reinvestigated by Bottomly and Tong, [14] who reformulated it as $[Ru_2(NH_3)_6Cl_4H_2O]Cl$ and were therefore the first workers to assign mixed oxidation states to the metal ions in the binuclear unit. They also

recorded a magnetic moment of 2.05 BM per molecule at 21°C, commensurate with one unpaired electron per two ruthenium atoms. Bottomly and Tong assigned a mono chloro-bridged structure to the complex, however, more recent work by Mercer and Gray [10] has shown that this was in fact not correct.

By analogy with the previously studied aquo complexes, in particular $[Ru_2Cl_3(H_2O)_6]^{2+}$, together with analytical results, electrochemical, magnetic and spectroscopic data, Mercer and coworkers assigned the by now familiar $RuCl_3Ru$ containing structure i.e. $[(NH_3)_3RuCl_3Ru(NH_3)_3]^{2+}$ to the complex produced on treatment of $[Ru(NH_3)_6]^{2+}$ with HCl [10]. Interestingly the dimer can be cleaved to $[Ru(III)Cl_3(NH_3)_3]$ on prolonged reaction with hydrochloric acid in the presence of oxygen at room temperature. This monomer was erroneously assigned as the mer isomer and the configuration was cited as evidence discounting the possibility of a triple-bridged dimer [14]. In fact the compound consists solely of the fac isomer as demonstrated by the X-ray crystal structure published in 1977 [15].

2.3.2 Results and Discussion

2.3.3 E.s.r. and Electrochemical Data Relating to the $[Ru_2Cl_3(NH_3)_6]^{2+}$ Cation

In our laboratory, once the blue cation $[Ru_2Cl_3(NH_3)_6]^{2+}$ had been prepared by the method of Mercer and Gray [10]; yielding an aqueous solution of the chloride salt, production of an organo-soluble salt proved to be a relatively simple matter. It was found that addition of an

aqueous solution containing a stoichiometric quantity of $Na[BPh_4]$ to an aqueous solution of the blue cation, resulted in the immediate precipitation of a dark blue solid, (see Experimental section).

The uv/visible spectrum of this salt, (soluble in thf MeCN and MeOH), in methanol was essentially similar to that published [10] for the chloride salt of $[Ru_2Cl_3(NH_3)_6]^{2+}$ in dilute acid, i.e. a broad absorption λmax = 582nm (ε = 4,300) producing the intense blue colouration, with no other appreciable absorptions in the region 800-300nm.

The esr spectrum of the chloride salt in water at 150K, apparently not discussed elsewhere, reveals a single broad absorption (width at half height = 230 gauss), as shown in Figure 2.4. However the esr spectrum of the $[BPh_4]^-$ salt, in MeOH, at 150K shows a much more clearly defined 2g value pattern $g_\perp$ = 2.10, $g_\parallel$ = 1.96, (see Figure 2.5), indicative of the expected highly axially symmetric structure postulated for $[Ru_2Cl_3(NH_3)_6]^{2+}$.

Mercer and Gray reported their observations on the polarography of $[Ru_2Cl_3(NH_3)_6]Cl_2$ in 1 molar solutions of HCl, KCl and H_2SO_4. An oxidation wave was observed in all these supporting electrolytes on both platinum and carbon paste electrodes, however a reduction wave could only be seen in KCl and H_2SO_4 and was closely followed by catalytic hydrogen discharge. Investigation of the electrochemistry of the cation is greatly facilitated, given access to the organo-soluble $[BPh_4]^-$ salt. Thus investigation of $[Ru_2Cl_3(NH_3)_6][BPh_4]_2$ in thf or MeCN with

Figure 2.4. E.s.r. Spectrum of $[Ru_2Cl_3(NH_3)_6]Cl_2$ in Aqueous Glass at 150K

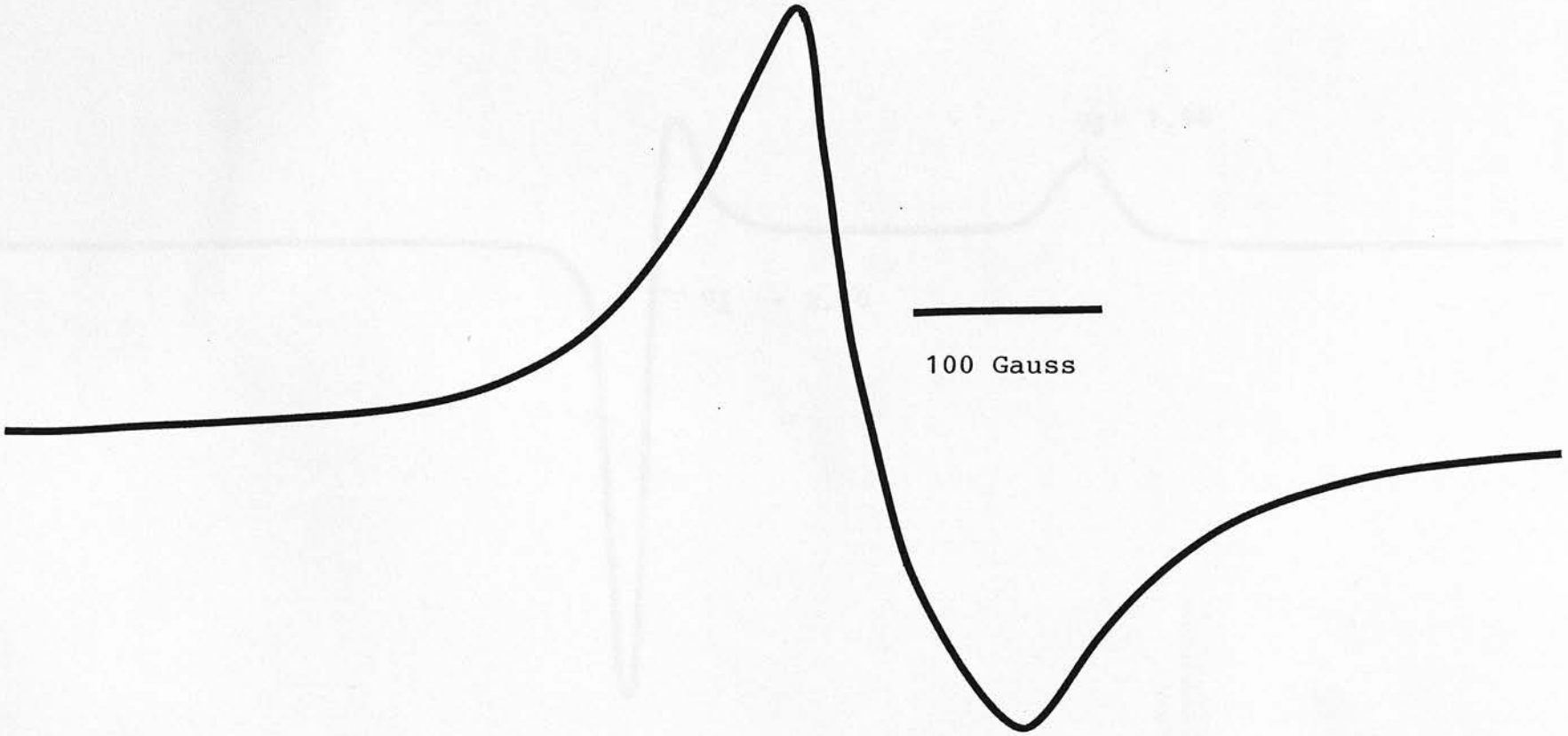

Figure 2.5 E.s.r. Spectrum of $[Ru_2Cl_3(NH_3)_6][BPh_4]_2$ in Methanol Glass at 150K

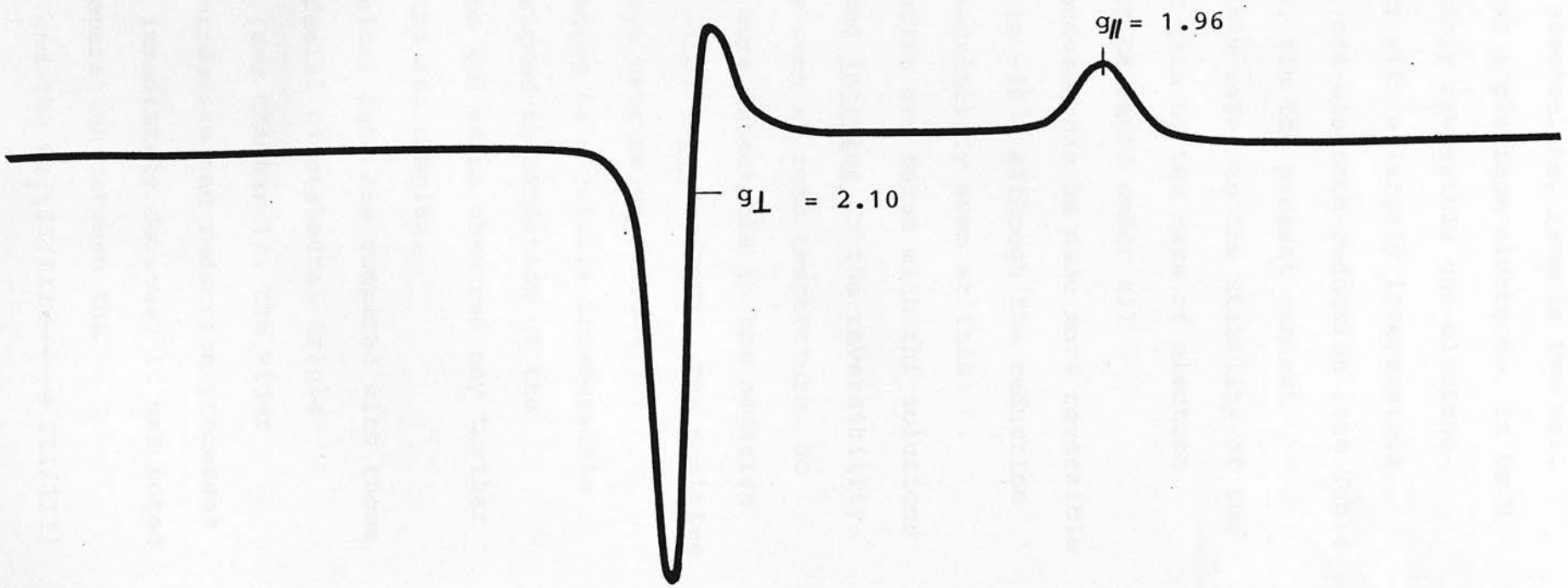

$[^{n}Bu_4N][BF_4]$ supporting electrolyte, reveals two well defined redox processes at a platinum electrode. In MeCN at room temperature a nearly reversible one-electron oxidation occurs together with a largely irreversible (very small return wave) one-electron reduction (see Table 2.1), (separation 1.23V). (In the present context reversible and irreversible refer to the stability of the electrode product rather than to the rate of electron transfer which appears to be rapid under all circumstances). Both processes can be made more reversible by cooling the solution to -40°C although the reduction does not attain full reversibility even at this temperature. Similar results are found with thf solutions although there is a marked <u>increase</u> in the reversibility of the reduction process even at room temperature. No further redox processes were detectable in the negative range to a potential of -2.0V (<u>vs.</u> Ag/AgCl). The positive range reveals a very large wave at <u>ca.</u> +0.60V (<u>vs.</u> Ag/AgCl) corresponding to a totally irreversible process, tentatively assigned to oxidation of the tetraphenylboronate anion and which obscured any further oxidation processes of the Ru_2 complex.

If these electrochemical data are compared with those for other symmetric confacial bioctahedral triple chloro-bridged systems, (see Chapter 1), the wider separation between the oxidation and reduction processes for $[Ru_2Cl_3(NH_3)_6]^{2+}$ is immediately obvious. It was noted in Chapter 1 that the separation between the Ru_2(II/II $\longleftrightarrow$ II/III) and the Ru_2(II/III $\longleftrightarrow$ III/III)

redox couples for these types of complex i.e. where there is exact or approximate matching of the ruthenium coordination spheres at either end, is of the order of 0.5V, (see Table 1). The uniformity of this parameter throughout the entire range of the compounds studied, was attributed to the ability of each of the terminal ligands concerned to withdraw electron density from the metal centres thus decreasing the electronic delocalisation between them. Thus as long as the ligands capacity for π-acceptance is of sufficient magnitude to inhibit covalent interaction between the centres, the actual identity of the particular ligand concerned has little effect on the separation of the two redox couples in question.

This phenomenon is no longer applicable to the $[Ru_2Cl_3(NH_3)_6]^{2+}$ ion. The observed redox couple separation of 1.23V indicates a very substantial increase when compared to the separations found for the complexes discussed in chapter 1. A possible explanation for the increase in redox couple separation is the enhancement of electron delocalisation between the two metal centres, due to the electronic nature of the six terminal NH_3 ligands. NH_3 has no π-acceptor capability unlike the tertiary phosphine and arsine ligands present in the complexes previously described. This would be expected to cause a relative rise in the electron density at the two metal centres, increasing the degree of electron delocalisation between those two centres. The oxidation and reduction of the ruthenium centres should be distinctly more difficult

when those two centres are interacting but only if electron delocalisation is present to allow 'communication' between the two metal ions. Reference to Table 2.1 showing the redox potentials for $[Ru_2Cl_x(H_2O)_{(9-x)}]$ (x=3,4,5) also suggests a similar potential separation between the two processes of not less than 0.93V and 0.99V in aqueous solution. The as yet unobtainable $E_{\frac{1}{2}}$ potentials for these redox processes in non-aqueous media would indeed be valuable.

2.3.4 Electronic Spectrocopic Measurements on the $[Ru_2Cl_3(NH_3)_6]^{2+/3+}$ and $[Ru_2Cl_x(H_2O)_{(9-x)}]^{(5-x)/(6-x)+}$ Series of Complexes

The first species investigated were the aquo complexes $[Ru_2Cl_x(H_2O)_{(9-x)}]^{(5-x)+}$ (x = 3,4,5). The spectra were run in aqueous HBF_4 solution of the appropriate concentration for the particular complex being studied (see Experimental section). The spectra were run at between 0°C and 4°C in a 0.05cm Infrasil quartz OTTLE cell fitted with a platinum gauze working electrode. Spectra were run over the entire range 2000-200nm (5000-50,000 cm^{-1}). After recording the spectrum of the mixed valence Ru_2(II/III) species, each complex was oxidized in turn to the yellow Ru_2(III/III) form and the change in the spectrum determined and proved to be reversible, supporting the view taken by Mercer of the oxidation product. The spectra of $[Ru_2Cl_3(H_2O)_6]^{2+/3+}$ are shown in Figure 2.6. It was found that the spectra for the three blue complexes show a remarkable similarity to one another in the range 450-1500nm, and that their yellow

Figure 2.6a. UV/Visible Spectra of $[Ru_2Cl_3(H_2O)_6]^{2+/3+}$

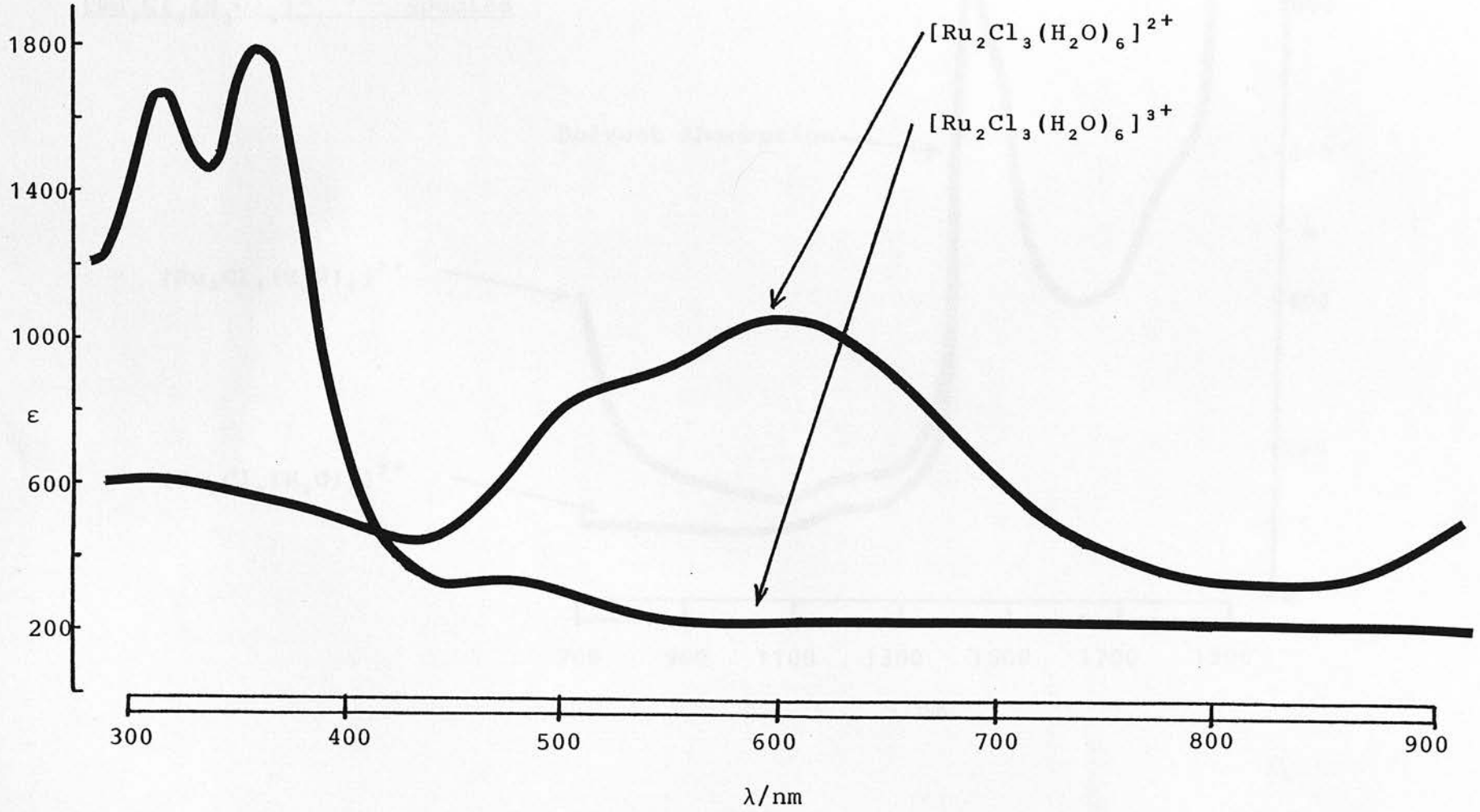

Figure 2.6b. Near infrared spectra of the $[Ru_2Cl_3(H_2O)_6]^{2+/3+}$ Species

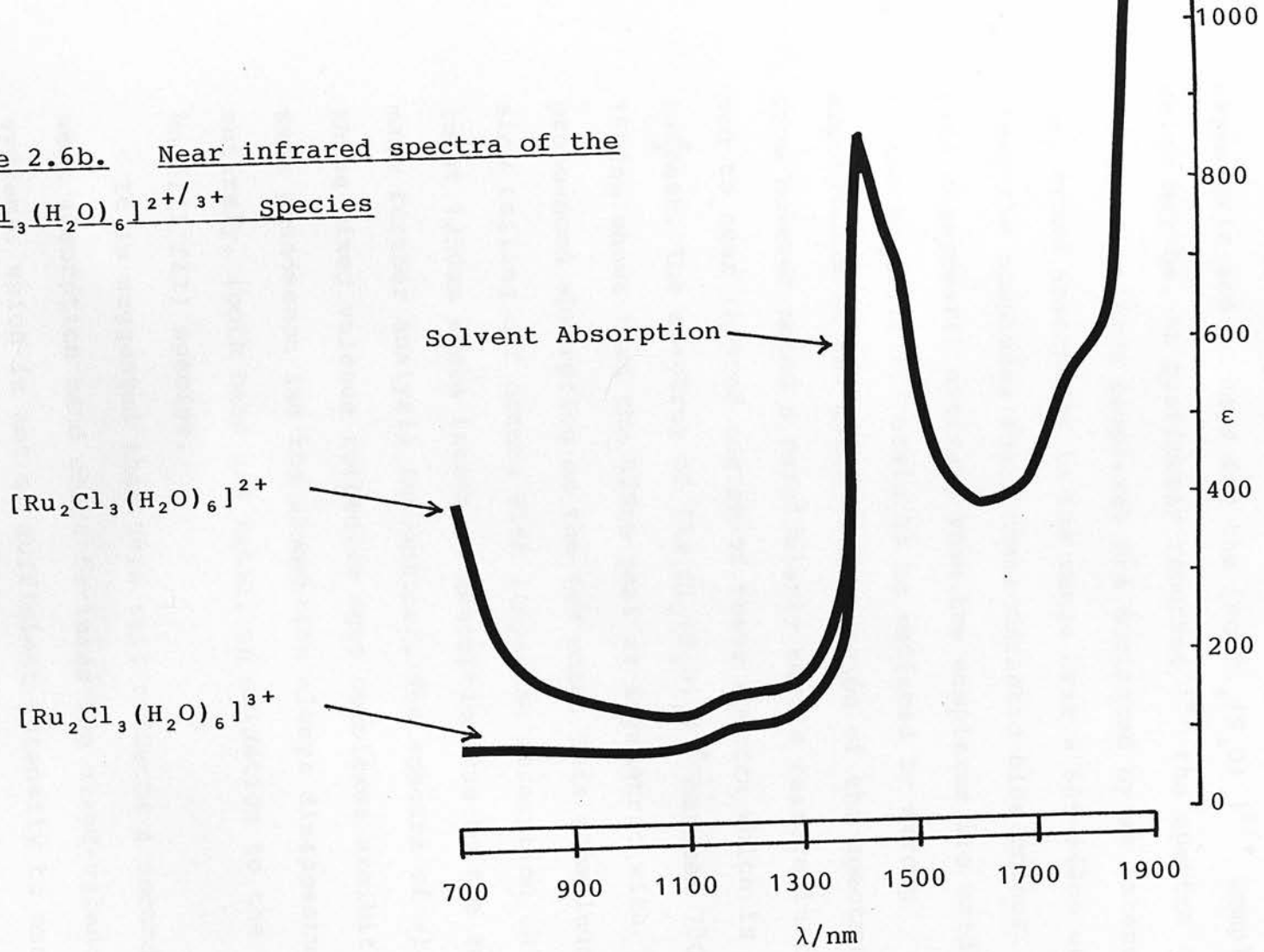

oxidised forms likewise show a striking resemblance to one another over the same range. This is an interesting result for the $[Ru_2Cl_4(H_2O)_5]^{+/2+}$ complex which must be asymmetric and perhaps for the $[Ru_2Cl_5(H_2O)_4]^{0/+}$ complex which may be. As previously reported [6] the spectra of the mixed valence complexes are dominated by an intense, very broad absorption in the range λmax = 605-640nm which gives the complexes their characteristic blue colour. This band disappears entirely when the complexes are oxidised to the Ru_2(III/III) state to be replaced by strong absorptions in the ultra violet region of the spectrum. We have however noted a particularly subtle feature in the red to near infared region of these spectra which is of interest. The spectrum of $[Ru_2Cl_3(H_2O)_6]^{2+}$ between 700 and 1500nm shows that the 605nm peak is asymmetric with pronounced absorption on the red edge. This anomalously slow tailing off occurs with lingering absorption until at least 1350nm where intrusive absorption due to the solvent make further analysis impractical. The spectra of all three mixed valence ruthenium aquo complexes exhibit this same phenomenon and the absorption always disappears entirely, (both band and tail), on oxidation to the Ru_2(III/III) species.

It is suggested that this tail reflects a second very weak absorption band characterising the mixed-valence systems, which is not of sufficient intensity to manifest itself as a distinct peak. No improvement in resolution could be achieved on the spectrum illustrated in Figure 2.6 despite repeated attempts to increase absorbance by

increasing the concentration of the solution or by changing the operating parameters of the instrument. We therefore turned our attention to the $[Ru_2Cl_3(NH_3)_6]^{2+}$ complex.

The spectrum of this complex was again recorded from 2000-200nm (5000-50,000 cm^{-1}) under the same operating conditions as for the aquo complexes described above, except that the solvent was changed to either MeCN or MeOH facilitating the use of the organosoluble $[BPh_4]^-$ salt. In both solvents the main dominating band exhibited by the complex was that responsible for its blue colour, centred at 582nm (17,180 cm^{-1}) in MeOH, and 583nm (17,150 cm^{-1}) in MeCN (cf. 585nm (17,090 cm^{-1}) reported for the water soluble dichloro salt in 0.50M H_2SO_4 by Mercer and Gray [10]).

However, crucially we also observe a weak distinct band, in both solvents, at 1355nm (7,380 cm^{-1}) in MeOH and 1350nm (7,140 cm^{-1}) in MeCN, (see Figure 2.7). The interpretation of the origin of these bands became of prime importance to the understanding of the electronic structure of this complex.

Two simple contrasting models may be considered in relation to the observations.

a) If the two ruthenium atoms prove to be equivalent with a common symmetry and an overall nominal oxidation state of +2.5, then molecular orbital theory may be invoked to produce a molecular orbital manifold, derived from the interacting t_2 sets, within which electronic transitions may be optically induced.

b) If the ruthenium atoms are considered as isolated

Figure 2.7a UV/Visible Spectrum of $[Ru_2Cl_3(NH_3)_6][BPh_4]_2$ in MeCN

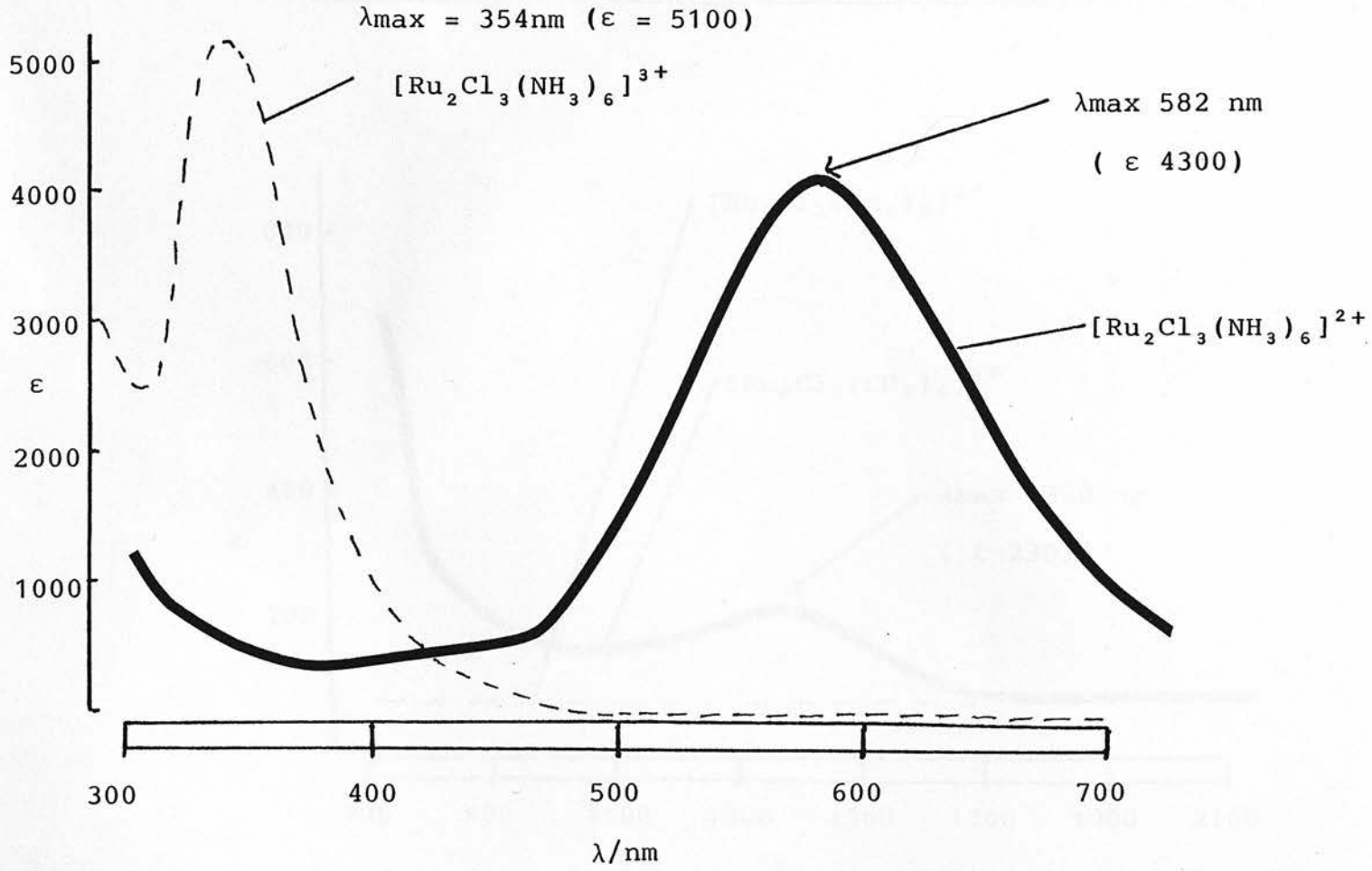

Figure 2.7b Near infrared Spectrum of $[Ru_2Cl_3(NH_3)_6][BPh_4]_2$ in MeCN

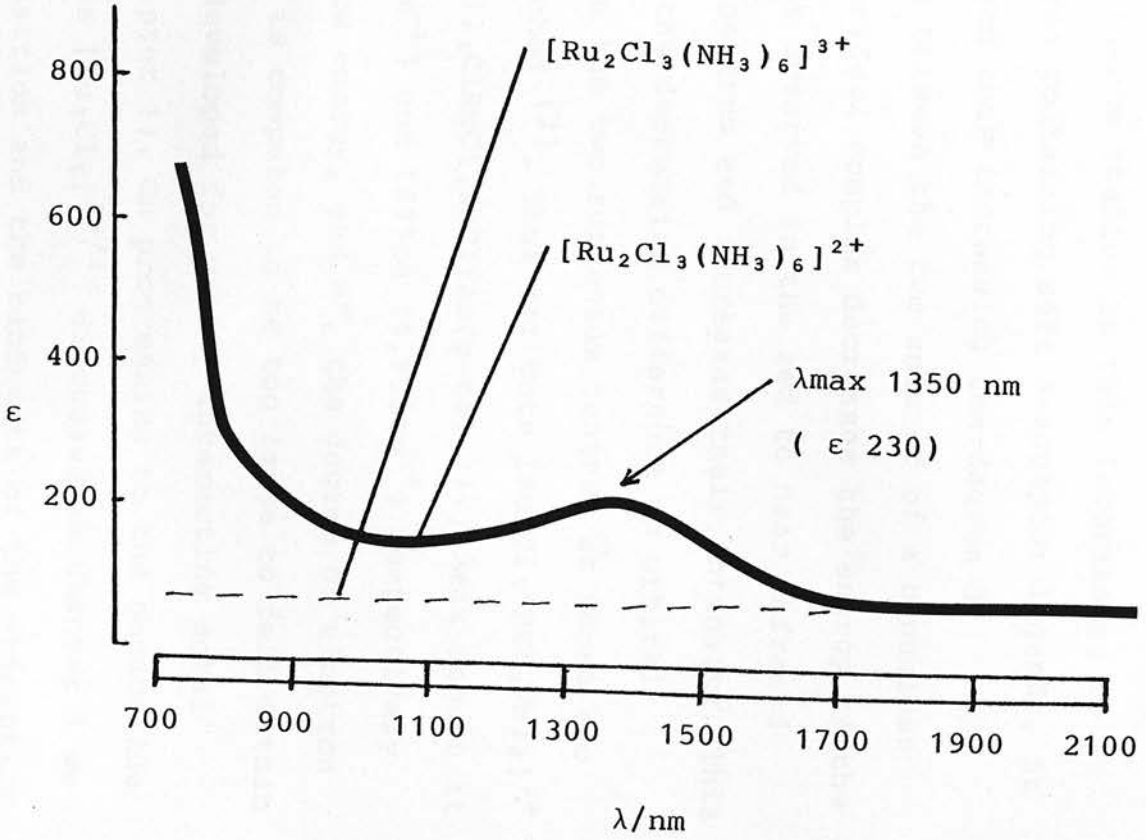

entities, with distinct geometries and differing oxidation states, i.e. +2 and +3 respectively, and in the first approximation, with non-interacting d orbitals, then a molecular orbital approach is inappropriate. This case amounts to the classic mixed-valency system where intervalence charge transfer rather than molecular orbital transitions can occur.

In interpreting the bands observed for $[Ru_2Cl_3(NH_3)_6]^{2+}$ there are a number of points to be kept in mind. In previous intervalence studies in this laboratory, on related complexes containing soft π-acceptor ligands, it has been observed that increasing the degree of ligand-matching between the two ends of of a binuclear triple chloro-bridged complex decreases the energy of the absorption bands observed in the red to near infrared region of the spectrum and increases their intensity. This trend reflects the decreasing difference in orbital energies between the two ruthenium centres as those two centres are matched [2]. Thus for both $[Ru_2Cl_3(PEt_2Ph)_6]^{2+}$ and $[(As\{p\text{-}tol_3\})_2ClRuCl_3RuCl(As\{p\text{-}tol_3\})_2]$ λmax occurs at 2,299nm (4350 cm^{-1}) and 1695nm (5,900cm^{-1}) respectively i.e. at very low energy, and α^2, the degree of electron delocalisation, is computed to be too large to fall within Hush's theory, developed for weakly interacting metal centres (see chapter 1). On progressing to the nonahalide complexes such as $[Ru_2Cl_9]^{3-/2-}$ discussed in Chapter 1 we find that the position and the bandwidth of the absorption believed to correspond to an intervalence charge-transfer transition for the Ru_2(III/IV) species which occurs at

970nm (10,310 cm^{-1}), just allows the complex to fit within the confines of Hush's weakly interacting model. Further reduction to the Ru_2(II/III) species would almost certainly take the description of the complex outside that model due to theincreased electron density of the 35 electron system, (cf. $[Ru_2X_9]^{2-}$ (33 electron system)).

From a different perspective, the proposed delocalisation of $[Ru_2Cl_9]^{4-}$ (35 e) in contrast to established localisation of $[Ru_2X_3(PR_3)_6]^{2+}$, (35 e), would reflect the high ruthenium d-electron density when π-basic Cl^- replaces π-acid PR_3. Equally if the triple chloro-bridged binuclear ruthenium complexes where the terminal ligands i.e. NH_3, H_2O or a mixture of H_2O and Cl^- are treated in the same manner, since the ligands in these cases are all π-donors and should increase the electron density on the metal centres, a comparatively large degree of metal-metal interaction is understandable. Thus the bands observed in the red region of the spectrum for the hexammine and hexaquo Ru_2(II/III) complexes, although almost cetainly due to their mixed valency in the most general sense, would be difficult to rationalise on the basis of intervalence charge transfer. The principal band is much too intense and of extremely high energy, (ca. 17,000 cm^{-1} cf. 5,000 cm^{-1}), and it is not proper to seize instead on the weaker band as evidence for the persistence of the localised model though its position and intensity are comparable. To do so would be to fail to offer any assignment of the major band which is not present in the iso-structural Ru_2(II/II) and Ru_2(III/III) systems and is

therefore intimately associated with the mixed valency. Moreover, the soft ligand systems which do adhere to the trapped valence model have no band comparable to the band at ca. 17,000 cm^{-1}. Thus a pronounced dichotomy seems evident, and as shown above this disparate behaviour may follow from the significant alteration in ruthenium d-electron density. One notes that there will be a clear dichotomy because at the molecular level the molecular geometry will depart abruptly from symmetry if the trapped valence conditions become operative.

Very recently, work published independently by Hush and others [16] has supported and strengthened this view. The results, giving electronic and spectroscopic data for $[Ru_2Cl_3(NH_3)_6]Cl_2$ and $[Ru_2Br_3(NH_3)_6]Br_2$ in a variety of solvents, likewise identify the previously unreported bands at 7150 cm^{-1} (1399nm) for $[Ru_2Cl_3(NH_3)_6]Cl_2$ in D_2O. They also observe bands at 6870 cm^{-1} (1456nm) for $[Ru_2Br_3(NH_3)_6]Br_2$ in D_2O, confirming that these bands are a true feature of these particular complexes.

The paper outlines a typical molecular orbital scheme for the interaction of the metal d-orbitals in a confacial bioctahedron and assigns the two absorptions in the red and near infrared regions of the electronic spectra to $\sigma \rightarrow \sigma^*$ and $\delta^* \longrightarrow \sigma^*$ transitions respectively as shown in Figure 2.8. Unfortunately although their intention is unambiguous, the authors persist in labelling these transitions as intervalence charge-transfer bands. The molecular orbital scheme given must imply the symmetric situation, all orbitals being 50% Ru (a) and 50% Ru (b).

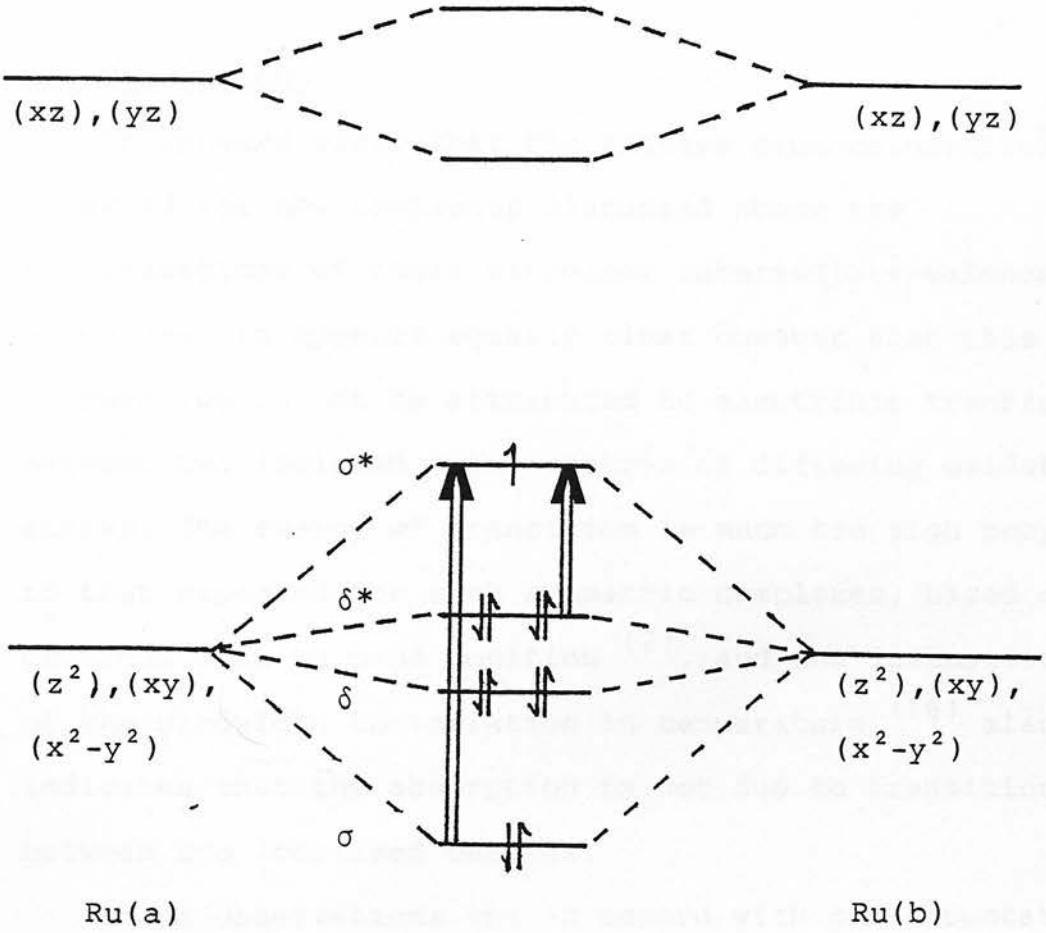

Figure 2.8 Proposed Qualitative Ru 4d-Ordering in Delocalised Confacial Bioctahedral Complexes (after Hush[16])

The proposed visible and near infrared electronic transitions of the $[Ru_2Cl_3(NH_3)_6]^{2+}$ Ion are indicated by the long and short arrows respectively.

There is no element of differential valency or charge transfer involved in this assignment and the reason for the rather misleading nomenclature is not clear.

2.4 Conclusions

It appears clear that the intense blue colouration observed for the complexes discussed above are manifestations of their binuclear intermediate-valence structure. It appears equally clear however that this colouration cannot be attributed to electronic transfer between two isolated metal centres of differing oxidation states. The energy of transition is much too high compared to that expected for such symmetric complexes, based on previous work on band position [2], and the insensitivity of the bandwidth to variation in temperature [16] also indicates that the absorption is not due to transition between two localised centres.

These observations are in accord with our expectation of the results of substituting π-basic for π-acidic ligands in confacial bioctahedral molecules of this type. The greater the degree of π-basicity exhibited by the terminal ligands the greater the degree of electron delocalisation that will be exhibited by the two metal centres.

2.5 Experimental

Electrosynthesis were performed in a standard three compartment cell with Pt gauze working and counter electrodes, (see Chapter 1), using a PAR 170 universal programmer and potentiostat and a saturated calomel reference electrode for all aqueous work. Ion exchange chromatography was employed using a 25 x 1 cm jacketed column, thermostated at 0°C using a Haake FX6Q refrigeration unit. Uv/visible/near ir spectra were recorded with Pye-Unicam SP8-400 and Beckmann Mk IV Acta spectrophotometers. The Optically Transparent Thin-Layer Electrode was of the previously described design (see Chapter 1) employing 0.05 cm Infrasil cells and a platinum gauze working electrode.

Materials

Commercial ruthenium trichloride, (Johnson Matthey plc). Ion exchange resins were Dowex 50-X8, 200-400 mesh, (H^+ form), and Dowex 1-X8, 100-200 mesh, (Cl^- form). The cation resin was washed with 6M HCl prior to use to remove iron impurities. $K_2[RuCl_5(H_2O)]$ was prepared by the method of Mercer and Buckley [17]. All procedures were performed under N_2 or Ar atmospheres using deoxygenated solvents.

Tri-μ-chloro(hexaquo)diruthenium (II/III) dichloride
Tri-μ-chloro(chloropentaquo)diruthenium (II/III) chloride
Tri-μ-chloro(dichlorotetraquo)diruthenium (II/III)

The complexes listed above were prepared by the method of Mercer and Dumas [6]. A solution of $K_2[RuCl_5(H_2O)]$ in 0.01 M acid solution was reduced by controlled potential

electrolysis at -0.50V *vs.* sce at room temperature until ruthenium metal was visible on the walls of the electrolysis cell. The resulting solution, intense blue in colour, was loaded onto a 25 x 1 cm column of Dowex 50-X8 cation exchange resin at 0°C. The column was then eluted with 0.01 M acid solution until the effluent was no longer blue. This eluent was kept at 0°C under nitrogen for later extraction of the neutral complex $[Ru_2Cl_5(H_2O)_4]$. The remaining two blue bands on the column comprise a very narrow (*ca.* 1 cm) band at the top consisting of the $[Ru_2Cl_3(H_2O)_6]^{2+}$ complex and a much more diffuse (*ca.* 10-20 cm) band containing the $[Ru_2Cl_4(H_2O)_5]^{+}$ complex. The latter could be eluted with 0.1 M acid whilst the more tightly held dication could be eluted from the column with 0.5 M acid solution. To obtain the neutral $[Ru_2Cl_5(H_2O)_4]$ complex, the eluent first washed from the cation exchange column was loaded onto a 25 x 1 cm column of Dowex 1-X8 anion exchange resin which was then thoroughly washed with distilled water. The required complex could then be eluted with 0.01 M acid solution. All the above manipulations including the chromatography, were performed at *ca.* 0°C under an inert gas atmosphere.

Tri-μ-chloro(hexammine)diruthenium (II/III) dichloride dihydrate

This was prepared by the method of Mercer and Gray [10] Hydrazine hydrate (85% 5ml) was added slowly to $RuCl_3.xH_2O$ dissolved in water (5ml). Following the initial vigorous reaction the solution was refluxed for 90 minutes under an

atmosphere of nitrogen. The resulting solution was filtered and cooled to 0°C whereupon 8 M HCl (10 ml) was added and the solution allowed to stand for 30 minutes at 0°C under N_2. Ethanol (20 ml) was then added and a blue solid precipitated from the solution. The solid was removed by filtration, washed with ethanol and diethyl-ether and air dried.

Yield 0.55g (85%)

Analysis Calc. for $H_{22}Cl_5N_6O_2Ru_2$:H 4.3; N 16.2%

Found :H 4.2; N 16.0%

Addition of a solution containing a stoichiometric amount of $Na[BPh_4]$ to a solution of $[Ru_2Cl_3(NH_3)_6]Cl_2$ in water yields the sky-blue solid, $[Ru_2Cl_3(NH_3)_6][BPh_4]_2$ in quantitative yield.

Analysis Calc. for $C_{48}H_{58}B_2Cl_3N_6Ru_2$:C 54.9; H 5.5; N 8.0%

Found :C 55.1; H 5.6; N 8.0%

References Chapter 2

1. A.J. Lindsay. Ph.D. Thesis, University of Edinburgh, 1982.
2. G.A. Heath, A.J. Lindsay, T.A. Stephenson and D.K. Vattis. J.Organometal.Chem , 1982, 233 353.
3. P.W. Armit and T.A. Stephenson. J.Organometal.Chem , 1974 73 C33.
4. R. Contreras, G.G. Elliot, R.O. Gould, G.A. Heath, A.J. Lindsay and T.A. Stephenson. J.Organometal.Chem , 1981, 215 C6.
5. V.T. Coombe, G.A. Heath, T.A. Stephenson and D.K. Vattis. J.Chem.Soc., Dalton Trans , 1983, 2307.
6. P.E. Dumas and E.E. Mercer. Inorg.Chem , 1971, 10 2755.
7. Yu A. Barbanel' and I.E. Starik. Russ.J.Inorg.Chem , 1961, 6 109.
8. R.M. Wallace. J.Phys.Chem , 1964, 68 2418.
9. D. Rose and G. Wilkinson. J.Chem.Soc., A , 1970, 1791.
10. L.W. Gray and E.E. Mercer. J.Am.Chem.Soc , 1972, 94 6426.
11. J.F. Endicott and H. Taube. J.Am.Chem.Soc , 1962, 84 4984.
12. J.F. Endicott and H. Taube. Inorg.Chem , 1965, 4 437.
13. F.M. Lever and A.R. Powell. J.Chem.Soc., A , 1969, 1477.
14. F. Bottomly and S.B. Tong. Can.J.Chem.Soc , 1971, 49 3739.
15. F. Bottomly. Can.J.Chem.Soc , 1977, 55 2788.

16. N.S. Hush, J.K. Beattie and V.M. Ellis. Inorg.Chem , 1984, 23 3339.

17. R.R. Buckley and E.E. Mercer. Inorg.Chem , 1965, 4 1692.

CHAPTER 3

Synthesis and Characterisation of Some New Bromo-Bridged Binuclear Complexes of Ruthenium

3.1 Introduction

Triple halide-bridged complexes of ruthenium containing chloride bridging ligands have been known since 1961 [1]. Initially the terminal ligands within these complexes consisted entirely of tertiary phosphine groups e.g. $[Ru_2Cl_3(PEt_2Ph)_6]^+$ [1] or a mixture of tertiary phosphine and halide ligand e.g. $[Ru_2Cl_4(PEt_2Ph)_5]$ [2,3].

The appearance of more varied examples dates from the early 1970's with species such as $[Ru_2Cl_4(PPh_3)_4(N_2)]$ [4] and $[Ru_2Cl_4(PPh_3)_4Y]$ (Y = CO,CS) [5,6] being reported. Much more recently binuclear compounds have been synthesised containing one of the ruthenium atoms in the +3 oxidation state in the form of mixed valence complexes e.g. $[Ru_2Cl_5(PPh_3)_4]$ [7].*

To date however, there are very few examples of isolable Ru_2(III/III) triple-bridged complexes of any type. Examples of these compounds are restricted to:

a) the $[Ru_2X_9]^{3-}$ (X = Cl,Br) species previously discussed, (see Chapter 1).

b) $[Ru_2(CH_2)_3(PMe_3)_6]$ which is diamagnetic and exhibits a short Ru-Ru bond distance of 2.650(1)A which probably indicates the presence of a metal metal bond [8].

c) $[Ru_2Cl_6(AsR_3)_3]$ species (R = Ph, p-tol) which will be discussed in detail below.

The introduction of AsR_3 in place of PR_3 in our

(* The first reported synthesis and characterisation of a mixed valence binuclear ruthenium compound of this type i.e. $[Ru_2Cl_5(P^nBu_3)_4]$ was reported in 1967 [9] however numerous attempts in our laboratory to repeat the work have been unsuccessful).

laboratory in the late 1970's created a new range of complexes including the Ru_2(III/III) $[Ru_2Cl_6(AsR_3)_3]$ complexes mentioned above and also the Ru_2(II/III) $[Ru_2Cl_5(AsR_3)_4]$ species (R = Ph, p-tol) [10].

Other Ru_2(III/III) species such as $[Ru_2Cl_3(PEt_2Ph)_6]^{3+}$ $[Ru_2Cl_4(PEt_2Ph)_5]^{2+}$, $[Ru_2Cl_5(PEt_2Ph)_4]^{+}$ and $[Ru_2Cl_5(As\{p\text{-}tol\}_3)_4]^{+}$ (various somers) may be <u>electrogenerated</u> and studied in situ [11] by spectroelectrochemical techniques but they have not been isolated due to their instability and the difficulty of separating them from the inert electrolyte of the electrochemical system. The magnetic and electrochemical properties of these complexes have been investigated and magnetic measurements on $[Ru_2Cl_6(AsPh_3)_3]$ and $[Ru_2Cl_6(As\{p\text{-}tol\}_3)_3]$ show essentially non interacting centres at room temperature <u>i.e.</u>

$[Ru_2Cl_6(AsPh_3)_3]$ = 2.81 BM/dimer (1.99 BM/Ru) at 267K

$[Ru_2Cl_6(As\{p\text{-}tol\}_3)_3]$ = 2.97 BM/dimer (1.95 BM/Ru) at 294K

However <u>variable temperature</u> measurements on complementary 34 electron <u>electrogenerated</u> systems indicate that the complexes all show depression of μeff with decreasing temperature and that, interestingly, the degree of interaction between the metal centres decreases as the degree of asymmetry between them increases [11] <u>e.g.</u>

$[(As\{p\text{-}tol\}_3)_3RuCl_3RuCl_2(As\{p\text{-}tol\}_3)]^{+}$ μeff = 2.01 BM/Ru at 233K

$[(As\{p\text{-}tol\}_3)_2ClRuCl_3RuCl_2(As\{p\text{-}tol\}_3)]$ μeff = 1.45 BM/Ru at 229K

$[(As\{p\text{-}tol\}_3)_2ClRuCl_3RuCl(As\{p\text{-}tol\}_3)_2]^{+}$ μeff = 0.91 BM/Ru at 233K.

(A final class of Ru_2(III/III) complexes containing hard Lewis bases may be generated from their Ru_2(II/III) precursors by electrochemical oxidation i.e. $[Ru_2Cl_3(NH_3)_6]^{3+}$[12], $[Ru_2Cl_3(H_2O)_6]^{3+}$, $[Ru_2Cl_4(H_2O)_5]^{2+}$ and $[Ru_2Cl_5(H_2O)_4]^{+}$ [13]. These are discussed in detail in Chapter 2).

The trend of increasing interaction with decreasing asymmetry is also reflected in the equivalent 35 electron Ru_2(II/III) species, by the observed position of the intervalence charge-transfer band in their visible/near ir spectra (but not by the measured magnetic moments which give μeff values consistent with one unpaired electron irrespective of the symmetry of terminal ligand ligation [11]. Very recently another complex of this type i.e. $[Ru_2(II/III)Cl_3L_2]^{2+}$ (L = 1,4,7-triazacyclononane) has been prepared by refluxing an aqueous suspension of $[RuCl_3L]$ [14]. Initial aqueous electrochemical measurements indicate that the deep blue 35 electron complex may be reversibly oxidised to the Ru_2(III/III) species but that only irreversible reduction occurs.

The study of analogous ruthenium bromo complexes has generally been hampered by the lack of a suitable bromide containing Ru(II) or Ru(III) precursor. Apart from the synthesis and preliminary investigation of $[Ru_2Br_4(PEt_2Ph)_5]$[3] produced by the reaction of $[RuBr_2(PPh_3)_4]$ [15] with PEt_2Ph in degassed light petroleum and more recently $[RuBr_2(CO)(PPh_3)_4]$ via. the reaction of $[RuBr_2(PPh_3)_3]$ and $[RuBr_2CO(PPh_3)_2dmf]$[16], the synthesis of ruthenium bromo binuclear complexes has

remained relatively unexplored. Such complexes were made by reaction of a chloro analogue or precursor under the appropriate conditions in the presence of a large excess of an inorganic bromide such as LiBr. It is now recognised that this reaction method leads to product mixtures containing both Br and Cl ligation.

With the production of a pure organo-soluble ruthenium bromo source, namely $M_3[Ru_2Br_9]$, (M = $[Ph_3PhCH_2P]^+$ or $[^nBu_4N]^+$ - see Chapter 1), a route to pure bromo-bridged compounds has been discovered as described in this chapter.

3.2 Results and Discussion

3.2.1 Synthesis and Characterisation of Ru (III/III) Complexes

Initial investigations, using the organo-soluble $[Ru_2Br_9]^{3-}$ anion as a source of the Ru-Br moiety under a range of reaction conditions, were based on the corresponding reactions undergone by commercial ruthenium trichloride ($RuCl_3xH_2O$) under the same conditions.

The first reaction investigated was that between $[Ph_3PhCH_2P]_3[Ru_2Br_9]$ and $AsPh_3$ in refluxing methanol (see Experimental section). Under these conditions $RuCl_3xH_2O$ produces the compound $[RuCl_3(AsPh_3)_2MeOH]$ [15], (with a labile methanolate group), which proved to be an excellent precursor for the synthesis of a wide range of monomeric Ru(III) complexes and also binuclear ruthenium complexes containing Ru(II) and/or Ru(III).

Thus in an analogous manner to the chloro complex,

reaction of the $[Ru_2Br_9]^{3-}$ anion with $AsPh_3$ in hot methanol gives the red-brown microcrystalline solid, $[RuBr_3(AsPh_3)_2MeOH]$, (see Experimental section). The MeOH group is labile and can be readily replaced with other solvent ligands, demonstrated by shaking the compound in acetone at room temperature for 24 hours. The black microcrystalline solid which is deposited after this time is pure $[RuBr_3(AsPh_3)_2(Me_2CO)]$ (cf. the reaction of $[RuCl_3(AsPh_3)_2MeOH]$ in acetone [15]).

The $[Ru_2Br_9]^{3-}$ anion has proved to be an excellent precursor to a number of other pure ruthenium-bromo complexes which have until now been difficult to prepare. For example treatment of $[Ph_3PhCH_2P]_3[Ru_2Br_9]$ with an excess of PPh_3 in refluxing MeOH under N_2 leads to quantitative yields of the red-brown microcrystalline product $[RuBr_2(PPh_3)_3]$ [17]. Like the analogous chloro-complex, $[RuCl_2(PPh_3)_3]$, the bromo-complex itself has also proven to be a very useful precursor from which solvates, such as $[RuBr_2CO(PPh_3)_2dmf]$,(made by stirring $[RuBr_2(PPh_3)_3]$ in warm dmf in the presence of CO gas), or $[RuBr_2CO(PPh_3)_2MeOH]$ (made by heating $[RuBr_2CO(PPh_3)_2dmf]$ under reflux in methanol), may be readily prepared. Ultimately, binuclear complexes e.g. $[Ru_2Br_4CO(PPh_3)_4]$ may be prepared from these solvates for example by reaction of equimolar quantities of $[RuBr_2(PPh_3)_3]$ and $[RuBr_2CO(PPh_3)_2MeOH]$ in refluxing acetone [17].

Electrochemical examination of the bromo methanolate complex again demonstrates its similarity in behaviour to the chloro analogue [18]. Thus a.c. voltammetric

measurements of the complex in a $CH_2Cl_2/[^nBu_4N][BF_4]$ medium initially show a single wave, corresponding to the expected one electron reduction to $[RuBr_3(AsPh_3)_2MeOH]^-$, at +0.17V (vs. Ag/AgCl). This wave however, rapidly disappears and is replaced by two new waves, (separation 0.96V), which both correspond to reversible one-electron reduction processes (vide infra).

This electrochemical behaviour strongly suggests spontaneous rearrangement to a binuclear diruthenium (III/III) complex capable of undergoing the two successive one electron reductions observed, (see Scheme 3.1).

Scheme 3.1

$2[RuX_3(AsPh_3)_2MeOH]$

non-polar solvent, -MeOH

$2'[RuX_3(AsPh_3)_2]'$

Binuclear halide bridged

Ru_2(III/III) complex (I)

Initially for X = Cl the binuclear product (I) was formulated as the double chloro-bridged complex $[Ru\ Cl_3(AsPh_3)_2]_2$[18], (see Figure 3.1)

Figure 3.1

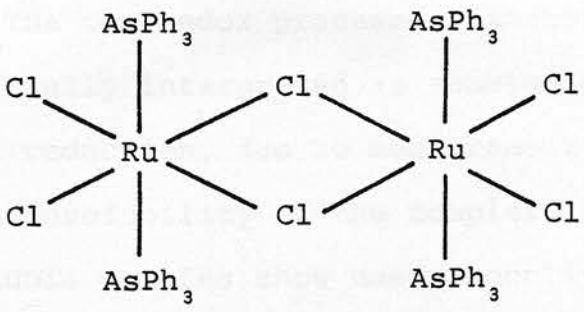

(I)

(or isomers with the $AsPh_3$ and terminal Cl groups interchanged)

The esr spectrum of (I) showing a 2g value pattern, was cited as evidence to support this centrosymmetric structure together with solid state magnetic measurements which indicated a value of 2.81 BM per dimer, (1.99 BM/Ru), corresponding to two unpaired electrons per molecule. Osmometric molecular weight measurements on the more soluble $[RuCl_3(As\{p\text{-}tol\}_3)_2]_n$ complex indicated n=2 and carbon and hydrogen analysis were consistent with this formulation [10]. The electrochemical behaviour of the analogous As(p-tolyl)$_3$ complexes also showed two reversible one electron reductions.

If $[RuCl_3(AsR_3)_2MeOH]$ (R = Ph, p-tol) are <u>heated under reflux</u> however,in non-polar solvents such as benzene, for one hour, brown microcrystalline materials are precipitated. Carbon and hydrogen analyses on these materials are consistent with the formulation $[Ru_2Cl_6(AsR_3)_3][0.5\ C_6H_6]$ and electrochemical measurements suggested two successive one electron reductions [10], (see Table 3.2). *

The electrochemical and esr, (<u>vide infra</u>), behaviour of these complexes is virtually identical to that of the proposed double chloro-bridged complexes $[Ru_2Cl_6(AsR_3)_4]$

(* The two redox processes exhibited by this compound were initially interpreted as showing a reversible <u>oxidation</u> [19] and reduction, due to measurement difficulties caused by the insolubility of the complex. However studies on more soluble samples show unequivocally that <u>both</u> processes correspond to one-electron reductions [10].)

cited earlier and indeed if samples of one are added to the other there is no discernible change in either redox or esr behaviour of the mixture when compared to either of the pure samples.

This suggests that it is likely, that the double-bridged $[Ru_2Cl_6(AsR_3)_4]$ (R = Ph, p-tol) complexes should be reformulated as the triple-bridged complexes $[Ru_2Cl_6(AsR_3)_3]AsR_3$ containing a molecule of free arsine ligand associated with each binuclear unit. In support of this conclusion, treatment of $[Ru_2Cl_6(AsR_3)_4]$ with HBF_4 in acetone, at room temperature, for several days leads to the formation of $[Ru_2Cl_6(AsR_3)_3]$ the HBF_4 presumably removing the loosely associated AsR_3 as $[HAsR_3]^+[BF_4]^-$. There are three possible isomeric structures consistent with a triple chloro-bridged structure for the $[Ru_2Cl_6(AsR_3)_3]$ complexes outlined above, (see Figure 3.2).

Esr measurements on the $[Ru_2Cl_6(AsPh_3)_3]$ complex show a 2g value spectrum indicating a plane of symmetry in the molecule. This excludes structure 1 (see Figure 3.2) as a possible model for the complex but still leaves two possible isomeric forms, (structures 2 & 3 - see Figure 3.2), either of which would exhibit an axially symmetric esr pattern. However previous, extensive studies into the electrochemical behaviour of these and related triple-bridged binuclear systems, (see Chapter 1 and references therein), have shown that the separation between the redox potentials for the expected two one-electron reductions, would be markedly dependent on

Figure 3.2 Possible Isomeric Structures for $[Ru_2X_6(AsR_3)_3]$ (X = Cl, Br; R = Ph, p-tolyl)

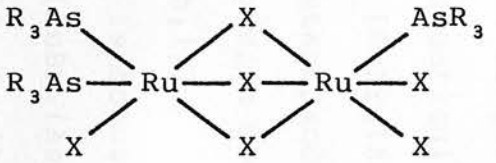

Structure 1

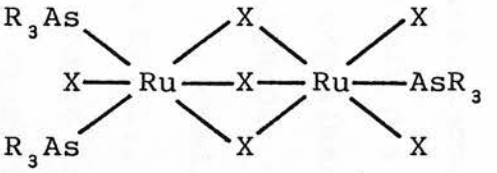

Structure 2

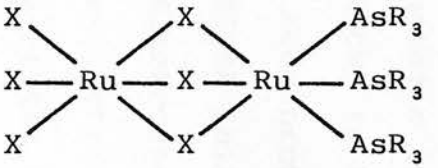

Structure 3

isomeric form. Isomer 2 should show a separation of *ca.* 0.95V and isomer 3 a separation of *ca.* 1.90V. Since the actual separation is *ca.* 0.95V the assignment of isomeric form 2 is clearly the more favourable. Isomer 2 is also the more favourable based on steric considerations, isomer 3 having three bulky $AsPh_3$ groups contained within one trigonal face.

Similar experiments have been carried out using the $[RuBr_3(AsPh_3)_2MeOH]$ complex as a starting material. As previously mentioned, the reactions of this complex when dissolved in CH_2Cl_2, can be monitored electrochemically, showing the change from a monomeric to a binuclear structure. If $[RuBr_3(AsPh_3)_2MeOH]$ is heated under reflux in benzene under nitrogen, a deep brown solution is produced from which a brown-black solid may be isolated, (see Experimental section). Electrochemical investigation of this solid reveals two one-electron reductions at potentials identical to those of the two new waves which appear when $[RuBr_3(AsPh_3)_2MeOH]$ is dissolved in CH_2Cl_2 and allowed to stand, and the carbon and hydrogen analyses fit very closely with those expected for the formulation $[Ru_2Br_6(AsPh_3)_3]$.

Thus it is concluded that the product formed on dissolving $[RuBr_3(AsPh_3)_2MeOH]$ in CH_2Cl_2 or on heating in benzene is $[Ru_2Br_6(AsPh_3)_3]$, by analogy with the previous experiments on the chloro compounds and in the light of the new data available on the carbon and hydrogen analyses of the bromo complexes and their electrochemical behaviour (see Table 3.2).

The expected esr signal for $[Ru_2Br_6(AsPh_3)_3]$ was not observed despite attempts at measurement in various solvents. This may be due to the insolubility of the complex rather than an inherent lack of unpaired electrons, (cf. the insolubility of $[Ru_2Cl_6(AsPh_3)_3]$[10])

Alleviation of this problem of insolubility, (achieved for the chloro-analogue by preparation of the more soluble $[Ru_2Cl_6(As\{p\text{-}tol\}_3)_3]$ complex), by the attempted preparation of $[Ru_2Br_6(As\{p\text{-}tol\}_3)_3]$, was unsuccessful, leading only to mixtures of products (vide infra).

The exact mechanism of formation of these triple bridged binuclear species is unknown although it seems probable that a likely first step would be the loss of the labile MeOH group from one or both monomeric ruthenium centres followed by cross coupling of the resulting coordinatively unsaturated species, (see Scheme 3.1). Eventual loss of the MeOH ligand from both ruthenium atoms would allow the formation of a double chloride-bridged intermediate which might then be followed by intramolecular rearrangement to form the triple bridged binuclear product, (see Scheme 3.2).

Scheme 3.2

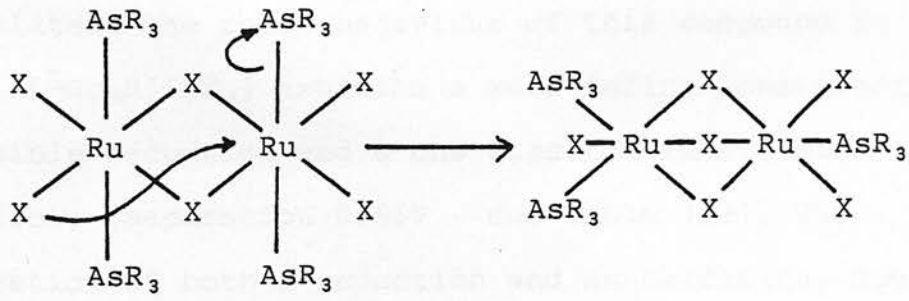

In proposing this mechanism, it must be noted that there is no evidence for the formation of the double

bridged species in the electrochemical data so far available, although a more thorough study of the electrochemical behaviour of the $[RuX_3(AsR_3)_2MeOH]$ complexes might yet provide useful insight.

3.2.2. Synthesis and Characterisation of Mixed-Valence Triple Bromo-Bridged Complexes of Ruthenium

Following the characterisation of $[Ru_2Br_6(AsPh_3)_3]$ obtained from $[RuBr_3(AsPh_3)_2MeOH]$ in non-polar non-coordinating solvents such as CH_2Cl_2 and C_6H_6, interest was focussed on reactions of the methanolate complex, together with those of the $[Ru_2Br_9]^{3-}$ anion, in more polar solvents in the presence of added tertiary arsine. This type of reaction has been examined for $[RuCl_3(AsR_3)_2MeOH]$ (R = Ph, p-tol) and '$RuCl_3xH_2O$', and a variety of interesting mixed-valence binuclear compounds have been produced, a number of which were later extensively investigated by electrochemical[10,12,16] and spectroelectrochemical[11] methods.

Thus if $[RuBr_3(AsPh_3)_2MeOH]$ is heated under reflux in degassed ethanol, with an excess of $AsPh_3$ for two hours, a deep purple-black solid, analysed as $[Ru_2Br_5(AsPh_3)_4]$, may be isolated. The redox behaviour of this compound in $CH_2Cl_2/[^nBu_4N][BF_4]$ exhibits a well defined one-electron reversible reduction and a one electron reversible oxidation, (separation 0.66V - see Table 3.2). The observation of both a reduction and an oxidation, together with the small separation of 0.66V between the two, is indicative that the compound is a mixed-valence one and

that there is a symmetric arrangement of terminal halide and tertiary arsine ligands i.e. one terminal halide and two arsine ligands at each end of the molecule, (cf. related studies on $[Ru_2Cl_5(AsPh_3)_4]$ [10]). Two structural isomers (4 & 5) are possible for this complex, (see Figure 3.3),

Figure 3.3.

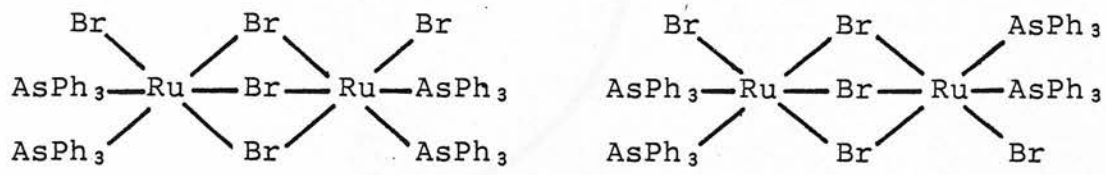

(4) (5)

and again esr spectroscopy can be used to determine the correct structure. Structure 4 should show a 2g value spectrum indicating the axial plane of symmetry of the molecule, whereas structure 5 lacks any plane of symmetry and would therefore be expected to exhibit a lower symmetry 3g value esr spectrum. The spectrum observed, (see Figure 3.4), shows three g values indicating structure 5 to be the one actually formed, this staggered structure also appears to be the more favourable sterically cf. $[Ru_2Cl_4CS(PPh_3)_4]$ [16,17].

As previously noted attempts to isolate the monomer $[RuBr_3(As\{p\text{-}tol\}_3)_2MeOH]$ in the same manner as $[RuBr_3(AsPh_3)_2MeOH]$, (readily prepared for the chloro analogue by heating a solution of '$RuCl_3xH_2O$' and $As(p\text{-}tol)_3$ in methanol [10]), were unsuccessful. Thus heating a solution of $[Ph_3PhCH_2P]_3[Ru_2Br_9]$ in methanol with an excess of $As(p\text{-}tol)_3$ for up to 8 hours produces a mixture of products which could not be separated. An

Figure 3.4 E.s.r. Spectrum of $[Ru_2Br_5(AsPh_3)_4]$ in CH_2Cl_2 at 150K

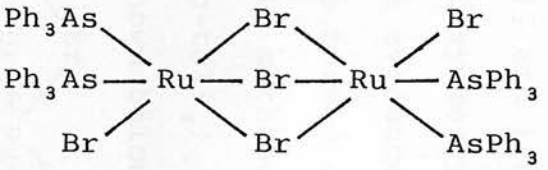

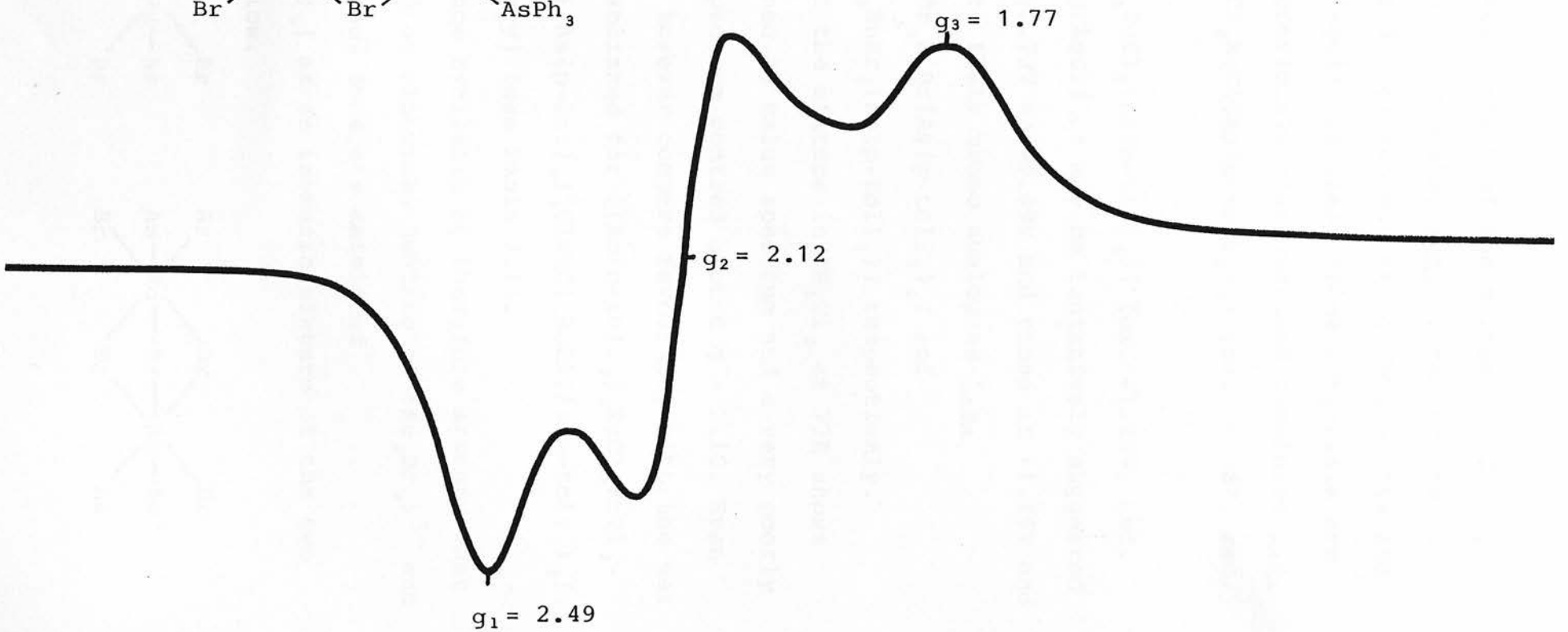

electrochemical investigation of the mixture in CH_2Cl_2 however, revealed 5 major peaks, i.e. 2 reductions at -0.20V and +0.09V and 3 oxidations at +0.79V, +1.16V and +1.32V (all vs. Ag/AgCl). If these redox potentials are compared with the previously characterised complexes i.e. $[(As\{p\text{-}tol\}_3)_2ClRuCl_3RuCl(As\{p\text{-}tol\}_3)_2]$ (ox. +0.78V, red. +0.05V) and [7] $[(As\{p\text{-}tol\}_3)_3RuCl_3RuCl_2(As\{p\text{-}tol\}_3)]$ (ox. +1.20V, red. -0.28V) (all vs. Ag/AgCl) it may be tentatively suggested that the peaks at +0.79V and+0.09V and those at +1.16V and -0.20V may be due to their bromo analogues i.e. $[(As\{p\text{-}tol\}_3)_2BrRuBr_3RuBr(As\{p\text{-}tol\}_3)_2]$ and $[(As\{p\text{-}tol\}_3)\ RuBr_3RuBr_2(As\{p\text{-}tol\}_3)]$ respectively.

Esr analysis of the mixture in CH_2Cl_2 at 77K shows only a poorly defined 2g value spectrum and a very poorly defined 3g value spectrum centred around g = 2.10. Even these limited data however compare favourably with the esr values already established for $[(As\{p\text{-}tol\}_3)_3RuCl_3RuCl_2$-$(As\{p\text{-}tol\}_3)]$ and $[(As\{p\text{-}tol\}_3)_2ClRuCl_3RuCl(As\{p\text{-}tol\}_3)_2]$, (no plane of symmetry) (see Table 3.1).

From the evidence available it therefore appears that the products formed on vigourous heating of $[Ru_2Br_9]^{3-}$ and $As(p\text{-}tol)_3$ in methanol consists mainly of $[Ru_2Br_5(As\{p\text{-}tol\}_3)_4]$ as an isomeric mixture of the two stuctures shown below.

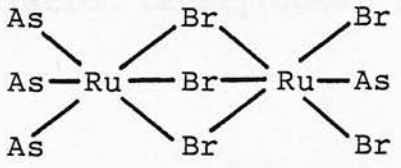

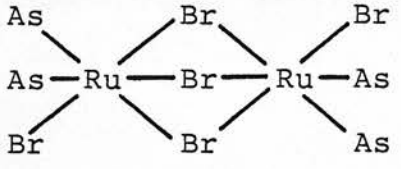

3.2.3 Reaction of $[Ru_2Br_9]^{3-}$ with Bidentate Ligands

In order to try to increase the range of triple bromo-bridged complexes, attempts were made to produce these types of complex by reaction of the organo-soluble $[Ru_2Br_9]^{3-}$ precursor with bidentate P and As donor ligands. Thus, when a solution of $[^nBu_4N]_3[Ru_2Br_9]$ in methanol is heated under reflux in the presence of an excess of $(Ph_2P)CH_2CH_2(Ph_2P)$ (dppe) for one hour a light orange solution is produced from which a pale orange precipitate could be isolated, analytically consistent with the formulation $[RuBr_2(dppe)_2]$, (see Experimental section). Electrochemical investigation of the precipitate in $CH_2Cl_2/[^nBu_4N][BF_4]$ at room temperature showed a single reversible one-electron oxidation at +0.67V *vs.* Ag/AgCl with no other redox processes occurring within the available potential range. The complex is shown to have the *trans-* configuration by $^{31}P\{^1H\}$ n.m.r spectroscopy which shows a singlet at δ= 41.6 ppm.

Similarly heating $[^nBu_4N]_3[Ru_2Br_9]$ with an excess of $(AsPh_2)CH_2CH_2(AsPh_2)$ (dpae) in bromoethane under reflux for 3 hours gives a deep green solution from which a small quantity of a pink microcrystalline material could be isolated. This material also exhibits a one-electron reversible oxidation at +0.67V *vs.* Ag/AgCl and the carbon and hydrogen analysis figures fit closely for the formulation $[RuBr_2(dpae)_2]$, (see Experimental section).

3.3 Conclusions

These studies have extended the available range of binuclear complexes of ruthenium, bridged by simple halide ligands. As well as new Ru_2(III/III) complexes, the new Ru_2-(II/III) mixed valence complexes also produced should prove useful in the investigation of the electronic behaviour of mixed valence complexes in general and triple halide-bridged complexes in particular. These investigations have already reached an advanced stage where the triple chloro-bridged analogues are concerned, with an excellent opportunity for variation in neutral terminal ligand character and in isomeric form. The same type of variation has now been shown to be available for triple bromo-bridged complexes of this type. The failure of other ligands such as bidentate phosphorus and arsenic donors to form such triple bridged complexes, can be ascribed to the facile reduction of Ru(III) to Ru(II) accompanied by the formation of six strong bonds which inhibits further reaction in the presence of an excess of such ligands.

See page 101 first.

Tribromobis(triphenylarsine)acetone ruthenium (III)

The complex $[RuBr_3(AsPh_3)_2MeOH]$ (0.27g) was shaken in acetone (30 ml) for 24 hours at room temperature. After this time the precipitate, black, microcrystalline solid was removed by filtration washed with acetone and diethyl-ether and air dried. 0.25g (90%).

Analysis	Found	C 46.1	H 3.5%
Calc. for $C_{39}H_{36}As_2Br_3ORu$		C 46.1	H 3.5%

$\nu CO = 1655\ cm^{-1}$

Dibromobis(bisdiphenylarsenoethane) ruthenium (II)

$[^{n}Bu_4N]_3[Ru_2Br_9]$ (0.50g) and $Ph_2As(CH_2)_2AsPh_2$ (0.74g) were heated under reflux in bromoethane (30 ml) for 3 hours. The solution colour changed from purple to deep green and a pink microcrystalline product was produced which was removed by filtration, washed with C_2H_5Br and diethyl-ether and air dried. 0.21g (28%).

Analysis:	Found	C 50.4	H4.0%
Calc. for $C_{52}H_{48}As_4Br_2Ru$		C 50.6	H3.9%

Dibromobis(bisdiphenylphosphenoethane) ruthenium (II)

$[^{n}Bu_4N]_3[Ru_2Br_9]$ (0.50g) and $Ph_2P(CH_2)_2PPh_2$ (0.60g) were heated under reflux in methanol (30 ml) for 1 hour. The solution colour changed from purple to a pale orange and a pale orange precipitate formed. This was removed by filtration, washed with methanol and diethyl-ether and air dried. 0.41g (64%).

Analysis:	Found	C 59.1	H 4.5%
Calc. for $C_{52}H_{48}Br_2P_4Ru$		C 59.0	H 4.5%.

3.4 Experimental Should precede page 100.

Materials

Commercial ruthenium trichloride (Johnson Matthey plc). Triphenylarsine, dppe, dpae (Aldrich Chemicals). Tri(4-methylphenyl)arsine (Maybridge Chemicals).

All physical measurements were carried out as in chapters 1 and 2.

Tri-μ-bromo-a,c,h-tribromotris(triphenylarsine) diruthenium (III/III)

$[RuBr_3(AsPh_3)_2MeOH]$ (0.25g) was dissolved in degassed benzene (50 ml) and heated for 6 hours under reflux in an atmosphere of nitrogen. After reduction of the solution volume the black precipitate produced was filtered off, washed with diethyl ether and air dried. 0.10g (60%).

Analysis: Found C 41.2 H 2.8%

Calc. for $C_{57}H_{48}As_3Br_6Ru_2$ C 41.7 H 2.9%

Tri-μ-bromo-a,i-dibromotetrakis(triphenylarsine) diruthenium (II/III)

$[RuBr_3(AsPh_3)_2MeOH]$ (0.20g) was dissolved in degassed ethanol (50 ml) together with $AsPh_3$ (0.80g) and the solution was heated under reflux in an atmosphere of nitrogen for 2 hours after which time a deep purple precipitate had formed. This was removed from the solution by filtration, washed with ethanol and diethyl-ether and air dried. 0.18g (49%)

Analysis: Found C 47.5 H 3.4

Calc. for $C_{72}H_{60}As_4Br_5Ru_2$ C 47.3 H 3.3

Tri-μ-bromo-a,i-dibromotetrakis (tri(4-methylphenyl)arsine) diruthenium (II/III) and Tri-μ-bromo-a,c-dibromotetrakis (tri(4-methylphenyl)arsine) diruthenium (II/III)

A solution of $[Ph_3PhCH_2P]_3[Ru_2Br_9]$ in degassed ethanol, together with excess $As(p\text{-}tol)_3$ was heated under reflux in an atmosphere of nitrogen for 8 hours. Reduction of the solution volume and trituration produces a brown powder which was removed by filtration, washed with diethyl-ether and air dried. (n.b. This product precipitates as a mixture consisting mainly of the 2 isomers above - see text).

Tribromobis(triphenylarsine)methanolate ruthenium (III)

The complex $[Ph_3PhCH_2P]_3[Ru_2Br_9]$ (0.32g) was heated under reflux in methanol (50 ml) for 30 minutes. After filtration through celite to remove any undissolved material the solution was added to a flask containing $AsPh_3$ (0.30g). After heating under reflux for 1 hour the microcrystalline, red-brown product was removed by filtration, washed with methanol and diethyl-ether and air dried. 0.26g (82%).

Analysis	Found	C 45.1	H 3.4%
Calc. for $C_{37}H_{34}As_2Br_3ORu$		C 45.1	H 3.5%

Table 3.1 E.s.r Data for Selected Triple Halide-Bridged Complexes of Ruthenium

Complex	Configuration	'g' values at 150K in CH_2Cl_2	Ref
$[Ru_2Cl_6(AsPh_3)_3]$	I	g 2.49 g not observed	10
$[Ru_2Br_6(AsPh_3)_3]$	I	not observed (see text)	
$[Ru_2Cl_5(As\{p\text{-}tol\}_3)_4]$	II	g 2.54 g 1.63	10
$[Ru_2Cl_5(As\{p\text{-}tol\}_3)_4]$	III	g_1 2.41 g_2 2.11 g_3 1.87	10
$[Ru_2Br_5(AsPh_3)_4]$	III	g_1 2.49 g_2 2.12 g_3 1.77	

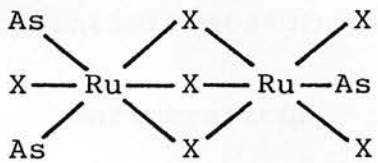

Configuration I

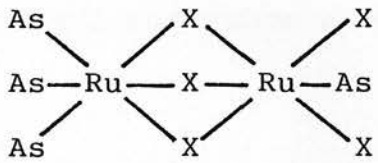

Configuration II

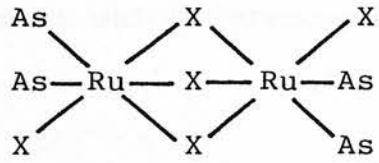

Configuration III

Table 3.2 Electrochemical Data for Some Selected Triple Halide-Bridged Complexes of Ruthenium

Ref	Complex	Configuration	(II/II)/(II/III)	(II/III)/(III/III)	Sep^n
10	$[Ru_2Cl_6(AsPh_3)_3]$	I	+0.57V	-0.49V	1.06V
10	$[Ru_2Cl_6(As\{p\text{-}tol\}_3)_3]$	I	+0.53V	-0.49V	1.02V
	$[Ru_2Br_6(AsPh_3)_3]$	I	+0.61V	-0.33V	0.94V
	$[Ru_2Br_5(AsPh_3)_4]$	II	+0.20V	+0.86V	0.66V
10	$[Ru_2Cl_5(AsPh_3)_4]$	II	+0.09	+0.85V	0.76V
10	$[Ru_2Cl_5(As\{p\text{-}tol\}_3)_4]$	II	+0.05V	+0.78V	0.73V
	$[Ru_2Br_5(As\{p\text{-}tol\}_3)_4]$	II	+0.09V	+0.79V	0.70V
10	$[Ru_2Cl_5(As\{p\text{-}tol\}_3)_4]$	III	-0.28V	+1.20V	1.48V
	$[Ru_2Br_5(As\{p\text{-}tol\}_3)_4]$	III	-0.20V	+1.16V	1.36V

(All potentials measured against Ag/AgCl reference electrode against which ferrocene oxidises at +0.55V)

Configurations

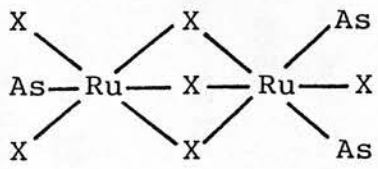

Configuration 1

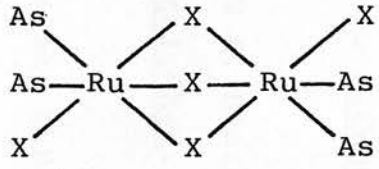

Configuration 2

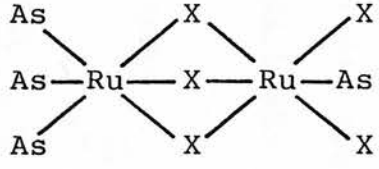

Configuration 3

Chapter 3 References

1. J. Chatt and R.G. Hayter. J.Chem Soc., 1961, 896.
2. R.H. Prince and K.A. Raspin. J.Inorg.Nucl.Chem., 1961, 31, 695.
3. P.W. Armit, A.S.F. Boyd and T.A. Stephenson. J.Chem.Soc. Dalton Trans., 1975, 1663.
4. L.W. Gosser, W.H. Knoth and G.W. Parshall. J.Am.Chem.Soc., 1973, 95, 3436.
5. P.W. Armit, T.A. Stephenson and E.S. Switkes. J.Chem.Soc. Dalton Trans., 1974, 1134.
6. P.W. Armit, W.J. Sime and T.A. Stephenson. J.Chem.Soc. Dalton Trans., 1976, 2121.
7. R. Contreras, G.G. Elliot, R.O. Gould, G.A. Heath, A.J. Lindsay and T.A. Stephenson. J.Organometal.Chem., 1981, 215, C6.
8. I.J. Colquohoun, W. McFarlane, A.M.R. Galas, M.B. Hursthouse, R.A. Jones and G. Wilkinson. J.Chem.Soc. Dalton Trans., 1980, 2480.
9. J.K. Nicholson. Angew.Chem., 1967, 6, 263.
10. R.A.C. Zarate. Ph.D. Thesis, University of Edinburgh. 1981.
11. G.A. Heath, A.J. Lindsay, T.A. Stephenson and D.K. Vattis. J.Organometal.Chem., 1982, 233, 353.
12. L.W. Gray and E.E. Mercer. J.Am.Chem.Soc., 1972, 94, 6426.
13. P.E.Dumas and E.E. Mercer. Inorg.Chem., 1971, 10, 2755.
14. W. Herrmann, M. Koppen and K. Wieghart. Z.Naturforsch., 1984, 39B, 1335.

15. T.A.Stephenson and G. Wilkinson. J.Inorg.Nucl.Chem., 1966, 28, 945.

16. P.W. Armit and T.A. Stephenson. J.Organometal.Chem., 1974, 73, C33.

17. A.J. Lindsay. Ph.D. Thesis, University of Edinburgh. 1982.

18. R. Contreras, G.A. Heath, A.J. Lindsay and T.A. Stephenson. J.Organometal.Chem., 1979, 179, C55.

19. T.Arthur, R. Contreras, G.A. Heath, G. Hefter, A.J. Lindsay, D.J.A. Riach and T.A. Stephenson. J.Organometal.Chem., 1979, 179, C49.

CHAPTER 4

Preparative Electrochemical Generation, and Characterisation of Some New Monomeric and Binuclear Osmium Complexes

4.1 Introduction

Following the pioneering work of Chatt and co-workers[1] in the early 1960's, many mono- and bi-nuclear complexes of osmium containing P-donor ligands have been synthesised. The propensity of osmium to form stable, octahedral, low-oxidation state complexes with 'soft' neutral ligands such as tertiary phosphines has opened up numerous avenues of exploration for the coordination chemist.

One of the first discovered and most stable of these types of compound were those of the $[Os_2Cl_3(PR_3)_6]^+$ family which possess the now well characterised confacial bioctahedral triple chloro-bridged structure. It was not until 7 years later however, that details of the preparation of the monomeric species mer-$[OsX_3(L)_3]$ (X = Cl, Br; L = monotertiary phosphine or arsine) were published [2]. Reaction of OsO_4 with a range of phosphine and arsine ligands was found to follow a general sequence (equation {1}).

$$[Os(VIII)O_4] \longrightarrow [LH]_2[Os(IV)X_6] \longrightarrow [Os(IV)X_4L_2] \longrightarrow [Os(III)X_3L_3] \longrightarrow [L_3Os(II)X_3Os(II)L_3]X \quad ..\{1\}$$

Thus when $[Os(VIII)O_4]$ was dissolved in ethanol containing the hydrohalic acid, (preventing volatilisation of the tetroxide by converting it to $H_2[Os(IV)X_6]$), treatment of the resulting solution with an excess of

phosphine or arsine led to the general sequence above. It was found that the $[OsX_4L_2]$ complexes were only isolable with the less reactive phosphines and with arsines, and it was claimed that in the special case of triphenylphosphine, a different reaction, yielding $[OsOCl_3(PPh_3)_2]$, took place. This latter result was found to be in error when it was discovered that the product of this reaction was actually a mixture of $[OsO_2Cl_2(PPh_3)_2]$ and trans-$[OsCl_4(PPh_3)_2]$ [3]. Reaction of $[OsCl_6]^{2-}$ with PPh_3 in either ethanol or a mixture of t-butanol and water produced the complex $[OsCl_2(PPh_3)_3]$ [4,5] although in our hands the products have been found to be somewhat variable and a more reliable method has been formulated involving the use of methanol as the solvent [6,7].

Since the discovery in 1967 by Shilov and co-workers[8] that the reduction of $[OsCl_6]^{2-}$ and OsO_4 by N_2H_4 yielded osmium complexes containing dinitrogen, much interest has been shown in the low-valent coordination complexes of osmium. In 1970 Chatt and co-workers[9] prepared a series of 12 dinitrogen complexes of the type cis-$[Os(II)X_2(QR_3)\ N_2]$ by zinc reduction of a solution of mer-$[OsX_3(QR_3)_3]$ (X = Cl, Br; QR_3 = tertiary phosphine or arsine) under dinitrogen. The possibility that these complexes might play some part in the fixation of dinitrogen in a catalytic reduction of the gas to ammonia was not ignored; however all attempts to reduce the dinitrogen in these complexes were unsuccessful. A year later many other complexes of the general type $[OsX_2Y(QR_3)_3]$ and $[OsX_2Y_2(QR_3)_2]$ (X = Cl, Br; Y = CO,

MeCN, PhCN, MeNC, PhNC; QR_3 = tertiary phosphine or $AsMe_2Ph$) were prepared [10], again by zinc reduction of mer-$[OsX_3(QR_3)_3]$ in the presence of Y.

In this chapter the results of electrochemically induced ligand substitution on the complex mer-$[OsCl_3(PMe_2Ph)_3]$ to form a range of new Os(II) complexes are discussed.

4.2 Results and Discussion

4.2.1 Electrochemistry in Non-Coordinating Solvents

The monomer, mer-$[OsCl_3(PMe_2Ph)_3]$ [1], when examined in CH_2Cl /0.5M $[^nBu_4N][BF_4]$ at 293K under argon, exhibited a cyclic voltammetric response as shown in Figure 4.1a. The oxidation was assigned as an Os(III)⟶Os(IV) electrode process and the reduction as an Os(III)⟶Os(II) electrode process with a rapid following chemical reaction accounting for the irreversibility of the process corresponding to this wave.

If the temperature of the solution is lowered to 233K, the cyclic voltammogram then appears as shown in Figure 4.1b, indicating that the chemical reaction following the reduction has been inhibited leading to a fully reversible redox process, (the anodic to cathodic peak separation is 50mV corresponding closely to the theoretical value for a one electron wave of 44mV at 233K), (see Chapter 1 for full reversiblity criteria). Thus on a cyclic voltammetric timescale it is possible to stabilise the $[OsCl_3(PMe_2Ph)_3]^-$ anion [2] simply by lowering the temperature.

It was also found that by altering the solvent or

Figure 4.1a Voltammetry of mer-$[OsCl_3(PMe_2Ph)_3]$ at room temperature in 0.5M $[^nBu_4N][BF_4]/CH_2Cl_2$

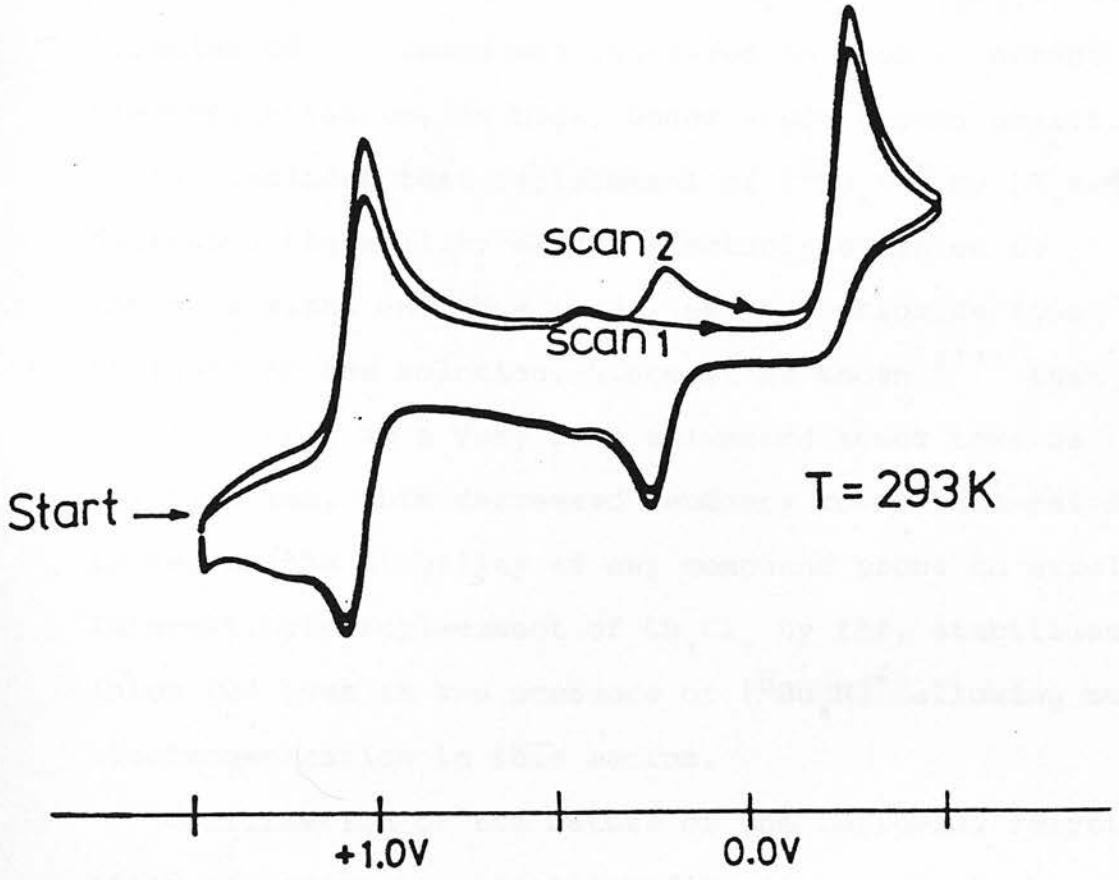

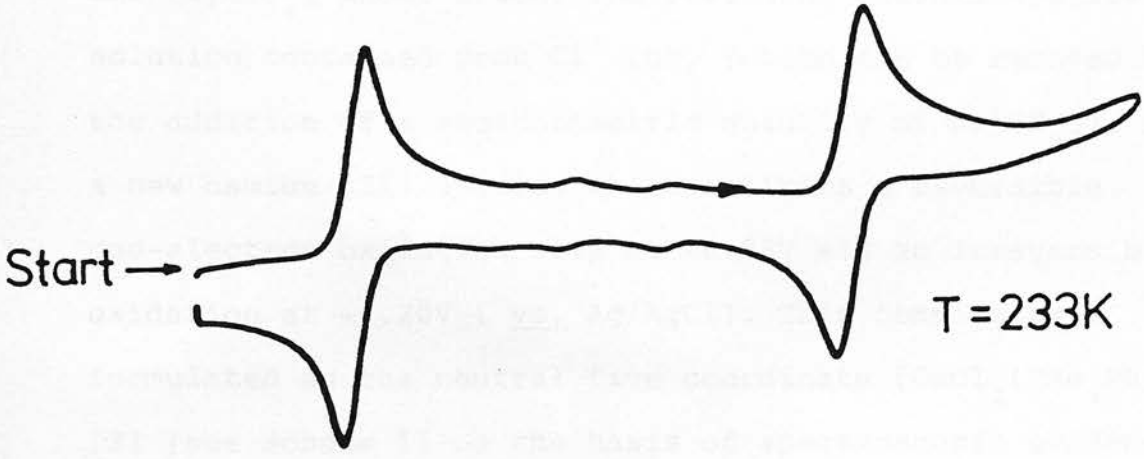

Figure 4.1b Voltammetry of mer-$[OsCl_3(PMe_2Ph)_3]$ at -40°C in 0.5M $[^nBu_4N][BF_4]/CH_2Cl_2$

electrolyte composition, the lifetime of the anion [2] could be increased substantially. Thus by replacing $[^{n}Bu_4N][BF_4]$ by $[R_3MeN][BF_4]$ ($R = C_8H_{17}$ to $C_{10}H_{21}$), the lifetime of the anion was increased to such an extent that electrogeneration, in bulk, under argon became possible. It is concluded that replacement of $[^{n}Bu_4N]^+$ by $[R_3MeN]^+$ decreases the ability of the electrolyte cation to ion-pair with, and thus stabilise, any chloride ions released to the solution. Since it is known [11] that CH_2Cl_2 itself is a very poor solvating agent towards chloride ion, this decreased tendency toward ion-pairing increases the stability of any compound prone to expel Cl^- Interestingly replacement of CH_2Cl_2 by thf, stabilises the anion [2] even in the presence of $[^{n}Bu_4N]^+$ allowing bulk electrogeneration in this medium.

Confirmation of the nature of the following reaction after reduction was established by carrying out the electrosynthesis at 298K in $CH_2Cl_2/[^{n}Bu_4N][BF_4]$ or thf/$Li[ClO_4]$ under argon. The resulting greenish-yellow solution contained free Cl^- ion, (which can be removed by the addition of a stoichiometric quantity of $Na[BF_4]$), and a new osmium (II) species which exhibits a reversible one-electron oxidation step at +0.03V and an irreversible oxidation at +1.20V (*vs.* Ag/AgCl). This complex is formulated as the neutral five coordinate $[OsCl_2(PMe_2Ph)_3]$ [3] (see Scheme 1) on the basis of spectroscopic evidence. Thus at 203K, the $^{31}P-\{^1H\}$ nmr spectrum shows a doublet centred at δ -32.8ppm and a triplet centred at δ -44.8ppm (J_{AB} 17.1 Hz) *cf.* the much studied $[RuCl_2(PPh_3)_3]$ complex

which has a square pyramidal structure in the solid state. Early crystallographic studies [12] on this ruthenium analogue indicated a close approach between the ruthenium atom and an ortho hydrogen on one of the phenyl rings. However it was concluded that there was no geometrical basis for metal-hydrogen interaction other than restricted rotation due to the preferred square pyramidal geometry, and that the stability of this five-coordinate complex arose from the blocking of the vacant site by the phenyl ring. Later studies [5] in solution supported this conclusion. $[RuCl_2(PPh_3)_3]$ exhibits fast intramolecular ligand scrambling in solution at room temperature, leading to a broad singlet in the $^{31}P-\{^1H\}$ nmr spectrum. On lowering the temperature however, the major pattern observed is that characteristic of the solid state structure i.e. magnetically inequivalent phosphines. $[OsCl_2(PPh_3)_3]$ also exhibits intramolecular scrambling at room temperature although with a comparatively slower rate of site exchange characteristic of third vs. second row transiton metal complexes [5]. Very recently, Green et al[13] have argued for an 'agostic' bonding interaction between the hydrogen and the metal as evidenced by nmr and other spectroscopic studies. In respect to complex [3], such a square pyramidal structure is consistent with the $^{31}P-\{^1H\}$ nmr spectrum of the complex, and with its further reactions.

Thus, if a concentrated (i.e. $> 4 \times 10^{-3}$ M) solution of $[OsCl_2(PMe_2Ph)_3]$ is electrogenerated in thf or CH_2Cl_2 under argon, then further reaction takes place to produce

the dimer $[Os_2Cl_4(PMe_2Ph)_6]$ and ultimately the binuclear cation $[Os_2Cl_3(PMe_2Ph)_6]$ (see Scheme 1). This complex can also be synthesised and isolated by a separate route (see Experimental section) and the species produced by the two methods have identical nmr and voltammetric properties, (i.e. $^{31}P-\{^1H\}$ nmr:- singlet at δ -36.7 ppm; voltammetry:- two reversible one-electron oxidations at +1.09V and +1.60V vs. Ag/AgCl). If the electrogeneration of this cation from mer-$[OsCl_3(PMe_2Ph)_3]$ is monitored, the intermediate species [4] is observed by $^{31}P-\{^1H\}$ nmr spectroscopy. This has a doublet centred at δ -40.0 ppm and a triplet centred at δ -46.9 ppm (see Figure 4.2). Voltammetry of the solution also shows a new wave corresponding to an oxidation at +0.48V vs. Ag/AgCl.

Recently Caulton et al [14] have photolysed $[OsH_4(PMe_2Ph)_3]$ in thf which produces $[Os_2H_4(PMe_2Ph)_6]$. This compound when dissolved in diethyl-ether undergoes further reaction to give the $[Os_2H_3(PMe_2Ph)_6]^+$ cation. They proposed loss of H_2 to give the reactive intermediate $[OsH_2(PMe_2Ph)_3]$, followed by dimerisation to give $[Os_2H_4(PR_3)_6]$ and then intramolecular rearrangement, with loss of H_2, to yield $[Os_2H_3(PR_3)_6]^+$. It is therefore reasonable to suggest that, in our case, the intermediate [4] is the doubly chloride-bridged $[Os_2Cl_4(PMe_2Ph)_6]$ complex which undergoes further intramolecular rearrangement to form the stable confacial bioctahedron $[Os_2Cl_3(PMe_2Ph)_6]^+$. This cation can also be formed by chemical reduction of mer-$[OsCl_3(PMe_2Ph)_3]$ using zinc amalgam in thf under argon, although again the

Figure 4.2 $^{31}P\{^{1}H\}$ n.m.r. Spectrum of $[Os_2Cl_4(PMe_2Ph)_6]$ in CH_2Cl_2

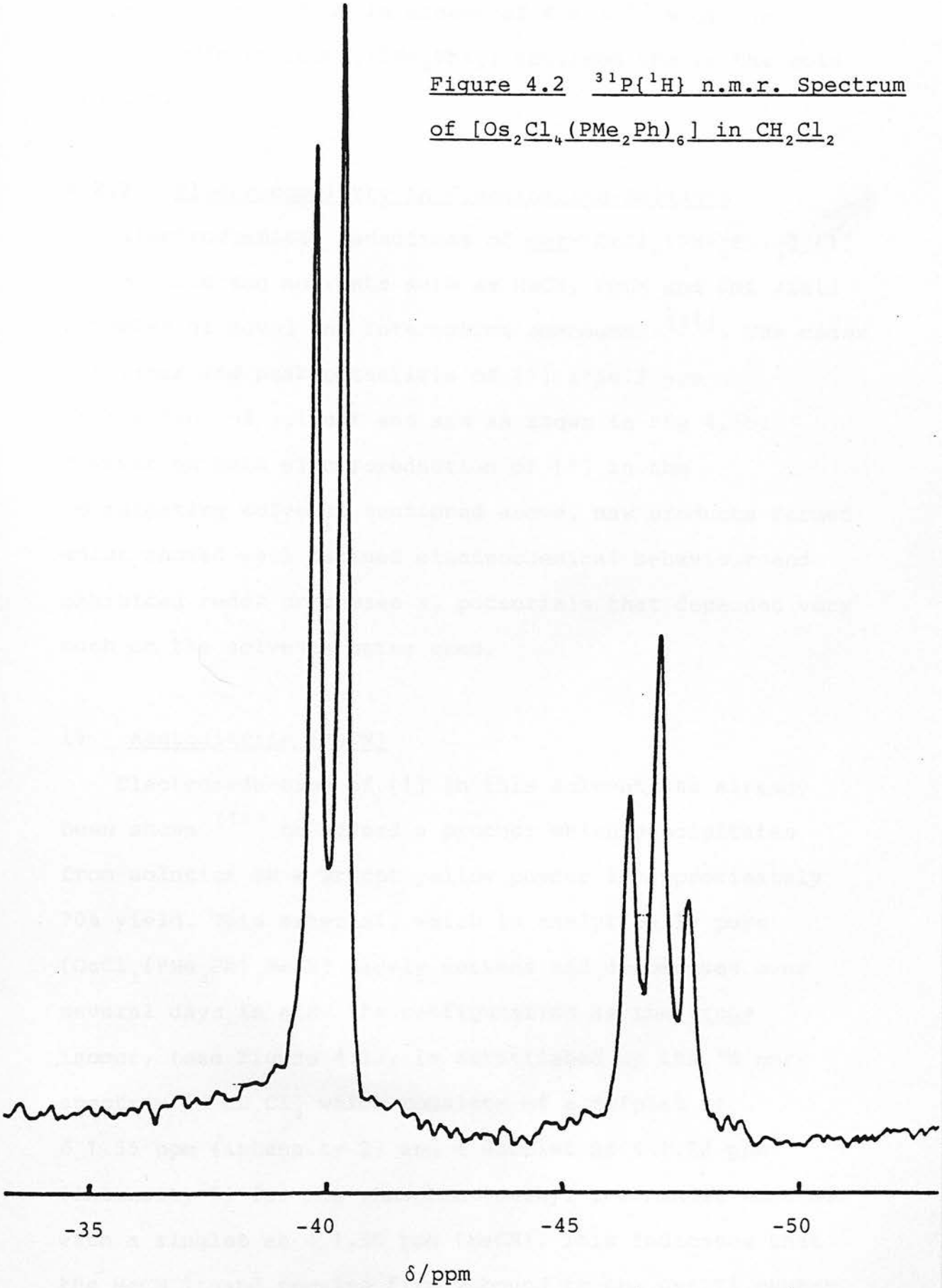

concentration must be in excess of 4×10^{-3} M or the five-coordinate $[OsCl_2(PMe_2Ph)_3]$ intermediate is the sole product.

4.2.2 Electrochemistry in Coordinating Solvents

Electrochemical reductions of mer-$[OsCl_3(PMe_2Ph)_3]$ [1] in coordinating solvents such as MeCN, PhCN and dmf yield a number of novel and interesting compounds [11]. The redox behaviour and peak potentials of [1] itself are independent of solvent and are as shown in Fig 4.1b. However on bulk electroreduction of [1] in the coordinating solvents mentioned above, new products formed which showed well-defined electrochemical behaviour and exhibited redox processes at potentials that depended very much on the solvents being used.

i) Acetonitrile (MeCN)

Electroreduction of [1] in this solvent has already been shown [11] to afford a product which precipitates from solution as a bright yellow powder in approximately 70% yield. This material, which is analytically pure $[OsCl_2(PMe_2Ph)_3MeCN]$ slowly darkens and decomposes over several days in air. Its configuration as the trans isomer, (see Figure 4.3), is established by its ^1H nmr spectrum in CD_2Cl_2 which consists of a triplet at δ 1.55 ppm (intensity 2) and a doublet at δ 1.72 ppm (intensity 1) for the phosphine methyl resonances together with a singlet at δ 1.30 ppm (MeCN). This indicates that the MeCN ligand remains firmly bound to the Os(II) centre

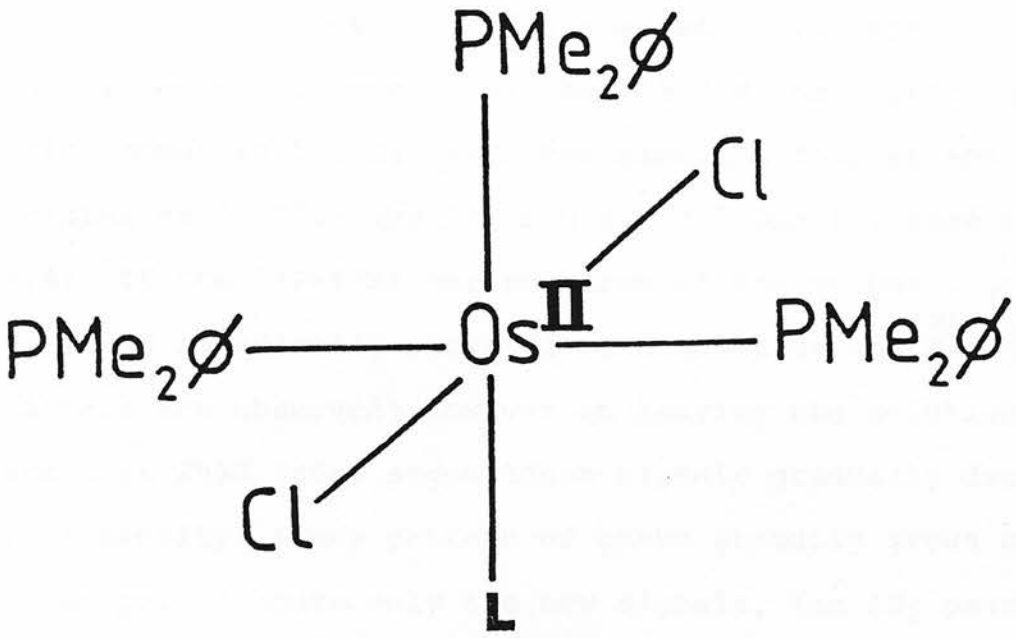

TRANS ISOMER

Figure 4.3 Cis- and Trans- Configurations of $[OsCl_2(PMe_2Ph)_3L]$ L = MeCN, dmf, N_2, CO, C_2H_4, PMe_2Ph

CIS ISOMER

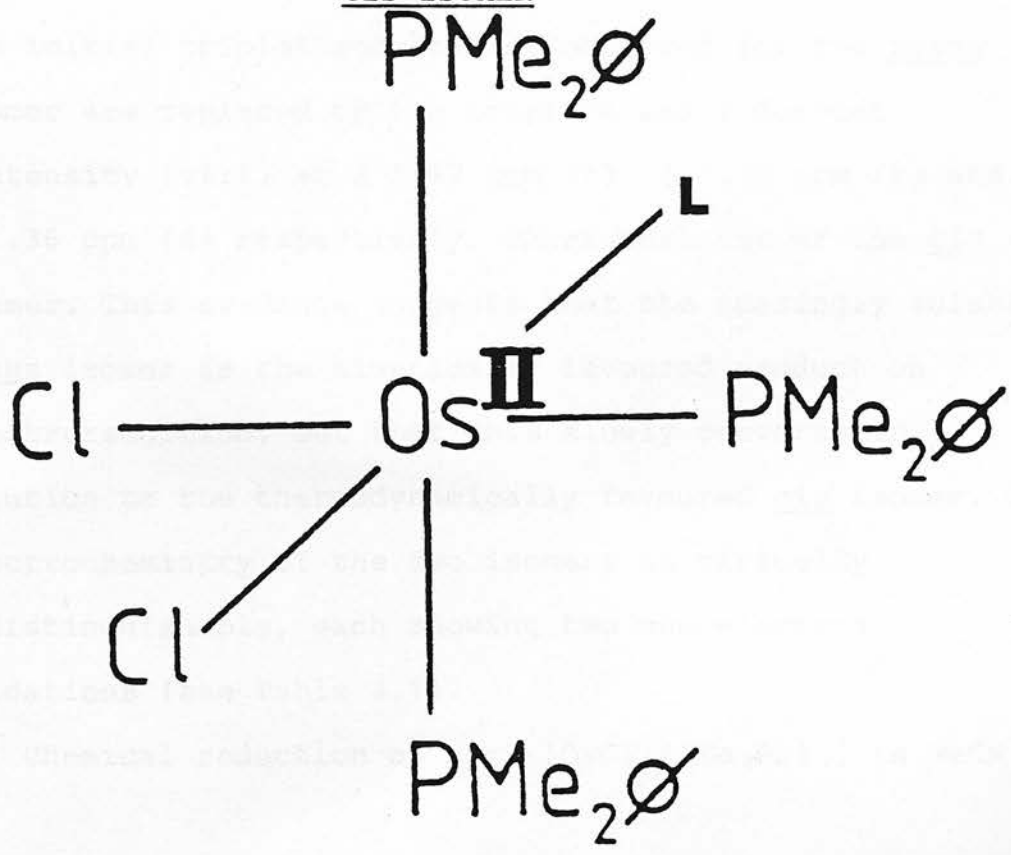

since there is no sign of a signal at δ 2.00 ppm corresponding to free MeCN. The $^{31}P-\{^{1}H\}$ nmr spectrum of this isomer in CH_2Cl_2 shows the expected doublet and triplet at δ -35.9 ppm (d) and δ -47.7 ppm (t) (see Figure 4.4). If the $^{31}P-\{^{1}H\}$ nmr spectrum of the mother liquor is examined immediately after electroreduction the same signals are observed; however on leaving the solution to stand at 293K under argon these signals gradually decrease in intensity. A new pattern of peaks steadily grows until after ca. 16 hours only the new signals, (an AB_2 pattern, see Figure 4.4), are present. This final solution is almost colourless and shows no sign of free PMe_2Ph or Cl^-, (beyond the one mole equivalent of Cl^- released during the electrosynthesis). The cis isomer configuration (see Figure 4.3) is confirmed by analysis of the phosphine methyl region of the ^{1}H nmr spectrum of an aged solution, generated by electrosynthesis in a $CD_3CN/Li[ClO_4]$ medium. The initial triplet and doublet observed for the trans isomer are replaced by two triplets and a doublet (intensity 1:1:1) at δ 1.87 ppm (t), δ 1.73 ppm (t) and δ 1.36 ppm (d) respectively, characteristic of the cis isomer. This evidence suggests that the sparingly soluble trans isomer is the kinetically favoured product on electroreduction, but that this slowly converts in solution to the thermodynamically favoured cis isomer. The electrochemistry of the two isomers is virtually indistinguishable, each showing two one-electron oxidations (see Table 4.1).

Chemical reduction of mer-$[OsCl_3(PMe_2Ph)_3]$ in MeCN

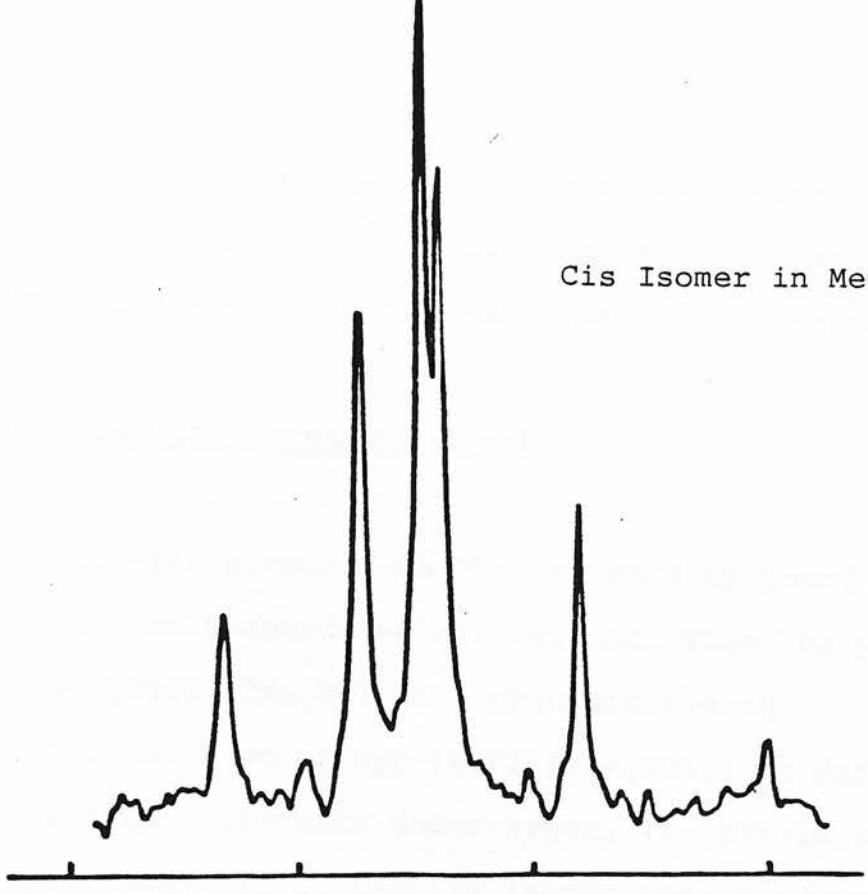

Figure 4.4 $^{31}P\{^{1}H\}$ nmr Spectra of cis- and trans-$[OsCl_2(PMe_2Ph)_3MeCN]$ at 298K

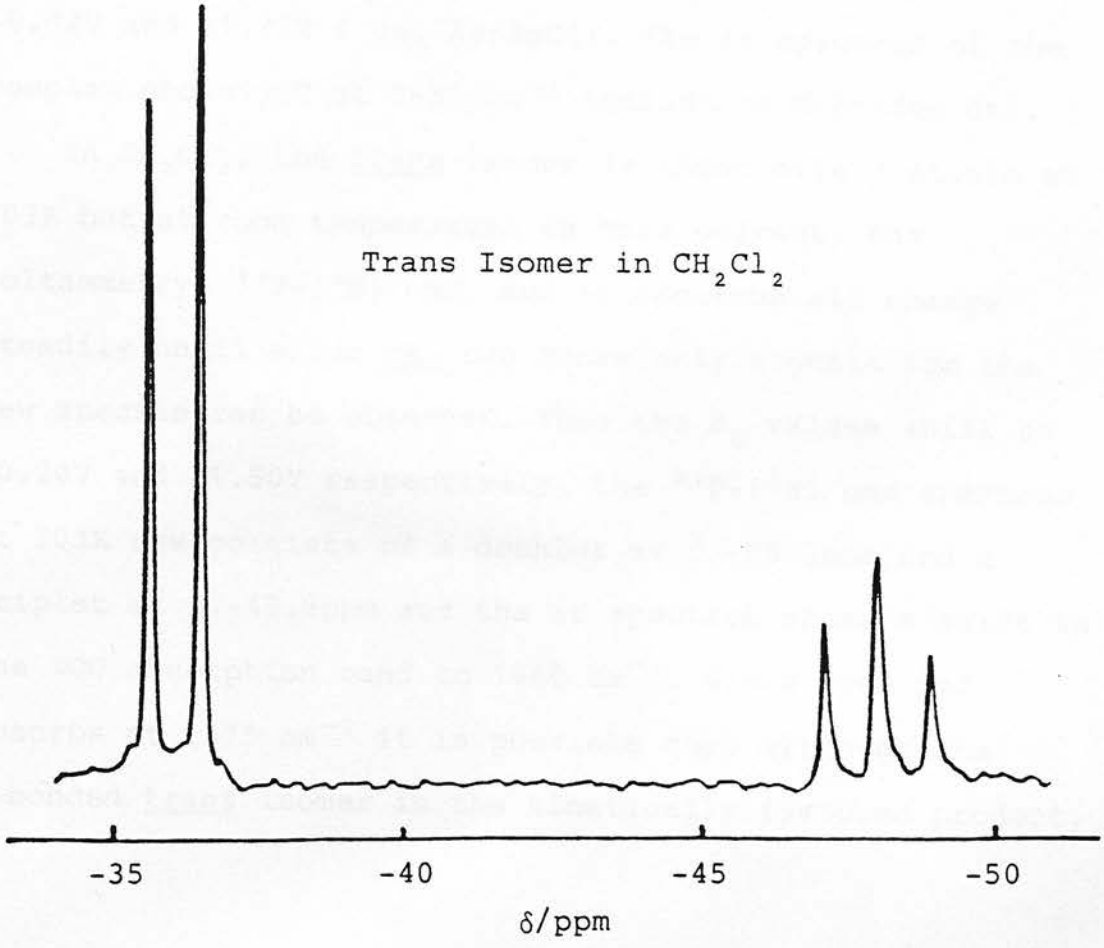

using zinc amalgam has led only to the formation of the trans complex [1] [10], due presumably to the short timescale over which the experiment was carried out.

ii) Dimethylformamide (dmf)

Behavior parallel to that of MeCN is found when dmf is used as the electrochemical solvent. Thus the yellow trans isomer $[OsCl_2(PMe_2Ph)_3dmf]$ precipitates on electroreduction of mer-$[OsCl_3(PMe_2Ph)_3]$ in dmf which may be removed by filtration under argon. If left in solution the complex converts to the cis isomer over a number of hours. The trans isomer, when dissolved in CH_2Cl_2, shows a $^{31}P-\{^1H\}$ nmr spectrum consisting of a doublet at δ-28.6ppm and a triplet at δ -47.5ppm and its electrochemistry reveals two reversible oxidations at +0.02V and +1.35V (vs. Ag/AgCl). The ir spectrum of the complex shows νCO at 1630 cm^{-1} indicating O-bonded dmf.

In CH_2Cl_2, the trans isomer is indefinitely stable at 203K but at room temperature in this solvent, the voltammetry, $^{31}P-\{^1H\}$ nmr, and ir spectrum all change steadily until after ca. two hours only signals for the new species can be observed. Thus the $E_{\frac{1}{2}}$ values shift to +0.20V and +1.50V respectively, the $^{31}P-\{^1H\}$ nmr spectrum at 203K now consists of a doublet at δ -36.2ppm and a triplet at δ -47.9ppm and the ir spectrum shows a shift in the νCO absorption band to 1660 cm^{-1}. Since free dmf absorbs at 1675 cm^{-1} it is possible that although the O-bonded trans isomer is the kinetically favoured product,

this rearranges fairly rapidly to the thermodynamically favoured N-bound product. The poor affinity of the Os(II) centre for O-donor ligands is also reflected in the fact that neither propylene carbonate or thf appear to bind to the five-coordinate $[Os(II)Cl_2(PMe_2Ph)_3]$.

A direct consequence of the reaction sequence postulated in Scheme 1 is that, since the products are formed by a dissociative mechanism rather than an associative one involving the solvent, the rate of chloride loss from the anion to form the five-coordinate intermediate should be independent of solvent. The rate of chloride loss (k_f) was measured by the cyclic triangular wave method of Nicholson and Shain [15], for charge transfer followed by an irreversible chemical reaction. When measured in $CH_2Cl_2/[^nBu_4N][BF_4]$, $MeCN/[^nBu_4N][BF_4]$ or $dmf/[^nBu_4N][BF_4]$ a constant rate of 5 s^{-1} at 288K was found. The following reaction, (uptake of L to form $[OsCl_2(PMe_2Ph)_3L]$), varied from very fast, where the five-coordinate intermediate could not be observed under any conditions, to rates at which the intermediate was detectable using fast scanning techniques. The rate of chloride loss can of course be retarded by decreasing the temperature as previously noted.

4.2.3 Electroreduction in the Presence of other Volatile Ligands

Other complexes of the type $[OsCl_2(PMe_2Ph)_3L]$ can be readily prepared by electroreduction of mer-$[OsCl_3(PMe_2Ph)_3$

in a solution of $CH_2Cl_2/[^nBu_4N][BF_4]$ which is continuously saturated by a stream of a coordinating gaseous ligand L.

i) Carbon Monoxide

Electroreduction in the presence of CO produces a clear yellow solution which appears from nmr and ir spectral data to consist of only one isomer i.e. the trans-$[OsCl_2(PMe_2Ph)_3CO]$ (see Figure 4.3 and Figure 4.5).

The $^{31}P-\{^1H\}$ nmr spectrum shows an AB_2 type pattern with no sign of any other signal. Unlike all other ligands L the trans complex does not rearrange to its cis analogue at room temperature. However this conversion can be accomplished by heating the solution under reflux for a number of hours.

The ir spectra showed the νCO trans = 1947 cm^{-1} and νCO cis = 1930 cm^{-1} (νCO gas = 1950 cm^{-1} in electrolyte solution). These results concur with those already published for this complex which is readily made chemically, in both its isomeric forms [10].

ii) Ethylene (C_2H_4)

Ethylene coordinates very readily to the five-coordinate complex [3] to produce results similar to those outlined above. Thus the $^{31}P-\{^1H\}$ nmr spectrum of the solution initially shows a well defined doublet and triplet at δ -39.1 ppm and δ -48.5 ppm respectively, assigned to the trans isomer (see Figure 4.3). Over a period of hours at room temperature this signal gradually gives way to an AB_2 type pattern at ca. δ -32 ppm (see

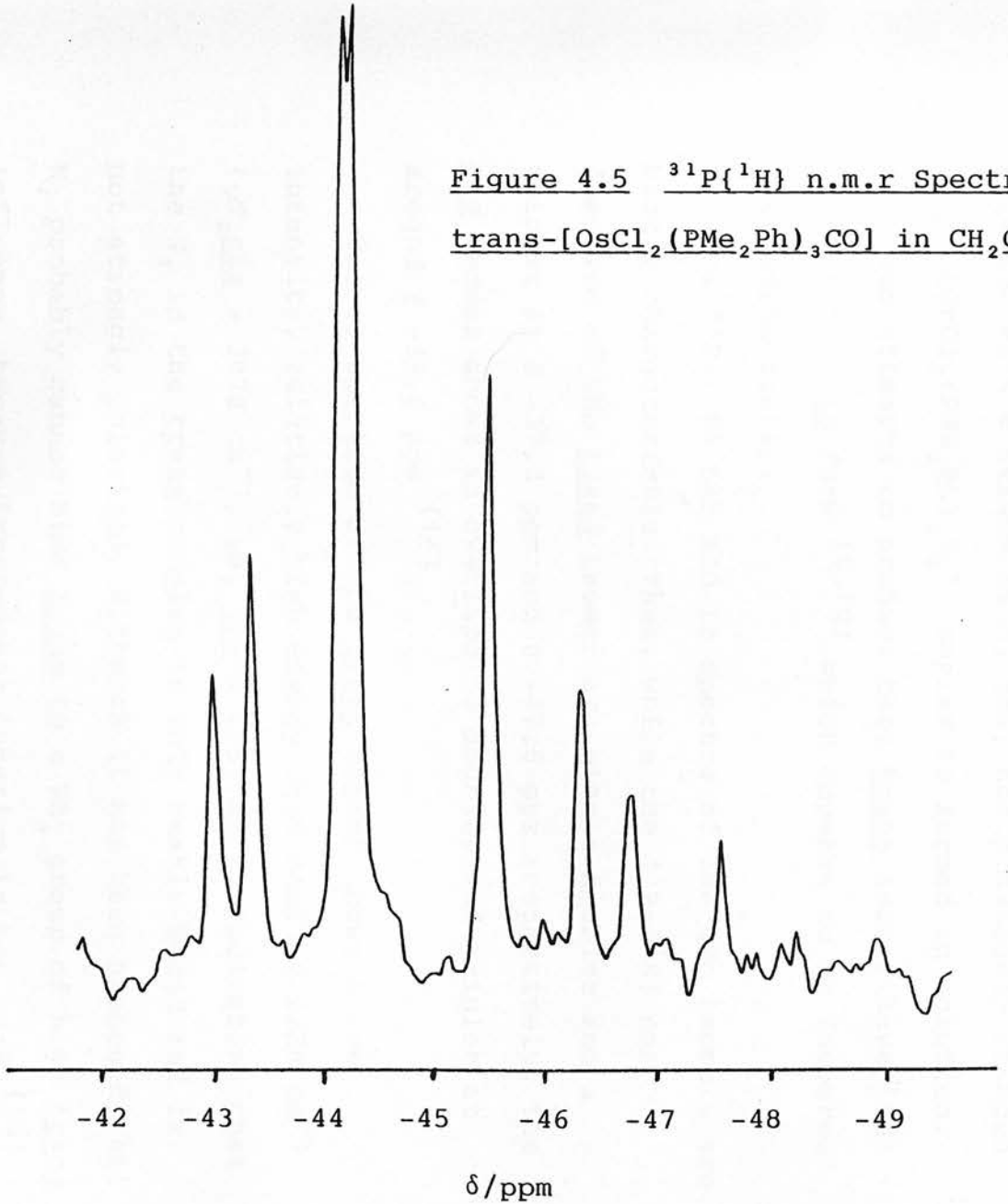

Figure 4.5 $^{31}P\{^{1}H\}$ n.m.r Spectrum of trans-$[OsCl_2(PMe_2Ph)_3CO]$ in CH_2Cl_2

Table 4.1) which is assigned to the more thermodynamically stable cis isomer (see Figure 4.3).

iii) Dinitrogen (N_2)

If a solution of mer-$[OsCl_3(PMe_2Ph)_3]$ in CH_2Cl_2/ $[^nBu_4N][BF_4]$ is electroreduced while saturating the solution with a stream of N_2 gas, the previously unknown trans-$[OsCl_2(PMe_2Ph)_3N_2]$ complex is formed in solution. Previous attempts to produce this trans isomer have led only to the cis form [9,10] which appears to be favoured thermodynamically.

The $^{31}P-\{^1H\}$ nmr and ir spectra of the two isomers are highly characteristic. Thus, while the $^{31}P-\{^1H\}$ nmr spectrum of the trans isomer exhibits a doublet and a triplet at δ -37.3 ppm and δ -47.8 ppm respectively, the cis isomer shows an overlapping doublet and triplet at around δ -34.6 ppm [16].

The ir spectrum of the trans isomer shows a low intensity, relatively high energy νN-N band at 2280 cm^{-1} (νN_2 cis = 2078 cm^{-1}, νN_2 gas = 2331 cm^{-1}) indicating that the N_2 in the trans complex is only weakly bound and is not strongly polarized. Although it has been proposed that N_2 probably cannot bind trans to a PR_3 group of high trans influence, because its σ-donor function is too weak [10], we have clearly established that such binding can be observed under the correct conditions even though the metal-nitrogen bond is considerably weaker than in the cis isomer.

Insertion of N_2 into the trans position is relatively

slow, and fast-scan techniques (ν = $100Vs^{-1}$ at 293K) show Os(II/III) couples for both the five-coordinate intermediate [3] and the trans N_2 adduct, (cf. MeCN insertion where no five-coordinate intermediate could be observed under any conditions tried).

Being so thermodynamically unstable, no attempt was made to try and isolate the trans-$[OsCl_2(PMe_2Ph)_3N_2]$ complex and its characterisation demonstrates the power of coupling electrochemistry with in-situ spectroscopic methods to elucidate the structure of otherwise intractable species.

Recently Armstrong and Walton [17] have described the electrochemistry of the related monomers mer-$[OsCl_3(PR_3)_3]$ (PR_3 = $PMePh_2$, $PEtPh_2$, PEt_2Ph, PEt_3, P^nPr_3 and P^nBu_3) in CH_2Cl_2. All of these complexes were reported to have a reversible (or near reversible) oxidation and an irreversible reduction similar to mer-$[OsCl_3(PMe_2Ph)_3]$ (Figure 4.1a). It was further noted, that following the reduction, an unidentified chemical product with a well defined electrochemistry, similar to that in Figure 4.1a, could be detected. Since all procedures were reported as being carried out under N_2, it is most probable that this unidentified product is in each case the trans-$[OsCl_2(PR_3)_3N_2]$ complex as outlined above.

In summary, for every L examined, the $[OsCl_2(PMe_2Ph)_3L]$ product formed initially by electroreduction is the trans isomer, (in accord with the trans effect), which converts to the thermodynamically stable cis isomer on standing or on heating. Chemical

reduction of mer-$[OsCl_3(PMe_2Ph)_3]$ and related systems generally does not offer this degree of control [10].

4.2.4 The Special Case of L = PMe_2Ph

If the electroreduction of mer-$[OsCl_3(PMe_2Ph)_3]$ is carried out in $CH_2Cl_2/[^nBu_4N][BF_4]$ to which an excess of free PMe_2Ph has been added, then as in all the other cases the red colour of the original compound is converted to bright yellow and a new compound can be identified by $^{31}P-\{^1H\}$ nmr spectroscopy and by voltammetry. This new compound was initially assumed to be the trans-$[OsCl_2(PMe_2Ph)_4]$ complex and thus the reaction was deemed to be consistent with the general pathway as shown in Scheme 1.

This assignment was reinforced by the separate experimental observations of the products of chemical reduction of mer-$[OsCl_3(PMe_2Ph)_3]$ in ethanol by zinc amalgam and direct reaction of $Na_2[OsCl_6]$ with PMe_2Ph, again in ethanolic solution, (see Experimental section). Both chemical reductions produced the same yellow solid, with spectroscopic and voltammetric properties indistinguishable from those of the yellow solution produced by electroreduction; namely a singlet at δ -52.5 ppm in the $^{31}P-\{^1H\}$ nmr spectrum at 298K, while cyclic voltammetry showed two reversible one electron oxidations at +0.28V and +1.54V vs. Ag/AgCl. This initially formed, electroreduced product, in common with most other trans-$[OsCl_2(PMe_2Ph)_3L]$ complexes, showed evidence of isomerisation over a period of a few hours at room

temperature to the well characterised cis derivative, showing a well defined A_2B_2 pattern $^{31}P-\{^1H\}$ nmr spectrum in $CDCl_3$. The cis isomer can also be independently prepared by a chemical method, (see Experimental section). Interestingly, in CD_2Cl_2 the $^{31}P-\{^1H\}$ nmr spectrum of the cis isomer exhibits only a singlet, which is ascribed to accidental degeneracy of the phosphorus resonances.

Perhaps the most intriguing aspect of this particular isomeric pair appears on examining their voltammetry and low temperature nmr spectra. Unlike the voltammetry of all the other $[OsCl_2(PMe_2Ph)_3L]$ complexes, where the redox potentials for both the cis and trans isomers are virtually superimposable, the redox couples for cis and trans-$[OsCl_2(PMe_2Ph)_4]$ are separated by more than 400mV. The first oxidation of the cis complex occurs at +0.75V vs. Ag/AgCl, ie. at a considerably more positive potential than that of its trans analogue.

Furthermore, the $^{31}P-\{^1H\}$ nmr signal of the trans isomer changes dramatically as the temperature is reduced (see Figure 4.6). At 193K the simple room temperature singlet at δ -52.5 ppm has become a sharp singlet at δ -50.0 ppm superimposed on a poorly defined complex pattern (ca. 1:3 intensity ratio). This process is reversible with temperature and is concentration independent. A variable temperature ^1H nmr study of the 'trans' complex shows only one set of signals in the methyl and phenyl regions at room temperature suggesting 4 magnetically equivalent phosphine ligands but as the temperature is lowered the spectrum becomes more

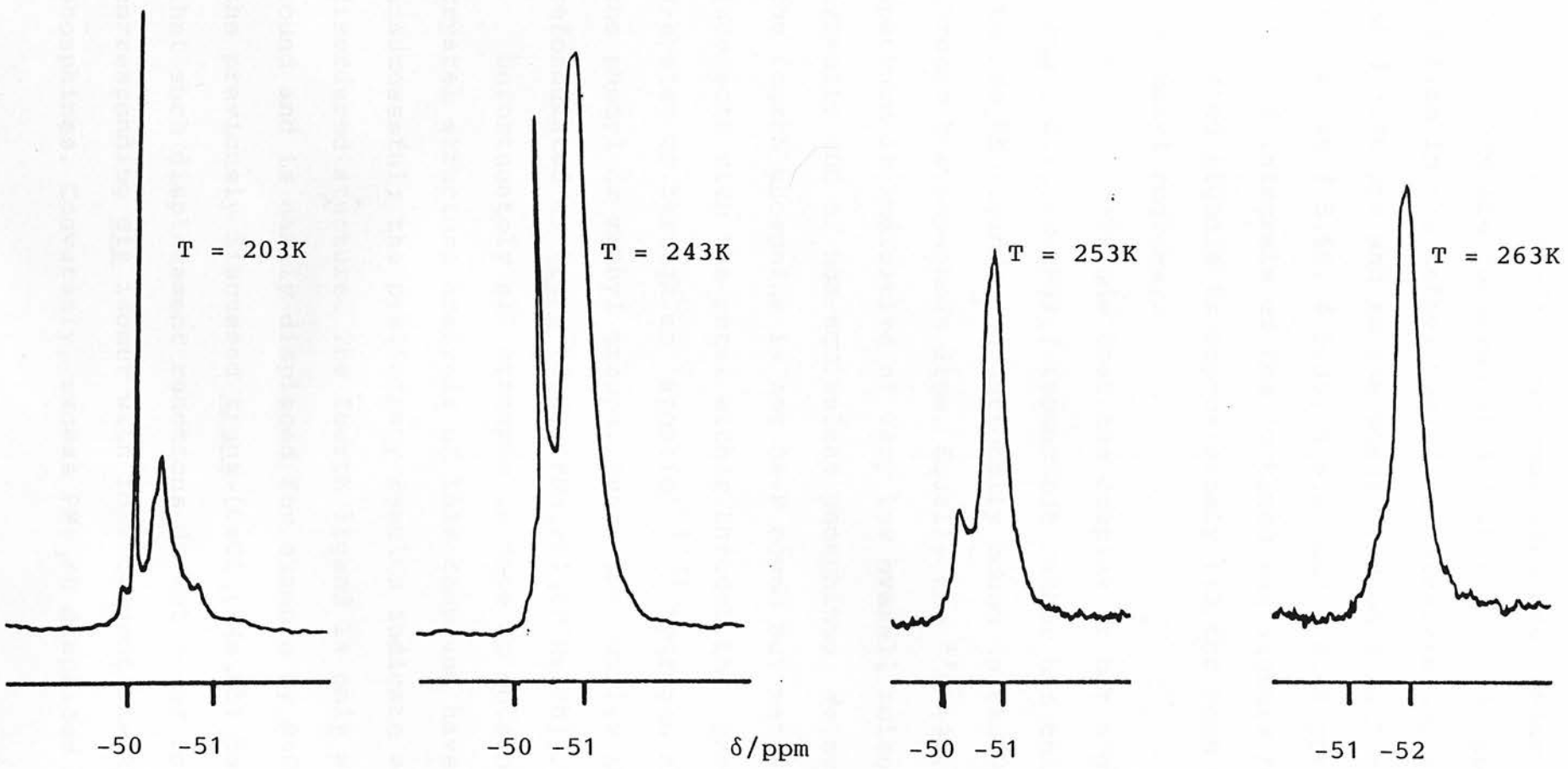

Figure 4.6 Variable Temperature $^{31}P\{^{1}H\}$ nmr Spectra of trans-$[OsCl_2(PMe_2Ph)_4]$ in CH_2Cl_2

complicated.

At 203K, signals whose positions are independent of temperature are observed at δ 1.60 and δ 7.37 ppm and in addition in the methyl region two singlets appear at δ0.68 and δ 1.90 ppm and in the phenyl region 4 multiplets centred at δ 5.65, δ 6.05, δ 6.65 and δ 8.46 ppm. The ratio of integrals of the combined new signals to the unshifted signals is approximately 1:3 for both the methyl and phenyl regions.

Thus we conclude that the complex is not a genuine trans-$[OsCl_2(PMe_2Ph)_4]$ isomer but rather has only three of its PMe_2Ph ligands conventionally bound to the Os centre through the phosphous atom. Equally the ^{13}C (90.2 MHz) nmr spectrum is indicative of very low overall molecular symmetry and of non-equivalent phosphines. We suggest that the fourth phosphine is not Os-P bound but rather interacts with the metal either through the phenyl ring π-system or through an 'agostic' [13] hydrogen atom from the phenyl or methyl groups. Hence the complex should be reformulated as trans $[OsCl_2(PMe_2Ph)_3(P'Me_2Ph)]$.

Unfortunately all attempts to date to obtain an X-ray crystal structure analysis of this compound have proved unsuccessful; the preliminary results indicate a highly disordered structure. The fourth ligand is only weakly bound and is easily displaced for example by MeCN, to give the previously discussed trans-$[OsCl_3(PMe_2Ph)_3MeCN]$. Note that such displacement reactions do not occur for the corresponding cis isomer with four conventionally bound phosphines. Conversely, excess PMe_2Ph displaces MeCN from

trans-$[OsCl_3(PMe_2Ph)_3MeCN]$ in CH_2Cl_2 yielding the pseudo trans isomer.

The failure to observe the true trans-$[MCl_2(PR_3)_4]$ isomer for trans-$[OsCl_2(PMe_2Ph)_4]$ is not restricted to this complex. Preliminary studies on trans-$[RuCl_2(PMe_2Ph)_4]$ also show similar $^{31}P-\{^1H\}$ and ^1H nmr behaviour. However genuine trans-$[MCl_2(PR_3)_4]$ complexes do exist; for example trans-$[OsCl_2(PMe_3)_4]$ shows a singlet $^{31}P-\{^1H\}$ nmr spectrum at all temperatures, consistent with its X-ray crystal structure [18] and thus the phenomenon must be intimately linked with the particular substituent groups on PMe_2Ph.

Table 4.1 Voltammetric and $^{31}P\{^{1}H\}$ n.m.r. Data for Various $[OsCl_2(PMe_2Ph)_3L]$ Complexes at 293K

Complex	Solvent	ν_A (ppm)	ν_B (ppm)	J_{AB}/Hz	OsII/OsIII	OsIII/OsIV (Where observed)
mer-$[OsCl_3(PMe_2Ph)_3]$	thf	-42.7	-45.1	12.2	-0.36	+1.20
trans-$[OsCl_2(PMe_2Ph)_3]$	¶thf	-44.8	-32.8	17.1	+0.03	+1.20
trans-$[OsCl_2(PMe\ Ph)_3MeCN]$	CH_2Cl	-47.7	-35.9	22.0	+0.25	+1.58
cis-$[OsCl_2(PMe_2Ph)_3MeCN]$	MeCN	-31.3	-31.9	20.6	+0.25	
trans-$[OsCl_2(PMe_2Ph)_3dmf]$	CH_2Cl	-47.5	-28.6	18.3	+0.02	+1.35
cis-$[OsCl_2(PMe_2Ph)_3dmf]$	dmf	-30.5	-31.3	15.0	+0.02	
trans-$[OsCl_2(PMe_2Ph)_3dmf]$*	CH_2Cl	-47.9	-36.2	22.0	+0.20	+1.50
trans-$[OsCl_2(PMe_2Ph)_3CO]$	CH_2Cl	-46.4	-43.5	30.1	+0.83	
trans-$[OsCl_2(PMe_2Ph)_3C_2H_4]$	CH_2Cl	-48.5	-39.1	15.9	+0.54	
cis-$[OsCl_2(PMe_2Ph)_3C_2H_4]$	CH_2Cl	-34.0	-30.9	18.3	+0.54	
trans-$[OsCl_2(PMe_2Ph)_3N_2]$	thf	-47.8	-37.3	22.0	+0.16	
cis-$[OsCl_2(PMe_2Ph)_3N_2]$	thf	-36.3	-34.9	15.1	--	
trans-$[OsCl_2(PMe_2Ph)_4]$	CH_2Cl	-52.5	--	--	+0.28	+1.54
cis-$[OsCl_2(PMe_2Ph)_4]$	CH_2Cl	-43.8	-44.9	13.4	+0.75	
$[Os_2Cl_4(PMe_2Ph)_6]$	¶CH_2Cl	-44.8	-40.0	17.1	+0.48	
$[Os_2Cl_3(PMe_2Ph)_6]$	CH_2Cl	-36.7	--	--	+1.09	+1.60

¶ Spectra measured at 203K

* N-bound dmf (see text)

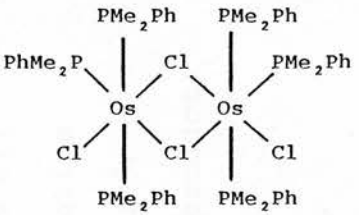

[4]

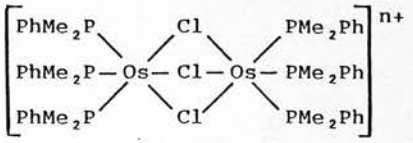

Scheme 4.1 Electroinduced Reactions of mer-$[OsCl_3(PMe_2Ph)_3]$

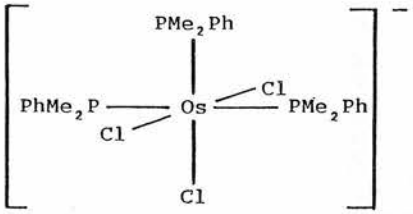

[2]

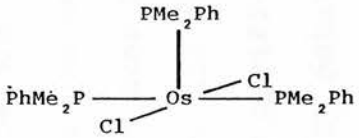

[3]

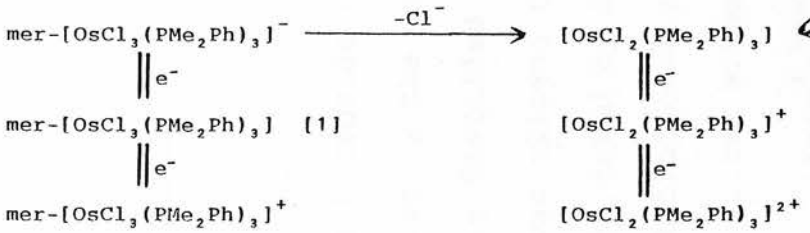

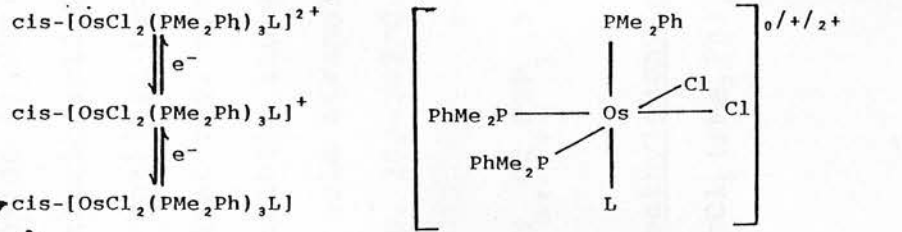

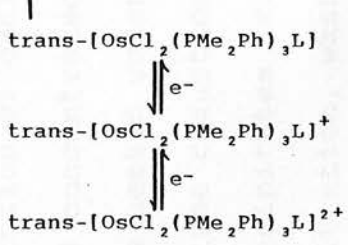

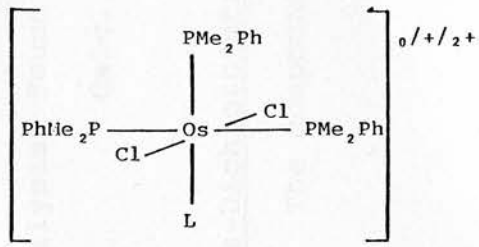

L = MeCN, dmf, N_2, C_2H_4, CO, PMe_2Ph (see text)

4.3 Experimental

Reagents

Osmium tetroxide (Johnson-Matthey plc). Acetonitrile was purified by the method of Walter and Ramaley [19] and was freshly distilled from P_2O_5 before use. Methylene chloride was allowed to stand for one week over KOH pellets and dried by distillation over P_2O_5. thf was dried by distillation over sodium wire. All other solvents were used as supplied without further purification. $[R_3MeN][BF_4]$ ($R = C_{8-10}\ H_{17-21}$) was prepared by metathesis of 'Adogen 464' ($[R_3MeN]Cl$) (Aldrich Chemicals) with $Na[BF_4]$ in MeCN. $Na_2[OsCl_6]$ was prepared by standard methods [20].

mer-Trichlorotris(dimethylphenylphosphine)osmium(III)

This was prepared by the literature method of Leigh et al. [2]. Dimethylphenylphosphine (3.00g) was added to a solution of osmium tetroxide (1.00g) in ethanol (50 ml) and concentrated hydrochloric acid (2 ml). The solution was heated under reflux until it became bright red. On volume reduction the bright red, microcrystalline product precipitates from the solution and was removed by filtration, washed with cold ethanol and air dried. [Yield 2.38g (85%)]. m.p. 200-202°C (decomp.)

Analysis: Found : C 40.8; H 4.6%

Calc. for $C_{24}H_{33}Cl_3OsP_3$: C 40.6; H 4.6%

cis-Dichlorotetrakis(dimethylphenylphosphine)osmium(II)

The compound mer-$[OsCl_3(PMe_2Ph)_3]$ (0.57g) and PMe_2Ph

(0.5ml) were refluxed in degassed 2-methoxyethanol (40ml) for 30 minutes until the red colour had completely changed to a golden yellow. On reduction of the volume and the addition of acetone, when cooled the pale cream product precipitates from the solution. This was removed by filtration, washed well with acetone and diethyl-ether and dried in vacuo [Yield 0.51g (60%)].

Analysis: Found : C 47.3; H 5.2%

Calc. for $C_{32}H_{44}Cl_2OsP_4$: C 47.2; H 5.4%

trans-Dichlorotetrakis(dimethylphenylphosphine)osmium(II)

The trans complex was prepared by a variant of the method of Bell et al [21]. Mer-$[OsCl_3(PMe_2Ph)_3]$ (2.20g), PMe_2Ph (0.90g) and Zn/Hg amalgam (3.2g) were shaken in thf (40ml) for 90 minutes. The yellow solution produced was filtered through celite and reduced in volume to ca. 8 ml whereupon degassed ethanol (20ml) was added and the solution cooled to 0°C. On standing the product precipitates from the solution as a yellow microcrystalline solid which was removed by filtration, washed with diethyl-ether and dried in vacuo [Yield: 2.02g (80%)].

Analysis: Found : C 46.7; H 5.4%

Calc. for $C_{32}H_{44}Cl_2OsP_4$: C 47.2; H 5.4%

Electrochemical preparations of trans-$[OsCl_2(PMe_2Ph)_3S]$ (S = MeCN or dmf)

These were prepared by a variation of the method of R.A.C. Zarate [11]. A solution containing

mer-$[OsCl_3(PMe_2Ph)_3]$ (0.10g) and 0.50M $[^nBu_4N][BF_4]$ in the appropriate solvent (5ml) was electroreduced at -0.60V vs. Ag/AgCl until the current decayed to <1% of its initial value. The products which precipitated were filtered off under nitrogen, well washed with diethyl-ether, then dried and stored in vacuo.

S = MeCN

[Yield: 0.07g (70%)].

Analysis: Found : C 42.4; H 5.0; N 1.9%

Calc. for $C_{26}H_{36}Cl_2NOsP_3$: C 43.5; H 5.0; N 1.9%

S = dmf

[Yield: 0.06g (57%)].

Analysis: Found : C 43.3; H 5.3; N 1.8%

Calc. for $C_{27}H_{40}Cl\ NOOsP_3$: C 42.9; H 5.3; N 1.9%

Tri-μ-chloro-hexakis(dimethylphenylphosphine) diosmium(II/II) chloride

The compound cis-$[OsCl_2(PMe_2Ph)_4]$ (0.14g) was heated under reflux in degassed iso-butanol (30ml) for 24 hours. On volume reduction and cooling, the pale yellow product precipitates as the chloride salt. [Yield: 0.095g (85%)].

Analysis: Found : C 42.8; H 4.8%

Calc. for $C_{48}H_{66}Cl_4Os_2P_6$: C 42.7; H 4.8%

Tri-μ-chloro-hexakis(dimethylphenylphosphine) diosmium(II/II) tetraphenylborate

This complex can also be precipitated from solution (prepared as for the chloride salt) in quantitative yield by the addition of a stoichiometric quantity of $Na[BPh_4]$

Analysis: Found : C 52.7; H 5.4%

Calc. for $C_{90}H_{86}BCl_3Os_2P_6$: C 52.9; H 5.3%

Chapter 4 References

1. J. Chatt and R.G Hayter, J.Chem.Soc.Dalton.Trans.,1961, 896.
2. J. Chatt, G.J. Leigh, D.M.P.Mingos and R.J. Paske, J.Chem.Soc.Dalton.Trans., 1968, 2636.
3. D.J. Salomon and R.A. Walton, Inorg.Chem., 1978, 17, 2379.
4. H. van Bekkum and O van Rantwijk, J.Coord.Chem., 1974, 4, 7.
5. K.G. Caulton and P.R. Hoffman, J.Am.Chem.Soc., 1975, 97, 4221.
6. T. Arthur, Ph.D. Thesis, University of Edinburgh, 1980.
7. J.A.S. Duncan, Ph.D. Thesis, University of Edinburgh, 1983.
8. Yu.G. Borodko, V.S. Bukreev, M.L. Khidekel, G.J. Kozub and A.E. Shilov, Zur.Strukt.Khim., 1967, 8, 542.
9. J. Chatt, G.J. Leigh and R.L. Richards, J.Chem.Soc., A, 1970, 2243.
10. J. Chatt, D.P. Melville and R.L. Richards, J.Chem. Soc., A, 1971, 1169.
11. R.A. Contreras-Zarate, Ph.D. University of Edinburgh, 1981.
12. J.A. Ibers and S.J. La Placa, Inorg.Chem., 1965, 4, 778.
13. M. Brookhart and M.L.H. Green, J.Organometal.Chem., 1983, 250, 395.
14. K.G. Caulton, M.A. Green and J.C. Huffman, J.Organometal.Chem., 1983, 243, C78.
15. R.S. Nicholson and I. Shain, Anal.Chem., 1964, 36, 706.

16. S. Donovan-Mtunzi, J. Mason and R.L.Richards, J.Chem.Soc., A, 1984, 469.

17. J.E. Armstrong and R.A. Walton, Inorg.Chem., 1983, 22, 1545.

18. A.S. Alves, R.A. Anderson, D.S. Moore and G. Wilkinson, Polyhedron, 1982, 1, 83.

19. L. Ramaley and M. Walter, Anal.Chem., 1973, 45, 165.

20. 'Handbook of Preparative Inorganic Chemistry' Vol. II, 2nd Edition, Academic Press. 1965.

21. B. Bell, J. Chatt and G.J. Leigh, J.Chem.Soc.Dalton.Trans., 1973, 997.

APPENDIX 1

Electrochemical Generation, and Characterisation of the Low-Spin Ruthenium (III) Nitrosyl Complex $[RuCl_5NO]^-$

A.1.1 Introduction

The formation of nitric oxide complexes is a marked feature of ruthenium chemistry and they are more numerous than for any other element. Any ruthenium compound that has been in contact with NO, NO_2 or HNO_3 must be suspected of containing an NO moiety, and their ease of formation led to the first simple halo-nitrosyl complex of ruthenium, $K_2[RuCl_5NO]$ being reported as long ago as 1888[1]

Much of the chemistry of ruthenium nitrosyl complexes is concerned with ligand substitution processes which leave the RuNO moiety intact, although a very important body of reactions modifying the coordinated NO ligand also exists [2]. The RuNO group is found in cationic and neutral complexes, as well as anionic ones, and bears an effective overall charge of +3; generally the most realistic assignment of metal oxidation state is Ru(II), associated with NO^+, (isoelectronic with CO). Ruthenium (II) nitrosyl compounds are identified by characteristically strong infrared absorptions with νNO between 1930 and 1830 cm^{-1}. The Ru(II)NO moiety exhibits extensive π-backbonding and thus the Ru(II) centre is uniquely favoured in these types of complexes.

However, it was recently reported [3] that the first example of a ruthenium (III) nitrosyl complex $NH_4[RuCl_5NO]$, [1] could be isolated as one of the products arising from reaction of $RuCl_3.xH_2O$ with NOCl in the presence of an excess of PPh_3. Magnetic measurements on this pink compound [1] were reported to give a magnetic

moment of 5.86 BM per ruthenium indicating a high spin d5 (t_2g3 eg2) configuration. The esr spectrum was consistent with a high spin configuration of [1] and indeed showed isotropic coupling to ^{101}Ru. Because this was the first report of a ruthenium (III) nitrosyl or indeed of any high spin ruthenium (III) system, and because the corresponding isoelectronic $[RuCl_5CO]^{2-}$ ion was well known to contain the expected low spin ruthenium (III) centre, we decided to investigate the properties of this novel complex.

A.1.2 Results and Discussion

In our hands all efforts to duplicate the results of Pandey et al [3] proved unsuccessful. Thus, shaking a solution of $RuCl_3.xH_2O$ and PPh_3 (1:8 molar ratio) with NOCl (1 atm) in CH_2Cl_2-EtOH resulted in the precipitation of an orange-brown solid which was found to be water-soluble. The infrared spectrum of the solid showed the presence of NH_4^+ ion, (apparently by reduction of NO^+), and no PPh_3; however esr and magnetic susceptibility studies indicated that only traces of paramagnetic material were present, and no evidence for the Ru(III) monoanion was found. Extensive variation of the reaction conditions at ambient temperature produced similar results, whereas under reflux conditions, the only product isolated was the well-known $[Ru(II)(NO)Cl_3(PPh_3)_2]$ [4].

In these circumstances it was decided to attempt a more logical preparation of $[RuCl_5NO]^-$, by direct

oxidation of the readily accessible $[RuCl_5NO]^{2-}$ anion [5]. Accordingly the well known salt $K_2[RuCl_5NO]$ was prepared but proved very poorly soluble in the non-aqueous solvents suited to electrosynthetic oxidation procedures. However metathesis of $K_2[RuCl_5NO]$ with $[Ph_3PhCH_2P]Cl$, $[^{n}Bu_4N]Cl$ or $[Ph_4As]Cl$ produce salts which are soluble in numerous organic solvents, allowing for the first time, survey and thorough fundamental study of its electrochemical behaviour.

The cyclic voltammetry (CV), linear a.c. voltammetry (acV) and stirred voltammetry (SV) of $[Ph_3PhCH_2P]_2[RuCl_5NO]$ are shown in Figure A1.1. Regardless of counter-cation the $[RuCl_5NO]^{2-}$ complex exhibits one, very well-defined redox process within the available voltammetric range, *i.e.* a one-electron oxidation at a fairly extreme positive potential of 1.48V *vs.* Ag/AgCl. This oxidation is fully chemically reversible(*vide infra*)but shows sluggish charge-transfer kinetics, (*i.e.* at 298K ip(anodic)/ip(cathodic) = 1 at all scan rates (ν) from 50 to 500 mVs^{-1} but the peak to peak separation Ep = 100mV at ν = 50 mVs^{-1} and 120 mV at ν = 200 mVs^{-1}). The one-electron nature of the process is indicated by the acV peak width at half height, (100 mV, independent of ω in the range 20 - 600 Hz), the charateristic diffusion coefficient, ($D = 5.0 \times 10^{-6}$ cm^2s^{-1} at 293K), [6] and was ultimately confirmed by coulometry.

Coulometric measurements at 223K on controlled potential electrogeneration of $[Ph_3PhCH_2P]_2[RuCl_5NO]$ at +1.80V *vs.* Ag/AgCl in CH_2Cl_2/0.5M $[^{n}Bu_4N][BF_4]$ show the

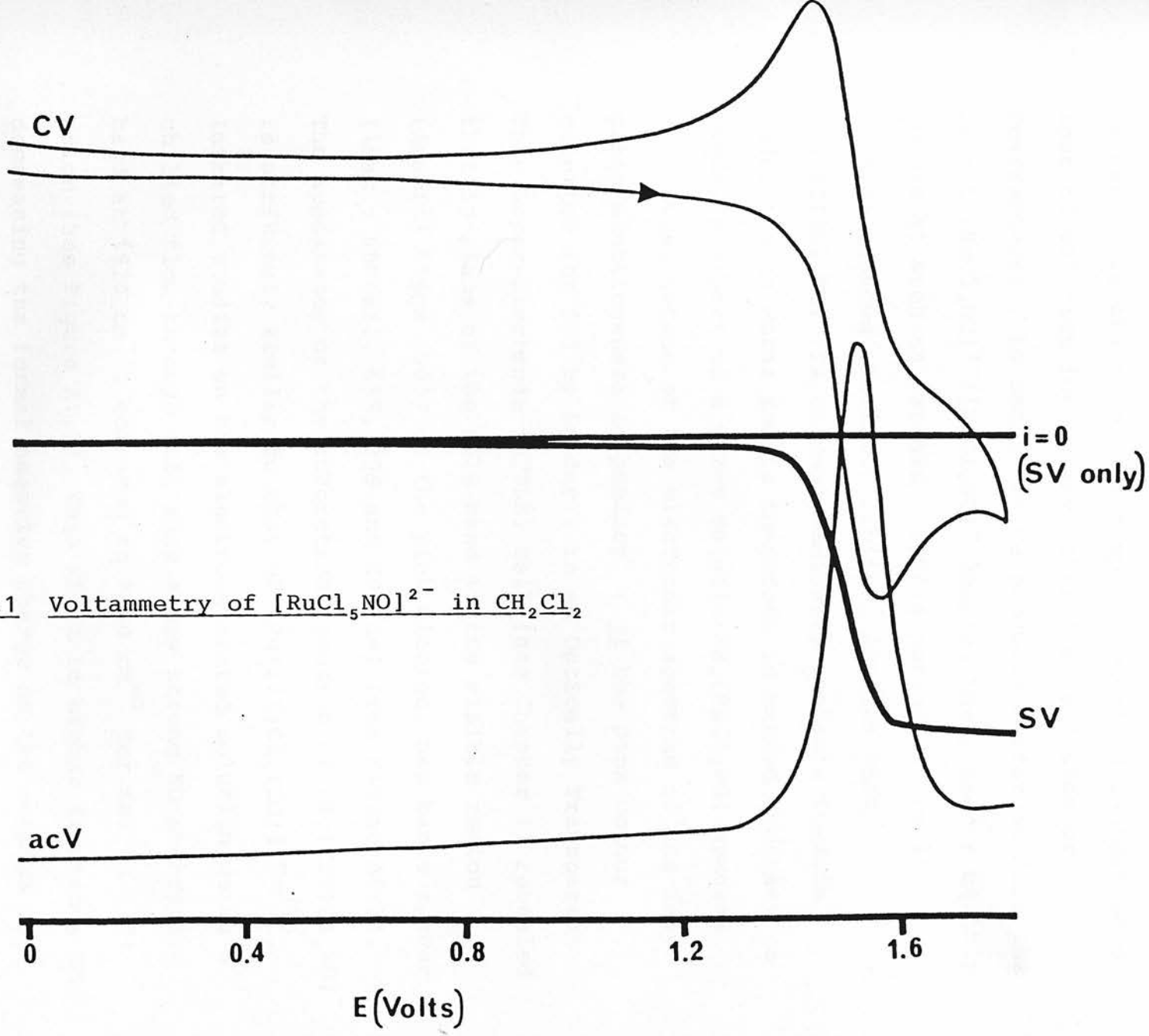

Figure A1.1 Voltammetry of $[RuCl_5NO]^{2-}$ in CH_2Cl_2

expected exponential decay of current and the loss of 1.0 electron per molecule of $[RuCl_5NO]^{2-}$. During bulk oxidation in the cold, the complex showed no indication of loss of chloride ion or any other fragmentation or rearrangement, to redox-active products different from the parent $[RuCl_5NO]^{2-}/[RuCl_5NO]^{-}$ couple. The presence of this couple at such an extreme positive potential, (well outside aqueous stability limits), implies that $[Ru(III)Cl_5NO]^{-}$ is thermodynamically unstable towards reduction by water and is therefore in marked contrast to Pandey's report of a water soluble $NH_4[RuCl_5NO]$ species.

Investigation of the electronic spectrum of the deep green electrogenerated product, (cf the pink colour reported for [1] by Pandey), in an Optically Transparent Thin-Layer-Electrode (OTTLE) cell (see Chapter 1) revealed that in place of the sole band in the visible region ($\lambda max(\varepsilon)$ 514nm (50)) of the pink dianion, new bands appear (λmax : 690(sh), 655, 398 and 294 nm) (see Figure A1.2). The appearance of the absorption spectrum of $[Ru(III)Cl_5NO]^{-}$ is strikingly similar to that of $[Ru(III)Cl_5(CO)]^{2-}$ [7]. Infrared studies on the electrogenerated solution using a chilled flow-through cell show a new strong NO absorption band at 1920 cm^{-1}, compared to 1850 cm^{-1} for the Ru (II) anion (See Figure A1.3). This shift to higher frequency on decreasing the formal negative charge on the complex is compatible with the behaviour observed in the related metal carbonyl compounds. As the d-π backbonding from the metal to the π-acceptor CO ligand decreases, so the M-C bond weakens, which in turn increases the bond order of

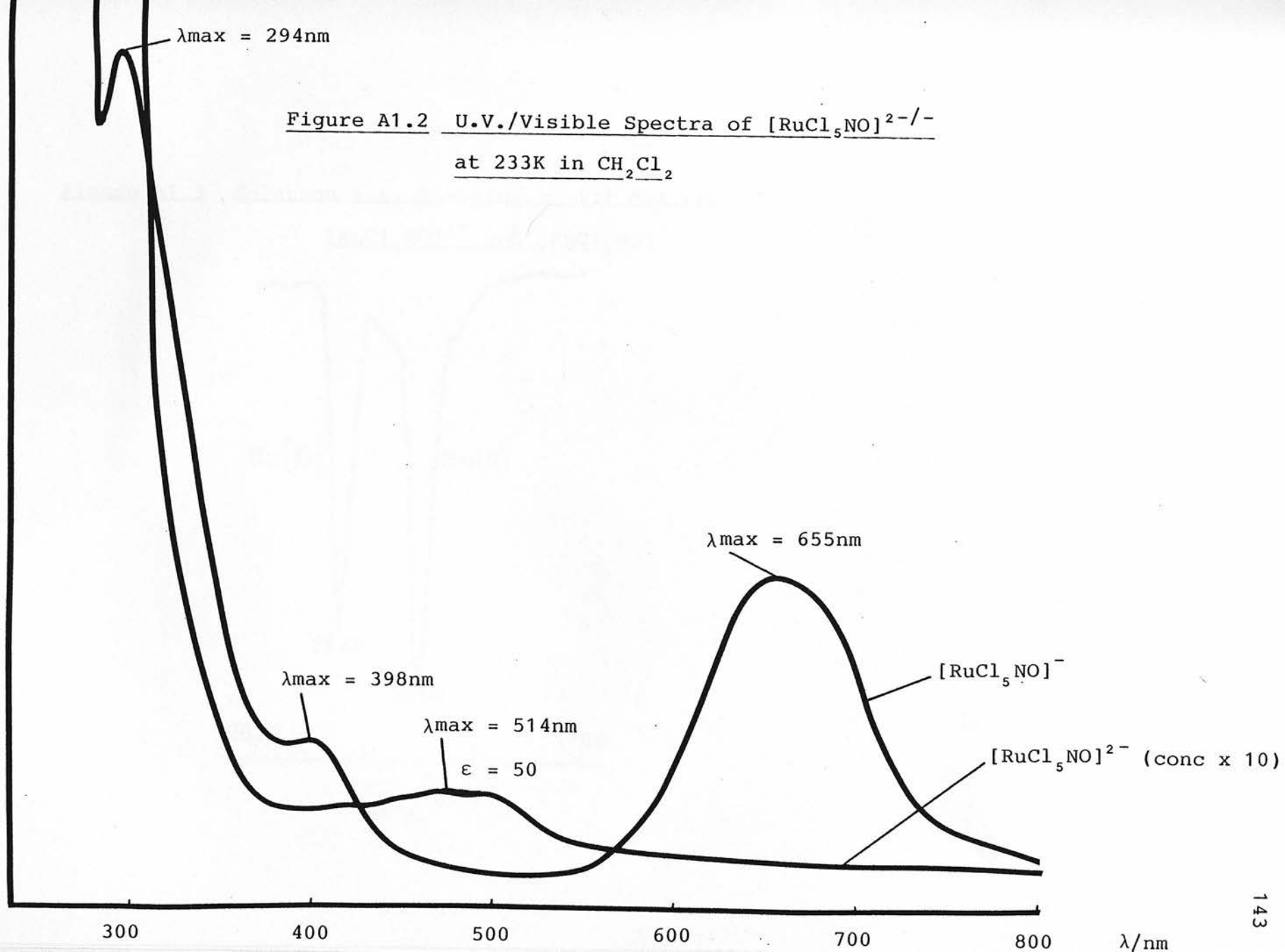

Figure A1.2 U.V./Visible Spectra of $[RuCl_5NO]^{2-/-}$ at 233K in CH_2Cl_2

Figure A1.3 Solution i.r. Spectrum of 1:1 Mixture of $[RuCl_5NO]^{2-}$ and $[RuCl_5NO]^{-}$

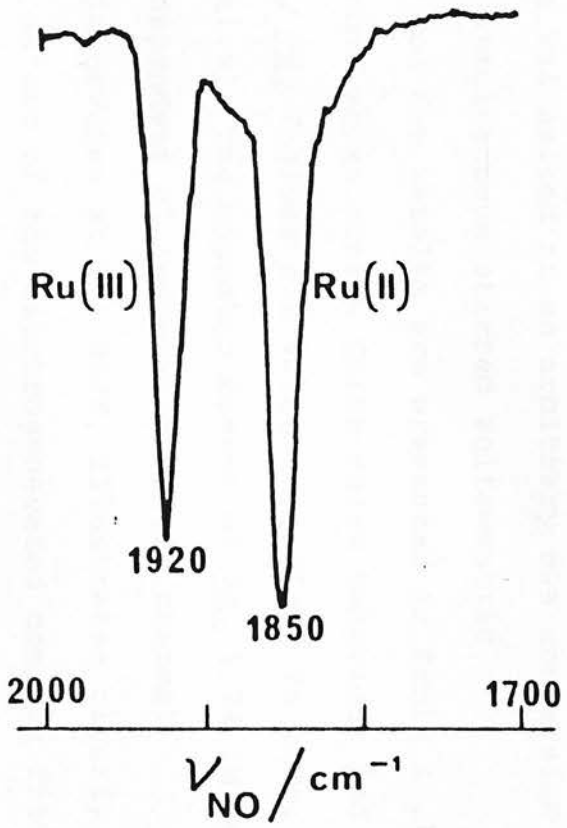

the C-O linkage, causing a rise in the corresponding infrared vibrational frequency. For the first time an exactly analogous process can be shown to occur for the NO^+ moiety.

The esr spectrum, (see Figure A1.4), is similar to those of many low spin ruthenium complexes [8,9] showing no sign of the hyperfine splitting previously reported for Pandey's pink compound. This indicates that the esr spectrum reported for [1] may in fact be due to an impurity such as Mn^{2+} ion.

Magnetic measurements were carried out using the Evans' method, [10] (see Appendix 3), on a chilled sample of the electrogenerated solution. The electrogeneration of the monoanion was halted at an arbitrary 80% conversion as monitored by simultaneous stirred voltammetric measurements and the results are presented in Table A1.1.

The compound shows strict Curie-Weiss behaviour and a plot of $1/\chi_m$, *vs.* T gives a θ value very close to zero, (see Figure A1.5). The magnetic moment of *ca.* 1.74 BM per molecule, independent of temperature until thermal degradation intervenes at T > 260K, illustrates clearly the low-spin nature of the electrogenerated complex This value compares well with the reported magnetic moment of the analogous $K_2[RuCl_5CO]H_2O$ complex (1.87 BM/molecule at 296K) [11]. Deviation from Curie-Weiss behaviour above 260K reveals that the paramagnetic monoanion reverts back to the diamagnetic dianion, as demonstrated independently by relaxation of the electronic and ir spectra and by successive stirred voltammograms.

Figure A1.4 E.s.r. Spectrum of $[RuCl_5NO]^-$ at 153K

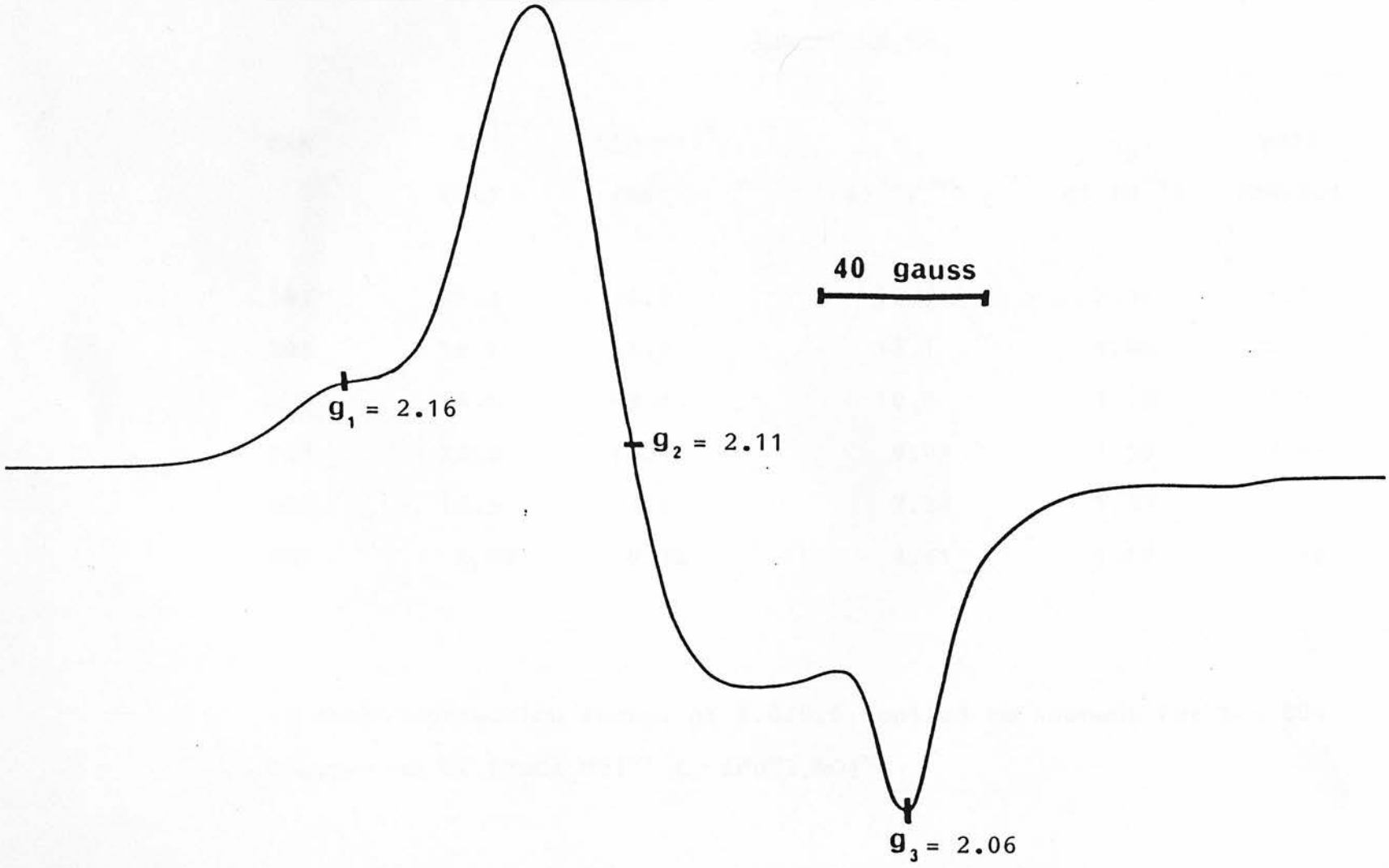

Table A1.1

Variable Temperature Evans' Magnetic Measurements on the $[RuCl_5NO]^-$ Ion in CH_2Cl_2

T/K	Δf (Hz)	Δf(corr)§ (Hz)	χ_g ($\div 10^{-6}$)	$\chi_{m'}$ ($\div 10^{-3}$)	μeff (BM/Ru)
183	21.2	26.5	13.8	2.03	1.73
203	18.2	22.7	12.1	1.86	1.74
223	15.5	19.4	10.5	1.70	1.75
243	13.2	16.4	9.09	1.55	1.74
263	10.5	13.1	7.34	1.37	1.71
283	6.69	8.36	4.61	1.10	1.58

(§ Note: correction factor of 1.0/0.8 applied to account for the 80% conversion of $[RuCl_5NO]^{2-}$ to $[RuCl_5NO]^-$)

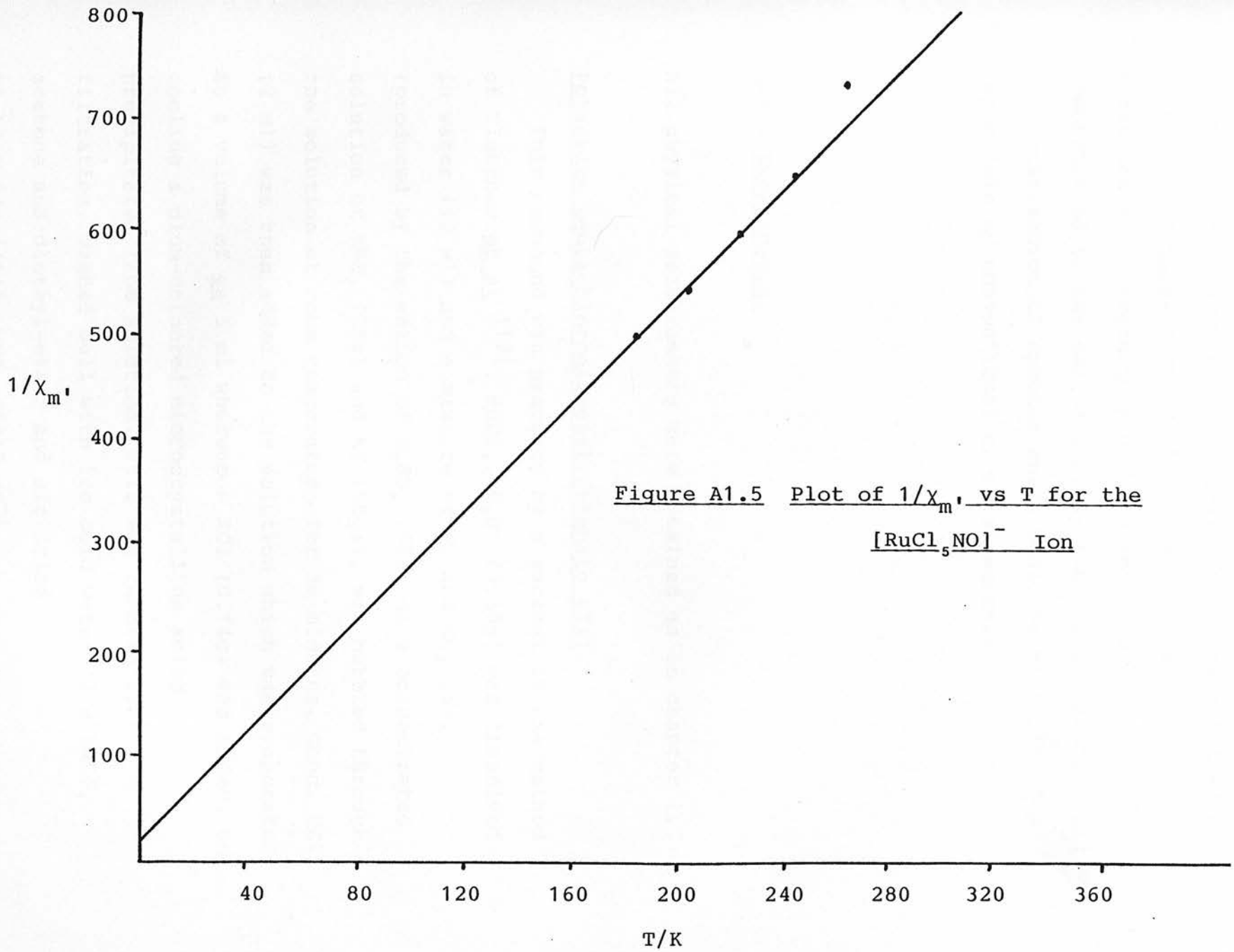

Figure A1.5 Plot of $1/\chi_m$' vs T for the $[RuCl_5NO]^-$ Ion

Thus there are serious discrepancies between the properties we deduce for $[RuCl_5NO]^-$ and those ascribed to it by Pandey et al however, the power of the electrochemical techniques we have employed are demonstrated by the generation, synthesis, observation and characterisation of species which would be virtually impossible by conventional chemical means.

A.1.3 Experimental

All physical measurements were obtained as in chapter 1.

Potassium pentachloronitrosylruthenate (II)

This compound was prepared by a variant if the method of Fletcher et al [12]. $RuCl_3.xH_2O$ (0.50g) was dissolved in water (10 ml) and a mixture of NO and NO_2 gas, (produced by the action of H_2SO_4 (50%) on a concentrated solution of KNO_2 (30g) and KI (15g)), was bubbled through the solution at room temperature for 30 minutes. Conc. HCl (2 ml) was then added to the solution which was evaporated to a volume of ca 5 ml whereupon KCl (0.14g) was added. On cooling a plum-coloured microcrystalline solid precipitated from solution. This was removed by filtration, washed well with ice cold water (2 x 5ml), acetone and diethyl-ether and air dried.

Yield 0.34g (41%) $\nu NO = 1915\ cm^{-1}$

Treatment of this potassium salt with a concentrated aqueous solution of triphenylbenzylphosphonium chloride produces the organic soluble, mauve coloured $[Ph_3PhCH_2P]_2$ $[RuCl_5NO]$ compound in quantitative yield.

Found: C 59.1; H4.3; N 1.4%

Calc. for $C_{50}H_{44}Cl_5NOP_2Ru$: C 59.1; H4.3; N 1.4%

νNO = 1836 cm^{-1}

Appendix 1 References

1. Joly, Compt.rend., 1888, 107, 994.
2. B.F.G. Johnson and J.A. McCleverty, Progr.Inorg Chem., 1966, 7, 277.
3. S.R. Ahuja, S. Bharti, K.K. Pandey and N.S. Poonia, J.Chem.Soc.Chem.Comm., 1982, 1268.
4. S.D. Robinson and M.F. Uttley, J.Chem.Soc.Dalton.Trans., 1972, 1.
5. W.M. Campbell jr., E.E. Mercer and R.M. Wallace, Inorg.Chem., 1964, 3, 1018.
6. A.J. Bard and L.R. Faulkner "Electrochemical Methods" John Wiley & Sons Inc. (New York) 1980 pp 153.
7. J. Halpern, B.R. James and A.L.W. Kemp, J.Am.Chem.Soc., 1966, 88, 5142.
8. B.G. Jeliazkowa and J.B. Raynor, J.Chem.Soc.Dalton.Trans., 1982, 1185.
9. R.E. DeSimone, J.Am.Chem.Soc., 1973, 95, 6238.
10. D.F. Evans, J.Chem.Soc. 1959, 2003.
11. J.E.Fergusson and A.M. Greenaway, Aust.J.Chem. 1978, 31, 497.
12. J.M. Fletcher, I.L. Jenkins, F.M. Lever, F.S. Martin, A.R. Powell and R. Todd, J.Inorg.Nucl.Chem., 1955, 1, 378.

APPENDIX 2

Redox Studies on Binuclear Osmium Carboxylate Complexes

A.2.1 Introduction

Although diruthenium carboxylate complexes have been known and studied extensively for some considerable time [1] it is only comparatively recently that the corresponding osmium systems have been synthesised and investigated [2,3,4].

If $RuCl_3.xH_2O$ is heated with carboxylic acid/acid anhydride mixtures for several hours under a stream of oxygen, ruthenium carboxylate complexes with a general formulation $[Ru_2(OCOR)_4Cl]$, (R = Me, Et, ^{n}Pr) are produced [1] the two ruthenium atoms having formal oxidation states of 2 and 3. At the time of their discovery, it was found that these complexes had surprisingly high magnetic moments of between 4.0 and 4.6 BM per molecule, quite incommensurate with the presence of only one unpaired electron per diruthenium unit. These findings were interpreted by Norman and co-workers [5] by invoking a ground state configuration of $\sigma 2\pi 4\delta 2\pi^* 2\delta^* 1$ (vide infra). The X-ray crystal structure of the tetra-n-butyrate complex also indicated a very short Ru-Ru bond distance in the molecule [6] of 2.281A, (closest approach in ruthenium metal is 2.65A), indicating a fairly extensive interaction between the ruthenium atoms. This is in keeping with what might be expected by comparison with other, analogous, compounds such as $[Mo_2(OCOR)_4]$ where a very strong quadruple bond is believed to exist [7] or $[Rh_2(OCOR)_4(H_2O)_2]$ which has a metal-metal bond order of only 1 [8,9,10].

An electrochemical study [11] of the $[Ru_2(OCO^nPr)_4Cl]$ complex in CH_2Cl_2 revealed two poorly defined reduction

waves at 0.00V and -0.34V *vs.* sce. The wave at 0.00V collapses on addition of excess Cl^-, and the scheme shown below has been proposed to account for these observations.

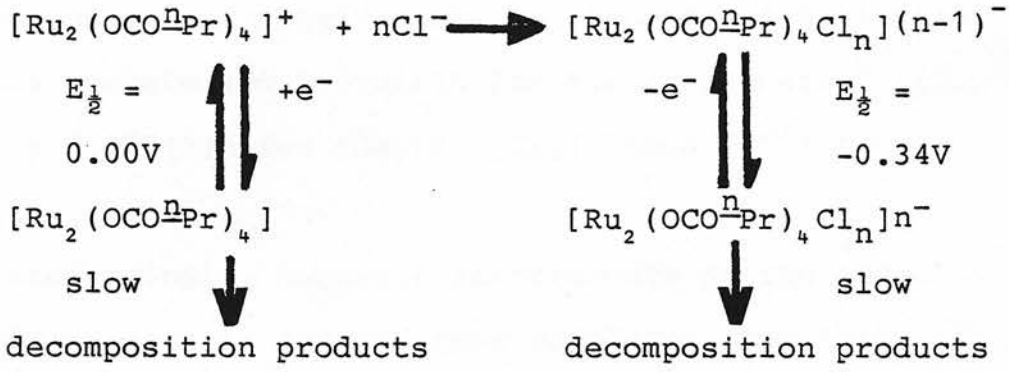

In view of this data and the discovery of synthetic routes to related osmium compounds *i.e.* $[Os_2(OCOR)_4Cl_2]$ [3] and $[Os_2(hp)_4Cl_2]$ [12] it was decided to investigate the redox-properties of the osmium compounds in more detail.

A.2.2 Results and Discussion

In 1981 Wilkinson and co-workers [2] found that the interaction of solutions of the $[OsCl_6]^{2-}$ ion with an acetic acid/acid anhydride mixture, plus HCl, at elevated temperatures produced the complex $[Os_2(OCOMe)_4Cl_2]$. In 1983, after improvements in the preparative method, [3] it was shown that the complex was a useful starting point for a number of exchange reactions. For example the homologues $[Os_2(OCOR)_4Cl_2]$ (R = Et, ^{n}Pr) were prepared by reaction of $[Os_2(OCOMe)_4Cl_2]$ with the appropriate carboxylic acid, and the hydroxypyridinato complex, $[Os_2(hp)_4Cl_2]$, by reaction with 2-hydroxypyridine. The X-ray diffraction data of the

butyrate complex [3] showed a short Os-Os distance of 2.301(1)A indicating, as expected, significant metal-metal interaction. The more recent X-ray data [13] for the acetate and propionate complexes concurs with this indication giving metal-metal bond lengths of 2.314(1)A for the acetate and 2.316(2)A for the propionate (cf Os-Os = 2.357(1)A for $[Os_2(hp)_4Cl_2].2MeCN$ [12]) (vide infra).

Interestingly, magnetic measurements on the more soluble propionate and butyrate complexes show that, unlike most comparable binuclear transition-metal carboxylates, both compounds are paramagnetic, although the small magnitude of μeff (e.g. 1.15 BM per Os at ca. 300K for R = ^{n}Pr) and the decrease in the value with decreasing temperature indicates that there is considerable antiferromagnetic interaction between the two Os(III) ions [3]

Of particular interest in our laboratory was the redox activity of these osmium systems. Initial electrochemical studies indicated that for the two complexes soluble enough for measurement, i.e. the propionate and butyrate compounds, each exhibited a facile one-electron reduction, at +0.52V and +0.48V (vs Ag/AgCl), respectively [4] . (N.B. These were initially thought to be one electron oxidations [3] but this conclusion has now been shown to be incorrect [4,14]). Each process was reversible with ip anodic/ip cathodic = 1 and a constant $ip/\nu^{1/2}$ ratio between the values of ν= 50-400 mVs^{-1} in accord with diffusion control. In addition, at room temperature the

propionate exhibits irreversible oxidation (+1.84V) and reduction (-1.37V) waves and the butyrate shows similar peaks at +1.79V and -1.05V.

Consistent with the interpretation that the redox process for each complex at ca. +0.50V corresponds to a one-electron reduction, controlled-potential electrolysis of the solution at 0.00V vs. Ag/AgCl produces a solution containing the monoanion $[Os_2(OCOR)_4Cl_2]^-$ (R = Et, ^nPr) which appears to be quite stable at room temperature.

Parallel investigations by Walton and co-workers [4] using chemical means indicate that cobaltocene is a good reductant in these circumstances. Treatment of a solution of either the propionate or the butyrate complexes in acetone with cobaltocene yields, after 30 minutes, an olive-green precipitate of $[Co(C_5H_5)_2][Os_2(OCOR)_4Cl_2]$. They likewise find that $[Os_2(hp)_4Cl_2]$ (hp = 2-hydroxypyridine), (a close electronic analogue of the osmium carboxylates, first discovered by Cotton and Thompson [12] and later made by substitution of $[Os_2(OCOMe)_4Cl_2]$ with 2-hydroxypyridine [3]) can be reduced chemically to the monoanion $[Co(C_5H_5)_2][Os_2(hp)_4Cl_2]$.

Since binuclear compounds containing the multiply bonded $(Os_2)^{6+}$ core and the previously unknown $(Os_2)^{5+}$ core were thus identified, a valuable opportunity existed for investigating the effect on bonding of altering the core charge. This study was undertaken using magnetic measurements on the electrogenerated solutions in the Edinburgh laboratory.

In the case of the ruthenium carboxylate compounds,

experimental [6] and theoretical [5] work has indicated that the π^* and δ^* energy levels are close, in energy terms, and that the ground state configuration of the $[Ru_2(OCOR)_4Cl]$ class of compounds should be assigned as $\sigma 2\pi 4\delta 2\pi^* 2\delta^* 1$ (thus giving rise to the experimentally observed, three unpaired electrons). Nonetheless other multiply bonded $(Ru_2)^{5+}$ compounds such as $[Ru_2L_2]^+$ where L = dibenzotetraza[14]annulene [6] exhibit ground states with $\pi^*$and δ^* orbital energy levels reversed i.e. $\sigma 2\pi 4\delta 2\delta^* 2\pi^* 1$.

In the case of the osmium carboxylates the situation is more complex. The neutral complexes $[Os_2(OCOR)_4Cl_2]$ and $[Os_2(hp)_4Cl_2]$ exhibit μeff values between 1.4 and 1.6 BM per molecule at room temperature indicating a ground state configuration with no unpaired electrons i.e. $\sigma 2\pi 4\delta 2\delta^* 2$ but with an appreciable contribution from the exited state with two unpaired elecrons, i.e. $\sigma 2\pi 4\delta 2\delta^* 1\pi^* 1$ or $\sigma 2\pi 4\delta 2\pi^* 2$

When the carboxylate complexes are reduced to their respective Os_2(II/III) monoanions, their magnetic moments increase (as measured by the Evans' method [15] (see Appendix 3)). Our results for both the butyrate complex, (μeff per molecule = 2.47 BM at 275K rising to 2.88 BM at 215K) and the propionate complex, (μeff per molecule = 2.65 BM at 240K rising to 2.85 BM at 190K) agree well with those of Walton and coworkers carrying out similar measurements using the same technique on their cobaltocene reduced derivatives (2.73 BM at 298K to 2.84 BM at 209K for R = ^{n}Pr).

This magnetic behaviour can be explained in terms of

the population of $\sigma 2\pi 4\delta 2\delta^{*}1\pi^{*}2$ (i.e. three unpaired electrons) and $\sigma 2\pi 4\delta 2\delta^{*}2\pi^{*}1$ or $\sigma 2\pi 4\delta 2\pi^{*}3$ (i.e. one unpaired electron) configurations, at room temperature, with a possible increase in the population of the spin-quartet state as the temperature is lowered. The overall depression of moments compared to those of the isoelectronic $[Ru_2(OCOR)_4Cl]$ complex (ca. 4.0 BM per molecule at 300K, temperature invariant to 60K) suggests that the spin-doublet state ($\sigma 2\pi 4\delta 2\pi^{*}3$ or $\sigma 2\pi 4\delta 2\delta^{*}2\pi^{*}1$) is more accessible for the $(Os_2)^{5+}$ complexes.

Solution magnetic measurements were also carried out on the hydroxypyridinate anion by Walton et al. and these showed behaviour comparable with the carboxylate complexes, (2.6 BM per molecule at 308K and 2.63 BM at 173K).

Electrochemical generation of the Os_2(II/III) carboxylate anions was followed spectroscopically in an Optically Transparent Thin-Layer-Electrode (OTTLE) cell (see Chapter 1). The resulting spectra are shown in Figure A2.1 and Figure A2.2. As can be seen, the spectra of the two anions are very similar with the very strong peak of the Os_2(III/III) species at 392nm being replaced by much smaller absorptions in the region ca. 380nm and ca. 340nm in each case. In addition a very weak shoulder grows at ca. 500nm for each complex. In the case of the propionate complex the absorption at 277nm collapses to a shoulder at ca. 285nm and the shoulder at 244nm becomes a definite peak at 237nm. For the butyrate complex the peak at 278nm collapses to a shoulder at ca. 280nm.

Figure A2.1 U.V./Visible Spectra of $[Os_2Cl_2(OCOEt)_4]^{0/-}$ in CH_2Cl_2 0.5M $[^nBu_4N][BF_4]$

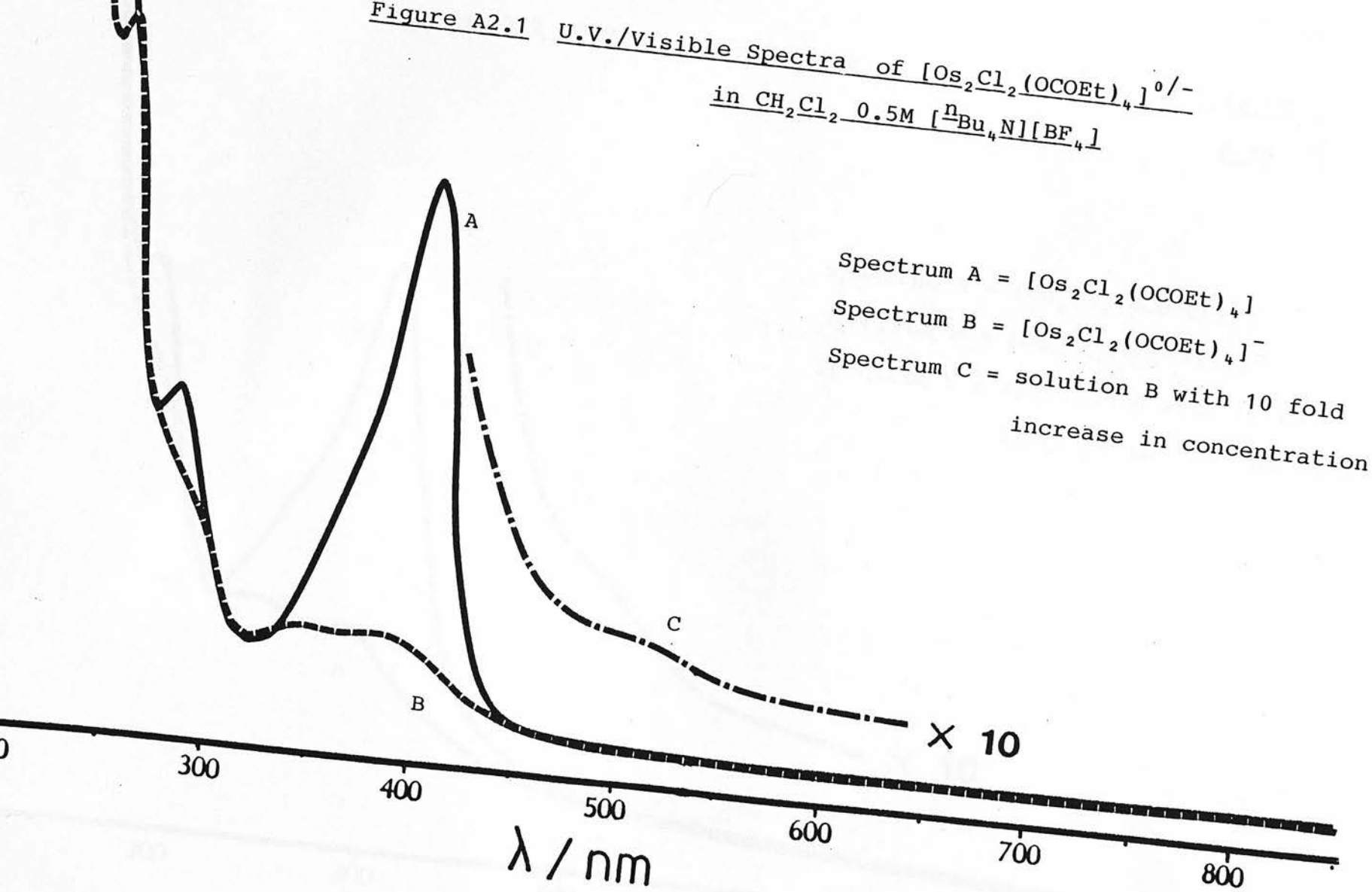

Spectrum A = $[Os_2Cl_2(OCOEt)_4]$

Spectrum B = $[Os_2Cl_2(OCOEt)_4]^-$

Spectrum C = solution B with 10 fold increase in concentration

Figure A2.2 U.V./Visible Spectra of $[Os_2Cl_2(OCO^nPr)_4]^{0/-}$ in CH_2Cl_2

0.5M $[^nBu_4N][BF_4]$

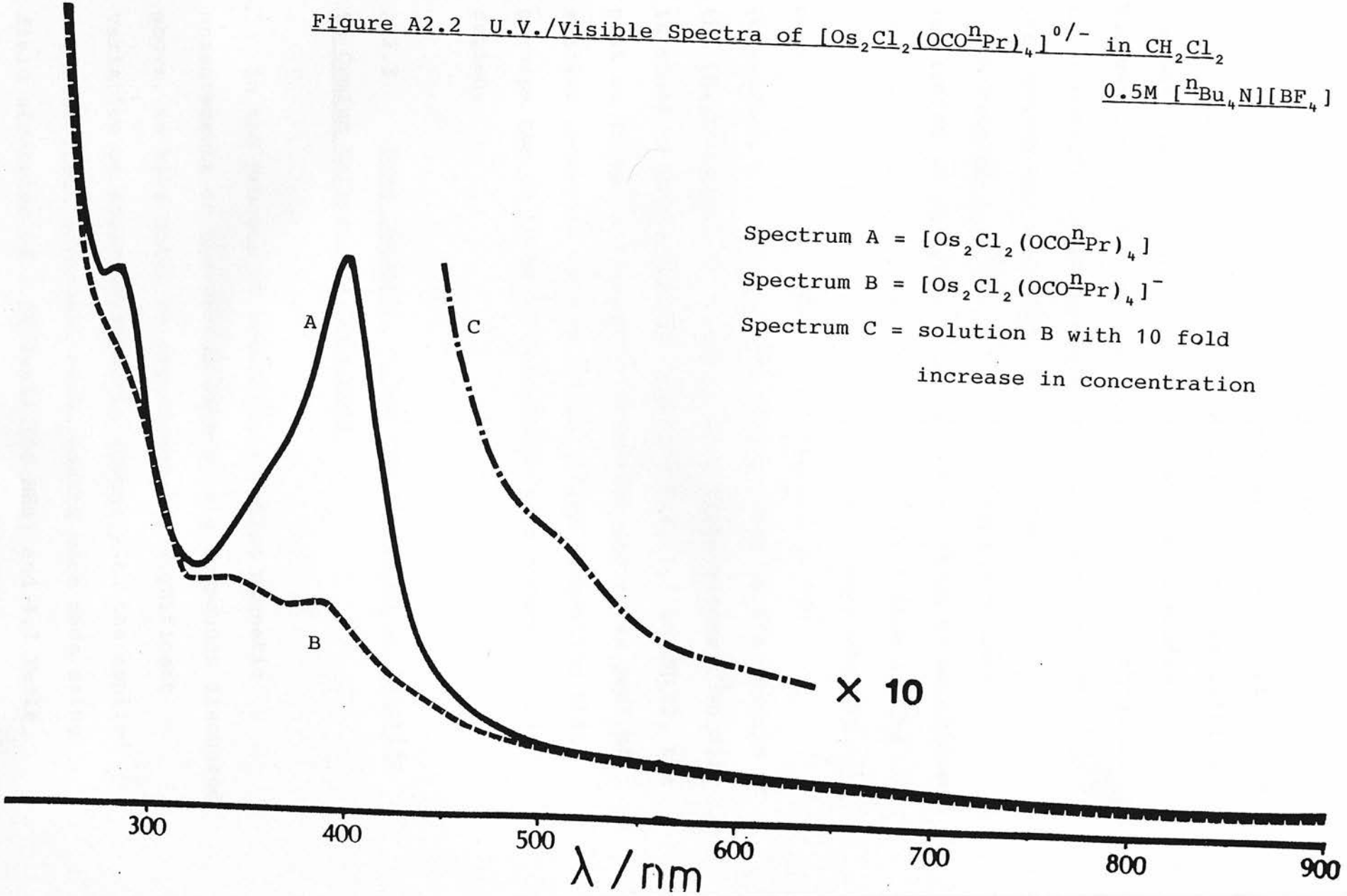

The interpretation of these spectra is not straightforward, particularly in view of the uncertainties in the exact description of the ground state composition for both neutral and anionic carboxylate molecules. However, if studies of the more intensively investigated $[Ru_2(OCOR)_4Cl]$ complexes are taken into account some assignments may be tentatively suggested.

Norman et al. [5] assign the single prominent absorption of the ruthenium complex at 463nm to an allowed $O\pi$ to $Ru_2\pi^*$ transition and a similar transition in the osmium complexes i.e. $O\pi \longrightarrow Os_2\pi^*$ may account for the bands seen at ca. 392nm in the spectra of the $[Os_2(OCOR)_4Cl_2]$ species and at ca. 380nm in the spectra of the $[Os_2(OCOR)_4Cl_2]^-$ species. If a large excess $[^nBu_4N]Br$ is added to a solution of $[Os_2(OCO^nPr)_4Cl_2]$ in CH_2Cl_2 the peak at 392nm is reduced in intensity and a new peak of similar intensity appears at ca. 442nm suggesting that perhaps the Cl to $Os_2\pi^*$ transition also occurs in this region.

A.2.3 Some Comments on the Evans' Method in Relation to Osmium Carboxylate Complexes

In the process of obtaining solution magnetic measurements on the osmium carboxylate compounds discussed above, we have noted an experimentally significant variation of apparent magnetic moment with the applied magnetic field strength. Measurements were made using field strengths of 1.88 Tesla (80 MHz) and 4.7 Tesla

(200 MHz), the 200 MHz machine employing a liquid helium temperature superconducting magnet. The differing axial field geometries of superconducting and non-superconducting magnets require a modification of the standard Evans method equation; i.e. for non-superconducting magnets:

$$\chi_g = \frac{3\Delta f(1-\alpha\Delta t)}{2\pi fm} + \chi_0 + \chi_0\frac{(d_0-d_s)}{m}$$

whereas superconducting magnets require

$$\chi_g = \frac{3\Delta f(1+\alpha\Delta t)}{4\pi fm} + \chi_0 + \chi_0\frac{(d_0-d_s)}{m}$$

where

Δf = frequency separation of lines in Hz

α = solvent expansion coefficient

Δt = T - 293 K

f = frequency of proton resonance in Hz

m = mass of substance in 1 ml solution (in g)

χ_0 = gram susceptibility of solvent

d_0 = density of solvent

d_s = density of solution

(see Appendix 3 for full explanation of this method)

However, even on correct application of these two forms of the equation, marked differences occurred in the apparent magnetic moments of the osmium carboxylate anions, as measured at the two different field strengths. Thus while at 80 MHz the measured magnetic moments for the butyrate anion (2.88 BM per molecule at 215K to 2.47 BM at 275K) and for the propionate anion (2.85 BM per molecule

at 190K to 2.65 BM at 240K) agree well with the results found elsewhere [4] , when measured at 200 MHz there was a significant increase in the apparent moment ($[Os_2(OCO^{n}Pr)_4Cl_2]$; μeff per molecule = 3.65 BM at 180K to 3.16 BM at 301K : $[Os_2(OCOEt)_4Cl_2]$; μeff per molecule = 3.97 BM at 198K to 3.51 BM at 284K).

Interestingly, the effect appears to have reached a maximum at or before 200 MHz and if even higher field strengths i.e. 360 MHz (8.46 Tesla) are employed no further increase in apparent magnetic moment is found.

The phenomenon occurs to a more limited extent with other osmium compounds. Thus the magnetic moment of mer-$[OsCl_3(PMe_2Ph)_3]$ also appears to increase with increasing field strength until reaching a plateau (see Table 1). The effect however seems minimal on mer-$[RuCl_3(PMe_2Ph)_3]$ and disappears entirely when the magnetic moments of complexes such as $Cr(acac)_3$ are measured at different field strengths by this method.

To date no satisfactory explanation for this phenomenon has been discovered and it is obvious that a much more extensive survey of the magnetic behaviour of compounds exposed to high applied field strengths is required before an interpretation of this phenomenon can be accomplished.

Experimental

All physical measurements were obtained as in Chapter 1. The OTTLE cell used was of a previously tested design (see Chapter 1 for full details)

Tetra-μ-2-hydroxypyridinato-dichlorodiosmium(III/III)

Tetra-μ-acetato-dichlorodiosmium(III/III)

Tetra-μ-propionato-dichlorodiosmium(III/III)

Tetra-μ-butyrato-dichlorodiosmium(III/III)

The above compounds were made by the published literature methods [3].

Table A2.1

Magnetic Measurements (Evans' Method) on mer-$[OsCl_3(PMe_2Ph)_3]$ in CH_2Cl_2 at Differing Field Strengths

Field Strength (Tesla)	Observed Magnetic Moment (BM/molecule)
1.41	1.78
1.88	1.85
4.70	2.09
8.46	2.10

Appendix 2 References

1. T.A. Stephenson and G. Wilkinson, J.Inorg.Nucl.Chem., 1966, 28, 2285.
2. A.S. Alves, D.S. Moore and G. Wilkinson, J.Chem.Soc.Chem.Comm., 1981, 1164.
3. T. Behling, T.A. Stephenson, D.A. Tocher, M.D. Walkinshaw and G. Wilkinson, J.Chem.Soc.Dalton.Trans., 1983, 2109.
4. V.T. Coombe, G.A. Heath, T.A. Stephenson, S.M. Tetrick and R.A. Walton, Inorg.Chem., 1984, 23, 4567.
5. D.A. Case, J.G. Norman Jr. and G.E. Renzoni, J.Am.Chem.Soc., 1979, 101, 5256.
6. F.A. Cotton and R.A. Walton, "Multiple Bonds Between Metal Atoms", John Wiley and Sons Inc. (New York), 1982.
7. J.V. Brencic and F.A. Cotton, Inorg. Chem., 1968, 8, 7.
8. M.A. Porai-Koshits and A.S. Antsyshkina, Dokl.Chem., 1962, 146, 902.
9. L. Dubicki and R.L. Martin, Inorg.Chem., 1970, 9, 673.
10. J.G. Norman and H.J. Kolari, J.Am.Chem.Soc., 1978, 100, 791.
11. F.A. Cotton and E. Pederson, Inorg.Chem., 1975, 14, 388.
12. F.A. Cotton and J.L. Thompson, J.Am.Chem.Soc., 1980, 102, 6437.
13. F.A. Cotton, A.R. Chakravarty, T.A. Stephenson and D.A. Tocher, Inorg.Chim.Acta., 1984, 87, 115.

14. T. Behling, T.A. Stephenson, D.A. Tocher, M.D. Walkinshaw and G. Wilkinson, J.Chem.Soc.Dalton.Trans., 1984, 305.

15. D.F. Evans, J.Chem.Soc., 1959, 2003.

APPENDIX 3

The Evans' Nuclear Magnetic Resonance Method for the Measurement of Solution Magnetic Susceptibility

Many years ago it was found [1,2] that the nmr resonance frequency of a proton in a molecule depends on, among other factors, the bulk magnetic susceptibility of the medium in which the molecule is situated. This phenomenon gives rise to the method of measuring magnetic susceptibility in solution by the method first described by Evans in 1959. This is accomplished by measuring the shift in the proton resonance frequency Δf of an inert compound, (in this case tetramethylsilane (TMS)), caused by the introduction of the paramagnetic compound to be studied. This may be carried out in a 5mm nmr tube containing a small reference capillary (see Figure A3.1).

The shift in the proton resonance frequency is given by the expression

$$\Delta H = (2\pi/3)\Delta k$$

where Δk is the change in volume susceptibility. The gram magnetic susceptibility of any paramagnetic substance may thus be determined using the following equation; (see below for changes arising from the differing field geometry appropriate for superconducting magnets).

$$\chi_g = \frac{3\Delta f(1+\alpha\Delta T)}{2\pi f m} \cdot \chi_0 + \chi_0 \frac{(d_0-d_s)}{m}$$

where

Δf = frequency separation in Hz

f = frequency of proton resonance in Hz

m = mass of paramagnetic substance per ml

χ_0 = gram susceptibility of the solvent

α = expansion coefficient of the solvent

Figure A3.1 N.m.r. Method for the Measurement of Solution Magnetic Susceptibilty

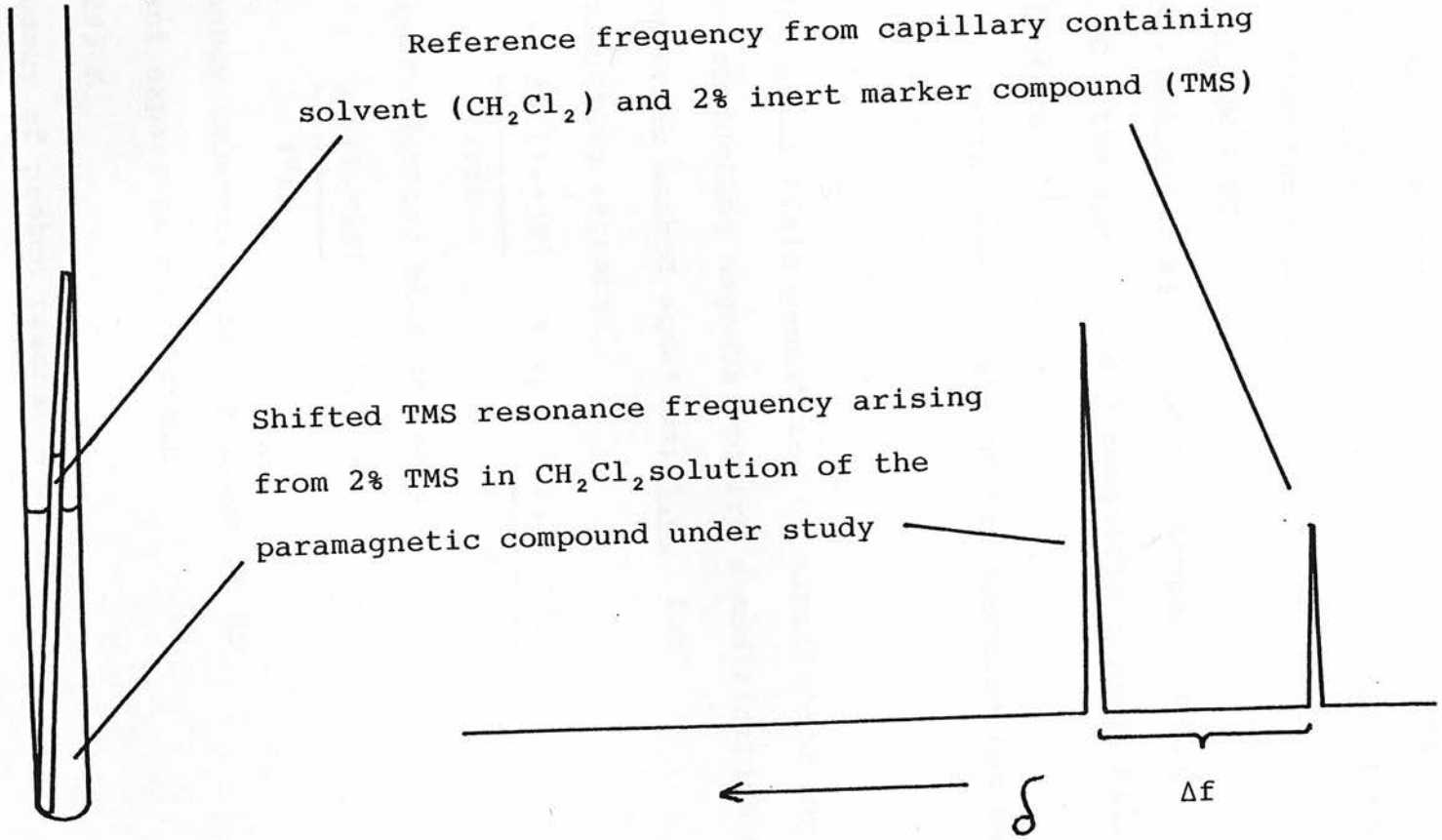

The last part of the expression relates to the densities of the solvent and the solution and for highly paramagnetic substances can be neglected without serious error. The corrected molar susceptibility, χ_m', can then be calculated from the expression

$$\chi_m' = \chi_g.MW + DC$$

where MW = the molecular weight of the compound being studied and DC = the sum of the diamagnetic susceptibility correction factors [3].

Finally the magnetic moment, eff of the compound can be calculated using the expression

$$\mu eff = 2.83[\chi_m'.T]^{\frac{1}{2}}$$

The differing axial field geometries of superconducting and non-superconducting magnets require a modification of the standard Evans method equation; i.e. for non-superconducting magnets:

$$\chi_g = \frac{3\Delta f(1+\alpha\Delta T)}{2\pi fm} + \chi_0 + \frac{\chi_0(d_0-d_s)}{m}$$

whereas superconducting magnets require

$$\chi_g = \frac{3\Delta f(1+\alpha\Delta T)}{4\pi fm} + \chi_0 + \frac{\chi_0(d_0-d_s)}{m}$$

Δf = frequency separation of the lines in Hz

α = solvent expansion coefficient

$\Delta T = T - 293$ K

Δf = frequency of proton resonance in Hz

m = mass of substance in 1 ml solution (in g)

χ_0 = gram susceptibility of solvent

d_0 = density of solvent

d_s = density of solution

Appendix 3 References

1. D.F. Evans, Proc.Chem.Soc , 1958, 115.

2. D.F. Evans, J.Chem.Soc , 1959, 2003.

3. "Theory and Applications of Molecular Paramagnetism", Wiley Interscience, New York,

Appendix 4 Abbreviations

acac	acetylacetonate
BM	Bohr magneton
^{n}Bu	normal butyl
dmf	dimethylformamide
dpae	(1,2-diphenylarseno)ethane
dppe	(1,2-diphenylphosphino)ethane
e.s.r.	electron spin resonance
Et	ethyl
hp	2-hydroxypyridinato
Hz	Hertz
ir	infrared
Me	methyl
MeCN	methyl cyanide (acetonitrile)
MP	melting point
n.m.r.	nuclear magnetic resonance
OTTLE	Optically transparent thin layer electrode
ϕ or Ph	phenyl
ppm	parts per million
^{n}Pr	normal propyl
thf	tetrahydrofuran
TMS	tetramethylsilane
p-tol	4-methylphenyl
UV	ultra violet

LIST OF COURSES ATTENDED

Computing Course

by Dr C.N.M. Pounder

Microcomputer Interfacing Methods

Imperial College London

Modern Aspects of Inorganic Chemistry

by Professor E.A.V. Ebsworth

Structural Methods in Chemistry

by Dr C. Glidewell

Fourier Transform Infrared Spectroscopy

by Dr A. Morrison, Dr J. Duncan and Dr S. Cradock

Modern Laser Techniques in Chemistry

by Professor R.Donovan

University of Strathclyde Inorganic Club Conferences

1981, 1982, 1983

2nd International Platinum Metals Conference 1984

Electrochemical One-electron Oxidation of $[Ru(NO)Cl_5]^{2-}$: Spectroscopic and Magnetic Evidence for the (t_{2g}^5) Ruthenium(III) Pentachloronitrosyl Complex Monoanion $[Ru(NO)Cl_5]^-$

Vyvyan T. Coombe, Graham A. Heath,* T. Anthony Stephenson,* and Derek A. Tocher
Department of Chemistry, University of Edinburgh, Edinburgh EH9 3JJ, Scotland

Voltammetric measurements establish a reversible one-electron oxidation for $[Ru(NO)Cl_5]^{2-}$ in CH_2Cl_2; the i.r. and e.s.r. spectra and magnetic properties of the electrogenerated deep green product are consistent with low-spin $[Ru(NO)Cl_5]^-$, and quite different from the properties recently attributed to this anion.

Reprinted from the Journal of The Chemical Society
Chemical Communications 1983

Electrochemical One-electron Oxidation of $[Ru(NO)Cl_5]^{2-}$: Spectroscopic and Magnetic Evidence for the (t_{2g}^5) Ruthenium(III) Pentachloronitrosyl Complex Monoanion $[Ru(NO)Cl_5]^-$

Vyvyan T. Coombe, Graham A. Heath,* T. Anthony Stephenson,* and Derek A. Tocher
Department of Chemistry, University of Edinburgh, Edinburgh EH9 3JJ, Scotland

Voltammetric measurements establish a reversible one-electron oxidation for $[Ru(NO)Cl_5]^{2-}$ in CH_2Cl_2; the i.r. and e.s.r. spectra and magnetic properties of the electrogenerated deep green product are consistent with low-spin $[Ru(NO)Cl_5]^-$, and quite different from the properties recently attributed to this anion.

Recently, Pandey *et al.*[1] have reported that NOCl reacts with hydrated ruthenium trichloride in the presence of an eightfold excess of triphenylphosphine to give, amongst other products, the pink ruthenium(III) complex $NH_4[Ru(NO)Cl_5]$ which is claimed to be the first example both of high-spin Ru^{III} and of a Ru^{III} nitrosyl complex. Since this would entail reappraisal of well established and soundly based expectations of low-spin behaviour in complexes of 4d tervalent metal ions {*cf.* the isoelectronic $[Ru(CO)Cl_5]^{2-}$ anion[2]}, we are prompted to report some relevant observations.

We have investigated a direct method of generating this species by controlled electrogeneration from the well known,[3] redox-related, 18-electron complex anion, $[Ru(NO)Cl_5]^{2-}$. Cyclic (C.V.) and linear a.c. voltammetry (a.c.V.) at a Pt electrode in CH_2Cl_2 (Figure 1) establish that $[Ph_3(PhCH_2)P]_2[Ru(NO)Cl_5]$ is resistant to oxidation except at extreme potentials where a well defined oxidation is observed. This oxidation is *chemically* reversible although apparently characterised by sluggish heterogeneous charge-transfer kinetics [*i.e.* at 293 K, i_p(anodic)/i_p(cathodic) ratio = 1 at all scan rates (ν) from 50 to 500 mV s^{-1}, but E_p = 100 mV at ν = 50 mV s^{-1} and 120 mV at ν = 200 mV s^{-1}]. The one-electron nature of the process is indicated by the a.c.V. peak width at half height (100 mV, independent of ω in the range 20—600

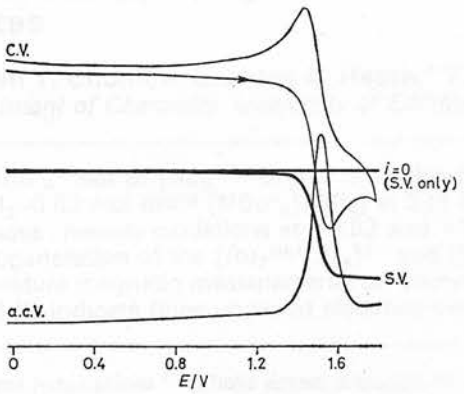

Figure 1. Voltammetry of $[Ru(NO)Cl_5]^{2-}$ in CH_2Cl_2. Scan rates: 100 mV s^{-1} (C.V.), 10 mV s^{-1} (S.V. and a.c.V.). Potentials *vs.* Ag/AgCl reference (against which ferrocene is oxidised at +0.55 V).

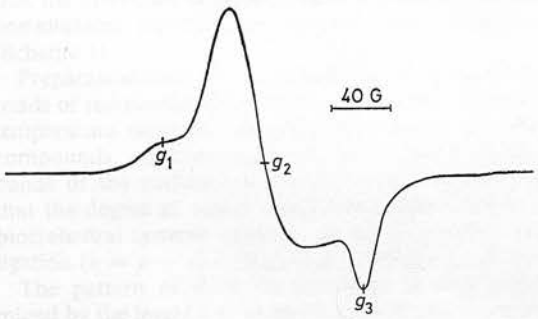

Figure 2. E.s.r. spectrum of $[Ru(NO)Cl_5]^-$ (see text) at 153 K, g_1, 2.16; g_2, 2.11; g_3, 2.06.

Hz), the characteristic diffusion coefficient ($D = 5 \times 10^{-6}$ cm^2 s^{-1} at 293 K),[4] and ultimately confirmed by coulometry (see below). Successive scans give no indication of expulsion of chloride or any other fragmentation/rearrangement to redox-active products other than the $[Ru(NO)Cl_5]^{2-}/[Ru(NO)Cl_5]^-$ couple.

Controlled potential electrolysis in CH_2Cl_2–0.50M$[Bu_4N]BF_4$ at +1.80 V and 223 K proceeds smoothly with the expected exponential decay of current. Percentage conversion was monitored by stirred voltammetry (S.V.) and the electrolysis was interrupted at an arbitrary 80% conversion. Simultaneous coulometric measurements establish that 1.0 electrons are lost per molecule of $[Ru(NO)Cl_5]^{2-}$.

The deep-green electrogenerated product [$\lambda_{max}(\epsilon)$: 690sh, 655 (4 300), 398 (2 100), and 294 nm (10 900)] present in 80% yield in the chilled anolyte solution has been characterised *in situ* as indicated below and its properties are completely consistent with its formulation as the *low-spin* $[Ru(NO)Cl_5]^-$ anion. Thus, magnetic measurements by the Evans' method[5] give $\mu = 2.28$ μ_B at 183 K, and a plot of $1/\chi_M$ *vs.* T in the range 263—183 K shows strict Curie–Weiss behaviour with $\theta = +28$ K {*cf.* $K_2[Ru(CO)Cl_5]H_2O$ where $\mu = 1.87$ μ_B at 296 K[2]}. The e.s.r. spectrum of the green product at 153 K (Figure 2) is typical of that observed for many low-spin ruthenium(III) complexes.[6] I.r. studies on the electrogenerated solution using a chilled flow-through cell reveal a strong NO band at 1920 cm^{-1}, compared to 1850 cm^{-1} for the ruthenium(II) anion (Figure 3). This shift to higher frequency on decrease in formal negative charge on the complex is compatible with the behaviour observed in related metal carbonyl compounds.

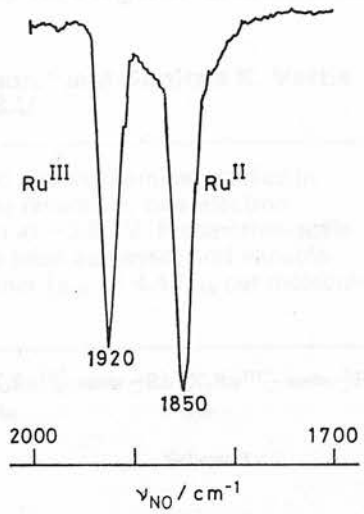

Figure 3. Solution i.r. spectrum of 1:1 mixture of $[Ru(NO)Cl_5]^{2-}$ and $[Ru(NO)Cl_5]^-$ (see text).

At temperatures above 260 K, the deep-green product exhibits 1:1 reversion to the mauve $[Ru(NO)Cl_5]^{2-}$ ion as demonstrated independently by relaxation of the solution i.r. and electronic spectra, and by successive stirred voltammograms. This offers strong circumstantial evidence for its formulation as the $[Ru(NO)Cl_5]^-$ anion.

The observed oxidation potential (+1.53 V) implies that, in contrast to Pandey's report,[1] the $[Ru(NO)Cl_5]^-$ anion is thermodynamically unstable towards reduction by water (or even free Cl^-), although it may be that under strict vacuum-line conditions the compound would be indefinitely stable at room temperature.

Hence, there are serious discrepancies between the properties we deduce for $[Ru(NO)Cl_5]^-$ and those ascribed to it by Pandey *et al.* Little experimental detail is given in their preliminary communication and, to date, all our attempts to reproduce their results have proved unsuccessful. Thus, although shaking a solution of '$RuCl_3.xH_2O$' and PPh_3 (1:8 molar ratio) with NOCl (1 atm) in CH_2Cl_2–EtOH resulted in the precipitation of an orange-brown, water-soluble material containing NH_4^+ ions and no PPh_3, e.s.r. and magnetic studies indicated that only traces of paramagnetic material were present. Under reflux conditions, the only product isolated was the well known $[Ru(NO)Cl_3(PPh_3)_2]$.[7]

We thank the S.E.R.C. for provision of electrochemical equipment (to G.A.H.) and for financial support (to V.T.C. and D.A.T.) and Johnson Matthey plc for loans of ruthenium trichloride.

Received, 29th December 1982; Com. 1479

References

1 K. K. Pandey, S. R. Ahuja, N. S. Poonia, and S. Bharti, *J. Chem. Soc., Chem. Commun.*, 1982, 1268.
2 See J. E. Fergusson and A. M. Greenaway, *Aust. J. Chem.*, 1978, **31**, 497 and references therein.
3 E. E. Mercer, W. M. Campbell, Jr., and R. M. Wallace, *Inorg. Chem.*, 1964, **3**, 1018.
4 A. J. Bard and L. R. Faulkner, 'Electrochemical Methods,' Wiley, New York, 1980, p. 153.
5 D. F. Evans, *J. Chem. Soc.*, 1959, 2003.
6 See J. B. Raynor and B. G. Jeliazkowa, *J. Chem. Soc. Dalton Trans.*, 1982, 1185 and references therein.
7 S. D. Robinson and M. F. Uttley, *J. Chem. Soc., Dalton Trans.*, 1972, 1.

Triple Halide-bridged Diruthenium Complexes in Higher Oxidation States

Vyvyan T. Coombe, Graham A. Heath,* T. Anthony Stephenson,* and Dimitris K. Vattis
Department of Chemistry, University of Edinburgh, Edinburgh EH9 3JJ

The $NBu^n_4{}^+$ salt of $[Ru_2^{III,III}Br_9]^{3-}$ is soluble in organic solvents and electrochemical studies in CH_2Cl_2–0.50 mol dm^{-3} $[NBu^n_4][BF_4]$ at 233 K show it to have three reversible, one-electron processes: namely oxidations at +0.83 and +1.36 V and a reduction at −0.60 V. Preparative-scale electrogeneration of the $[Ru_2^{III,IV}Br_9]^{2-}$ and $[Ru_2^{IV,IV}Br_9]^{-}$ ions has been achieved, and variable-temperature magnetic measurements on anolyte solutions of the former ($\mu_{eff.}$ = 4.40 μ_B per molecule at 273 K) indicate three unpaired electrons per molecule.

In recent publications [1] we have drawn attention to the occurrence in three distinct oxidation levels, ranging from $Ru_2^{II,II}$ to $Ru_2^{III,III}$, of various triple chloro-bridged binuclear complexes of general form $[L_{3-x}Cl_xRuCl_3RuCl_yL_{3-y}]^z$ where L are neutral ligands such as PR_3, AsR_3, CO, *etc.*[1] and NH_3 [2] and H_2O.[3] Furthermore, extensive voltammetric studies have established that the individual complexes generally display two reversible one-electron transfers to connect these oxidation levels (Scheme 1).[1]

Preparative-scale electrogeneration of a number of such triads of redox-related species has been achieved and variable-temperature magnetic measurements on the diruthenium(III) compounds, together with the intervalence charge-transfer bands of the ruthenium(II)ruthenium(III) compounds, reveal that the degree of metal–metal interaction in these confacial bioctahedral systems increases as the asymmetry in chloride ligation ($u = y - x$) in $[L_{3-x}Cl_xRuCl_3RuCl_yL_{3-y}]^z$ decreases.[1]

The pattern of electrode potentials is also largely determined by the level ($y + x$) and asymmetry ($y - x$) of terminal halide binding. For example, substitution of PMe_2Ph by chloride in $[(PMe_2Ph)_3RuCl_3Ru(PMe_2Ph)_3]^{3+}$ causes shifts in the first reduction potential of −0.75 V for each additional chloride at the redox-active centre and −0.25 V for attachment at the remote ruthenium.[1,4] Unrefined extrapolation to exhaustively substituted $[Ru_2X_9]^{3-}$ ions (X = Cl or Br) suggests that the $E_{\frac{1}{2}}(Ru_2^{III,III}$–$Ru_2^{II,III})$ couple could shift by a remarkable −3.0 V compared to $[(PMe_2Ph)_3RuCl_3Ru(PMe_2Ph)_3]^{3+/2+}$. From the limited number of analogues available, *e.g.* $[(PMe_2Ph)_3RuBr_3Ru(PMe_2Ph)_3]^{+/2+/3+}$, it appears that the corresponding bromo-systems have very similar electrochemical behaviour, in accord with Scheme 1.[4]

We now describe the electrochemical behaviour of the highly symmetrical $[Br_3Ru^{III}Br_3Ru^{III}Br_3]^{3-}$ ion and report the bulk electrogeneration of the new redox-related $[Ru_2Br_9]^{n-}$ ions (n = 2 or 1) which are respectively the first examples of diruthenium 33 and 32 valence-electron, triple halide-bridged systems.

Results and Discussion

The salt $K_3[Ru_2Br_9]$ was readily prepared by the method described by Fergusson and Greenaway,[5] namely reaction of '$RuCl_3 \cdot xH_2O$' with a concentrated HBr–ethanol mixture followed by addition of KBr. This material is freely soluble only in water (in which electrochemical studies are very limited). However, we find that treatment of the aqueous solution with $[NBu^n_4]Br$ induces precipitation of $[NBu^n_4]_3[Ru_2Br_9]$ which dissolves readily in organic solvents. The $PPh_3(CH_2Ph)^+$ salt was similarly prepared.

The constitution of these $M_3[Ru_2Br_9]$ compounds was confirmed by elemental analyses and conductivity measurements (see Experimental section).

$$\rangle Ru^{II}X_3Ru^{II}\langle \rightleftharpoons \rangle Ru^{II}X_3Ru^{III}\langle \rightleftharpoons \rangle Ru^{III}X_3Ru^{III}\langle$$
36e 35e 34e

Scheme 1.

Magnetochemistry of $[NBu^n_4]_3[Ru_2Br_9]$.—For $Cs_3[Ru_2Br_9]$ [5] the reported solid-state magnetic moment $\mu_{eff.}$ is 1.01 μ_B per Ru at 296 K. From susceptibility measurements by the Evans method [6] on $[NBu^n_4]_3[Ru_2Br_9]$ in CH_2Cl_2, we calculate $\mu_{eff.}$ = 1.19 μ_B per Ru at 299 K, confirming that the effective magnetic moment per ruthenium atom is depressed from that characterising monomeric ruthenium(III) complexes. This evidence establishes the presence of significant interactions between the paramagnetic centres within the symmetric binuclear complex, (*cf.* $[\{As(C_6H_4Me\text{-}p)_3\}_2ClRu^{III}Cl_3Ru^{III}Cl\{As(C_6H_4Me\text{-}p)_3\}_2]^+$ (u = 0) [1] where $\mu_{eff.}$ = 0.91 μ_B per Ru at 233 K). Comparison may be made with the lower symmetry $[\{As(C_6H_4Me\text{-}p)_3\}_2ClRu^{III}Cl_3Ru^{III}Cl_2\{As(C_6H_4Me\text{-}p)_3\}]$ (u = 1) [1] where $\mu_{eff.}$ = 1.45 μ_B per Ru at 229 K and 1.61 μ_B per Ru at 297 K, and $[\{As(C_6H_4Me\text{-}p)_3\}_3Ru^{III}Cl_3Ru^{III}Cl_2\{As(C_6H_4Me\text{-}p)_3\}]^+$ (u = 2) [1] where $\mu_{eff.}$ = 2.01 μ_B per Ru even at 233 K.

The measured Ru–Ru internuclear distances of 2.86 Å in $Cs_3[Ru_2Br_9]$ (powder diffraction data) [5] and 2.725 (3) Å in the recently reported $Cs_3[Ru_2Cl_9]$ (three-dimensional single-crystal diffraction data) [7] are in keeping with the magnetic data for these symmetric systems.

In the case of $[Ru_2Cl_9]^{3-}$, Cotton and co-workers [8] have calculated by the SCF-Xα-SW method that the ground-state valence-electron structure is $a_1'^2e'^4e''^4$. The reported magnetic moment of $Cs_3[Ru_2Cl_9]$ is particularly low ($\mu_{eff.}$ = 0.51 μ_B per Ru at 300 K) and indeed has been attributed to temperature-independent paramagnetism rather than to contributions from thermally accessible triplet states.[7]

Voltammetry of $[NBu^n_4]_3[Ru_2Br_9]$.—Cyclic voltammetry (c.v.) and linear stirred voltammetry (s.v.) together with a.c. voltammetry (a.c.v.) at platinum electrodes in CH_2Cl_2 establish that at 233 K $[NBu^n_4]_3[Ru_2Br_9]$ undergoes reversible, stepwise oxidations at +0.83 and +1.36 V and a quasi-reversible reduction at −0.60 V (Figure).† Unlike the two oxidations, the reduction step shows no c.v. return wave at room temperature due to rapid breakdown of $[Ru_2Br_9]^{4-}$.

† All potentials are corrected to 293 K and were measured in CH_2Cl_2–0.50 mol dm^{-3} $[NBu^n_4][BF_4]$ *vs.* a Ag–AgCl reference at which ferrocene is oxidised at +0.55 V.

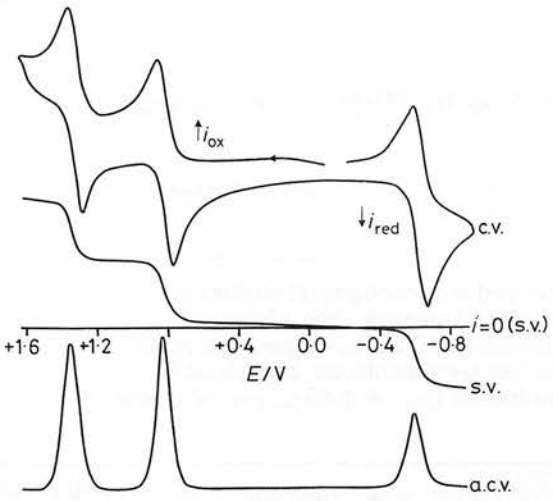

Figure. Voltammetry of $[NBu^n_4]_3[Ru_2Br_9]$ in CH_2Cl_2 at 233 K. Scan rates: 100 mV s^{-1} (c.v.); 10 mV s^{-1} (s.v. and a.c.v.). Potentials *vs.* Ag–AgCl reference (against which ferrocene is oxidised at +0.55 V)

The one-electron nature of these steps is indicated by the equal heights of the low-temperature s.v. waves, the a.c.v. peak widths at half-height at 233 K (72 mV, independent of the a.c. frequency (ω) in the range 40—400 Hz), the characteristic diffusion coefficient ($D = 4.73 \times 10^{-6}$ cm^2 s^{-1} at 285 K, measured at +1.0 V),[9] and finally by coulometric measurements which show that the first oxidation step corresponds to the loss of 1.0 electron per molecule of $[Ru_2Br_9]^{3-}$. These features have been separately confirmed for the $PPh_3(CH_2Ph)^+$ salt.

$$[Ru_2^{II,III}Br_9]^{4-} \underset{}{\overset{-0.60\ V}{\rightleftharpoons}} [Ru_2^{III,III}Br_9]^{3-} \overset{+0.83\ V}{\rightleftharpoons}$$
35e 34e

$$[Ru_2^{III,IV}Br_9]^{2-} \overset{+1.36\ V}{\rightleftharpoons} [Ru_2^{IV,IV}Br_9]^{-}$$
33e 32e

Scheme 2.

Hence, these observations establish the sequence of metal-based redox interconversions shown in Scheme 2. The $[Ru_2Br_9]^{3-}$ ion is reported [5] to undergo chemical oxidation in solutions containing excess of bromide ion to form $[Ru^{IV}Br_6]^{2-}$ (*i.e.* $[Ru_2Br_9]^{3-} + Br^- + Br_2 \rightleftharpoons 2[RuBr_6]^{2-}$). Electrochemical studies on $[PPh_3(CH_2Ph)]_2[RuBr_6]$ in CH_2Cl_2–0.20 mol dm^{-3} $[NBu^n_4][BF_4]$ show a reduction wave at +0.20 V (irreversible at 300 K but reversible at 233 K) and an oxidation wave at +1.55 V (irreversible at all temperatures). Hence this species is clearly *absent* in the electrochemical oxidation of $[Ru_2Br_9]^{3-}$ described above.

It is interesting to note that the cumulative effect of exhaustive bromo-substitution has made the 33- and 32-electron species accessible while shifting the 34–35 electron couple *ca.* −2.5 V with respect to that of $[Ru_2Cl_3(PMe_2Ph)_6]^{3+/2+}$.

Magnetic Studies on Electrogenerated $[Ru_2Br_9]^{n-}$ *Ions.*—In order to explore further the structural and electronic changes which might accompany these stepwise electron-transfer processes in the $[Ru_2Br_9]^{3-}$ ions, we have sought to electrogenerate the $[Ru_2Br_9]^{n-}$ ions (n = 4, 2, or 1) on a preparative scale. Unfortunately, bulk electrosynthesis of the $[Ru_2Br_9]^{4-}$ ion has not been accomplished even at 200 K because of the very low stability of the material.

Table. Magnetic measurements on $[NBu^n_4]_2[Ru_2Br_9]$

T/K	$10^6\chi_M$(corr)	$1/\chi_M$(corr)	$\mu_{eff.}(\mu_B)$ per molecule
273	8 792	113.7	4.40
263	9 146	109.3	4.40
252	9 425	106.1	4.38
242	9 592	104.3	4.33
231	9 851	101.5	4.28
220	9 962	100.4	4.20
210	10 231	97.7	4.16
200	10 429	95.9	4.10
190	10 479	95.4	4.01

However, controlled-potential electrolysis in CH_2Cl_2–0.50 mol dm^{-3} $[NBu^n_4][BF_4]$ at +1.0 V and 223 K of $[NBu^n_4]_3[Ru_2Br_9]$ proceeds smoothly with the expected exponential decay of current. The percentage conversion was monitored by stirred voltammetry and essentially quantitative conversion into the $[Ru_2Br_9]^{2-}$ ion was achieved. This anion is quite stable in solution up to 273 K although ready decomposition occurs at higher temperatures. Magnetic studies were made on the anolyte solution between 190 and 273 K by the Evans method. From duplicate measurements on separately electrogenerated solutions, we calculate that for the $[Ru_2Br_9]^{2-}$ ion a plot of $1/\chi_M$(corr) *vs.* T is linear with intercept $\theta = -234$ K, and $\mu_{eff.} = 4.40$ μ_B per molecule at 273 K decreasing to 4.01 μ_B at 190 K.

These results imply that $[Ru_2Br_9]^{2-}$ possesses *three* unpaired electrons per molecule (whereas one unpaired electron might have been anticipated following oxidation of either $a_1'^2e'^4e''^4$ or $a_1'^2e'^4e''^3a_2''^1$ states of $[Ru_2Br_9]^{3-}$). Thus, in contrast to $[Ru_2Br_9]^{3-}$, it appears that the oxidised complex contains only loosely coupled ruthenium(III) (d^5) and ruthenium(IV) (d^4) centres, having one and two unpaired electrons respectively. The striking possibility exists that the 33-electron complex $[Ru_2Br_9]^{2-}$ might have a flickering asymmetric geometry with 'trapped' spin centres [as demonstrated for the related 35-electron ruthenium(II)ruthenium(III) complexes discussed earlier [1]].

In any event the much smaller Ru–Ru interaction in $[Ru_2Br_9]^{2-}$, compared to $[Ru_2Br_9]^{3-}$, is in accord with the decreased metal *d*-electron density in higher oxidation states. This view receives strong support from very recent structural studies by Cotton *et al.*[10] on the related $[W_2Cl_9]^{n-}$ ions (n = 2 or 3). They find that the internuclear distance in $[W_2Cl_9]^{2-}$ [2.540(1) Å] is 0.122(9) Å longer than in $[W_2Cl_9]^{3-}$, and attribute this effect largely to the increased mean oxidation state of the metal atoms, whereby the *d* orbitals contract leading to weaker σ bonding.

From a molecular orbital viewpoint, increased Ru–Ru separation due to such effects in $[Ru_2Br_9]^{2-}$ could result in near degeneracy in the valence-orbital manifold [11] and hence a readily accessible spin-quartet state $a_1'^2e'^4e''^2a_2''^1$. In the limit of negligible bonding, the two ruthenium centres could become almost independent as suggested above, although the orthodox molecular orbital description implies a symmetrical charge distribution for such binuclear complexes.

Electrogeneration of the diruthenium(IV) complex $[Ru_2Br_9]^-$ proceeds smoothly to *ca.* 80% conversion at 200 K and examination of the resulting solution by s.v. and c.v. establishes the formation of the stable monoanion. However the electrosynthesis appears to halt abruptly and reproducibly at this point. This is presumably due to the fact that the requisite oxidation potential is substantially more positive than that of free bromide and even 1% dissociation of the complex

would make 80% electrolysis the thermodynamic limit. Magnetic measurements confirm the compound is less paramagnetic than the $[Ru_2Br_9]^{2-}$ precursor but, in the circumstances, quantitative discussion is unwarranted.

Studies in collaboration with Professor F. A. Cotton are now in hand to evaluate the alternative descriptions of these systems. These include further SCF-Xα-SW calculations on the $[Ru_2X_9]^{n-}$ ions, together with electrochemical examination of the chloride system and attempts to isolate single crystals for $n = 2$ or 1.* A detailed comparison of the electronic spectra of the various electrogenerated anions will also be described.

Experimental

Microanalyses were by the Butterworth Micro Analytical Consultancy and the University of Edinburgh Chemistry Department. Infrared spectra were recorded in the region 4 000—200 cm^{-1} on a Perkin-Elmer 557 grating spectrometer using Nujol mulls on caesium iodide plates. Solution magnetic measurements (Evans method) were obtained on a Varian HA 100 n.m.r. spectrometer equipped with a variable-temperature probe. Electronic spectra were obtained on a Pye-Unicam SP8-400 spectrophotometer. Conductivity measurements were made in CH_3NO_2 at 303 K using a model 310 Portland Electronics conductivity bridge. Melting points were determined with a Köfler hot-stage microscope and are uncorrected.

Investigative electrochemistry was performed using a PAR model 170 potentiostat and programmer and $[NBu^n_4][BF_4]$ solutions (0.50 mol dm^{-3}) in CH_2Cl_2 (293—200 K) with platinum working and auxiliary electrodes and an Ag–AgCl reference electrode (against which ferrocene is oxidised at $E_{\frac{1}{2}} = +0.55$ V, which is *ca.* 50 mV removed from the s.c.e. values). All electrosyntheses were carried out using a Hi-Tek type DT2101 potentiostat in conjunction with a Hi-Tek type PPR1 waveform generator and associated bipotentiostat module for voltammetric monitoring.

Potassium Tri-μ-bromo-hexabromodiruthenate(III).—The compound ' $RuCl_3 \cdot xH_2O$ ' (0.50 g) was dissolved in 100 cm^3 of a mixture (1 : 1 v/v) of concentrated HBr (48%) and ethanol and heated under reflux under a nitrogen atmosphere for 2 h. A stoicheiometric amount of KBr (0.34 g) was then added and on concentration and cooling of the solution the black microcrystalline product precipitated. This was filtered off, washed with ethanol and diethyl ether, and dried *in vacuo*, yield 0.80 g (81%). Electronic spectrum (in water) (40 000—10 000 cm^{-1}): 35 710 ($\varepsilon = 21\,090$), 32 050 (14 140), 24 390 (3 970), and 20 330 cm^{-1} (4 540 $dm^3\ mol^{-1}\ cm^{-1}$).

Tetra-n-butylammonium Tri-μ-bromo-hexabromodiruthenate(III).—This was prepared from the potassium salt by treatment of an aqueous solution of the latter with an excess of $[NBu^n_4]Br$. The precipitated purple solid was washed with water and diethyl ether and dried *in vacuo* at 40 °C, m.p. 194 °C. The yield was almost quantitative (Found: C, 35.1; H, 6.6; N, 2.7. Calc. for $C_{48}H_{108}Br_9N_3Ru_2$: C, 34.9; H, 6.6; N, 2.6%); Λ (0.95×10^{-3} mol dm^{-3}) in CH_3NO_2 = 177 S $cm^2\ mol^{-1}$. Electronic spectrum (in CH_2Cl_2) (40 000—10 000 cm^{-1}): 34 720 ($\varepsilon = 26\,740$), 30 960 (18 200), 23 360 (4 120), and 19 720 cm^{-1} (6 050 $dm^3\ mol^{-1}\ cm^{-1}$).

Benzyltriphenylphosphonium Tri-μ-bromo-hexabromodiruthenate(III).—This was similarly prepared by treatment of aqueous solutions of $K_3[Ru_2Br_9]$ with an excess of $[PPh_3(CH_2Ph)]Cl$, m.p. 135—137 °C (decomp.) (Found: C, 44.3; H, 3.4; Br, 36.3; P, 4.4. Calc. for $C_{75}H_{66}Br_9P_3Ru_2$: C, 45.4; H, 3.3; Br, 36.3; P, 4.6%); Λ (1×10^{-3} mol dm^{-3}) in CH_3NO_2 = 232 S $cm^2\ mol^{-1}$. Electronic spectrum (in CH_2Cl_2) (40 000—10 000 cm^{-1}): 34 970 cm^{-1} ($\varepsilon = 27\,460$), 31 250 (19 350), 23 470 (4 970), and 19 680 cm^{-1} (6 270 $dm^3\ mol^{-1}\ cm^{-1}$).

Acknowledgements

We thank Johnson Matthey PLC for loans of ' $RuCl_3 \cdot xH_2O$ ', Professor F. A. Cotton of Texas A and M University for preprints of refs. 8 and 10 and for other helpful comments, and the S.E.R.C. for financial support (to V. T. C. and D. K. V.) and provision of electrochemical equipment (to G. A. H.). D. K. V. thanks the University of Patras, Greece, for leave of absence.

References

1 See G. A. Heath, A. J. Lindsay, T. A. Stephenson, and D. K. Vattis, *J. Organomet. Chem.*, 1982, **233**, 353 and refs. therein.
2 E. E. Mercer and L. W. Gray, *J. Am. Chem. Soc.*, 1972, **94**, 6426.
3 E. E. Mercer and P. E. Dumas, *Inorg. Chem.*, 1971, **10**, 2755.
4 A. J. Lindsay, Ph.D. Thesis, University of Edinburgh, 1982.
5 J. E. Fergusson and A. M. Greenaway, *Aust. J. Chem.*, 1978, **31**, 497.
6 D. F. Evans, *J. Chem. Soc.*, 1959, 2003.
7 J. Darriet, *Rev. Chim. Miner.*, 1981, **18**, 27.
8 B. E. Bursten, F. A. Cotton, and A. Fang, *Inorg. Chem.*, submitted for publication.
9 A. J. Bard and L. R. Faulkner, ' Electrochemical Methods,' Wiley, New York, 1980, p. 153.
10 F. A. Cotton, L. R. Falvello, G. N. Mott, R. R. Schrock, and L. G. Sturgeoff, *Inorg. Chem.*, submitted for publication.
11 F. A. Cotton, personal communication.

Received 2nd March 1983; *Paper* 3/333

* *Note added at proof:* we have now prepared $[NBu^n_4]_3[Ru_2Cl_9]$ and shown that it has closely comparable redox behaviour, with E_{red} (1) = −0.57, E_{ox} (1) = +0.92, and E_{ox} (2) = +1.58 V, in CH_2Cl_2.

Reprinted from Inorganic Chemistry, 1984, *23*, 4567

Contribution from the Departments of Chemistry, Purdue University, West Lafayette, Indiana 47907, and University of Edinburgh, Edinburgh EH9 3JJ, U.K.

Redox Chemistry of Multiply Bonded Diosmium Complexes: Preparation and Characterization of Complexes Containing Osmium–Osmium Bonds of Order 2.5

STEPHEN M. TETRICK,[1a] VYVYAN T. COOMBE,[1b] GRAHAM A. HEATH,[1b] T. ANTHONY STEPHENSON,*[1b] and RICHARD A. WALTON*[1a]

Received June 5, 1984

The complexes $Os_2(O_2CR)_4Cl_2$ (R = C_2H_5 or C_3H_7) and $Os_2(hp)_4Cl_2$ (hp is the monoanion of 2-hydroxypyridine) each possess a reversible one-electron reduction at $E_{1/2} \simeq +0.3$ V (for the carboxylates) or +0.1 V (for the hp derivative) vs. SCE. These reductions can be accomplished chemically by using cobaltocene as the reducing agent to produce $[(\eta\text{-}C_5H_5)_2Co][Os_2(O_2CR)_4Cl_2]$ and $[(\eta\text{-}C_5H_5)_2Co][Os_2(hp)_4Cl_2]$. These complexes are the first derivatives of the Os_2^{5+} core to have been isolated and have been characterized by cyclic voltammetry, electronic absorption spectroscopy, ESR spectroscopy, and magnetic susceptibility measurements. They are believed to contain Os–Os multiple bonds of order 2.5 with the configurations $\sigma^2\pi^4\delta^2\delta^{*1}\pi^{*2}$ ($S = {}^3/_2$) and $\sigma^2\pi^4\delta^2\delta^{*2}\pi^{*1}$ and/or $\sigma^2\pi^4\delta^2\pi^{*3}$ ($S = {}^1/_2$) being the principal contributors to the ground state at room temperature.

Introduction

Recently, various strategies have been explored for the synthesis of diosmium carboxylates, especially with a view to the isolation of compounds that might contain osmium–osmium multiple bonds. One such approach involved the use of the complexes *trans*-$OsO_2X_2(PR'_3)_2$ as synthetic starting materials,[2] and this led to the isolation and structural characterization of the novel, diamagnetic diosmium(IV) species $Os_2(\mu\text{-}O)(\mu\text{-}O_2CR)_2X_4(PR'_3)_2$.[3,4] Among the properties of note for this class of complexes (R = CH_3 or C_2H_5; X = Cl or Br; PR'_3 = PPh_3 or PEt_2Ph) is the occurrence of a very accessible one-electron reduction ($E_{1/2}$ values in the range +0.09 to +0.23 V vs. SCE) to give the paramagnetic $Os^{III}Os^{IV}$ monoanions.[4] On the other hand, when recourse was made to a different osmium starting material, namely, the hexachloroosmate(IV) ion, then reaction with acetic acid–acetic anhydride was found to give the diosmium(III) acetate $Os_2(O_2CCH_3)_4Cl_2$.[5] Subsequently, other diosmium(III) carboxylates $Os_2(O_2CR)_4Cl_2$ (R = Et, *n*-Pr, or CH_2Cl) were discovered[6,7] and the crystal structures of the acetate, propionate and butyrate were determined,[6-8] thereby establishing that these complexes are derivatives of the multiply bonded Os_2^{6+} core.[9]

We have explored the redox chemistry of these diosmium(III) complexes with a view to understanding their relationship to the well-established class of diruthenium carboxylates[10] and various derivatives that contain the isoelectronic triply bonded Re_2^{4+} core.[11,12] We provide in this report details of the redox chemistry of these diosmium(III) species which establish quite clearly that they undergo a facile one-electron reduction to give compounds that contain the hitherto unknown Os_2^{5+} core.

Experimental Section

Materials. All solvents were dried over molecular sieves, distilled, and purged with nitrogen gas for 30 min prior to use. Cobaltocene was purchased from Strem Chemicals, Inc., and was used as received. The *n*-propionate and *n*-butyrate complexes of the type $Os_2(O_2CR)_4Cl_2$ were prepared from $[OsCl_6]^{2-}$ solutions by using the procedure described previously.[7]

Reaction Procedures. All syntheses were carried out under an atmosphere of nitrogen.

$Os_2(hp)_4Cl_2 \cdot 2H_2O$. This complex, where Hhp = 2-hydroxypyridine, was prepared by a modification of the existing procedure.[7] A mixture of $Os_2(O_2CC_3H_7)_4Cl_2$ (112.7 mg, 0.141 mmol) and Hhp (116.7 mg, 1.23 mmol) was refluxed in 10 mL of ethanol for 45 min. The deep red solution was cooled to room temperature, and the solvent was removed by evaporation in an N_2 stream. Dichloromethane was then added to dissolve the dark red residue, and this solution was filtered through a medium-porosity frit. The volume of this solution was reduced to approximately 5 mL, and 5 mL of diethyl ether was added to initiate precipitation of the product. This mixture was refrigerated

(1) (a) Purdue University. (b) Edinburgh University.
(2) Armstrong, J. E.; Walton, R. A. *Inorg. Chem.* **1983**, *22*, 1545.
(3) Armstrong, J. E.; Robinson, W. R.; Walton, R. A. *J. Chem. Soc., Chem. Commun.* **1981**, 1120.
(4) Armstrong, J. E.; Robinson, W. R.; Walton, R. A. *Inorg. Chem.* **1983**, *22*, 1301.
(5) Moore, D. C.; Alves, A. S.; Wilkinson, G. *J. Chem. Soc., Chem. Commun.* **1981**, 1164.
(6) Stephenson, T. A.; Tocher, D. A.; Walkinshaw, M. D. *J. Organomet. Chem.* **1982**, *232*, C51.
(7) Behling, T.; Wilkinson, G.; Stephenson, T. A.; Tocher, D. A.; Walkinshaw, M. D. *J. Chem. Soc., Dalton Trans.* **1983**, 2109.
(8) Cotton, F. A.; Chakravarty, A. R.; Tocher, D. A.; Stephenson, T. A. *Inorg. Chim. Acta* **1984**, *87*, 115.
(9) Cotton, F. A.; Walton, R. A. "Multiple Bonds Between Metal Atoms"; Wiley: New York, 1982.
(10) Reference 9, pp 192–198.
(11) Reference 9, pp 184–191.
(12) Ebner, J. R.; Walton, R. A. *Inorg. Chem.* **1975**, *14*, 1987.

0020-1669/84/1323-4567$01.50/0

overnight to afford a high yield of the dark red product $Os_2(hp)_4Cl_2 \cdot 2H_2O$; yield 102.5 mg (84%). Anal. Calcd for $C_{20}H_{20}Cl_2N_4O_6Os_2$: C, 27.81; H, 2.34. Found: C, 28.10; H, 2.62. The presence of water in the complex was confirmed by ^1H NMR spectroscopy. Note that the present procedure utilizes $Os_2(O_2CC_3H_7)_4Cl_2$ rather than $Os_2(O_2CCH_3)_4Cl_2$,[7] a modification that results in an appreciable increase in the product yield (from 51% to 84%).

In our hands, recrystallized samples of this complex could be obtained as a wide variety of solvates. ^1H NMR spectroscopy of various samples showed the presence of small amounts of lattice ethanol, diethyl ether, or dichloromethane, in addition to water. Indeed, Cotton and Thompson,[13] who first prepared and structurally characterized this complex, had commented previously upon its propensity to form solvates.

$[(\eta\text{-}C_5H_5)_2Co][Os_2(O_2CC_3H_7)_4Cl_2]$. A quantity of $Os_2(O_2CC_3H_7)_4Cl_2$ (83.1 mg, 0.104 mmol) was added to 10 mL of acetone and the resulting solution treated with a close to stoichiometric amount of cobaltocene (23.2 mg, 0.123 mmol). The reaction mixture was then stirred at room temperature for 30 min, and the yellow-green precipitate that had formed was filtered off, washed with several portions of acetone and diethyl ether, and then dried; yield 86.4 mg (84%). Anal. Calcd for $C_{26}H_{38}Cl_2CoO_8Os_2$: C, 31.58, H, 3.88. Found: C, 31.70; H, 3.95.

$[(\eta\text{-}C_5H_5)_2Co][Os_2(O_2CC_2H_5)_4Cl_2]$. This complex was prepared by using a procedure analogous to that described for the butyrate; yield 82%. Anal. Calcd for $C_{22}H_{30}Cl_2CoO_8Os_2$: C, 28.33; H, 3.25. Found: C, 28.07; H, 3.28.

$[(\eta\text{-}C_5H_5)_2Co][Os_2(hp)_4Cl_2]$. Cobaltocene (30.1 mg, 0.159 mmol) was placed in a three-necked round-bottomed flask fitted with a rubber septum, an inlet for the influx of nitrogen gas or application of a vacuum, and a filter frit. After this system was purged with dinitrogen, a 10-mL solution of $Os_2(hp)_4Cl_2$ (115.1 mg, 0.139 mmol) in dichloromethane was added via a cannula. Within 15 min, the color of this solution had changed from dark red to olive green. After 30 min, 15 mL of deoxygenated diethyl ether was added to induce precipitation of the product, $[(\eta\text{-}C_5H_5)_2Co][Os_2(hp)_4Cl_2]$. The reaction mixture was filtered under dinitrogen to remove the olive green solid, which was washed several times with diethyl ether and then was vacuum-dried for 20 min; yield 103.6 mg (73%). Anal. Calcd for $C_{30}H_{26}Cl_2CoN_4O_4Os_2$: C, 35.43; H, 2.58. Found: C, 35.34; H, 2.75.

This complex is extremely air sensitive, especially in solution but also in the solid state, and must be stored and manipulated under nitrogen or argon gas at all times.

Physical Measurements. Electronic absorption spectra were obtained on dichloromethane solutions with an IBM Instruments Model 9420 (Purdue University) or Beckman Acta MIV (Edinburgh University) spectrophotometer. In the near-IR region appropriate background corrections were imposed. X-Band ESR spectra were obtained on toluene/dichloromethane glasses (5/2, v/v) at −160 °C with a Varian E-109 spectrometer. Magnetic susceptibilities were determined by the Evans method[14] on dichloromethane solutions with a Perkin-Elmer R32 (Purdue University) or Bruker WP805Y (Edinburgh University) NMR spectrometer. Routine cyclic voltammetry experiments were carried out on solutions in 0.2 M n-Bu_4NPF_6–CH_2Cl_2 and were performed as described previously.[15] The electrochemical generation of anions for subsequent spectroscopic characterization was carried out at 293 K by controlled-potential electrolysis at 0.00 V (vs. a Ag/AgCl reference electrode) of n-Bu_4NF–CH_2Cl_2 solutions of the complexes in an OTTLE cell (with a Pt-gauze working electrode and Infrasil windows).[16]

Elemental microanalyses were performed by Dr. H. D. Lee of the Purdue University Microanalytical Laboratory.

Results and Discussion

Cyclic voltammetric measurements on 0.2 M tetra-n-butylammonium hexafluorophosphate (TBAH)–dichloromethane solutions of the propionate and butyrate complexes $Os_2(O_2CR)_4Cl_2$ show that each complex exhibits a reversible one-electron couple[17,18] at $E_{1/2}$ = +0.29 and +0.30 V, respectively, vs. SCE (see Figure 1a). For each couple, $i_{p,a}/i_{p,c} = 1$ and $i_p/v^{1/2}$ ratios were constant in the sweep rate range 50–400 mV/s, in accord with diffusion control. At v = 200 mV/s, the potential separation ΔE_p between the anodic and cathodic peaks was 100 mV and increased slightly with increase in scan rate. A second couple is observed at $E_{1/2} \simeq$ +1.75 V vs. SCE upon extending the scan to +2.0 V. This process corresponds to a one-electron oxidation. While electrochemical behavior similar to that described above is observed in 0.1 M TBAH–acetonitrile, the oxidation now appears to be electrochemically irreversible ($i_{p,c}/i_{p,a} < 1$) although it occurs at a very similar potential ($E_{p,a}$ = +1.78 V in the case of R = n-Pr).

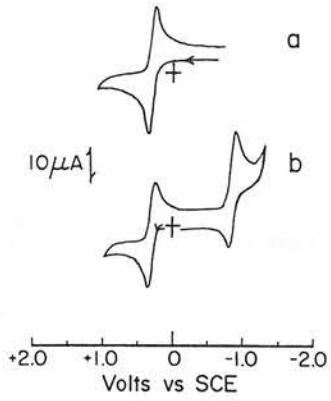

Figure 1. Cyclic voltammograms (measured at 200 mV/s in 0.2 M TBAH–CH_2Cl_2 at a Pt-bead electrode): (a) $Os_2(O_2CC_3H_7)_4Cl_2$; (b) $[(C_5H_5)_2Co][Os_2(O_2CC_3H_7)_4Cl_2]$.

The couple at $E_{1/2} \simeq$ +0.3 V corresponds to a one-electron reduction.[19] Consistent with our interpretation, we find that the controlled-potential electrolysis of such solutions at +0.20 V ($n = 1.0 \pm 0.1$ by coulometry) generates solutions containing the quite stable monoanion. Attempts to do this reduction chemically by using sodium or magnesium yielded intractable products. However, cobaltocene, which has been successfully used as a reducing agent[20,21] and which has a suitable reduction potential (−0.94 V vs. SCE in acetonitrile),[22] proved to be an ideal reductant. Thus, treatment of acetone solutions of $Os_2(O_2CR)_4Cl_2$ (R = C_2H_5 or C_3H_7) with cobaltocene yielded (after 30 min) an olive green precipitate of $[(C_5H_5)_2Co][Os_2(O_2CR)_4Cl_2]$. Cyclic voltammetry on 0.2 M TBAH–CH_2Cl_2 solutions of these complexes shows two reversible one-electron couples (Figure 1b): that at +0.30 V vs. SCE corresponds to the *oxidation* of the anion, while the reduction of the cobaltocenium ion is associated with the couple at −0.90 V vs. SCE.

We find that the reaction of $Os_2(O_2CC_3H_7)_4Cl_2$ with 2-hydroxypyridine (Hhp) in refluxing ethanol yields the dark

(13) Cotton, F. A.; Thompson, J. L. *J. Am. Chem. Soc.* **1980**, *102*, 6437.
(14) Evans, D. F. *J. Chem. Soc.* **1959**, 2003.
(15) Brisdon, B. J.; Conner, K. A.; Walton, R. A. *Organometallics* **1983**, *2*, 1159.
(16) Coombe, V. T.; Heath, G. A.; Stephenson, T. A.; Vattis, D. K. *J. Chem. Soc., Dalton Trans.* **1983**, 2307.
(17) We define reversibility in terms of a comparison with the behavior of known reversible couples such as $(C_5H_5)_2Fe/(C_5H_5)_2Fe^+$ and $Ru(bpy)_3^{2+}/Ru(bpy)_3^{3+}$. The characteristics of these latter systems obtained by using our experimental set-up and the 0.2 M TBAH–CH_2Cl_2 solvent system are described elsewhere.[18]
(18) Zietlow, T. C.; Klendworth, D. D.; Nimry, T.; Salmon, D. J.; Walton, R. A. *Inorg. Chem.* **1981**, *20*, 947.
(19) An earlier study[7] had led to the belief that this process actually corresponded to a one-electron oxidation, an interpretation that is now known to be incorrect; see: Behling, T.; Wilkinson, G.; Stephenson, T. A.; Tocher, D. A.; Walkinshaw, M. D. *J. Chem. Soc., Dalton Trans.* **1984**, 305. In this previous report,[7] electrode potentials were quoted vs. a Ag/AgI reference electrode whereas those here are referenced to the SCE. Exact comparison requires subtraction of 0.17 V from the data of ref 7, on the basis of the observations that, for the ferrocene/ferrocenium couple, $E_{1/2}$ = +0.60 V vs. Ag/AgI and $E_{1/2}$ = +0.43 V vs. the SCE in the present work.
(20) Gagné, R. R.; Ingle, D. M. *Inorg. Chem.* **1981**, *20*, 420.
(21) Gagné, R. R.; Ingle, D. M. *J. Am. Chem. Soc.* **1980**, *102*, 1444.
(22) Geiger, W. E., Jr. *J. Am. Chem. Soc.* **1974**, *96*, 2632.

red complex $Os_2(hp)_4Cl_2$ in 84% yield. While we have found that the analogous acetate complex can also be used as the precursor to $Os_2(hp)_4Cl_2$,[7] the yield is appreciably lower than when the butyrate is used. This diosmium(III) complex is the same as that which Cotton and Thompson[13] prepared from the reaction between $OsCl_3$ and 2-hydroxypyridine. Indeed, the electrochemical properties of these materials are the same,[23] an irreversible one-electron oxidation being observed at +1.20 V and a reversible one-electron reduction (n = 1.05) at +0.10 V vs. SCE (using a Pt-bead electrode in 0.2 M TBAH–CH_2Cl_2). As was the case with the diosmium(III) carboxylates, we were able to reduce $Os_2(hp)_4Cl_2$ to its monoanion using acetone solutions of cobaltocene, thereby confirming the close electronic relationship between $Os_2(O_2CR)_4Cl_2$ and $Os_2(hp)_4Cl_2$. The olive green complex $[(C_5H_5)_2Co][Os_2(hp)_4Cl_2]$ is much more sensitive to trace amounts of water and oxygen than its carboxylate analogues. Its solution in 0.2 M TBAH–CH_2Cl_2 displays a very characteristic cyclic voltammogram with two one-electron oxidations, with $E_{1/2}$ values of +1.19 and +0.03 V and a couple at −0.90 V vs. SCE due to $(C_5H_5)_2Co^+/(C_5H_5)_2Co$.

The electrochemical and chemical redox behavior we observe for $Os_2(O_2CR)_4Cl_2$ is in accord with that which might be expected on the basis of that for the related ruthenium systems.[9] The difference lies in the greatly enhanced stability of the Ru_2^{5+} core, as is present in $Ru_2(O_2CR)_4Cl$, over that of Ru_2^{6+}; the diruthenium(III) carboxylates $Ru_2(O_2CR)_4Cl_2$ are at present unknown.[24] This trend reflects the general tendency for an increase in the stability of the higher oxidation states as a transition group is descended; i.e. $Os_2^{6+} > Os_2^{5+}$ but $Ru_2^{6+} < Ru_2^{5+}$.

In the case of diruthenium complexes containing the Ru_2^{6+} or Ru_2^{5+} cores, it is apparent that the π^* and δ^* orbitals are close in energy, so that a precise assignment of the electronic structures of such species requires care. Thus, for the carboxylates $Ru_2(O_2CR)_4Cl$, the ground-state configuration is $\sigma^2\pi^4\delta^2\pi^{*2}\delta^{*1}$, on the basis of both experimental[9] and theoretical[25] results. On the other hand, the electronic structures of the species $[Ru_2L_2]^+$ and $[Ru_2L_2]^{2+}$, where L represents the dibenzotetraaza[14]annulene $[C_{22}H_{22}N_4]^{2-}$ ligand, are best described in terms of the ground-state configurations $\sigma^2\pi^4\delta^2\delta^{*2}\pi^{*1}$ and $\sigma^2\pi^4\delta^2\delta^{*2}$, respectively.[9,26]

For the Os_2^{6+} and Os_2^{5+} cores, as present in the carboxylate complexes, the situation becomes more complicated than this. The magnetic properties of the neutral complexes $Os_2(O_2CR)_4Cl_2$ and $Os_2(hp)_4Cl_2$ ($\mu_{eff} \approx 1.4$–1.6 μ_B/Os_2 unit at room temperature)[7] indicate that a $\sigma^2\pi^4\delta^2\delta^{*2}$ configuration with an appreciable contribution from the spin-triplet state $\sigma^2\pi^4\delta^2\delta^{*1}\pi^{*1}$ may be the best description. When $Os_2(O_2CR)_4Cl_2$ is reduced to its monoanion, we find that the magnetic moment increases. In the case of $[(C_5H_5)_2Co][Os_2(O_2CC_3H_7)_4Cl_2]$, its magnetic moment at 298 K (in CH_2Cl_2 by the Evans method) is $\mu_{eff} \simeq 2.73$ μ_B, a value that increases to 2.84 μ_B when the solution is cooled to 209 K. This accords with the configurations $\sigma^2\pi^4\delta^2\delta^{*1}\pi^{*2}$ (i.e. three unpaired electrons; cf. Ru_2^{5+}) and $\sigma^2\pi^4\delta^2\delta^{*2}\pi^{*1}$ or $\sigma^2\pi^4\delta^2\pi^{*3}$ (one unpaired electron) being the principal contributors to the ground state at room temperature. To further investigate this behavior, we have carried out magnetic measurements on solutions of the electrochemically generated anions. Both the propionate and butyrate $[Os_2(O_2CR)_4Cl_2]^-$ anions were electrogenerated at 0.00 V (vs. a Ag/AgCl reference electrode) at 293 K until such time as the current dropped to <1% of its initial value. The composition of the medium in both cases was 0.5 M n-Bu_4NBF_4 in CH_2Cl_2/CD_2Cl_2 (80/20, v/v). Tetramethylsilane (2%) was added after electrogeneration, and variable-temperature magnetic susceptibilities were determined by the Evans method. Allowance was made for the diamagnetic correction of the ligands and of the solvent. The data in Table I clearly show that, in spite of the technical difficulties involved in the in situ study of the magnetic properties of the air-sensitive electrogenerated diosmium anions, there is rather good agreement with the data obtained for $[(C_5H_5)_2Co][Os_2(O_2CC_3H_7)_4Cl_2]$. The reduced magnetic moments of these $[Os_2(O_2CR)_4Cl_2]^-$ anions and the form of the temperature dependence of μ_{eff} compared to that of isoelectronic $Ru_2(O_2CC_3H_7)_4Cl$ ($\mu_{eff} \approx 4$ μ_B/molecule at 300 K)[27] may arise from a larger separation of the π^*/δ^* orbitals in Os_2^{5+}, thereby producing a greater population of the spin-doublet state.

Table I. Magnetic Properties of Electrochemically Generated $[Os_2(O_2CR)_4Cl_2]^-$

R	μ_{eff} (temp)[a]
C_2H_5	2.47 (275), 2.77 (245), 2.88 (215)
C_3H_7	2.65 (240), 2.70 (210), 2.82 (200), 2.85 (190)

[a] μ_{eff} in Bohr magnetons; temperature in Kelvins.

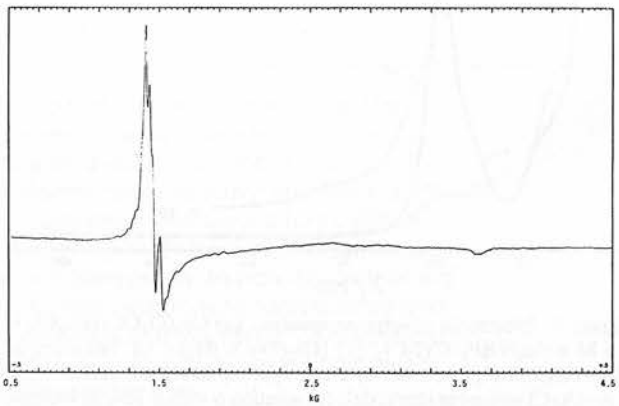

Figure 2. X-Band ESR spectrum of $[(C_5H_5)_2Co][Os_2(hp)_4Cl_2]$ in toluene/CH_2Cl_2 (5/2, v/v) at −160 °C.

A more limited study on $[(C_5H_5)_2Co][Os_2(hp)_4Cl_2]$ revealed that this complex displays comparable behavior.[28] The magnetic moment of this complex (recorded in CH_2Cl_2 by the Evans method) was 2.68 μ_B at 308 K and 2.63 μ_B at 173 K, and while μ_{eff} for this complex did not reveal the same temperature dependence as for $[Os_2(O_2CR)_4Cl_2]^-$, the magnitude of the moment is fully in accord with the population of both $\sigma^2\pi^4\delta^2\delta^{*1}\pi^{*2}$, and $\sigma^2\pi^4\delta^2\delta^{*2}\pi^{*1}$ (or $\sigma^2\pi^4\delta^2\pi^{*3}$).

The magnetic properties of the Os_2^{5+} complexes indicate that there is a major $S = {}^3/_2$ contribution to the ground state. Consequently, the ESR spectra of these complexes should be similar to that obtained for $Ru_2(O_2CC_3H_7)_4Cl$ by Cotton and Pedersen.[27] These authors concluded that this species exhibits an appreciable zero-field splitting; $2D$ is defined as the separation between the $|\pm{}^3/_2\rangle$ and $|\pm{}^1/_2\rangle$ states at zero magnetic field. If $D > 0$, then the $|\pm{}^1/_2\rangle$ states are lower in energy, while if $D < 0$, then the $|\pm{}^3/_2\rangle$ states are lower. Since spin–orbit coupling for a third-row transition metal is greater than that for the corresponding second-row element, $|2D|$ should then be greater for these Os_2^{5+} complexes as the zero-field

(23) Cyclic voltammetric data for $Os_2(hp)_4Cl_2$ as prepared from $OsCl_3$ are reported elsewhere: see: Armstrong, J. E. Ph.D. Thesis, Purdue University, 1982; p 79.
(24) Electrochemical studies of $Ru_2(O_2CR)_4Cl$ show that reduction to Ru_2^{4+} is much more favored than oxidation to Ru_2^{6+}.[9]
(25) Norman, J. G., Jr.; Renzoni, G. E.; Case, D. A. *J. Am. Chem. Soc.* **1979**, *101*, 5256.
(26) Warren, L. F.; Goedken, V. L. *J. Chem. Soc., Chem. Commun.* **1978**, 909.
(27) Cotton, F. A.; Pedersen, E. *Inorg. Chem.* **1975**, *14*, 388.
(28) We were unable to prepare by electrochemical means a sufficiently pure sample of $[Os_2(hp)_4Cl_2]^-$ to study the magnetic properties of this species when generated in this fashion.

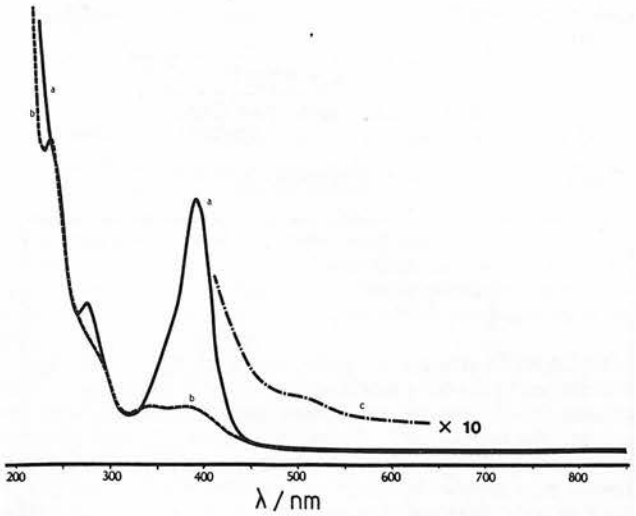

Figure 3. Electronic absorption spectra: (a) $Os_2(O_2CC_2H_5)_4Cl_2$ in 0.5 M n-Bu_4NBF_4–CH_2Cl_2; (b) $[Os_2(O_2CC_2H_5)_4Cl_2]^-$ following its electrochemical generation by electrolysis of solution a at 0.0 V (vs. a Ag/AgCl reference electrode); (c) solution b with a 10-fold increase in concentration. Spectra were recorded at 293 K in an OTTLE cell (with a Pt-gauze working electrode and Infrasil windows).

splitting is a function of the spin–orbit coupling constant. In exploring the X-band ESR spectra of the cobaltocenium salts prepared in the present investigation, we found that the complex $[(C_5H_5)_2Co][Os_2(hp)_4Cl_2]$ exhibits a rather well-defined spectrum in a toluene/dichloromethane glass (5/2, v/v) at −160 °C (see Figure 2).[29] Hyperfine splitting, which we believe is due to ^{14}N of the hydroxypyridinato ligands, is observed for both $g_\parallel$ and $g_\perp$. The g values are $g_\parallel \simeq 2.14$ and $g_\perp \simeq 2.20$, with the magnitude of $A(^{14}N)$ being in the neighborhood of 50 G. A very weak feature at 3600 G is observed in this spectrum and may be due to the parallel orientation lines.[27] These lines are expected to be very weak relative to those centered in the neighborhood of 1500 G.

Spectral simulations of $S = {}^3/_2$ systems by Pedersen and Toftlund[30] indicate that, in the limit of large D values, spectra qualitatively similar to that observed for this complex should be obtained. Indeed, the spectrum of $Ru_2(O_2CC_3H_7)_4Cl$ was fitted by assuming that $|2D|$, the zero-field splitting, was greater than 2.2 cm^{-1}.[26] Accordingly, a similar spectrum might be expected for $[(C_5H_5)_2Co][Os_2(hp)_4Cl_2]$ and related Os_2^{5+} species since the zero-field splitting should be at least as large as that observed for the diruthenium(II,III) complex.

The electrochemical generation of the carboxylate anions $[Os_2(O_2CR)_4Cl_2]^-$ was followed spectroscopically in an OTTLE cell. For the propionate (see Figure 3), the original very strong peak at 392 nm (ϵ = 10 800) and shoulder at 360 nm are replaced in the anion by peaks at 380 nm (ϵ = 1900) and 340 nm (ϵ = 2000). In addition, a new weak shoulder appears at 500 nm, the absorption at 277 nm (ϵ = 5800) collapses to a shoulder at ca. 285 nm, and the shoulder at 244 nm becomes a definite peak at 237 nm (ϵ = 12 000). In the case of the butyrate complex, very similar changes are observed on one-electron reduction. The strong peak at 392 nm (ϵ = 10 400) and shoulder at 364 nm are replaced by bands at 385 nm (ϵ = 2600) and 340 nm (ϵ = 3400). A new weak shoulder appears at 510 nm, and the peak at 278 nm (ϵ = 6100) collapses to a shoulder at ca. 280 nm.[31] Note that these are strictly reversible processes since in each case electrogeneration of the original compounds, with no loss of band intensity, is readily achieved.

A detailed interpretation of these electronic spectra is inappropriate, particularly in view of the uncertainties associated with an exact description of the ground-state composition of both the Os_2^{6+} and Os_2^{5+} cores. However, by analogy with related studies on Ru_2^{5+} carboxylato complexes,[25,33] the main component of the broad absorption band at 392 nm (Os_2^{6+}) and ca. 380 nm (Os_2^{5+}) can probably be assigned to an $O(\pi) \rightarrow Os_2(\pi^*)$ charge-transfer transition. The qualitative observation that the addition of a large excess of n-Bu_4NBr to $Os_2(O_2CC_3H_7)_4Cl_2$ reduces the intensity of the peak at 392 nm and produces an extra peak of comparable intensity at 442 nm suggests that $Cl \rightarrow Os_2(\pi^*)$ charge transfer also occurs in this region.

The profound modification of this prominent charge-transfer absorpion upon reduction from Os_2^{6+} to Os_2^{5+} is as expected for increased occupancy of the diosmium molecular orbital manifold. This behavior and the absence of intervalence bands in the near-infrared region of the Os_2^{5+} system (for both the propionate and butyrate anions no new absorptions with intensities (ϵ) >50 $dm^3\ mol^{-1}\ cm^{-1}$ were observed at wavelengths > 1000 nm) are fully consistent with the delocalized nature we ascribe to the intermediate valence anion. Further discussion of the origin of the other bands in these spectra must be deferred until more experimental and theoretical information such as single-crystal polarized absorption spectra and SCF–Xα–SW calculations is obtained.

The present work, which provides an accurate appraisal of the redox properties of triply bonded diosmium(III) and diosmium(III,II) complexes and their relationship to the analogous diruthenium species, will hopefully serve as an incentive for studies of the redox properties of more exotic diosmium species, such as the fascinating diosmium(II) porphyrin dimers that have been isolated very recently by Collman and co-workers.[34]

Acknowledgment is made to the donors of the Petroleum Research Fund, administered by the American Chemical Society, for support of this research through a grant to R.A.W. Also, we wish to thank Johnson Matthey PLC for loans of OsO_4, the SERC for financial support (to V.T.C.), and Napier College, Edinburgh, for the use of their Beckman Acta MIV spectrophotometer.

Registry No. $Os_2(hp)_4Cl_2$, 74718-48-2; $[(\eta\text{-}C_5H_5)_2Co][Os_2(O_2CC_3H_7)_4Cl_2]$, 93474-02-3; $[(\eta\text{-}C_5H_5)_2Co][Os_2(O_2CC_2H_5)_4Cl_2]$, 93474-03-4; $[(\eta\text{-}C_5H_5)_2Co][Os_2(hp)_4Cl_2]$, 93529-97-6; $Os_2(O_2CC_3H_7)_4Cl_2$, 83292-95-9; $Os_2(O_2CC_2H_5)_4Cl_2$, 89742-24-5; $(\eta\text{-}C_5H_5)_2Co$, 1277-43-6; Os, 7440-04-2.

(29) Less satisfactory spectral data were obtained for $[Os_2(O_2CR)_4Cl_2]^-$ and so are not discussed here. While the signals were much weaker than were those of the 2-hydroxypyridine complex, we note that the X-band ESR spectra of $[(C_5H_5)_2Co][Os_2(O_2CC_3H_7)_4Cl_2]$ and electrochemically generated $[Os_2(O_2CC_3H_7)_4Cl_2]^-$ were, as expected, identical. The spectra were recorded at −160 °C on toluene/CH_2Cl_2 (5/2, v/v) solutions and show two reasonably intense signals at 2460 and 2840 G, with a weaker feature at 4600 G. It may be that differences between the ESR spectra of $[Os_2(hp)_4Cl_2]^-$ and $[Os_2(O_2CR)_4Cl_2]^-$ reflect a change in the sign of the zero-field splitting parameter. This may also explain the differences in the temperature dependence of the magnetic moments of these complexes.

(30) Pedersen, E.; Toftlund, H. *Inorg. Chem.* **1974**, *13*, 1603.

(31) Similar spectral features were observed upon measuring the electronic absorption spectra of $[(C_5H_5)_2Co][Os_2(O_2CC_3H_7)_4Cl_2]$, although in this instance allowance has to be made for cobaltocenium absorptions.[32] Dichloromethane solutions of this salt show bands at 348, 393, and 510 (sh) nm that clearly have counterparts in the spectra of the electrochemically generated samples. Also, two much weaker features were observed at ~620 (br, sh) and ~850 nm, both possessing $\epsilon \lesssim 100$.

(32) Sheats, J. E.; Rausch, M. D. *J. Org. Chem.* **1970**, *35*, 3245.

(33) Martin, D. S.; Newman, R. A.; Vlasnik, L. M. *Inorg. Chem.* **1980**, *19*, 3404.

(34) Collman, J. P.; Barnes, C. E.; Woo, L. K. *Proc. Natl. Acad. Sci. U.S.A.* **1983**, *80*, 8784.

Electrochemically induced Ligand Substitutions on $[OsCl_3(PMe_2Ph)_3]$: Rational Pathways to Osmium(II) Complexes

Vyvyan T. Coombe, Graham A. Heath, T. Anthony Stephenson, John D. Whitelock, and Lesley J. Yellowlees*
Department of Chemistry, University of Edinburgh, Edinburgh EH9 3JJ

Following electroreduction of $[OsCl_3(PMe_2Ph)_3]$ it is possible to stabilise and characterise the reactive monoanion $[OsCl_3(PMe_2Ph)_3]^-$. This monoanion readily releases chloride to give a detectable five-co-ordinate intermediate which further reacts with a donor solvent or available ligands to produce $[OsCl_2(PMe_2Ph)_3L]$ (L = MeCN, dimethylformamide, dimethyl sulphoxide, PhCN, CO, N_2, or C_2H_4), initially as the *trans* isomer. The latter can be converted into the *cis* form. When L = PMe_2Ph, the '*trans* isomer' formed is not *trans*-$[OsCl_2(PMe_2Ph)_4]$ and should be formulated as *trans*-$[OsCl_2(PMe_2Ph)_3(P'Me_2Ph)]$ with a unique weakly bound phosphine. In non-co-ordinating media, concentrated solutions of $[OsCl_2(PMe_2Ph)_3]$ undergo further reactions to form doubly and triply bridged binuclear species such as $[Os_2Cl_4(PMe_2Ph)_6]$ and $[Os_2Cl_3(PMe_2Ph)_6]^+$. This series of electroinitiated reactions of *mer*-$[OsCl_3(PMe_2Ph)_3]$ has so far yielded over 20 separate complexes individually identified by both spectroscopic methods and voltammetric data.

In order to complement detailed studies on redox-active binuclear ruthenium complexes in this laboratory,[1–3] we have examined the chemistry of *mer*-$[OsCl_3(PMe_2Ph)_3]$ (**1**) as a possible starting point for rational syntheses of triply halide-bridged diosmium complexes such as $[(PMe_2Ph)_3OsCl_3Os(PMe_2Ph)_3]^+$ and $[(PMe_2Ph)_2ClOsCl_3Os(PMe_2Ph)_3]$. Chemical reduction of (**1**) results ultimately in the triply halide-bridged diosmium complex.[4] However, the mechanistic pathway is unknown and the chemical by-products complicate identification of the reduction products. Thus we have used electrochemical methods in parallel with spectroscopic techniques to elucidate the problem.

The monomer (**1**) has a rewarding electrochemical response, and we have been able to prepare the anion *mer*-$[OsCl_3(PMe_2Ph)_3]^-$ (**2**) together with several $[OsCl_2(PMe_2Ph)_3L]$ complexes [where L = dimethylformamide (dmf), PhCN, MeCN, *etc.*] in both *cis*- and *trans*-dichloro-forms. The *trans* isomer is that initially formed by electrogeneration, in contrast to chemical reduction which generally yields only the thermodynamically favoured *cis* isomers. Furthermore, under appropriate conditions diosmium complexes are indeed the ultimate products. All the various osmium(II) compounds have been individually characterised by i.r., n.m.r., and voltammetric measurements.

Results and Discussion

A cyclic voltammogram of *mer*-$[OsCl_3(PMe_2Ph)_3]$ in CH_2Cl_2 under argon at room temperature is shown in Figure 1(*a*). The oxidation [A in Figure 1(*a*)] is assigned as an $Os^{III} \longrightarrow Os^{IV} + e$ electrode process and the reduction (B) as an $Os^{III} + e \longrightarrow Os^{II}$ electrode process with a rapid 'chemical' (*i.e.* homogeneous) subsequent reaction. Figure 1 also shows that when the solution temperature is decreased to 233 K then the reduction becomes totally reversible (the ratio of the anodic to cathodic peak currents is 1.0 and the anodic-to-cathodic peak separation is 50 mV, compared with the theoretical value of 44 mV for a Nernstian one-electron wave at 233 K). It is therefore possible to stabilise the anion $[OsCl_3(PMe_2Ph)_3]^-$ (**2**) for some seconds simply by altering the temperature. However, adequate characterisation of the anion demands a much longer lifetime, and this has been achieved by variation of the solvent/electrolyte composition. A fully reversible voltammogram [resembling

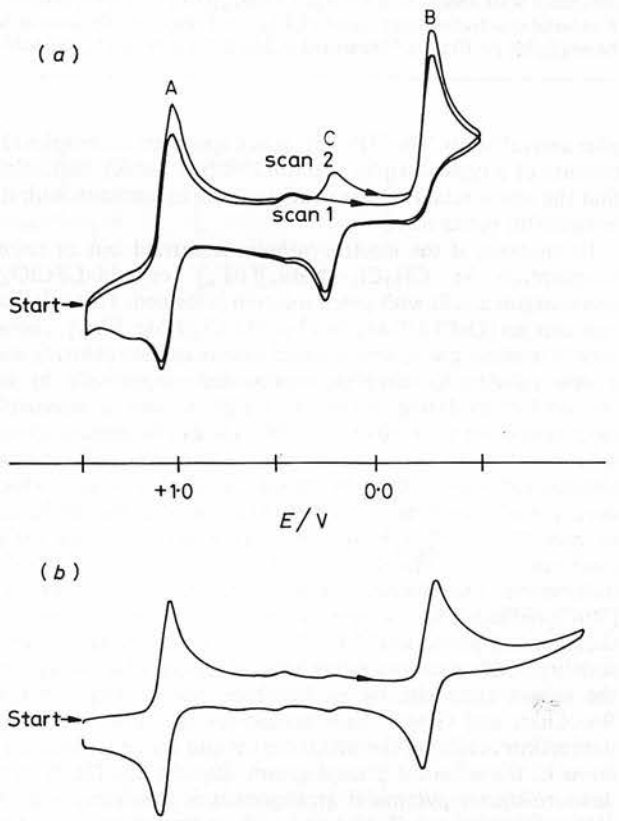

Figure 1. Cyclic voltammograms of *mer*-$[OsCl_3(PMe_2Ph)_3]$ in CH_2Cl_2–$[NBu_4][BF_4]$ under argon *vs.* Ag–AgCl (scan rate 100 mV s^{-1}) at 293 (*a*) and 233 K (*b*)

Figure 1(*b*)] can be obtained at room temperature in CH_2Cl_2 by replacing the supporting electrolyte $[NBu_4][BF_4]$ by $[NR_3Me][BF_4]$ (R = C_8H_{17} to $C_{10}H_{21}$), or by using tetrahydrofuran (thf) with $[NBu_4][BF_4]$. Remarkably, either system allows bulk electrogeneration under argon of (**2**) which is bright yellow [(**1**) is dark red], with no loss of the product even

Table. N.m.r. and electrochemical data for derivatives of $[OsCl_3(PMe_2Ph)_3]$

Compound	Solvent	^{31}P-$\{^1H\}$ N.m.r. [a] δ_A/p.p.m.	δ_B/p.p.m.	J_{AB}/Hz	$E_{\frac{1}{2}}$ (Os^{II}–Os^{III}) [b]
trans-$[OsCl_3(PMe_2Ph)_3]^-$	thf [c]	−42.7	−45.1	12.2 [d]	−0.36
trans-$[OsCl_2(PMe_2Ph)_3]$	CH_2Cl_2 [e]	−46.7	−33.6	22.0 [d]	+0.03
	thf [c]	−44.8	−32.8	17.1 [d]	+0.03
cis-$[OsCl_2(PMe_2Ph)_3]$	thf [c]	−49.4	−27.6	17.1 [d]	
trans-$[OsCl_2(PMe_2Ph)_3(MeCN)]$	CH_2Cl_2	−47.7	−35.9	22.0 [d]	+0.25
cis-$[OsCl_2(PMe_2Ph)_3(MeCN)]$	MeCN	−31.3	−31.9	20.6 [f]	+0.25
trans-$[OsCl_2(PMe_2Ph)_3(dmf)]$	CH_2Cl_2	−47.5	−28.6	18.3 [d]	+0.02
cis-$[OsCl_2(PMe_2Ph)_3(dmf)]$	dmf	−30.5	−31.3	15.0 [f]	+0.02
trans-$[OsCl_2(PMe_2Ph)_3(dmso)]$	dmso	−44.1	−38.7	17.1 [d]	+0.02
trans-$[OsCl_2(PMe_2Ph)_3(PhCN)]$	PhCN	−47.3	−38.3	22.0 [d]	*ca.* +0.26
cis-$[OsCl_2(PMe_2Ph)_3(PhCN)]$	PhCN	−31.3	−31.5	n.a.	*ca.* +0.26
trans-$[OsCl_2(PMe_2Ph)_3(CO)]$	CH_2Cl_2	−46.4	−43.5	30.1 [f]	+0.83
trans-$[OsCl_2(PMe_2Ph)_3(C_2H_4)]$	CH_2Cl_2	−48.5	−39.1	15.9 [d]	+0.54
trans-$[OsCl_2(PMe_2Ph)_3(N_2)]$	thf	−47.8	−37.3	22.0 [d]	+0.16
cis-$[OsCl_2(PMe_2Ph)_3(N_2)]$	thf	−36.3	−34.9	15.1 [f]	
trans-$[OsCl_2(PMe_2Ph)_4]$	CH_2Cl_2	−52,5 [g]			+0.28
cis-$[OsCl_2(PMe_2Ph)_4]$	CH_2Cl_2	−43.8	−44.9	13.4 [f]	+0.75
$[Os_2Cl_4(PMe_2Ph)_6]$	CH_2Cl_2 [e]	−44.8	−40.0	17.1 [d]	+0.48
$[Os_2Cl_3(PMe_2Ph)_6]^+$	CH_2Cl_2	−36.7 [g]			+1.09

[a] All resonances lie to high frequency of the H_3PO_4 reference. All values determined at room temperature (except where specified). [b] All values are measured with respect to a Ag–AgCl, $[NBu_4][BF_4]$–CH_2Cl_2 reference electrode, against which ferrocene is oxidised at +0.55 V in CH_2Cl_2. Values measured in solvents other than CH_2Cl_2 (see Table) include uncorrected junction potentials. The latter were checked in MeCN and dmf and found to be negligible (< 10 mV). [c] Measured at 230 K. [d] Triplet (δ_A) and doublet (δ_B) at 24.2 MHz. [e] Measured at 200 K. [f] AB_2 pattern at 24.2 MHz. [g] Singlet.

after several hours. The ^{31}P-$\{^1H\}$ n.m.r. spectrum of complex (**2**) consists of a typical triplet and doublet (see Table), indicating that the anion retains a *mer* configuration, in common with its osmium(III) precursor.

In contrast, if the electrosynthesis is carried out at room temperature in CH_2Cl_2–$[NBu_4][BF_4]$ or thf–$Li[ClO_4]$ under argon a yellowish green solution is formed. This solution contains no $[OsCl_3(PMe_2Ph)_3]$ or $[OsCl_3(PMe_2Ph)_3]^-$; however, it is diamagnetic and is found to contain free chloride and a new osmium(II) complex, represented respectively by an irreversible oxidation wave at +1.20 V and a reversible oxidation wave at +0.03V. The chloride can be removed from solution by addition of 1 mol equivalent of sodium tetrafluoroborate. Thus the rapid chemical reaction which occurs after reduction of complex (**1**) is loss of a chloride ligand to give $[OsCl_2(PMe_2Ph)_3]$, (**3**). The exact nature of (**3**) is uncertain but our various observations (see below) support the monomeric formulation shown. The analogous complex $[RuCl_2(PPh_3)_3]$ has square-pyramidal co-ordination both in the solid and in solution.[5,6] La Placa and Ibers [5] suggest that the stability of this structure arises from intramolecular blocking of the vacant sixth site by a phosphine phenyl ring, whereas Brookhart and Green [7] have argued for an 'agostic' bonding interaction involving the metal centre and an *ortho*-hydrogen atom of the adjacent phenyl group. Equally for (**3**), a *trans* dichloro-square-pyramidal arrangement is consistent with its ^{31}P n.m.r. spectrum (Table) and with its further reactions (see below). The designation 'five-co-ordinate' herein should be taken to embrace the possibility of special axial interactions. In thf, where the n.m.r. spectroscopic data are better defined, a further clear-cut rearrangement of complex (**3**) is observed. This is tentatively assigned to the *trans*- to *cis*-dichloro-conversion of (**3**) in to (**4**) (Scheme), although weak binding of thf is not excluded by the available data. In summary, as shown in the Scheme, *mer*-$[OsCl_3(PMe_2Ph)_3]$ on reduction loses the chloride ligand *trans* to phosphine to give the intermediate species (**3**), which exhibits its own distinctive redox behaviour [see Table and process C in Figure 1(*a*)]. This is an example of an electrochemical e.c.e. mechanism, *i.e.* an electron transfer, followed by a chemical change, followed by an electron transfer.[8]

We have extended our electrochemical studies of compound (**1**) to a variety of co-ordinating solvents such as acetonitrile (MeCN), dimethylformamide (dmf), dimethyl sulphoxide (dmso), and benzonitrile (PhCN). The redox behaviour and the peak potentials for the Os^{III}–Os^{IV} and Os^{II}–Os^{III} couples of (**1**) itself are independent of solvent and the voltammograms are similar in appearance to those in Figure 1. However, when determined by slow-scan voltammetry or after bulk reduction of compound (**1**), $E_{\frac{1}{2}}$ for the Os^{II}–Os^{III} couple of the *chemically altered* osmium(II) product is dependent on the solvent, occurring for example at +0.02 V in dmf but at 0.26 V in PhCN (Table). Conveniently, the product formed by electroreduction of (**1**) in MeCN largely precipitates from solution. This yellow product, with stoicheiometry $[OsCl_2(PMe_2Ph)_3(MeCN)]$, darkens and decomposes over several days in air. Its configuration is established as the *trans* isomer (Scheme) from its ^1H n.m.r. spectrum in CD_2Cl_2 which shows a triplet (intensity 2) and a doublet (intensity 1) for the methyl resonances (see Experimental section).[9] The MeCN ligand remains firmly bound to the osmium(II) centre as shown by the singlet ^1H n.m.r. signal at δ 1.30 p.p.m. and there is no evidence for free MeCN (singlet at δ 2.00 p.p.m.). The ^{31}P-$\{^1H\}$ n.m.r. spectrum of the *trans* isomer in CH_2Cl_2 shows the expected doublet and triplet [Table, Figure 2(*a*)]. The same signals are observed in the mother-liquor immediately after electroreduction of compound (**1**) since the *trans* product is slightly soluble in MeCN. However, if the solution is left standing at 293 K in the absence of air, these signals decrease in intensity and new ones steadily emerge until only the new signals [an AB_2 pattern, Figure 2(*b*)] are present after 16 h. This final, almost colourless, solution shows no evidence of free PMe_2Ph or Cl^- (beyond the 1 mol equivalent released during the electrosynthesis) and has an electrochemistry almost indistinguishable from the *trans* isomer. This indicates that the sparingly soluble *trans* isomer is the kinetically favoured product and this slowly converts in solution into the thermodynamically favoured *cis* isomer. Accordingly, in the ^1H

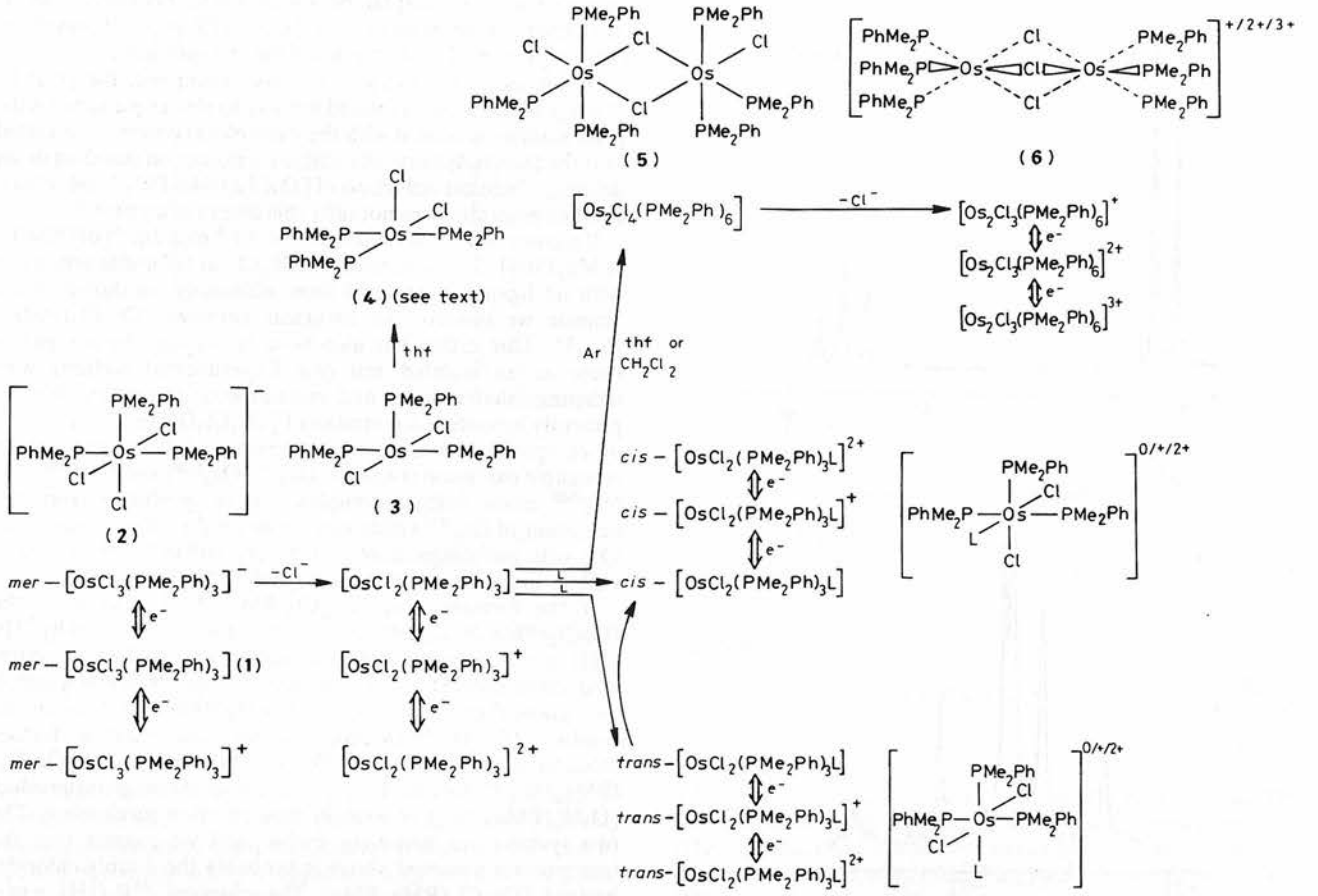

Scheme. L = PMe_2Ph (see text), PhCN, MeCN, dmf, N_2, C_2H_4, CO, or dmso

n.m.r. spectrum in CD_3CN[9] the initial triplet and doublet for the *trans* isomer are replaced by two triplets and a doublet (intensity 1:1:1) characteristic of the *cis* isomer (see Experimental section). The *cis* isomer was not isolated but it is noticeably more stable towards aerial oxidation in solution than the *trans* isomer.

Parallel behaviour is found when dmf is used as the electrochemical solvent. Thus the yellow *trans* isomer $[OsCl_2(PMe_2Ph)_3(dmf)]$ precipitates as electroreduction of (**1**) proceeds but the material remaining in solution converts into the *cis* isomer over several hours. N.m.r. and voltammetric data for both isomers are given in the Table. The i.r. spectrum of the *trans* isomer [ν(CO) 1 630 cm^{-1}] indicates O-bonded dmf. In CH_2Cl_2 at *ca.* 200 K the dmf isomer is indefinitely stable, however at room temperature the voltammetry, $^{31}P-\{^1H\}$ n.m.r. and i.r. spectra all change steadily until, after *ca.* 2 h, only signals for a new species are observed. Thus the $E_{\frac{1}{2}}$ value shifts from +0.02 to +0.20 V, the $^{31}P-\{^1H\}$ n.m.r. spectrum now consists of a doublet at δ −36.2 and a triplet at −47.9 p.p.m., and the i.r. spectrum shows the ν(CO) band shifted to 1 660 cm^{-1}. Since free dmf absorbs at 1 675 cm^{-1}, we tentatively suggest that the dmf ligand is no longer oxygen-bound, but rather nitrogen-bound to the osmium atom. A similar phenomenon is observed in dmso; the initial, presumably oxygen-bound, dmso in the *trans* complex quickly arranges to the thermodynamically favoured sulphur-bound *trans* analogue. The poor affinity of the osmium(II) centre for O-donor ligands is also reflected in the observation that neither thf nor propylene carbonate binds to complex (**3**).

A direct consequence of the reaction sequence postulated in the Scheme is that the rate of chloride loss from the anion (**2**) to form the five-co-ordinate $[OsCl_2(PMe_2Ph)_3]$ (**3**) should be independent of solvent (*i.e.* the products are formed *via* a dissociative mechanism, rather than by an associative mechanism involving solvent co-ordination). The rate of chloride loss (k_f) was measured according to the method of Nicholson and Shain[10] in CH_2Cl_2–$[NBu_4][BF_4]$, MeCN–$[NBu_4][BF_4]$, or dmf–$[NBu_4][BF_4]$ and in every case k_f = 5 s^{-1} at 288 K. The 'following reaction',[8] uptake of L to form $[OsCl_2(PMe_2Ph)_3L]$, ranges from very fast (when L = MeCN, where the five-co-ordinate intermediate could not be observed under any conditions) to rates at which the intermediate was detectable using fast-scanning techniques (*e.g.* L = N_2, see below). The rate of chloride loss can of course be retarded by decreasing the temperature, as noted above.

Other complexes of type $[OsCl_2(PMe_2Ph)_3L]$ (L = CO, N_2, or C_2H_4) can readily be prepared from solutions of electrogenerated (**3**) in CH_2Cl_2–$[NBu_4][BF_4]$ continuously saturated with the relevant gas (see Table for $^{31}P-\{^1H\}$ n.m.r. and voltammetric data). When L = CO, the *trans* isomer is formed [ν(CO) 1 950 cm^{-1} in electrolyte solution; lit.,[4] ν(CO) 1 947 (*trans*), 1 930 cm^{-1} (*cis*)]. There is no evidence of rearrangement even after several days in solution at ambient temperature, but on heating the solution the *cis* isomer is readily produced.

Previous attempts to prepare *trans*-$[OsCl_2(PMe_2Ph)_3(N_2)]$ have been unsuccessful, with only the *cis* isomer being formed.[4,11] This failure was ascribed to the dinitrogen having too weak a σ-donor function to bind *trans* to a high *trans*-influence ligand such as PMe_2Ph. However we find that on

Chemicals.—Acetonitrile was purified by the method of Walter and Ramaley[18] and was freshly distilled from P_2O_5 before use. Methylene chloride was allowed to stand for 1 week over KOH pellets and dried by distillation over P_2O_5. Tetrahydrofuran was dried by distillation over sodium wire. All other solvents were used as supplied without further purification. The salts $[NR_3Me][BF_4]$ ($R = C_8H_{17}$ to $C_{10}H_{21}$) were prepared by metathesis of Adogen 464, $[NR_3Me]Cl$ (Aldrich Chemicals), with $Na[BF_4]$ in MeCN. Osmium tetroxide was supplied by Johnson Matthey Chemicals Ltd. and Na_2OsCl_6 was prepared by standard methods.

mer-*Trichlorotris*(*dimethylphenylphosphine*)*osmium*(III).—This was prepared by the literature method of Leigh and co-workers[19] (Found: C, 40.8; H, 4.5. Calc. for $C_{24}H_{33}Cl_3OsP_3$: C, 40.6; H, 4.6%).

cis-*Dichlorotetrakis*(*dimethylphenylphosphine*)*osmium*(II).—The complex *mer*-$[OsCl_3(PMe_2Ph)_3]$ (0.57 g) and PMe_2Ph (0.5 cm^3) were heated under reflux in degassed 2-methoxyethanol (40 cm^3) for 30 min until the red colour had completely changed to a golden yellow. After volume reduction, addition of acetone, and cooling, the pale cream product precipitated and was washed well with acetone and diethyl ether and dried. Yield of *cis*-$[OsCl_2(PMe_2Ph)_4]$: 0.51 g, (60%) (Found: C, 47.3; H, 5.2. Calc. for $C_{32}H_{44}Cl_2OsP_4$: C, 47.2; H, 5.4%).

trans-*Dichlorotetrakis*(*dimethylphenylphosphine*)-*osmium*(II).—The *trans* complex was prepared by a variation of the method of Bell *et al.*,[16] namely; Na_2OsCl_6 and PMe_2Ph were heated under reflux in aqueous ethanol for 1 h (Found: C, 46.7; H, 5.4. Calc for $C_{32}H_{44}Cl_2OsP_4$: C, 47.2; H, 5.4%).

trans-*Dichlorotris*(*dimethylphenylphosphine*)(*methyl cyanide*)-*osmium*(II).—The complex *mer*-$[OsCl_3(PMe_2Ph)_3]$ (0.1 g) was dissolved in degassed MeCN–0.1 mol dm^{-3} $[NBu_4][BF_4]$ (10 cm^3) and electroreduced at −0.60 V until the current decayed to <5% of its initial value. The yellow product which precipitated was filtered off under nitrogen, washed with diethyl ether, dried and stored *in vacuo*. Yield of $[OsCl_2(PMe_2Ph)_3(MeCN)]$: 0.07 g (70%) (Found: C, 42.4; H, 5.0; N, 1.9. Calc. for $C_{26}H_{36}Cl_2NOsP_3$: C, 43.5; H, 5.0; N, 1.9%). ^1H N.m.r. spectra: *trans*-$[OsCl_2(PMe_2Ph)_3(MeCN)]$ in CD_2Cl_2, δ = 1.72 (d), 1.55 (t), and 1.30 p.p.m. (s, MeCN); *cis*-$[OsCl_2(PMe_2Ph)_3(CD_3CN)]$ in CD_3CN, δ = 1.87 (t), 1.73 (t), and 1.36 (d) p.p.m.

Tri-μ-*chloro-hexakis*(*dimethylphenylphosphine*)*diosmium*(II,II) *Chloride.*—The complex *cis*-$[OsCl_2(PMe_2Ph)_4]$ (0.135 g) was heated under reflux in degassed Bu^tOH (30 cm^3) for 24 h. On reduction in volume and cooling, the pale yellow product precipitated as the chloride salt. Yield of $[Os_2Cl_3(PMe_2Ph)_6]Cl$: 0.095 g (85%) (Found: C, 42.8; H, 4.8. Calc. for $C_{48}H_{66}Cl_4Os_2P_6$: C, 42.7; H, 4.8%).

Acknowledgements

We thank the S.E.R.C. for financial support (to V. T. C., J. D. W., and L. J. Y.) and Johnson Matthey plc for generous loans of OsO_4.

References

1 G. A. Heath, G. T. Hefter, D. R. Robertson, W. J. Sime, and T. A. Stephenson, *J. Organomet. Chem.*, 1978, **152**, C1 and refs. therein; T. Arthur, R. Contreras, G. A. Heath, A. J. Lindsay, D. J. A. Riach, and T. A. Stephenson, *ibid.*, 1979, **179**, C49; R. Contreras, G. G. Elliot, R. O. Gould, G. A. Heath, A. J. Lindsay, and T. A. Stephenson, *ibid.*, 1981, **215**, C6; G. A. Heath, A. J. Lindsay, T. A. Stephenson, and D. K. Vattis, *ibid.*, 1982, **233**, 353; V. T. Coombe, G. A. Heath, T. A. Stephenson, and D. K. Vattis, *J. Chem. Soc., Dalton Trans.*, 1983, 2307.
2 P. W. Armit, A. S. F. Boyd, and T. A. Stephenson, *J. Chem. Soc., Dalton Trans.*, 1975, 1663.
3 R. A. Contreras (Zarate), Ph.D. Thesis, University of Edinburgh, 1981.
4 J. Chatt, D. P. Melville, and R. L. Richards, *J. Chem. Soc. A*, 1971, 1169.
5 S. J. La Placa and J. A. Ibers, *Inorg. Chem.*, 1965, **4**, 778.
6 P. R. Hoffman and K. G. Caulton, *J. Am. Chem. Soc.*, 1975, **97**, 4221.
7 M. Brookhart and M. L. H. Green, *J. Organomet. Chem.*, 1983, **250**, 395.
8 A. J. Bard and L. R. Faulkner, 'Electrochemical Methods,' Wiley, New York, 1980, p. 462.
9 B. L. Shaw and A. C. Smithies, *J. Chem. Soc. A*, 1968, 2784.
10 R. S. Nicholson and I. Shain, *Anal. Chem.*, 1964, **36**, 706.
11 J. Chatt, G. J. Leigh, and R. L. Richards, *J. Chem. Soc. A*, 1970, 2243.
12 S. Donovan-Mtunzi, R. L. Richards, and J. Mason, *J. Chem. Soc., Dalton Trans.*, 1984, 469.
13 J. E. Armstrong and R. A. Walton, *Inorg. Chem.*, 1983, **22**, 1545.
14 V. T. Coombe, G. A. Heath, D. McMillan, T. A. Stephenson, and L. J. Yellowlees, unpublished work.
15 M. A. Green, J. C. Huffman, and K. G. Caulton, *J. Organomet. Chem.*, 1983, **243**, C78.
16 B. Bell, J. Chatt, and G. J. Leigh, *J. Chem. Soc., Dalton Trans.*, 1973, 997.
17 A. S. Alves, D. S. Moore, R. A. Anderson, and G. Wilkinson, *Polyhedron*, 1982, **1**, 83.
18 M. Walter and L. Ramaley, *Anal. Chem.*, 1973, **45**, 165.
19 J. Chatt, G. J. Leigh, D. M. P. Mingos, and R. J. Paske, *J. Chem. Soc. A*, 1968, 2636.

Received 15*th May* 1984; *Paper* 4/800